

Photoredox-catalyzed ATRA reactions and related processes in a new light

Dissertation

Zur Erlangung des Doktorgrades der Naturwissenschaften

Dr. rer. nat.

der Fakultät für Chemie und Pharmazie
der Universität Regensburg



vorgelegt von

Peter Ehrnsberger

aus Berg bei Neumarkt i. d. OPf.

Regensburg 2021

Die Arbeit wurde angeleitet von: Prof. Dr. Oliver Reiser

Promotionsgesuch eingereicht am: 14.09.2021

Promotionskolloquium am: 18.10.2021

Prüfungsausschuss: Vorsitz: Prof. Dr. Alkwin Slenczka

1. Gutachter: Prof. Dr. Oliver Reiser

2. Gutachter: Prof. Dr. Julia Rehbein

3. Prüfer: Prof. Dr. Robert Wolf

Der experimentelle Teil der vorliegenden Arbeit wurde in der Zeit von Juni 2016 bis März 2020 unter der Leitung von Herrn Prof. Dr. Oliver Reiser am Institut für Organische Chemie der Universität Regensburg angefertigt.

Besonders bedanken möchte ich mich bei Herrn Prof. Dr. Oliver Reiser für die Aufnahme in seinen Arbeitskreis, die Überlassung des vielseitigen Themas, die anregenden Diskussionen und seine Unterstützung.

Für meine Familie

Abbreviations

A	acceptor	<i>dr</i>	diastereomeric ratio
Ac	acetyl	dtbbpy	4,4'-di- <i>tert</i> -butyl-2,2'-bipyridine
AIBN	azobisisobutyronitrile	E	electrophile
Anhyd.	anhydrous	$E_{1/2}$	standard reduction potential
Aq.	aqueous	EA	ethyl acetate
Ar	aryl	Ed.	editor
ATRA	atom transfer radical addition	EDG	electron-donating group
ATRC	atom transfer radical cyclization	<i>ee</i>	enantiomeric excess
ATRP	atom transfer radical polymerization	e. g.	<i>exempli gratia</i> , for example
binc	bis(2-isocyanophenyl)	EPR	electron paramagnetic resonance
Bn	benzyl	equiv.	equivalents
Boc	<i>tert</i> -butoxycarbonyl	ESI	electrospray ionization
Bodipy	boron-dipyrromethene	<i>et al.</i>	and co-workers
bpy	2,2'-bipyridyl	Et	ethyl
Bu	butyl	EtOH	ethanol
°C	degrees Celsius	EWG	electron-withdrawing group
CFL	compact fluorescent lamp	FG	functional group
cm ⁻¹	wavenumbers	FRET	Förster resonance energy transfer
COD	1,5-cyclooctadiene	GABA	γ-aminobutyric acid
D	donor	h	hour(s)
d	day(s)	hν	light
dap	2,9-bis(<i>p</i> -anisyl)-1,10-phenanthroline	HMPA	hexamethylphosphoramide
DBU	1,8-diazabicyclo[5.4.0]undec-7-ene	HOMO	highest occupied molecular orbital
DCE	1,2-dichloroethane	HPLC	high-performance liquid chromatography
DCM	dichloromethane	HRMS	high-resolution mass spectrometry
DIOP	2,3- <i>O</i> -isopropylidene-2,3-dihydroxy	Hz	hertz
	-1,4-bis(diphenylphosphino)butane	IR	infrared
DIPEA	<i>N,N</i> -diisopropylethylamine	ISC	intersystem crossing
DMF	<i>N,N</i> -dimethylformamide	<i>J</i>	coupling constant
dmp	2,9-dimethyl-1,10-phenanthroline	L	ligand
DMSO	dimethyl sulfoxide	LED	light emitting diode
dpp	2,9-diphenyl-1,10-phenanthroline	LUMO	lowest unoccupied molecular orbital

μ	micro	THF	tetrahydrofuran
M	metal	TLC	thin-layer chromatography
M^+	parent molecular ion	TMS	tetramethylsilyl
Me	methyl	Ts	tosyl
MeCN	acetonitrile	TTET	triplet-triplet energy transfer
MeOH	methanol	UV	ultraviolet
Mes	mesityl	V	volt
MHz	megahertz	VLIH	visible-light induced homolysis
min	minute(s)	vs.	versus
MLCT	metal to ligand charge transfer	W	watt
mmol	millimole(s)	λ	wavelength
mp	melting point	δ	chemical shift (ppm) downfield from TMS
m/z	mass to charge ratio		
NBS	<i>N</i> -bromosuccinimide		
nm	nanometer		
NMR	nuclear magnetic resonance		
ns	nanosecond		
Nu	nucleophile		
PC	photocatalyst		
Ph	phenyl		
Phen	1,10-phenanthroline		
ppm	parts per million		
ppy	2-phenylpyridine		
Pr	propyl		
pybox	pyridine linked bisoxazoline		
R	arbitrary moiety		
R_f	retention factor		
rt	room temperature		
SET	single electron transfer		
t	time		
TBAF	tetra- <i>n</i> -butylammonium fluoride		
Tf	triflate		
TFA	trifluoroacetic acid		

Table of contents

A Introduction	1
1. The concept of atom efficiency	1
2. Developments of atom transfer radical additions (ATRA)	2
3. Photocatalysis – historical and photophysical background	8
4. Advancements in visible light-mediated ATRA chemistry	13
B Visible light mediated ATRA reactions and related processes	25
1. Visible light mediated allylation reactions with allylsilanes	25
1.1 Literature background	25
1.2 Visible light mediated allylations of α -halo carbonyls	27
1.3 Visible light mediated allylations of sulfonyl chlorides	33
1.4 Visible light mediated allylations of <i>N</i> -chloro-amines	38
1.5 Proposed mechanism	40
1.6 Conclusion	41
2. Visible light mediated ATRA reactions with vinylsilanes – Access to and utilization of α -haloalkylsilanes	42
2.1 Literature background and attempts towards photochemical vinylation	42
2.2 Common synthesis methods of α -haloalkylsilanes	45
2.3 α -haloalkylsilanes in organic synthesis	46
2.4 Atom transfer radical additions with vinyltrimethylsilane	50
2.5 Applications of photoredox-catalytically formed α -haloalkylsilanes	54
2.5.1 (<i>E</i>)-trimethyl(2-tosylvinyl)silane as synthon for acetylene in cycloaddition reactions	54
2.5.2 Peterson Olefination	57
2.5.3 Formation of silyl-substituted cyclopropanes and steps towards their ring-opening	58
2.6 Conclusion and outlook	64
3. Synthesis of cyclic γ -amino acids <i>via</i> visible light mediated ATRA reactions and cyclizations	65
3.1 Cyclic GABA-analogs	65
3.2 Visible light mediated ATRA reactions of <i>tert</i> -butyl allylcarbamate	67
3.3 Cyclization reactions	69
3.4 Conclusion	71
4. Visible light mediated ATRA reactions with oxabicyclic alkenes	72
4.1 7-Oxanorbornane derivatives in nature and organic synthesis	72
4.2 ATRA reactions with 7-oxanorbornenes	74
4.3 Testing different ring-opening strategies	80
4.4 Conclusion	84

C Summary	85
D Zusammenfassung	87
E Experimental Part	89
1. General information	89
1.1. Synthesis of literature known compounds and reagents	89
2. Visible light mediated allylations of α -halo carbonyls	90
3. Visible light mediated allylations of sulfonyl chlorides	94
4. Visible light mediated allylations of <i>N</i> -chloro-amines	103
5. Atom transfer radical additions with vinyltrimethylsilane	104
6. Formation of silyl-substituted cyclopropanes	112
7. Atom transfer radical additions with <i>tert</i> -butyl allylcarbamate	113
8. Atom transfer radical additions with oxabicyclohexenes	118
F References	124
G Appendix	134
1. NMR spectra	134
H Acknowledgement	188
I Declaration	190

A Introduction

1. The concept of atom efficiency

One of the foundation pillars of organic synthesis is the transformation of readily available raw materials and fine chemicals into complex target molecules. Scientists have ever been working on overcoming the main obstacle of these transformations which is the problem of selectivity. Generally, selectivity can be characterized into four categories: chemoselectivity (differentiation between functional groups), regioselectivity (orientational control), diastereoselectivity (control of relative stereochemistry) and enantioselectivity (control of absolute stereochemistry).^[1,2]

But one basic principle of organic synthesis has mostly been ignored for a long time: the concept of atom economy. The production of waste and unwanted side-products has long been underestimated both by scientists and industry. It was Trost who promulgated the concept of atom economy (sometimes called atom efficiency) in 1991.^[2] The core principle of atom economy is to look into how many atoms of the starting materials actually end up in the desired product and is calculated by dividing the molecular mass of the desired product by the sum of the molecular masses of all products that are formed (see equation 1).^[3]

$$\text{atom economy (\%)} = \frac{\text{mass of desired product}}{\text{mass of all formed products}} \times 100$$

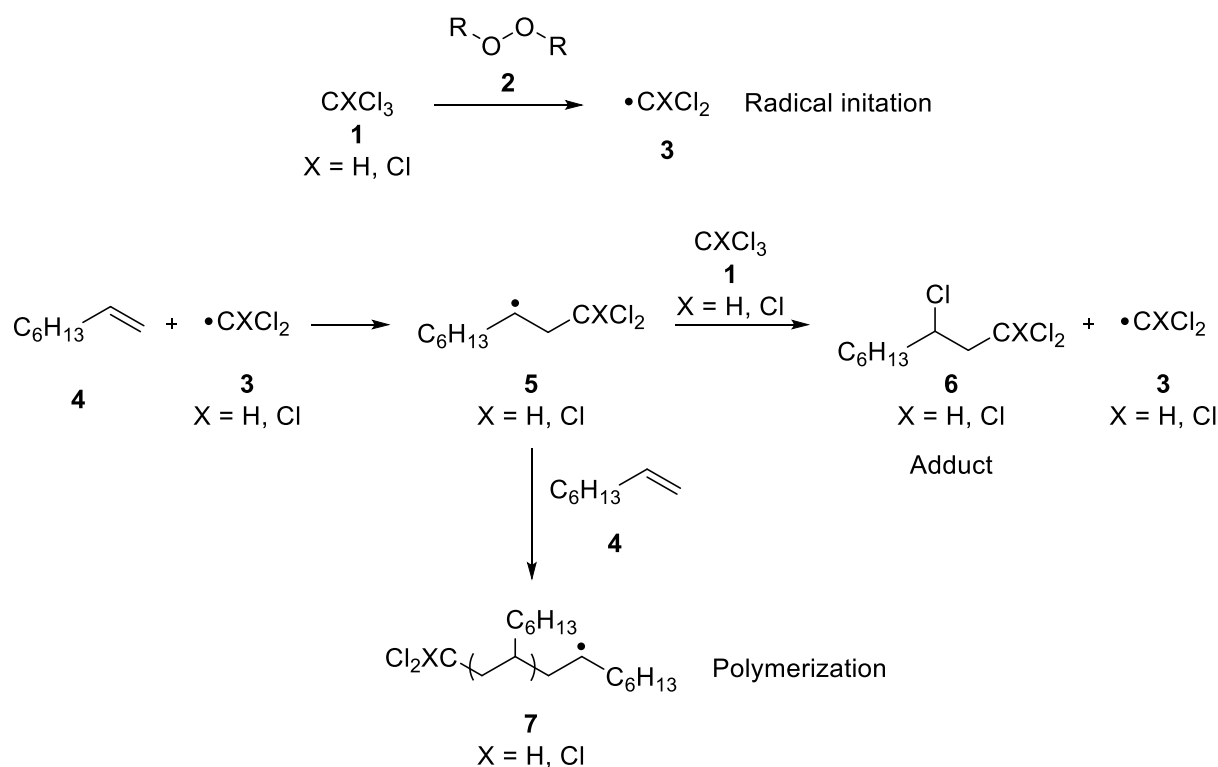
Equation 1. Calculation of the atom economy.

While atom economy is merely a theoretical value since it leaves out factors such as the yield of the reaction or use of excess starting materials, it is still a very elegant way of quickly determining the sustainability of reactions and it led to a rethinking in the scientific community. Since then, many new principles have been established to determine the sustainability of processes, for example the E factor which also takes the amount of used solvents, process aides and yields into account.^[4] Another example are the 12 principles of green chemistry established by Anastas and Warner.^[5]

Still, finding reactions with a high or even perfect atom economy is of great importance.^[6] There are several processes where every atom of the starting materials is present in the target molecule without any side products. These include cycloadditions like the Diels-Alders reaction, rearrangements, isomerizations, hydroformylations, hydrogenations or simple addition reactions.^[6]

2. Developments of atom transfer radical additions (ATRA)

One of these addition reactions with a perfect atom economy is the atom transfer radical addition reaction, also simply called ATRA. It goes back to the work of Kharasch and co-workers in the 1940s. After their investigation of an unprecedented *anti*-Markovnikov addition of HBr to alkenes with peroxides as radical initiators,^[7] they found out that this method could also be applied to polyhalogenated compounds in a radical chain reaction.^[8] In presence of small amounts of dibenzoyl or diacetyl peroxide as radical initiator **2**, the polyhalogenated carbons **1** were successfully added to 1-octene (**4**). In the radical initiation, the radical **3** is formed which then adds to 1-octene (**4**) to form the radical intermediate **5**. This radical can then either react with another 1-octene (**4**) to form polymerized side-products **7** or abstract a chlorine radical from **1** to form the desired adduct **6** (scheme 1).^[8]



Scheme 1. Kharasch reaction of tetrachloromethane and chloroform with 1-octene (**4**) in presence of a radical initiator **2**.^[8]

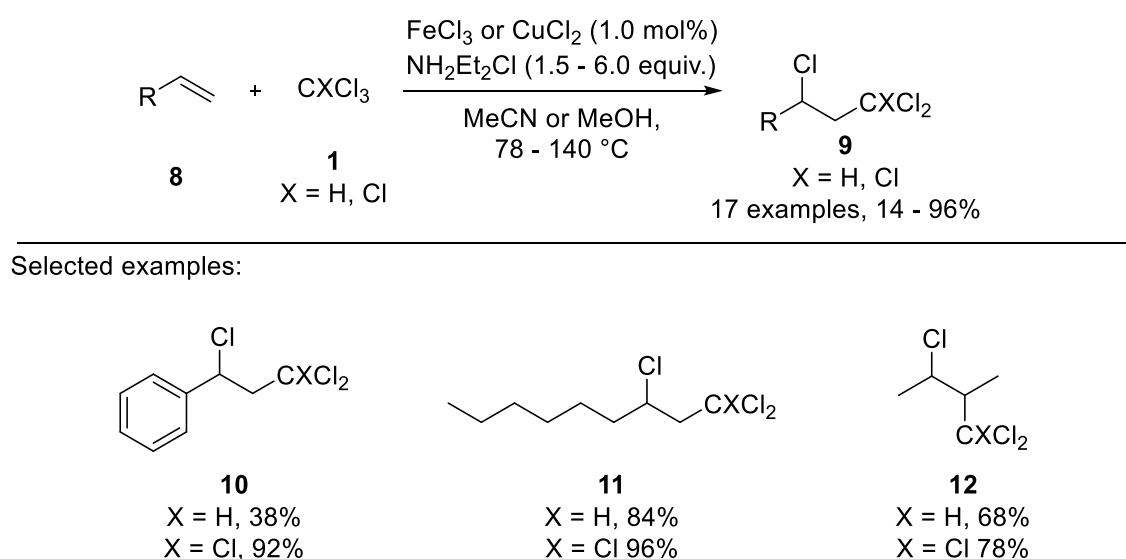
Shortly after, Kharasch *et al.* were able to expand this reaction to chlorinated acetic acids and this type of reaction is since been called the Kharasch reaction.^[9] The reaction has a high atom economy since the substrate is fully added to the alkene in good yields and only small amounts of radical initiator are needed. However, due to the radical chain mechanism of the reaction, the formation of telomerized and polymerized side products is unavoidable.

A Introduction

In the 1950s Minisci and co-workers observed that during the polymerization of acrylonitrile in halogenated solvents, the formation of the addition product of the halocarbons and acrylonitrile can be observed in a considerable amount.^[10] They later found out that this reaction is catalyzed by an iron species originating from corrosion of the reactor vessel.^[11]

These findings laid the groundwork for the first transition-metal-catalyzed Kharasch reactions and therefore the atom transfer radical addition (ATRA).

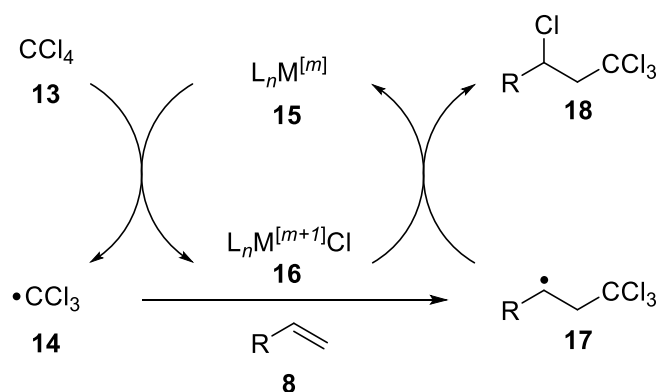
The first metal-catalyzed ATRA reaction was reported by Asscher and Vofsi in 1963. Using either iron(III)- or copper(II)-chloride as metal catalyst and diethylammoniumchloride as reductant, they were able to perform the ATRA reaction of tetrachloromethane and chloroform onto various alkenes (scheme 2).^[12]



Scheme 2. First transition-metal-catalyzed ATRA reaction by Asscher and Vofsi.^[12]

The proposed mechanism of this reaction starts with a single electron transfer from the metal salt **15** to tetrachloromethane (**13**) to generate the radical **14** and the oxidized metal halide **16**. The radical **14** then adds to the double bond of **8**, producing the carbon radical **17** which is then oxidized by the metal species **16** and takes up the chloride to yield the adduct **18** to close the catalytic cycle by regenerating the catalyst **15** (scheme 3).

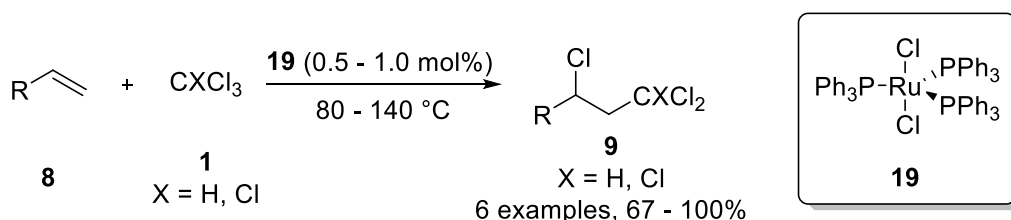
A Introduction



Scheme 3. Proposed mechanism for the ATRA reaction of CCl_4 (**13**) and olefins **8**.^[12]

Since then, a lot of work has been put into expanding the use of copper^[13] and iron^[14] complexes for ATRA reactions. But also complexes of manganese,^[15] chromium,^[16] nickel,^[17] but also toxic and hazardous compounds such as organotin reagents^[18] or triethylboranes^[19] have been used as radical initiators for ATRA reactions.

However, the by far the most efficient and active metal-complexes are based on ruthenium. The first example of ruthenium-based catalysts for ATRA reactions have been reported by Nagai *et al.* in 1973. The ruthenium(II)-triphenylphosphine complex $[\text{RuCl}_2(\text{PPh}_3)_3]$ (**19**) was shown to be a very effective catalyst for the addition of CCl_4 and chloroform to several olefins and styrene in good yields at a low catalyst-loading of 0.5 mol% and with very little telomerization side reactions (scheme 4).^[20]



Scheme 4. First $[\text{RuCl}_2(\text{PPh}_3)_3]$ (**19**) catalyzed ATRA reaction reported by Nagai *et al.*^[20]

Intensive effort has been put into developing ruthenium-based catalysts for ATRA reactions^[21] and the most commonly used classes consist of half-sandwich ruthenium complexes **20**^[22] and Grubbs-type complexes **21**^[23] (figure 1).

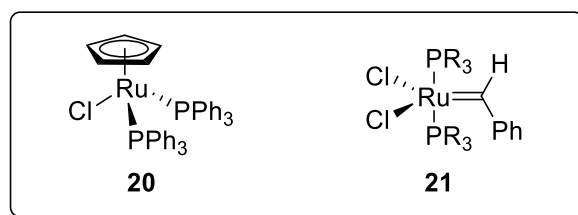
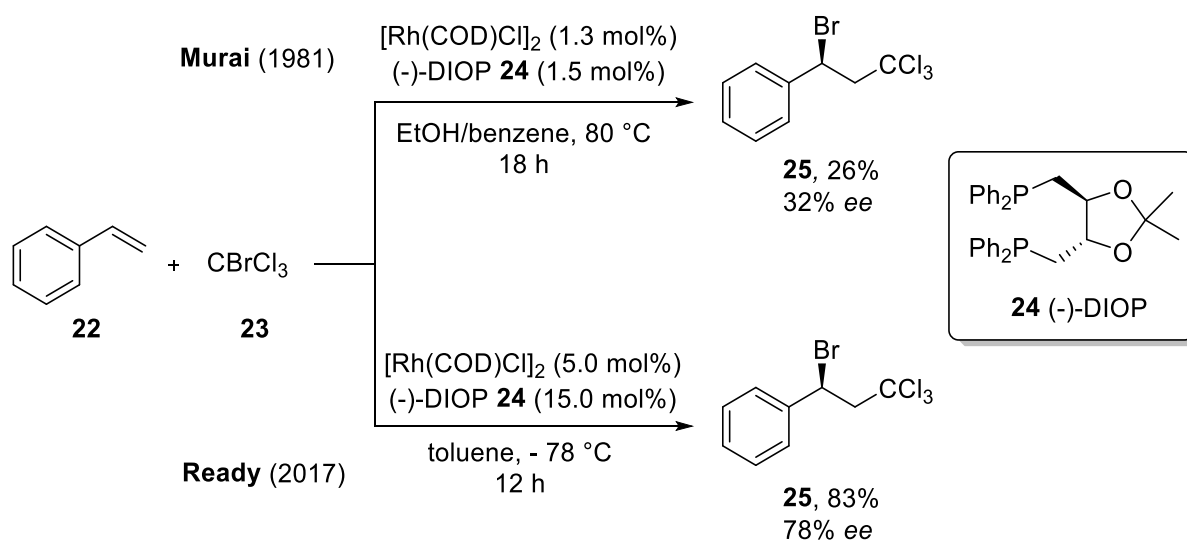


Figure 1. Half-sandwich ruthenium complexes **20** and Grubbs-type complexes **21** used in ATRA reactions.

A Introduction

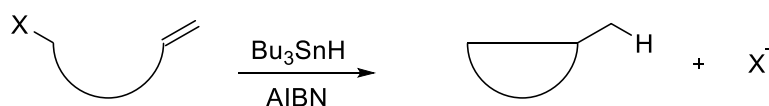
In 1981, Murai and co-workers showed the first example of an asymmetric atom transfer radical addition. Using a chiral (-)-DIOP ligand (**24**) in combination with ruthenium, the asymmetric addition of CBrCl_3 (**23**) was achieved with styrene (**22**) as trapping reagent. Only an enantiomeric excess of 32% of **25** was achieved at a poor overall yield of 26% at these harsh reflux conditions.^[24] Ready *et al.* could demonstrate that this reaction can be improved by changing the reaction conditions to low temperatures and higher loading of catalyst (scheme 5). With modified DIOP ligands even higher stereoselectivity and yields were achieved for various styrenes.^[25] This shows that chiral ruthenium-complexes can be a powerful tool to access the interesting group of chiral halides.^[26]



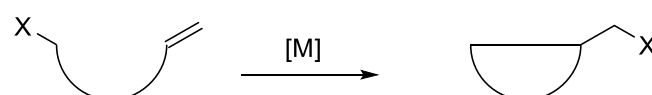
Scheme 5. Asymmetric ATRA reaction of CBrCl_3 (**23**) and styrene (**22**) using chiral ruthenium complexes.^[24,25]

Another transformation that has seen great use in synthetic chemistry that is closely related to the ATRA reaction is the atom transfer radical cyclization (ATRC). While reductive cyclizations have long been used in organic chemistry for a great number of transformations, its disadvantages lie in the use of toxic and hazardous organotin reagents as well as in a poor atom economy due to the loss of the halide.^[27] In comparison, the atom economy of the ATRC remains at 100% and transition-metal catalyzed systems can be applied. (scheme 6).

Reductive cyclization:



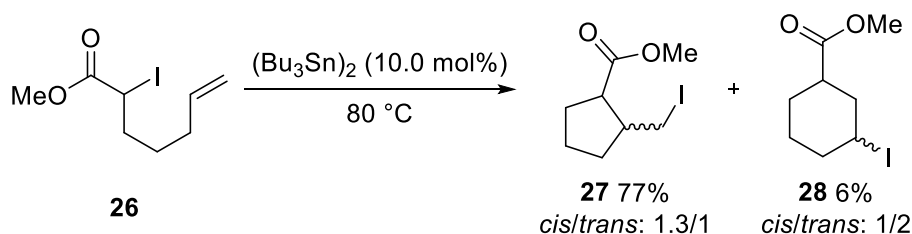
ATRC:



Scheme 6. Comparison of reductive cyclization using Bu_3SnH and transition-metal-catalyzed ATRC.

A Introduction

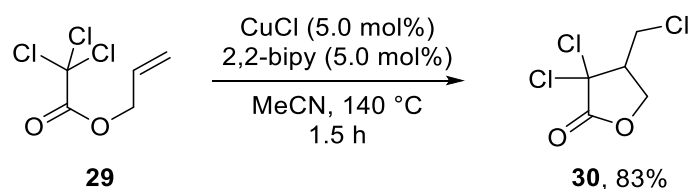
The first work regarding ATRC was done by Curran *et al.* in 1987. Cyclization of α -iodo-carbonyl compounds with terminal olefins such as **26** was achieved with $(\text{Bu}_3\text{Sn})_2$ as radical initiator. Selectivity of this reaction was still low with both the 5-*exo* **27** and 6-*endo* product **28** being formed in a mixture of *cis*- and *trans*-isomers (scheme 7).^[28]



Scheme 7. Atom transfer radical cyclization of α -iodo-carbonyl compound **26**.^[28]

Transition-metal catalyzed ATRC reactions have been applied in many useful transformations in organic synthesis and especially copper-complexes were numerous used for the cyclization of halogenated compounds to generate cyclic compounds and heterocycles with ring-sizes ranging from 4 up to 18.^[29]

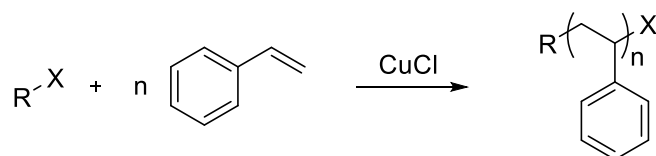
For example, Tsuji *et al.* used CuCl in combination with a bipy ligand to cyclize allyl 2,2,2-trichloroacetate (**29**) to the lactone **30** in good yield (scheme 8).^[30]



Scheme 8. ATRC of allyl 2,2,2-trichloroacetate (**29**) with CuCl .^[30]

Another very important process closely related to ATRA is the atom transfer radical polymerization (ATRP). Discovered independently by both Sawamoto and Matyjaszewski in the 1990s,^[31] it has become one of the most effective methods for controlled radical polymerizations. Again, copper has shown to be the best transition-metal to catalyze these reactions, allowing for the synthesis of well-defined polymers and copolymers with an easy way to control the molecular weight. The reaction starts with the addition of the radical derived from an alkyl halide to a monomer followed by a radical polymerization (scheme 9). Various monomers with C-C double bonds, such as acrylates, acrylamides, acrylonitrile or styrenes can be used and the reaction is very tolerant towards many solvents, functional groups and impurities.^[32,33]

A Introduction

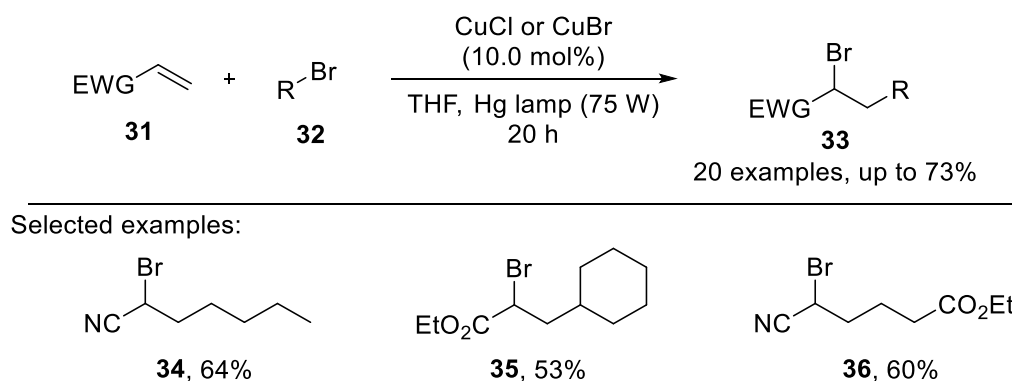


Scheme 9. General procedure for the ATRP of styrene.^[32]

The typical conditions of ATRA reactions and related processes often involve activation through high temperatures. But already back in 1947, Kharasch discovered that various light sources can be used to initiate the radical reaction of halogenated methanes, however only with unsatisfying results.^[34]

Further, perfluoroalkyl iodides can also be activated with UV light and added to electron-deficient alkenes.^[35]

By combining copper(I)-chloride or -bromide with UV light from a mercury lamp, Hitani *et al.* developed a photoredox-catalyzed ATRA reaction of alkyl bromides **32** and electron-deficient alkenes **31** with very promising results (scheme 10).^[36,37]



Scheme 10. Photoredox-catalyzed ATRA reaction using UV light activation and copper(I) salts.^[37]

While atom transfer radical additions and related processes have been established as a powerful tool in synthetic chemistry over the years,^[38] it still suffers from drawbacks such as the need for high temperatures and therefore high energy consumption, use of toxic and hazardous reagents or the need for very high energy UV light sources. It wasn't until the emergence of a new field in organic chemistry that led to a renaissance of ATRA chemistry: the arise of visible light mediated photocatalysis.

3. Photocatalysis – historical and photophysical background

It was the Italian chemist Giacomo Ciamician (1857 - 1922) who envisioned the use of sunlight as a main energy source for mankind and as an efficient tool in organic synthesis early in the 20th century.^[39]

In times where fossil fuels still seemed to be an infinite resource and the dangers of climate change and environmental pollution were neglected, his vision could only be seen as revolutionary. Already in 1886, he and Paul Silber could demonstrate that sunlight can promote the transformation of nitrobenzene to aniline and quinone to hydroquinone in presence of ethanol.^[40]

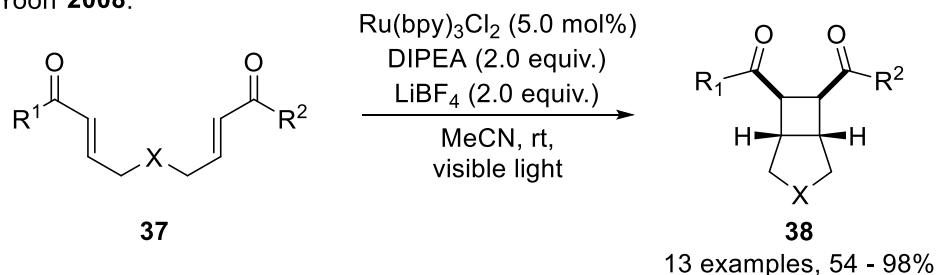
The use of visible light possesses one major challenge, namely the fact that most organic molecules do not absorb photons in the visible region of the electromagnetic spectrum. Therefore, in the 20th century, the use of UV light in organic chemistry has gained lots of attention.^[41] But the spectrum of sunlight reveals that only roughly 3% of it are in the UV region and therefore making use of sunlight for these transformations is very inefficient.^[42] The use of UV light sources and glassware is expensive, comes with safety hazards and reactions can also suffer from unwanted side-reactions, selectivity problems or even decomposition *via* unwanted bond-cleavage.^[43]

A way to overcome these obstacles is to use organic or metal-organic molecules that are able to absorb photons in the visible region and which are further able to act as catalysts in their excited states. The first pioneering work in this field was done in the late 1970s and early 1980s when Kellogg discovered that sensitizers like eosin Y (**51**) or Ru(bpy)₃Cl₂ (**46**) can accelerate the reduction of dihydropyridins under visible light irradiation.^[44] Other ground-breaking work was done by Deronzier,^[45] Okada,^[46] Sauvage,^[47] and others during that time.^[48] While photoredox catalysis has been used extensively in the field of solar-cells,^[49] CO₂ reduction^[50] and water splitting^[51] since then, it stayed mostly unexplored in organic synthesis for almost 30 years.

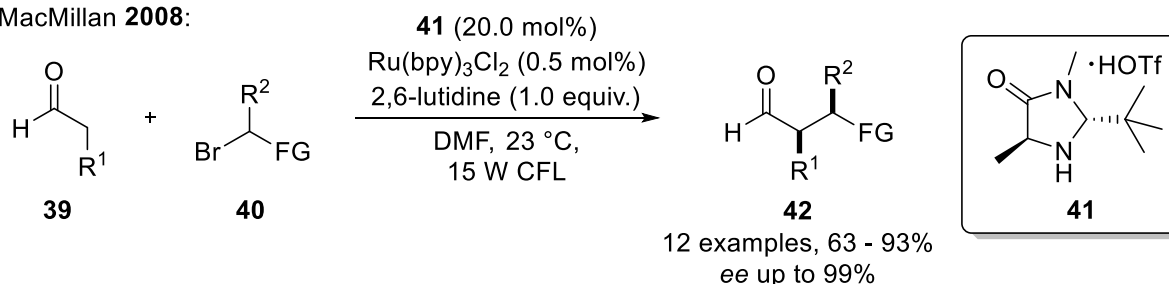
In 2008, the group of Yoon showed the successful use of visible light photocatalysis for the [2 + 2] cycloaddition of enones **37**,^[52] while MacMillan *et al.* could demonstrate a remarkable combination of photoredox catalysis and organocatalysis to achieve the asymmetric alkylation of aldehydes **39**.^[53] Together with Stephenson's protocol for the hydrodehalogenation^[54] (scheme 11), these publications laid the groundwork for modern photoredox catalysis in organic synthesis.

A Introduction

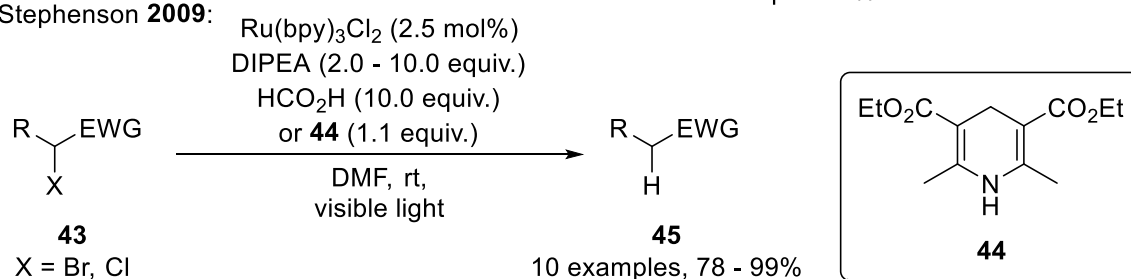
Yoon **2008**:



MacMillan **2008**:



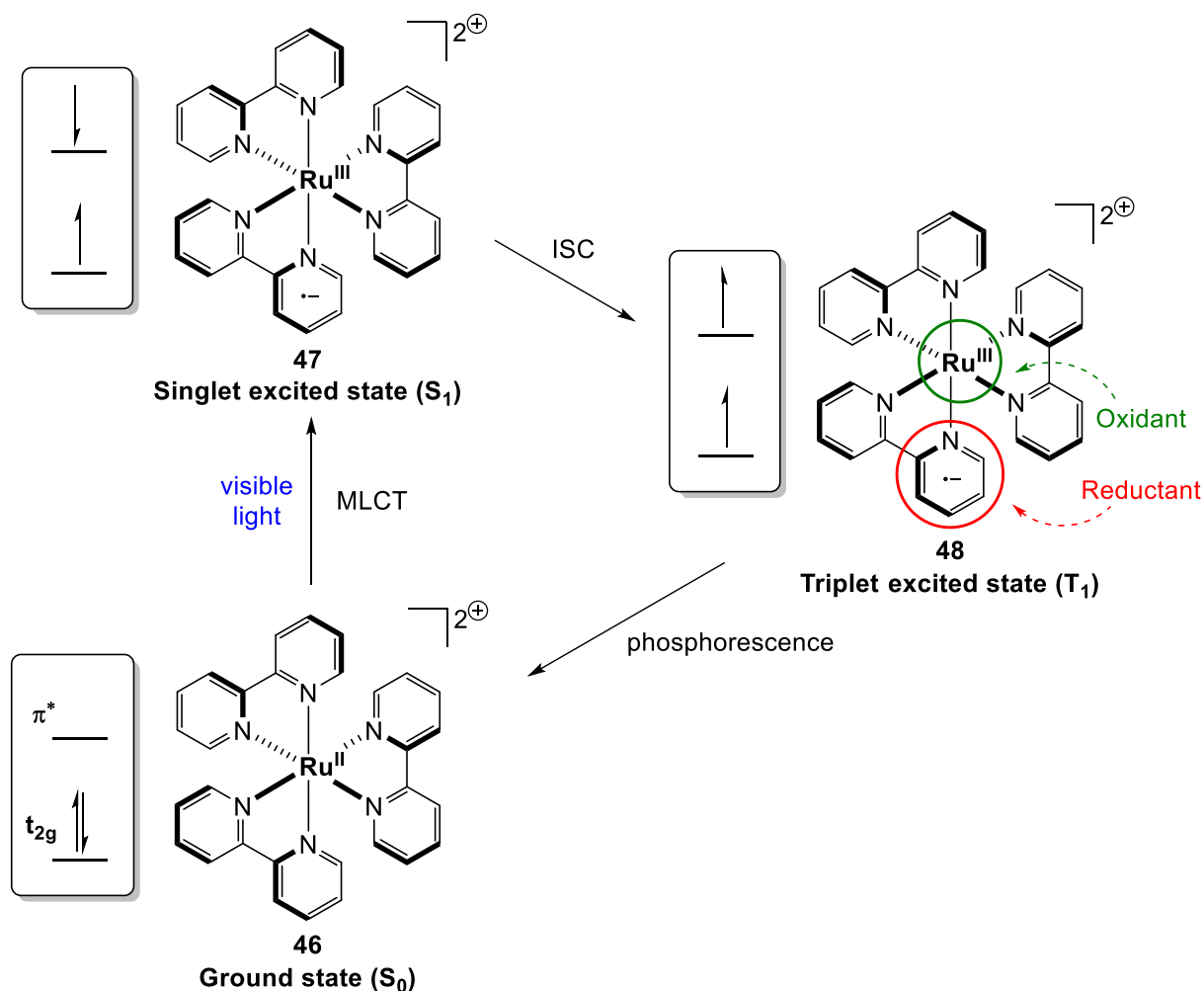
Stephenson **2009**:



Scheme 11. Photoredox-catalyzed transformations by Yoon, MacMillan and Stephenson.^[52-54]

These astonishing transformations all relied on the ruthenium-based transition-metal complex $\text{Ru(bpy)}_3\text{Cl}_2$ (**46**) acting as the photocatalyst. The photochemistry and -physics of these transition-metal complexes have been thoroughly investigated for decades^[55] and polypyridyl complexes of ruthenium and iridium are amongst the most widely used photocatalysts today.^[56] In the ground state (S_0) of these complexes like $\text{Ru(bpy)}_3\text{Cl}_2$ (**46**), an electron pair is set in the metal-centered t_{2g} orbital. Upon irradiation with visible light, one electron is promoted to the ligand-centered π^* orbital in a process called metal-to-ligand charge-transfer (MLCT). In this singlet excited state (S_1) **47** the metal-center has changed its oxidation state from (II) to (III) while a negative charge is located in the 2,2'-bipyridine (bpy) ligand. After a process called intersystem crossing (ISC) which is defined by a spin flip of the electron in the π^* orbital the complex is now in its lowest energy triplet-excited state (T_1) **48**. This triplet-excited state is long-lived enough ($t = 1100 \text{ ns}$)^[57] to allow for single electron-transfer (SET) events to undergo with organic molecules.^[58] Two different SET events can be achieved in this state. Either the metal-center can act as an oxidant and take up an electron from an organic compound or the negative charge located in the ligand can act as a reductant (scheme 12).^[59]

A Introduction

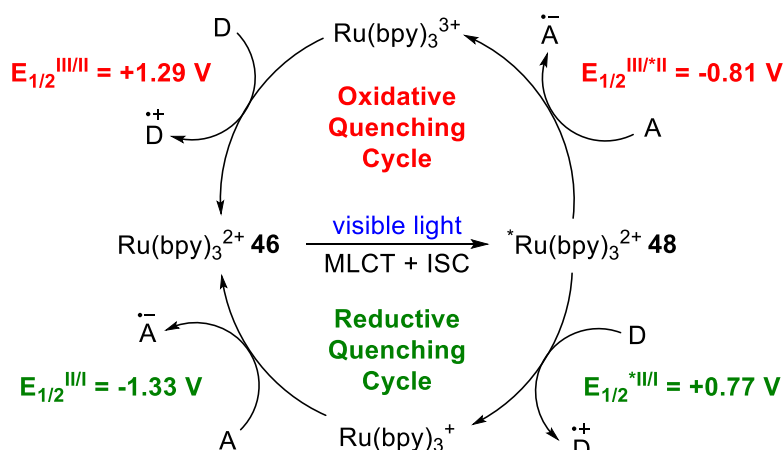


Scheme 12. Excitement of $\text{Ru}(\text{bpy})_3\text{Cl}_2$ (**46**) with visible light followed by MLCT and ISC to give the triplet-excited state (T_1) **48**.^[59]

The possibility of the triplet-excited state (T_1) of $\text{Ru}(\text{bpy})_3^{2+}$ **48** to act either as an oxidant or reductant leads to two photocatalytic cycles being accessible in photoredox-catalyzed reactions. In the oxidative quenching cycle, the excited catalyst $^*\text{Ru}(\text{bpy})_3^{2+}$ **48** can transfer the electron from the ligand-centered π^* orbital to an acceptor molecule (**A**). Commonly used sacrificial acceptor molecules are persulfates ($\text{S}_2\text{O}_8^{2-}$), Ar-NO_2 compounds or metal cations. A product of the reaction can also act as an acceptor molecule. After this step a $\text{Ru}(\text{III})$ -species is formed which has a very high oxidation potential ($E_{1/2}^{\text{III/II}} = +1.29 \text{ V}$) which is then reduced by a donor molecule (**D**) to regenerate the catalyst $\text{Ru}(\text{bpy})_3^{2+}$ **46**.

In the reductive quenching cycle, $^*\text{Ru}(\text{bpy})_3^{2+}$ **48** takes up an electron from a donor molecule (**D**) into its metal-centered orbital. Commonly used sacrificial donors are bases like NEt_3 and DIPEA or ascorbate but again, the products can also act as a donor. This step generates a highly reducing $\text{Ru}(\text{I})$ -species ($E_{1/2}^{\text{II/I}} = -1.33 \text{ V}$) that can reduce an acceptor compound (**A**) (scheme 13).^[59]

A Introduction



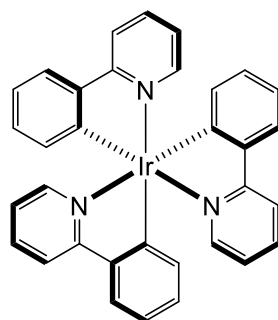
Scheme 13. General scheme of the oxidative and reductive quenching cycle of $\text{Ru}(\text{bpy})_3^{2+}$.^[59]

Other than these two electron-transfer pathways, a third pathway for decay of photoexcited states is also possible. It can also engage in an energy transfer with organic or inorganic substrates. The triplet-excited state (T_1) $^*\text{Ru}(\text{bpy})_3^{2+}$ **48** can perform a triplet-triplet energy transfer (TTET) with an acceptor molecule. Two different sensitization mechanisms are possible. In the Förster resonance energy transfer (FRET) the excited catalyst funnels its relaxation energy to the substrate if both catalyst and substrate are closer in range than 10 nm. This leads to the excitation of the substrate and one electron is shifted from its HOMO to its LUMO orbital while the catalyst returns to its ground state (S_0) **46**.

In case of the Dexter electron-transfer, the excited catalyst and the substrate are coming into physical contact with each other, which means their orbitals are overlapping. The electron from the π^* orbital of $^*\text{Ru}(\text{bpy})_3^{2+}$ **48** is transferred to the LUMO of the substrate while one electron from the HOMO of the substrate is transferred to the t_{2g} of the catalyst which results in the triplet-excited state of the substrate and the return of the catalyst to its ground state (S_0) **46**.^[60] Even though visible light mediated photoredox catalysis is still the major field in photocatalysis, energy transfer catalysis has also been used frequently in recent years.^[61]

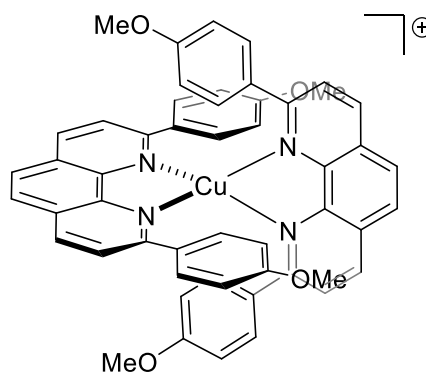
While $\text{Ru}(\text{bpy})_3\text{Cl}_2$ (**46**) was one of the first broadly applicable photocatalysts in organic synthesis, a great number of other catalysts have been widely used and studied since then. Iridium-based complexes are frequently used, like for example the neutral Ir(III)-complex *fac*-Ir(ppy)₃ (**49**) which has very good reducing abilities. Copper(I)- and copper(II)-complexes also gained lots of attention in recent years^[62] with $\text{Cu}(\text{dap})_2\text{Cl}$ (**50**) being the first commonly used one. Organic dyes have also seen broad application with eosin Y (**51**) being one of the most common ones.^[63] In recent years, *Mes*-Acridinium (**52**) (also called Fukuzumi dye) and other organic dyes have gathered great interest due to its high oxidation potentials (scheme 14).^[64]

A Introduction



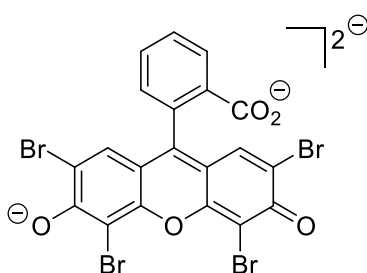
fac-Ir(ppy)₃
49

$$E_{1/2}(\text{Ir(III}^*)/\text{Ir(IV)}) = -1.73 \text{ V}$$



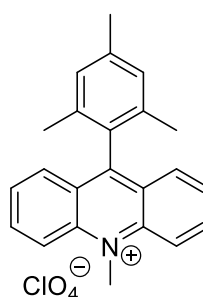
Cu(dap)₂Cl
50

$$E_{1/2}(\text{PC}^*/\text{PC}^{\bullet+}) = -1.43 \text{ V}$$



Eosin Y
51

$$E_{1/2}(\text{PC}^*/\text{PC}^{\bullet+}) = -1.11 \text{ V}$$



Mes-Acr
52

$$E_{1/2}(\text{PC}^{\bullet+}/\text{PC}) = +1.88 \text{ V}$$

Scheme 14. Commonly used photocatalysts and their oxidation and reduction potentials.^[64]

Over the last 15 years, photocatalysis has rapidly been evolved into a widely used field in organic synthesis and industry. Development in these processes is still ongoing, resulting in a variety of publications every year. Visible light has been applied for a great number of transformations in organic chemistry such as C-C or C-heteroatom bond formations, α -amino functionalizations, cycloadditions, decarboxylative couplings or fluorinations.^[64] Recently, the merger of photocatalysis with other fields in organic synthesis has tracked lots of attention. Dual metal-photocatalysis has been widely used for cross-coupling reactions.^[65] The combination of organo- and photocatalysis has been used for stereoselective transformations^[66] and even examples of bio-photocatalysis have emerged.^[67] Photo-electrocatalysis could have great potential in accessing new transformations and could eradicate some of the disadvantages of photoredox catalysis such as the occasional need for stoichiometric reductants or oxidants.^[68]

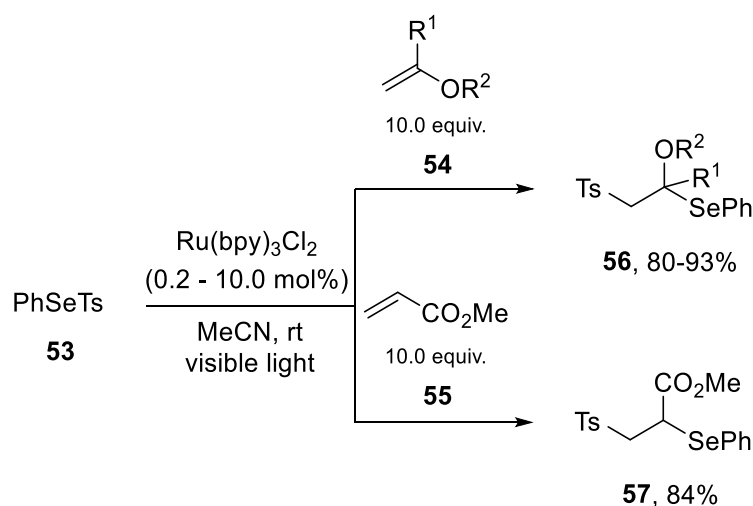
While recently, new ways to access intermediates such as carbocations,^[69] carbanions^[70] or carbene-types^[71] have been explored in photochemistry, the generation of radical anions is still the core principle at the heart of photoredox catalysis. Therefore, photoredox catalysis is perfectly suited

A Introduction

for atom transfer radical addition chemistry and related processes and since the reemergence of visible light mediated photocatalysis, the field of ATRA reactions has entered a new golden era.

4. Advancements in visible light mediated ATRA chemistry

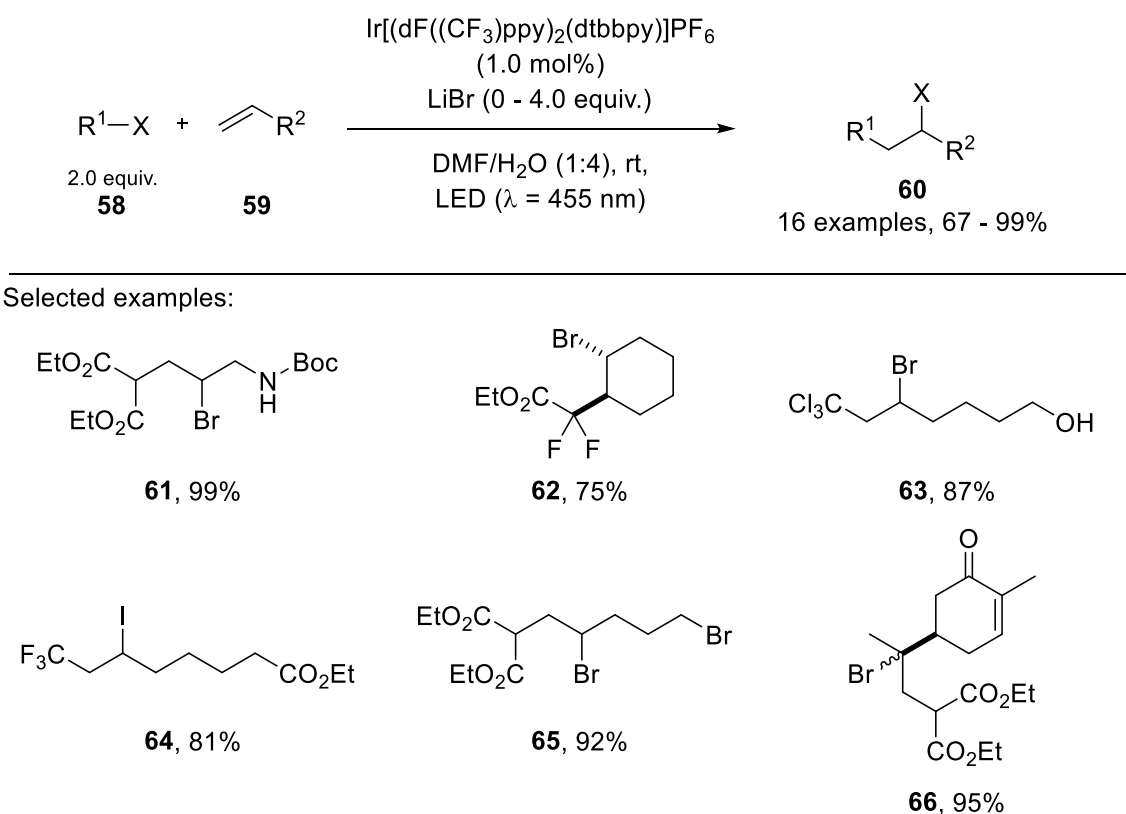
One of the earliest examples where visible light mediated photoredox catalysis was used for ATRA reactions was reported by Barton and co-workers in 1994. Employing $\text{Ru}(\text{bpy})_3\text{Cl}_2$ (**46**) as catalyst, phenylselenium sulfonate (**53**) was successfully added to various vinyl ethers **54** and methyl acrylate (**55**) to generate β -phenylselenosulfones **56** and **57** in very good yields (scheme 15). In the proposed mechanism, the excited photocatalyst performs a SET to the phenylselenium sulfonate (**53**) which leads to the formation of a tosyl radical which then adds to the alkene. The hereby generated radical can react with the starting phenylselenium sulfonate (**53**) to propagate the chain reaction.^[72]



Scheme 15. Visible light mediated ATRA reaction using phenylselenium sulfonate (**53**) and $\text{Ru}(\text{bpy})_3\text{Cl}_2$ (**46**) as photocatalyst.^[72]

Despite these remarkable early results, the topic of visible light mediated ATRA reactions remained unexplored for many years. It was not until 2011 when the ground-breaking work of Stephenson *et al.* brought ATRA reactions back into the spotlight. The Kharasch addition of haloalkanes and α -halo carbonyls **58** to olefins **59** was achieved under visible light irradiation with blue LED strips and the Ir(III)-complex $\text{Ir}[(\text{dF}((\text{CF}_3)\text{ppy})_2(\text{dtbbpy}))]\text{PF}_6$ as photocatalyst. Under mild reaction conditions very good yields were achieved and several functional groups were tolerated. The soft Lewis acid LiBr was needed to assist the reaction in most cases (scheme 16).^[73]

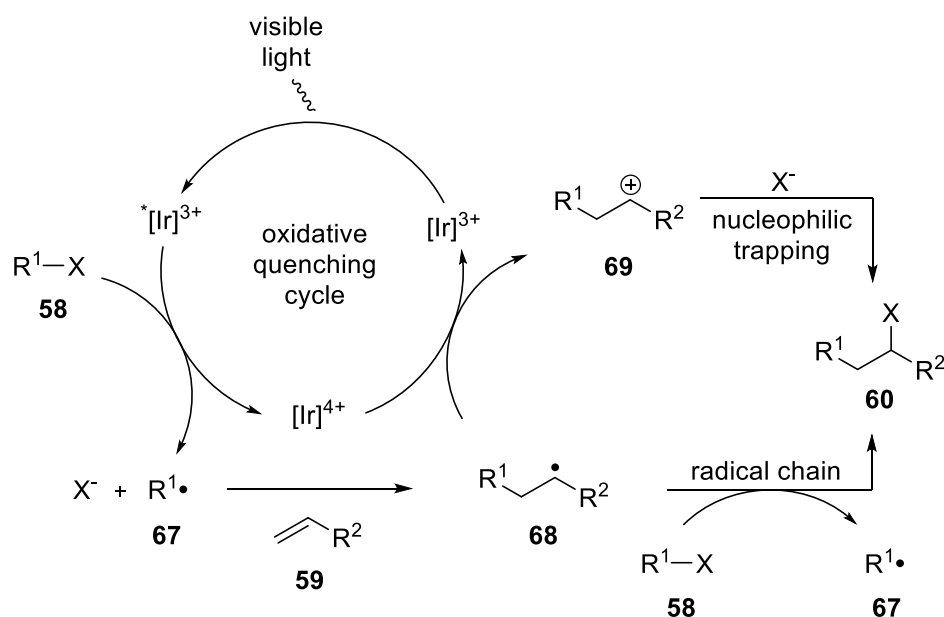
A Introduction



Scheme 16. Visible light mediated ATRA reaction using Ir[(dF((CF₃)ppy)₂(dtbbpy)]PF₆ (**X**) as photocatalyst.^[73]

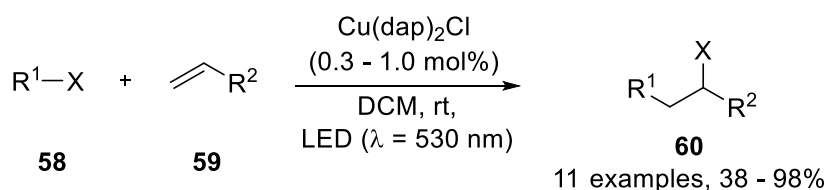
Similar to the mechanism proposed by Barton^[72], the reaction begins with the Ir(III)-catalyst getting excited *via* visible light irradiation. The excited catalyst is then able to transfer an electron to the haloalkane **58** in a SET to generate the alkyl radical **67** and a halide anion. The radical is then added to the double bond of the olefin **59**, leading to the formation of radical species **68**. This radical can then abstract a halide from the haloalkane, leading to the desired product **60** and another alkyl radical **67** in a typical ATRA radical chain mechanism. Additionally, Stephenson *et al.* proposed a second pathway in which the radical **68** is oxidized to the carbocation **69**. In this step, the Ir(IV)-species is reduced back to the photocatalyst and therefore the catalytic oxidative quenching cycle is being closed. The carbocation is then trapped by the halide to also yield the desired product **60** (scheme 17).^[73]

A Introduction

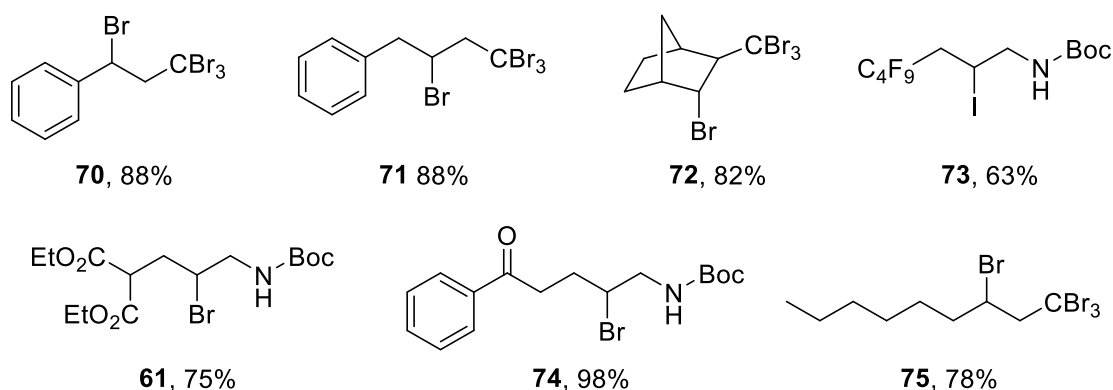


Scheme 17. Proposed mechanism for the photoredox-catalyzed ATRA reaction after Stephenson *et al.*^[73]

One year later, Reiser *et al.* demonstrated that the copper(I)-complex $\text{Cu}(\text{dap})_2\text{Cl}$ (**50**), which was initially discovered by Sauvage in 1987^[47] but has been rather unexplored since then, is also capable of catalyzing ATRA reactions under visible light irradiation. Haloalkanes such as CBr_4 , bromomalonate, α -bromoacetophenone and perfluorobutyl iodide were added to various alkenes **59** under irradiation of $\text{Cu}(\text{dap})_2\text{Cl}$ (**50**) with green light (scheme 18).^[74]



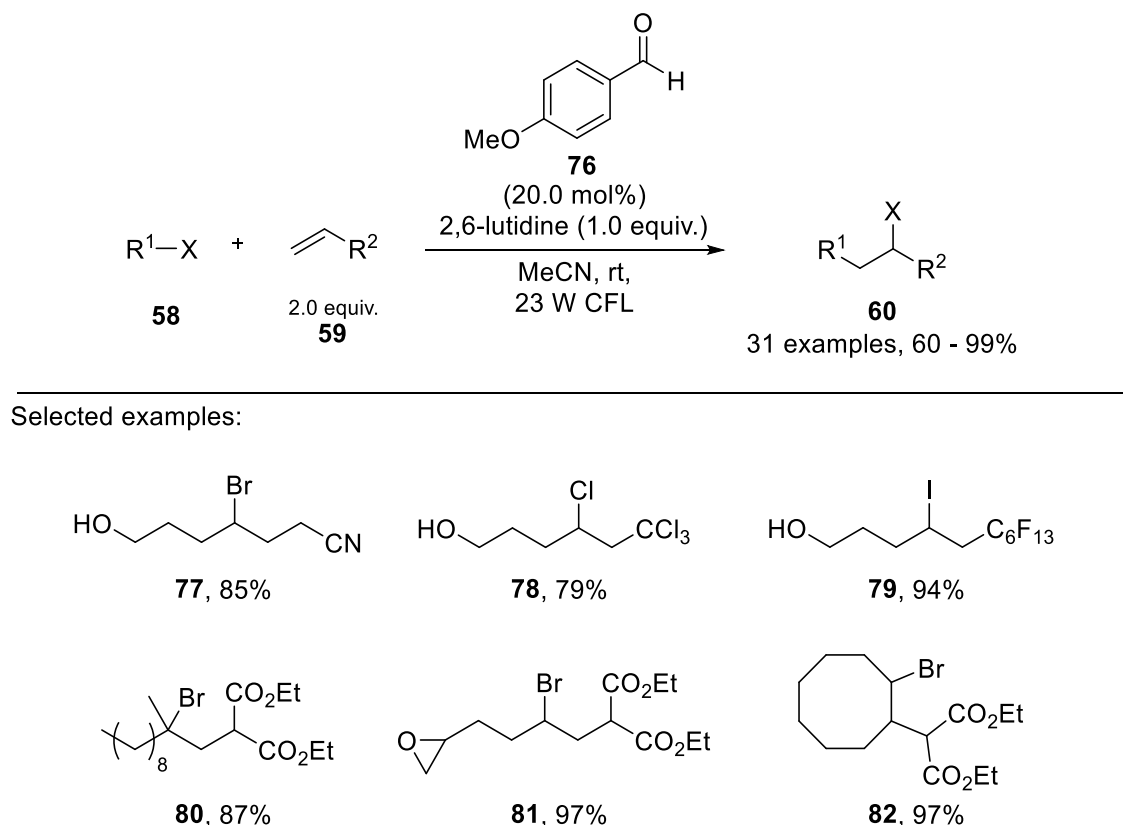
Selected examples:



Scheme 18. Visible light mediated ATRA reaction using $\text{Cu}(\text{dap})_2\text{Cl}$ (**50**) as photocatalyst.^[74]

A Introduction

Apart from these transition-metal-catalyzed ATRA reactions with photocatalysts derived from ruthenium-, iridium- or copper-salts, organic sensitizers, dyes or photocatalysts can also be used for these reactions as it was shown by the group of Melchiorre in 2014. The simple and inexpensive organic molecule *p*-anisaldehyde (**76**) was able to perform ATRA reactions of bromomalonate and other haloalkanes with various alkenes and alkynes in very good yields under mild conditions under irradiation with a 23 W CFL. The base 2,6-lutidine was necessary to neutralize traces of HBr that were formed in this reaction (scheme 19).^[75]



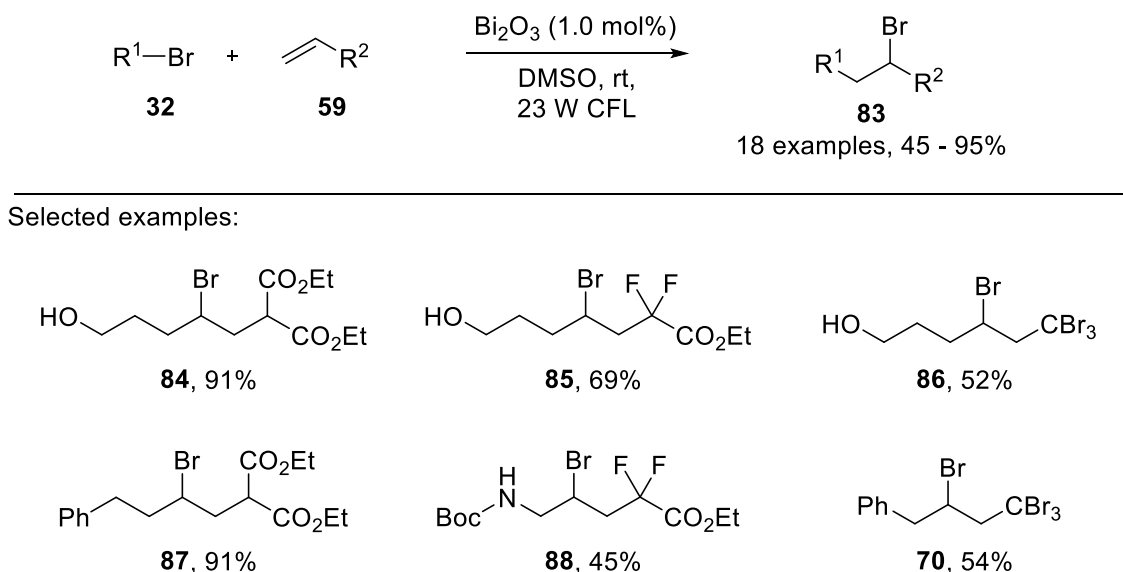
Scheme 19. Visible light mediated ATRA reaction using *p*-anisaldehyde (**76**) as photocatalyst.^[75]

From a mechanistic point of view, it was suggested that *p*-anisaldehyde absorbs a photon to reach its excited-singlet state. After intersystem crossing (ISC) to the triplet state, an energy transfer to the haloalkane takes place. The photosensitized haloalkane then undergoes homolytic C-X cleavage to generate an alkyl radical which then initiates the radical chain reaction.^[75]

Other organic sensitizers like 2-bromophenol,^[76] iodo-Bodipy,^[77] phenylglyoxylic acid^[78] or perylene diimides^[79] have since been successfully used in ATRA reactions.

Another inexpensive alternative to homogeneous transition-metal based catalysts is the use of heterogeneous semiconductors as it was shown by Pericas *et al.* in 2013 with the use of Bi_2O_3 as photocatalyst. Organobromides **32** and terminal olefins **59** could be used in the atom transfer radical addition under visible light irradiation of 1 mol% of bismuth oxide (scheme 20).^[80]

A Introduction

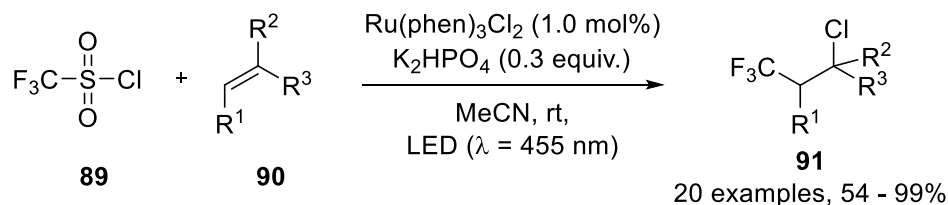


Scheme 20. Visible light mediated ATRA reaction using Bi₂O₃ as photocatalyst.^[80]

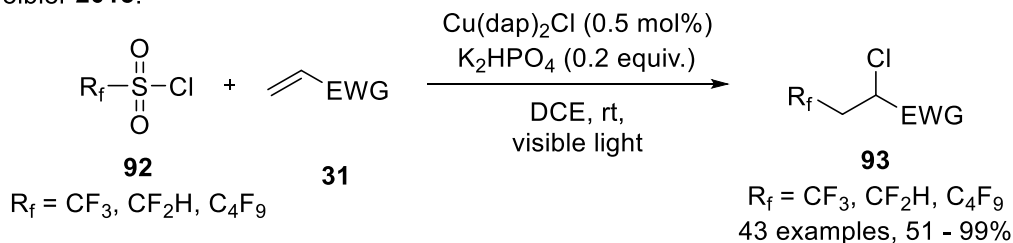
A reaction that has gained a lot of attention over the last years is the photocatalyzed di- and trifluoromethylation of alkenes and alkynes. Trifluoromethyl (CF₃) and difluoromethyl (CF₂H) groups are very useful motifs in the agrochemical and pharmaceutical industry. Various fluoromethylating reagents such as Umemoto-, Togni- or Hu-reagent are used for photochemical fluoromethylations.^[81] One of the cheapest trifluoromethyl sources is trifluoromethanesulfonyl chloride (**89**). In 2014, Jung and Han used a ruthenium phenanthroline complex to achieve the chlorotrifluoromethylation of alkenes with trifluoromethanesulfonyl chloride (**89**) under blue light irradiation. During the reaction SO₂ is eliminated.^[82] Similar results were found by the group of Dolbier when they used Cu(dap)₂Cl (**50**) for chlorotrifluoromethylations of electron-poor olefins **31**.^[83] In the same year, the group of Reiser showed that when Cu(dap)₂Cl (**50**) is used for the ATRA reaction of trifluoromethanesulfonyl chloride (**89**) and unactivated olefins **94**, no extrusion of SO₂ takes place (scheme 21). An unprecedented trifluoromethylchlorosulfonylation was achieved that way, showing the first evidence for the unique catalyst properties of copper complexes in ATRA reactions.^[84] This method was then later used for the synthesis of trifluoromethylated sultones from alkenols.^[85]

A Introduction

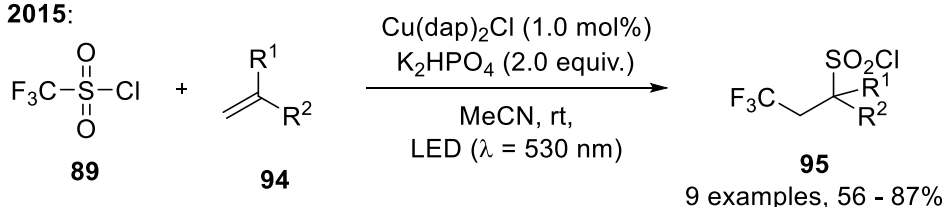
Jung, Han **2014**:



Dolbier **2015**:

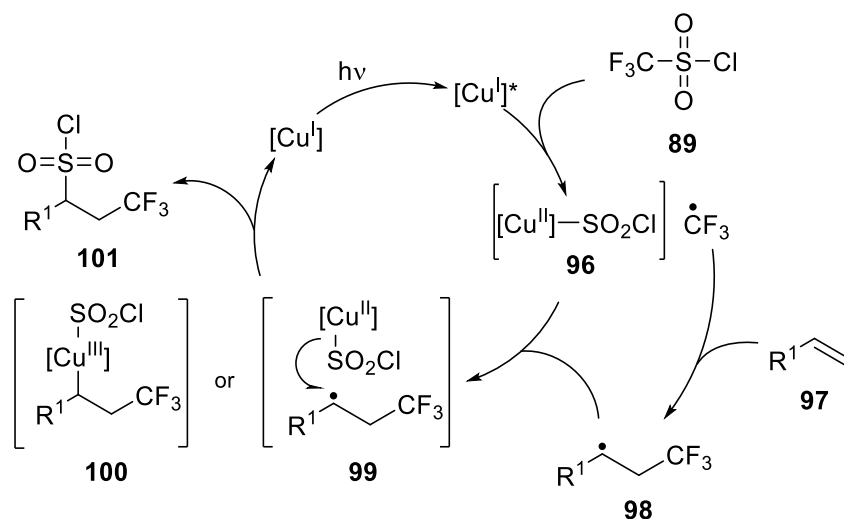


Reiser **2015**:



Scheme 21. Different visible light mediated trifluoromethylations of alkenes.^[82-84]

These findings from the Reiser group indicate that copper-catalyzed photoredox reactions can proceed in an inner-sphere mechanism and therefore open up new reaction pathways for ATRA reactions compared to other common photocatalysts, where reactions proceed in their outer sphere.



Scheme 22. Proposed inner-sphere mechanism for the trifluoromethylchlorosulfonylation of alkenes with $\text{Cu(dap)}_2\text{Cl}$ (**50**).^[86]

The proposed reaction mechanism for the trifluoromethylchlorosulfonylation of alkenes starts with a SET from the excited Cu(I)-species to the triflyl chloride (**89**) to generate the CF_3 radical and the

A Introduction

unstable SO_2Cl fragment that is stabilized by coordination to a Cu(II) -species **96**. The CF_3 radical adds to the alkene **97** to generate the radical **98**. There are now two possible pathways for the product formation: the Cu(II) -species **96** can either transfer its SO_2Cl ligand to the radical **98** (via **99**) or the radical **98** could bind to the Cu(II) -complex **96** to form a Cu(III) -intermediate **100** which can then undergo reductive elimination to the product **101** (scheme 22).^[84,86]

In recent years, the Reiser group also developed and used some copper(II)-complexes as photocatalysts like Cu(dap)Cl_2 (**102**)^[87] (figure 2) or $[\text{Cu(dmp)}_2\text{Cl}]\text{Cl}$ (**113**).^[88]

In 2018, the oxo-azidation of vinyl arenes **104** was reported using the copper(II)-complex Cu(dap)Cl_2 (**102**) (scheme 23). Spectroscopic analysis confirmed the formation of an aza-bridged Cu(II) -dimer with $\lambda_{\text{max}} = 525 \text{ nm}$.^[87] In 1962 Kochi showed that copper(II)-chloride undergoes homolytic cleavage of the Cu-Cl bond under UV light irradiation to generate copper(I)-chloride and a Cl radical.^[89] Based on this observation, it was proposed that the aza-bridged Cu(II) -complex can undergo visible light induced homolysis (VLH) to generate an azide radical.^[87]

Other unique transformations of copper photocatalysts involved the ATRA reaction of perfluoroalkyl iodides **106** with styrenes and phenylacetylenes **107**. While ATRA reactions of perfluoroalkyl iodides and olefins have been reported with common ruthenium- and iridium-based photocatalysts^[90] as well as organic dyes,^[91] the reaction of styrenes has never been successful under these conditions. The unique character of the copper catalyst with its ability to involve inner-sphere cycles and Cu(III) -intermediates was attributed to the success of this transformation.^[92] Cu(dap)Cl_2 (**102**) was also shown to be very effective for the chlorosulfonylation of olefins **59**^[93] and the ATRA reaction of iodoform (**111**)^[94] (scheme 23). In both cases common photocatalysts were not effective and inner-sphere mechanisms of copper-species were proposed.

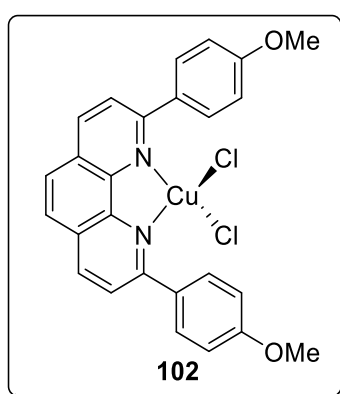
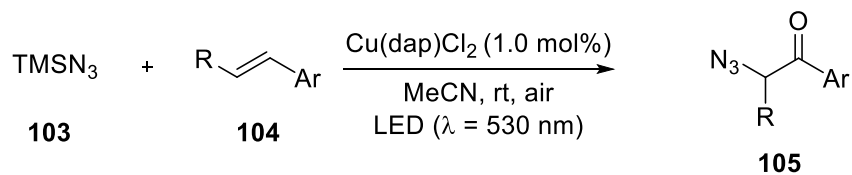


Figure 2. The copper(II)-complex Cu(dap)Cl_2 (**102**) developed by Reiser *et al.*^[87]

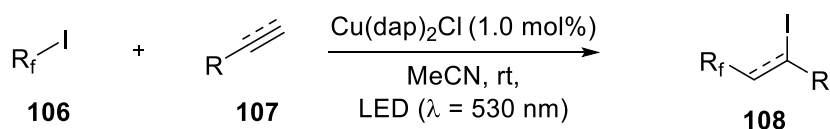
A Introduction

Reiser **2018**:



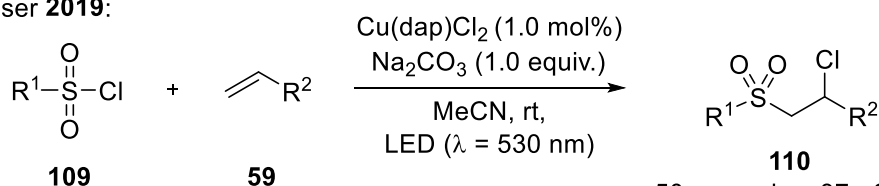
28 examples, 10 - 85%

Reiser **2018**:



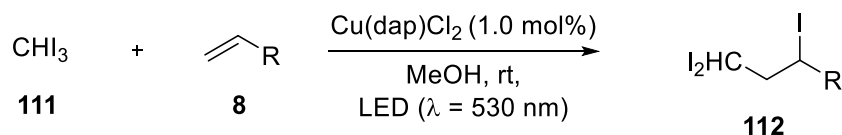
29 examples, 40 - 93%

Reiser **2019**:



50 examples, 37 - 99%

Reiser **2020**:

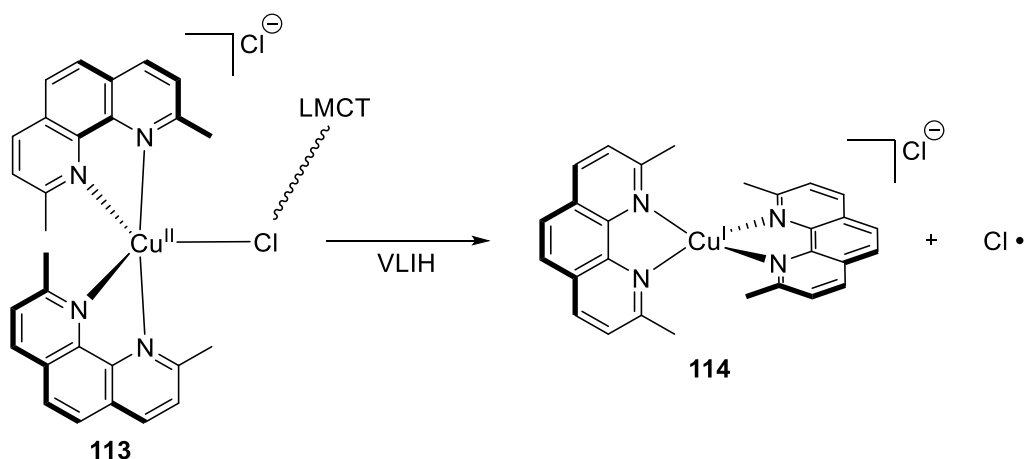


23 examples, 61 - 97%

Scheme 23. Copper-catalyzed ATRA reactions and related transformations developed by Reiser *et al.*^[87,92-94]

Recently, direct evidence for the visible light induced homolysis (VLH) of [Cu(dmp)₂Cl]Cl (**113**) was published by Reiser and Castellano. Static spectroscopic investigations, ultrafast transient absorption and electron paramagnetic resonance (EPR) spin experiments showed that homolytic bond cleavage of the Cu-Cl bond occurs under blue light irradiation ($\lambda_{\text{ex}} = 427$ or 470 nm). This cleavage corresponds to a Cl \rightarrow Cu(II) ligand-to-metal charge-transfer (LMCT) and leads to the formation of the copper(I)-species [Cu(dmp)₂]Cl (**114**) and a Cl radical (scheme 24).^[95]

A Introduction

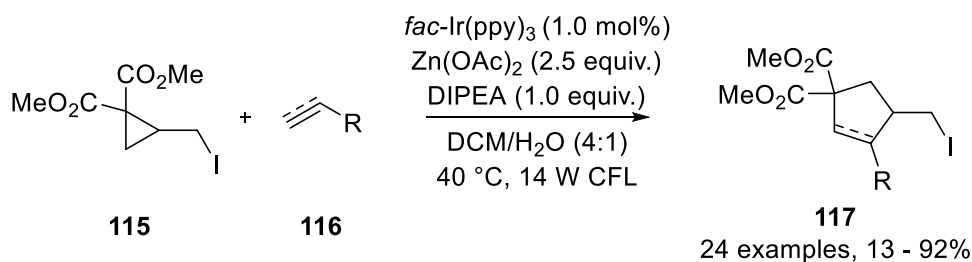


Scheme 24. Visible light induced homolysis (VLIH) of [Cu(dmp)₂Cl]Cl (**113**).^[95]

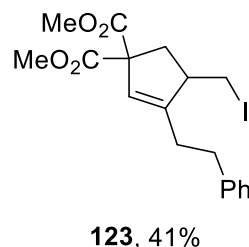
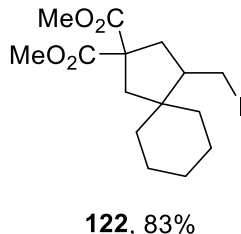
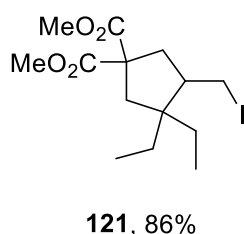
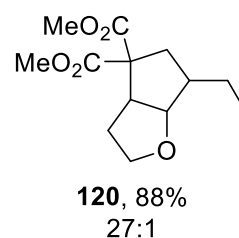
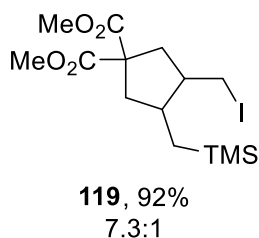
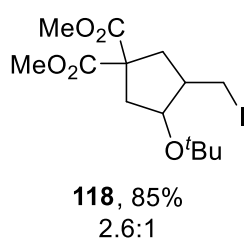
As these examples have shown, visible light mediated photoredox catalysis using transition-metal complexes or organic photocatalysts can be widely used for atom transfer radical additions and led to the discovery of various new ATRA reactions.^[96,97]

But visible light photoredox catalysis can also be applied to ATRA-related processes. Photocatalytic atom transfer radical cyclizations (ATRC) are challenging because the quenching cycle of the catalyst can lead to the formation of reduced products and therefore the halogen functionalities can be lost. Nevertheless, in 2013 Yao *et al.* have shown that the oxidative quenching cycle of *fac*-Ir(ppy)₃ (**49**) can be used for the intermolecular [3 + 2] ATRC reaction of dimethyl-2-(iodomethyl)cyclopropane-1,1-dicarboxylate (**115**) with olefins **116** to generate cyclopentane/cyclopentene derivatives **117** under mild conditions. For unactivated alkenes the use of Zn(OAc)₂ as Lewis acid was needed. (scheme 25).^[98]

A Introduction

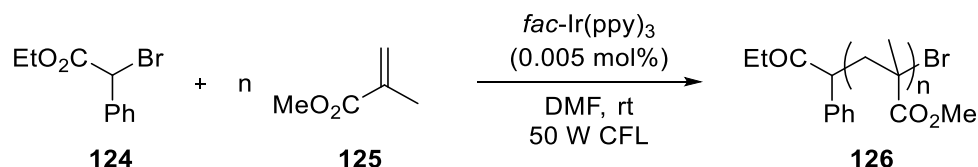


Selected examples:



Scheme 25. Visible light mediated ATRC of dimethyl-2-(iodomethyl) cyclopropane-1,1-dicarboxylate (**115**) and olefins **116**.^[98]

Since then, various catalytic systems have been applied for ATRC to afford a number of ring-systems.^[99] In 2012, the Hawker group could demonstrate that $fac\text{-Ir(ppy)}_3$ (**49**) can be used for the atom transfer radical polymerization (ATRP) of methyl methacrylate (**125**) with ethyl- α -bromophenylacetate (**124**) as initiator. Only ppm amounts of catalyst were needed to perform a living radical polymerization that allows for excellent spatial and temporal control over the chain-growth process (scheme 26).^[100]

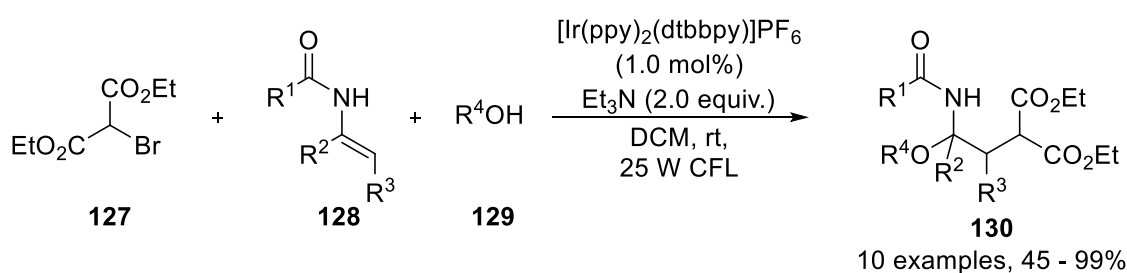


Scheme 26. Visible light mediated ATRP of methyl methacrylate (**125**) with ethyl- α -bromophenylacetate (**124**) as initiator.^[100]

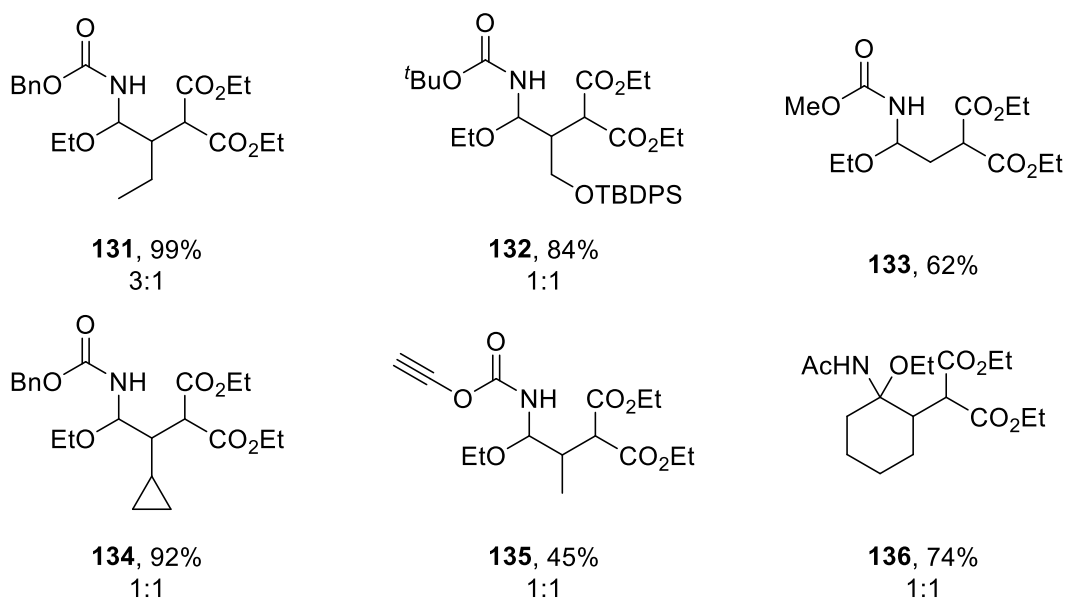
In photoredox-catalyzed ATRA reactions of olefins, the generation of a carbocation plays an important role. This intermediate is usually trapped by the halide that is formed in the mechanism of a typical ATRA reaction, but trapping by numerous other nucleophiles added to the reaction is also plausible. This way, multicomponent ATRA reactions could give access to a large variety of vicinal difunctionalized molecules. Even though these multicomponent reactions do not give a perfect atom economy anymore, the ability to synthesize heavily functionalized compounds in a single step is of great interest.

A Introduction

In 2012, the work group of Masson developed a three-component oxyalkylation reaction using a visible light mediated ATRA approach. The reaction of enecarbamates **128** with diethyl bromomalonate (**127**) and alcohols **129** was performed using $[\text{Ir}(\text{ppy})_2(\text{dtbbpy})]\text{PF}_6$ as photocatalyst in a reductive quenching cycle with Et_3N as sacrificial electron donor. In the reaction, a malonate radical is formed which then adds to the enecarbamate **128**. The resulting radical is oxidized by a Ir(III)-species to generate an iminium-ion which is trapped by the alcohol to yield a β -alkylated α -carbamidoether **130** (scheme 27).^[101]



Selected examples:



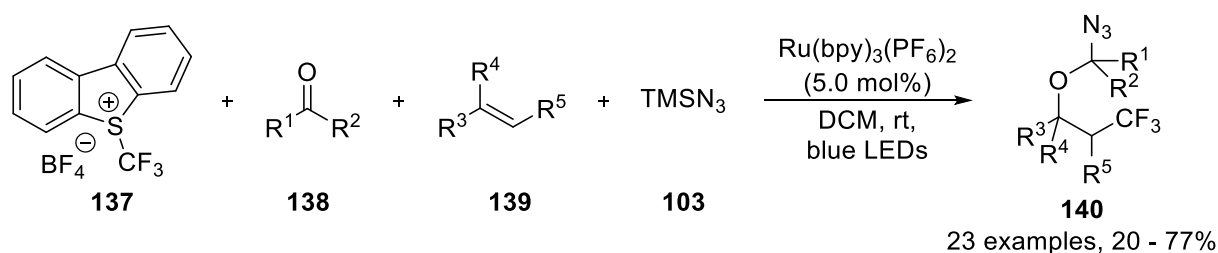
Scheme 27. Visible light mediated three-component ATRA reaction of enecarbamates **128** with diethyl bromomalonate (**127**) and alcohols **129**.^[101]

Using this method of three-component photoredox-catalyzed ATRA reactions, a plethora of interesting transformations like oxytrifluoromethylations of styrenes^[102] and enecarbamates,^[103] the hydroxytrifluoromethylation of styrenes,^[104] hydrotrifluoromethylation of alkenes,^[105] aminotrifluoromethylation^[106] or carbotrifluoromethylation^[107] were achieved.

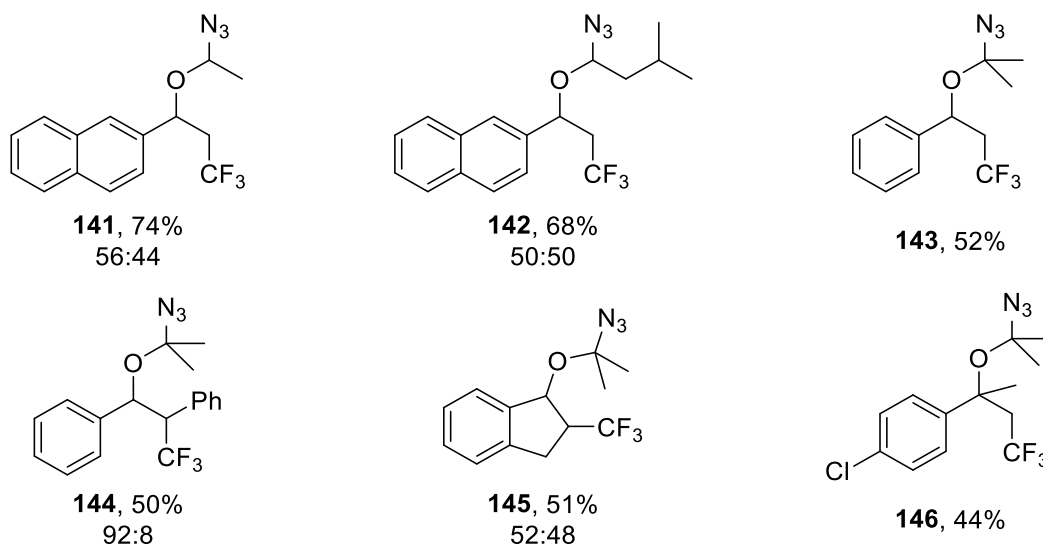
Going even one step further, Masson *et al.* could demonstrate a four-component ATRA reaction using visible light mediated photocatalysis. The azidoalkoxytrifluoromethylation of alkenes was achieved using $\text{Ru}(\text{bpy})_3(\text{PF}_6)_2$ as photocatalyst. Umemoto's reagent (**137**) was used as CF_3 radical source which

A Introduction

was trapped by an alkene **139** and the formed carbocation was trapped with a carbonyl compound **138** which then got attacked by an azide **103**. Overall, a sequence of C-C-, C-O- and C-N-bond formations was achieved in one step to generate highly functionalized compounds (scheme 28).^[108]



Selected examples:



Scheme 28. Visible light mediated four-component ATRA reaction of alkenes **139** with Umemoto's reagent (**137**), carbonyl compounds **138** and TMSN₃ (**103**).^[108]

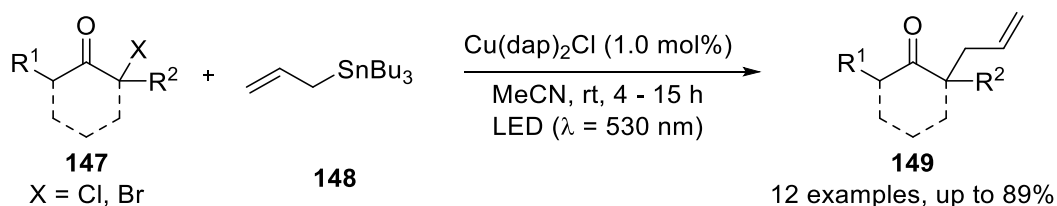
With the reinvigoration of visible light mediated photoredox catalysis, ATRA chemistry has been developed into a powerful tool for the difunctionalization of alkenes and alkynes. ATRA reactions developed in the middle of the 20th century usually required harsh conditions, hazardous or toxic reagents and suffered from poor selectivity. With photoredox catalysis, ATRA reactions can now be performed under mild conditions with high selectivity and good catalytic efficiency. The unique properties of photocatalysts originating from various compound classes such as organic dyes, semiconductors and most importantly transition-metal complexes of iridium, copper and ruthenium have led to new ways to perform highly efficient and ambitious ATRA transformations. ATRA processes are highly atom-economical and with its ability to create complex structures in one step they have the potential to become a useful method for the synthesis of natural products and pharmaceuticals.^[96]

1. Visible light mediated allylation reactions with allylsilanes

1.1 Literature background

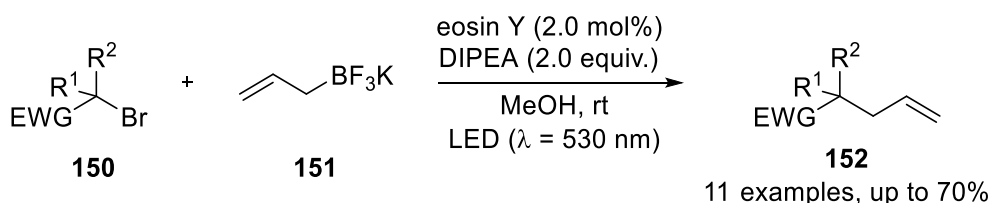
The introduction of the allyl functionality into organic molecules plays an important role due to its various further useful transformations such as dihydroxylation, epoxidation, ozonolysis, olefin metathesis and more. The allylation of organohalides is one of these powerful tools for introducing the allyl functionality.^[109] There are many reagents that can be used for the allylation *via* C-C bond formation such as allyl halides,^[110] allyl boranes and boronates^[111] or allyl Grignards.^[112] Another potent allylation reagent is allyl tributyltin (**148**) which can be used for the allylation of organohalides by radical initiation *via* azobisisobutyronitrile (AIBN), Et₃B or under photochemical conditions.^[113]

In 2012, the Reiser group showed that the copper photocatalyst Cu(dap)₂Cl (**50**) is able to catalyze the allylation of various α -halo carbonyl compounds **147** with allyl tributyltin (**148**) as allylating reagent under visible light irradiation (scheme 29).^[74]



Scheme 29. Visible light mediated allylation of α -halo carbonyls **147** with allyl tributyltin (**148**).^[74]

Since then, a variety of approaches for photoredox-catalyzed allylations have been established.^[114] In 2017 Leonori *et al.* showed that allyl-BF₃K (**151**) can be used as allylating agent for electrophilic radicals generated from bromomalonates and benzylbromides under visible light using eosin Y (**51**) as photocatalyst (scheme 30).^[115]

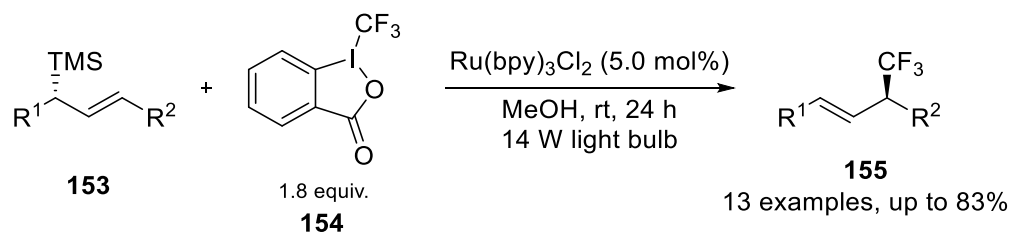


Scheme 30. Visible light mediated allylation of α -halo carbonyls **150** with allyl-BF₃K (**151**).^[115]

Already in 2012, the Reiser group tried to look for more ecologically benign alternatives to allyl tributyltin as allylating reagent. It was shown that allyltrimethylsilane (**159**) can also be used for the visible light mediated allylation using Cu(dap)₂Cl (**50**) as catalyst but only one example was met with

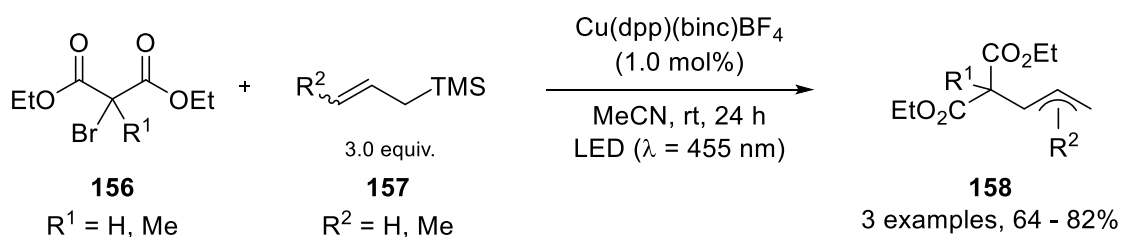
B Main Part

success.^[74] Shortly after, the Gouverneur group used more complex allylsilanes **153** in photoredox-catalyzed trifluoromethylations with Togni's reagent (**154**) as CF₃-source and Ru(bpy)₃Cl₂ (**46**) as catalyst (scheme 31).^[116]



Scheme 31. Visible light mediated trifluoromethylation of allylsilanes **153** with Togni's reagent (**155**).^[116]

The Reiser group also tried to expand the allylation reaction using allylsilanes **157** with the new copper(I)-bisisonitrile complex Cu(dpp)(binc)BF₄ and could show in three examples that diethyl bromomalonates **156** can also be used in this reaction (scheme 32).^[117]



Scheme 32. Visible light mediated allylation of α-halo carbonyls **156** with allylsilanes **157**.^[117]

1.2 Visible light mediated allylations of α -halo carbonyls

So, it was shown that allylsilanes can in fact be used in photoredox-catalyzed allylation reactions but only on few selected examples.^[74,117] Therefore this reaction was further explored by finding the best catalysts and conditions while expanding the scope of the allylsilanes, carbohalides and α -halo carbonyls. Furthermore, investigation into other radical sources were carried out. As a starting point for the investigation of the photoredox-catalyzed allylation using allylsilanes the reaction of diethyl 2-bromomalonate (**127**) and allyltrimethylsilane (**159**) was chosen (table 1).

Table 1. Optimization of the reaction of diethyl 2-bromomalonate (**127**) and allyltrimethylsilane (**159**).

$\text{EtO}_2\text{C}-\text{CH}(\text{Br})-\text{CO}_2\text{Et}$ (**127**) + $\text{CH}_2=\text{CH}-\text{CH}_2\text{TMS}$ (**159**, 3.0 equiv.) $\xrightarrow[\text{solvent, rt}]{[\text{PC}] (0.5 \text{ mol}\%)}$ $\text{EtO}_2\text{C}-\text{CH}(\text{CH}_2\text{CH}=\text{CH}_2)-\text{CO}_2\text{Et}$ (**160**)

Entry	Catalyst	Light	Solvent	Time	Yield
1	Cu(dap)Cl ₂	530 nm	MeCN	40 h	75%
2 ^[a]	Cu(dap)Cl ₂	530 nm	MeCN	40 h	74%
3	Cu(dap)Cl ₂	530 nm	MeCN	24 h	55%
4	-	530 nm	MeCN	40 h	-
5	Cu(dap)Cl ₂	-	MeCN	40 h	-
6	Cu(dap)Cl ₂	455 nm	MeCN	40 h	60%
7 ^[b]	Cu(dap)Cl ₂	530 nm	MeCN	40 h	62%
8 ^[c]	Cu(dap)Cl ₂	455 nm	MeCN	40 h	55%
9	Cu(dap)Cl ₂	530 nm	DMF	40 h	32%
10	Cu(dap)Cl ₂	530 nm	DMF/H ₂ O (1:4)	40 h	34%
11	Cu(dap)Cl ₂	530 nm	DCM	40 h	-
12	Cu(dap) ₂ Cl	530 nm	MeCN	40 h	68%
13	Cu(binc)(dpp)BF ₄	455 nm	MeCN	40 h	57%
14	Ru(bpy) ₃ Cl ₂	455 nm	MeCN	40 h	48%
15	<i>fac</i>-Ir(ppy)₃	455 nm	MeCN	24 h	93%
16	Ir[dF(CF ₃)ppy] ₂ (dtbbpy)PF ₆	455 nm	MeCN	24 h	91%

Standard reaction conditions: **127** (0.5 mmol), **159** (1.5 mmol), photocatalyst (0.5 mol%), solvent (1 mL), N₂ atmosphere, rt. ^[a]1.0 mol% of photocatalyst. ^[b]2.0 equiv. of **159**. ^[c]1.0 equiv. of Na₂CO₃ was added.

B Main Part

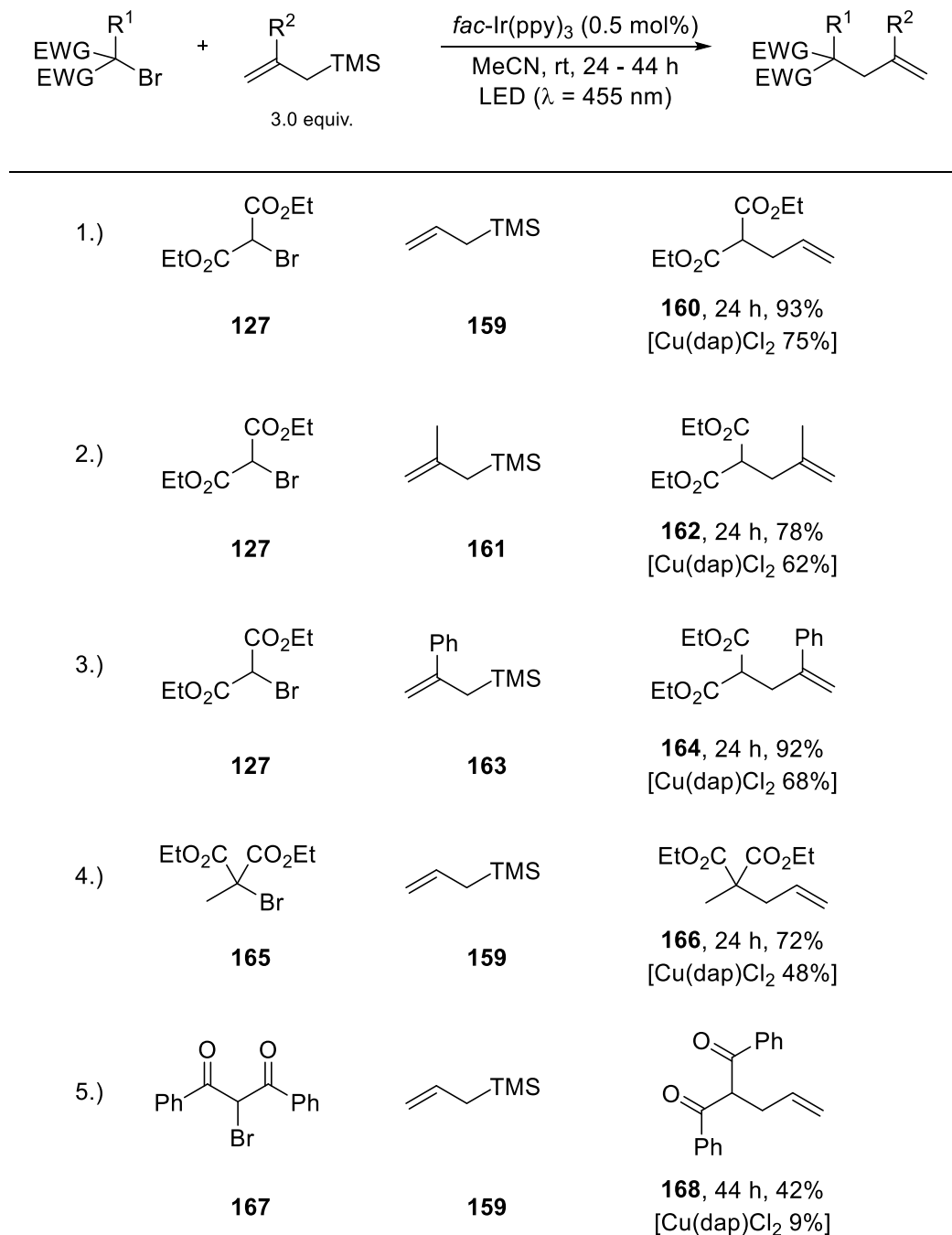
The reaction of **127** with three equivalents of the allylsilane **159** using 0.5 mol% of the newly discovered copper(II)-complex Cu(dap)Cl₂ (**102**)^[87] under green light irradiation ($\lambda = 530$ nm) gave the product **160** in good yield of 75% after 40 h.

Increasing the catalyst loading to 1.0 mol% did not benefit the reaction (entry 2). Changing the solvent from MeCN to other commonly used solvents also didn't increase the yields (entries 9 – 11). Surprisingly, the reaction did not proceed at all in DCM (entry 11). When the light source was changed to blue light ($\lambda = 455$ nm), the yield decreased to 60% (entry 6). Trying to lower the amount of **159** from three to two equivalents also gave lower yields, indicating that an excess of the allylsilane **159** is necessary. The addition of the base Na₂CO₃, which was previously shown to improve some Cu(dap)Cl₂-catalyzed reactions^[93] did however give a reduced yield of 55% (entry 8). Control experiments revealed that both the catalyst and light irradiation are necessary for the reaction (entry 4 & 5).

Comparing these results with some well-established catalysts shows that the copper(I)-complex Cu(dap)₂Cl (**50**) and the copper-bisisonitrile complex Cu(binc)(dpp)BF₄^[117] give lower yields than the new copper(II)-complex Cu(dap)Cl₂ (**102**) (entries 12 & 13). The ruthenium-based catalyst Ru(bpy)₃Cl₂ (**46**) also only gives the product in 48% yield (entry 14). Employing common iridium-based catalysts such as *fac*-Ir(ppy)₃ (**49**) and Ir[dF(CF₃)ppy]₂(dtbbpy)PF₆ not only raised the yield to 91% and 93%, respectively, but also lowered the reaction times from 40 to 24 h. Therefore, *fac*-Ir(ppy)₃ (**49**) seems to be the best catalyst for these transformations.

B Main Part

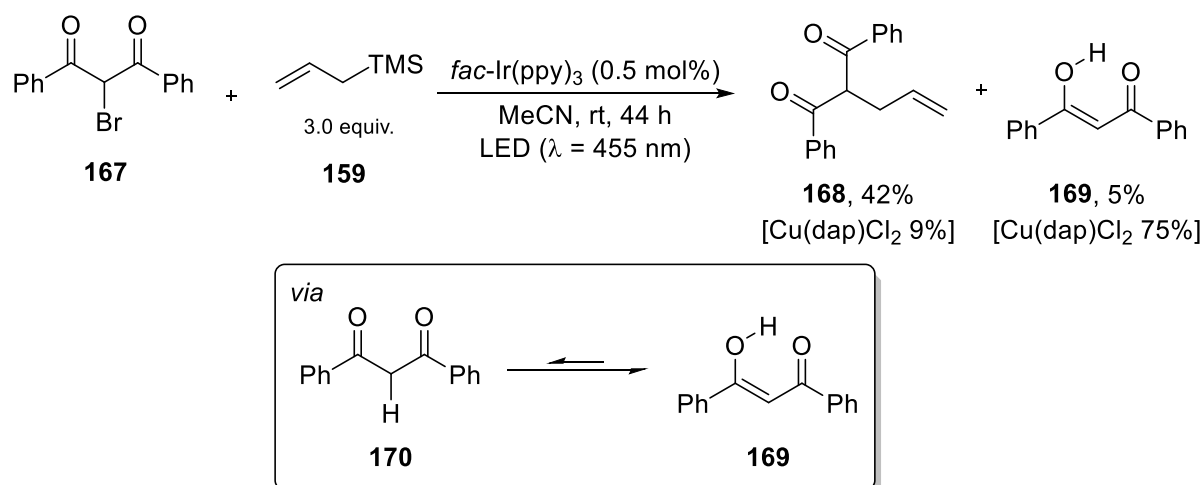
With these optimized reaction conditions at hand, the substrate scope was expanded using some more carbohalides bearing two electron-withdrawing groups and some substituted allylsilanes (scheme 33).



Scheme 33. Substrate scope of different carbohalides and allylsilanes; Comparison between *fac*-Ir(ppy)₃ (**49**) and Cu(dap)Cl₂ (**102**).

B Main Part

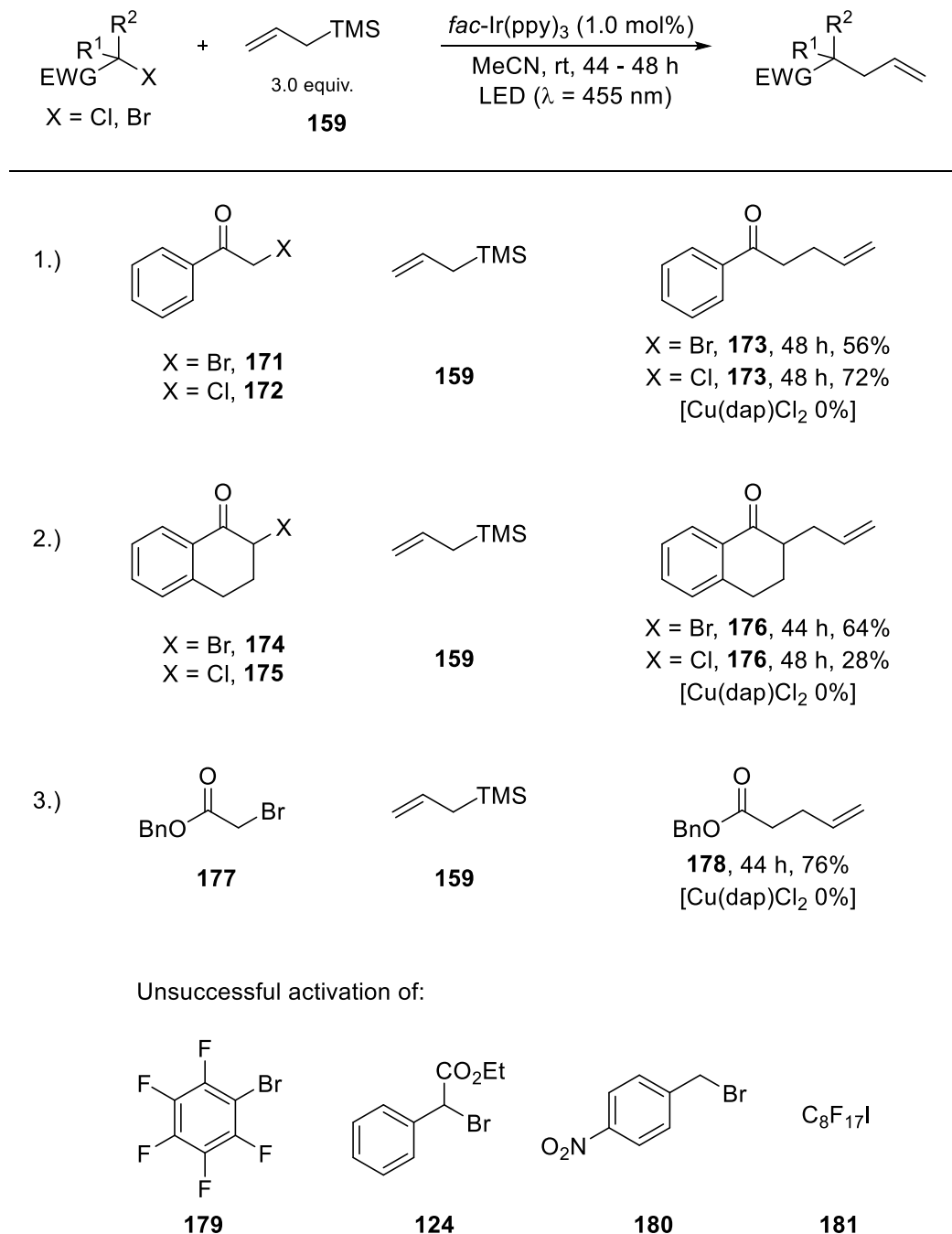
All reactions were performed with both *fac*-Ir(ppy)₃ (**49**) at blue light irradiation and Cu(dap)Cl₂ (**102**) at green light irradiation to get a good comparison of these two metal-based catalysts in these reactions. When trimethyl(2-methylallyl)silane (**161**) was reacted with **127**, the product **162** with a methyl-substituted allyl-group was obtained in good yield (78%) using *fac*-Ir(ppy)₃ (**49**), while the copper-catalyzed reaction gave lower yields (entry 2). Using an allylsilane with a phenyl substituent **163** in the same position gave excellent results (92%) with the iridium catalyst (entry 3). Changing to diethyl 2-bromo-2-methylmalonate (**165**) gave the product **166** in good yield (entry 4) but considerably lower than without the additional methyl-substituent (entry 1) indicating that an increased steric hinderance at the radical center and its better stabilization could affect the reaction. When the ester moieties were replaced by benzoyl groups **167** (entry 5) the yield dropped drastically (42%), especially in the case of Cu(dap)Cl₂ (**102**) (9%). This can be explained by a dehalogenation of the starting material **167** followed by a favored keto-enol tautomerization to form (Z)-3-hydroxy-1,3-diphenylprop-2-en-1-one (**169**) which is stabilized by an expanded conjugated π -system (scheme 34). In case of the iridium-catalyzed reaction only 5% of this side-product were observed while in the case of copper 75% were received, explaining the low yield of the desired product.



Scheme 34. Reaction of 2-bromo-1,3-diphenylpropane-1,3-dione (**167**) and allyltrimethylsilane (**159**); formation of side-product **169**.

B Main Part

Next, some halides that only bear one electron-withdrawing group were used for the allylation (scheme 35).



Scheme 35. Substrate scope of different α -halo carbonyls; unsuccessful substrates.

These compounds are more difficult to activate, therefore the catalyst loading had to be increased to 1 mol% to achieve full conversion of the starting materials and longer reaction times were necessary. With 2-bromoacetophenone (**171**), the allylated product **173** was obtained in 56% yield (entry 1). Surprisingly, the reaction did not proceed with Cu(dap)Cl₂ (**102**) even though this compound has been used in copper-catalyzed ATRA reactions before.^[74] Interestingly, when the bromine was replaced by

B Main Part

chlorine the same product **173** was obtained in even higher yield of 72%. This would not be expected since the chloride should be a lot harder to activate but in literature the same counterintuitive reactivity was also observed when the allylation was performed using tributylallyltin (**148**) and Cu(dap)₂Cl (**50**).^[74] The α -bromo- and α -chloro-derivative of 1-tetralone were synthesized (**174** and **175**) and the outcome of the reaction showed that in this case the bromo compound gave more than twice the yield of **176** than the chloro compound (entry 2). This is contrary to entry 1, but also again in accordance with what was reported in literature for these two compounds.^[74] When the α -bromo-ester **177** was used the product **178** was obtained in good yield of 76% (entry 3).

Trying to expand the substrate scope beyond α -halo carbonyl-compounds showed the limits of this reaction. Activation of the electron-deficient bromo-benzene derivative **179** was not possible with the iridium-catalyst. Ethyl 2-bromo-2-phenylacetate (**124**) which seems to be a suitable substrate to generate a radical in benzylic position did however not undergo the allylation. Instead, only decomposition of the starting material was observed. The electron-deficient 4-nitrobenzyl bromide (**180**) which was already used in ATRA related processes^[118] also did not give the desired product and instead only partial consumption of the starting material was observed giving rise to the dimerization product of the generated radical in traces. This has been observed for both Cu(dap)Cl₂ (**102**) and *fac*-Ir(ppy)₃ (**49**). In the case of the perfluorinated iodide **181** both catalysts only gave traces of product.

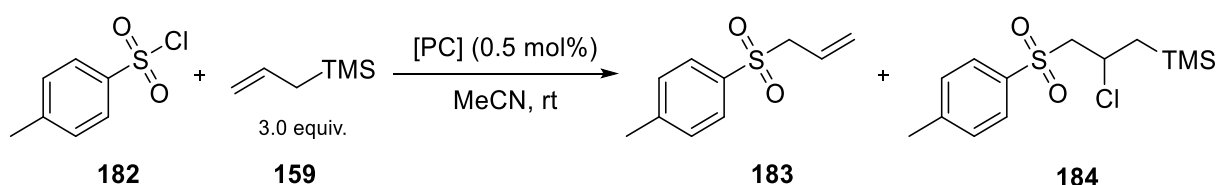
B Main Part

1.3 Visible light mediated allylations of sulfonyl chlorides

The generation of sulfur radicals has been developed as a useful tool in the formation of various C-S bonds.^[119] In the Reiser group, sulfonyl chlorides were already used for various photoredox-catalyzed processes.^[84,93,120] Sulfones are a very important compound class which can be found amongst various biologically active molecules and drugs and are used in many useful reactions.^[121] Especially allyl sulfones have been used in organic chemistry for a variety of transformations.^[122] Therefore, it was tested if this approach for the photochemical allylation would also be feasible for sulfonyl chlorides. With that, a new synthetic route for useful allyl sulfones under very mild conditions starting from benign and abundant starting materials could be accomplished.

As a starting point for this investigation, the reaction of tosyl chloride (**182**) and allyltrimethylsilane (**159**) in MeCN was screened (table 2).

Table 2. Optimization of the reaction of tosyl chloride (**182**) and allyltrimethylsilane (**159**).



Entry	Catalyst	Additives	Work-up	Light	Time	Yield	
						183	184
1	Cu(dap)Cl ₂	-	-	530 nm	48 h	53%	-
2	Cu(dap) ₂ Cl	-	-	530 nm	48 h	46%	-
3	<i>fac</i> -Ir(ppy) ₃	-	-	455 nm	48 h	28%	-
4	Cu(dap)Cl ₂	-	-	530 nm	48 h	18% ^[a]	59% ^[a]
5	Cu(dap)Cl ₂	-	KOH (4 equiv.) in H ₂ O at rt	530 nm	48 h	71%	-
6	Cu(dap)Cl ₂	-	NaF (2 equiv.) in H ₂ O at 50 °C	530 nm	48 h	75%	-
7	Cu(dap) ₂ Cl	-	NaF (2 equiv.) in H ₂ O at 50 °C	530 nm	48 h	68%	-
8	<i>fac</i> -Ir(ppy) ₃	-	NaF (2 equiv.) in H ₂ O at 50 °C	455 nm	48 h	39%	-
9	Cu(dap)Cl₂	Na₂CO₃ (1 equiv.)	NaF (2 equiv.) in H₂O at 50 °C	530 nm	18 h	90%	-
10	Cu(dap)Cl ₂	K ₂ HPO ₄ (1 equiv.)	NaF (2 equiv.) in H ₂ O at 50 °C	530 nm	26 h	77%	-
11	Cu(dap)Cl ₂	Na ₂ CO ₃ (1 equiv.)	-	530 nm	18 h	29% ^[a]	63% ^[a]

B Main Part

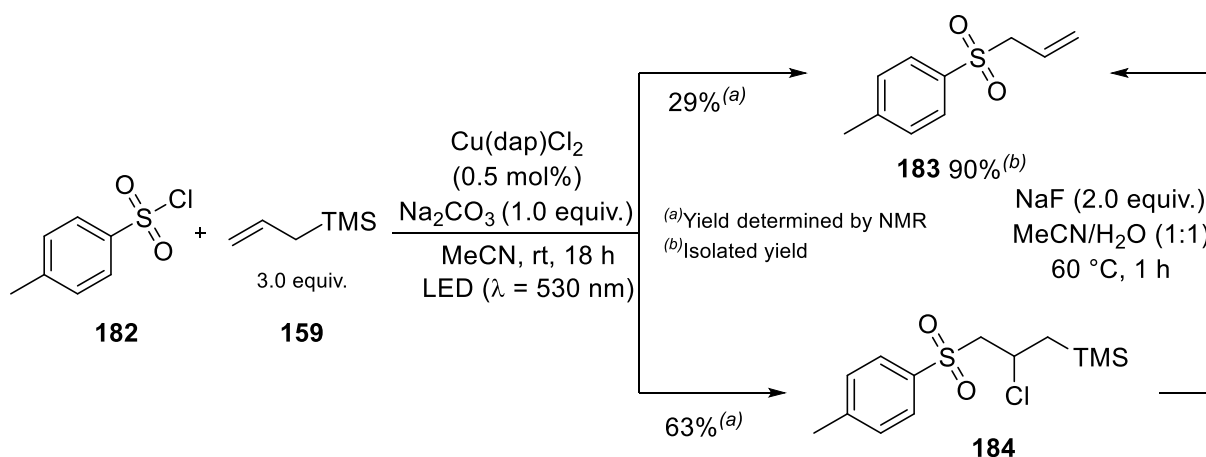
12	<i>fac</i> -Ir(ppy) ₃	Na ₂ CO ₃ (1 equiv.)	NaF (2 equiv.) in H ₂ O at 50 °C	455 nm	18 h	57% ^[a]	-
13	-	Na ₂ CO ₃ (1 equiv.)	NaF (2 equiv.) in H ₂ O at 50 °C	530 nm	48 h	-	-
14	Cu(dap)Cl ₂	Na ₂ CO ₃ (1 equiv.)	NaF (2 equiv.) in H ₂ O at 50 °C	-	48 h	-	-

^[a]Yield determined using 1,3,5-trimethoxybenzene as internal NMR-standard.

The reaction only gave moderate yields of 53% and 46% when the two copper catalysts Cu(dap)Cl₂ (**102**) and Cu(dap)₂Cl (**50**) (entry 1 & 2) were used. The yield was even lower with *fac*-Ir(ppy)₃ (**49**) which only gave 28% (entry 3). During the reaction, a second product was observed on the TLC and in the crude NMR this side product was found to be the actual ATRA product **184**. However, this compound could not be isolated by column chromatography. Therefore, the yield of the allylated product **183** and the ATRA product **184** were determined by adding 1,3,5-trimethoxybenzene as internal standard to the crude mixture and subjecting it to NMR spectroscopy (entry 4). That way, a yield of 18% for product **183** and 59% for the ATRA product **184** were found. This is surprising since the isolated yield of the reaction after column chromatography gives a higher yield of 53%. This indicates that during the chromatography the ATRA product **184** actually undergoes elimination to form the allylated product **183**. The combined NMR yields of both products in entry 4 would add up to a total of 77%. This means that conversion of the ATRA product **184** to the allylated product **183** undergoes with a loss of about 24%. To avoid that, it was tested if this elimination could be achieved before purification to avoid loss of product. Adding an aqueous solution of KOH after irradiation was complete and letting it stir at room temperature for an additional hour led to an increase of received allylated product **183** to 71%. Since silicon atoms are known to form bonds with fluorine rather easily it was also checked if NaF could also be able to eliminate the TMS group from the ATRA product **184**. In case of NaF, the reaction temperature had to be increased to 50 °C to get full elimination but with this method a yield of 75% could be achieved which is almost the maximum of the yield that would be possible after the photoreaction (entry 6). During the investigation of this reaction, it was found in the Reiser group that addition of inorganic bases, such as Na₂CO₃, to photoreactions of sulfonyl chlorides with copper catalysts can lead to much higher yields.^[93] And in fact, the addition of one equivalent of Na₂CO₃ to the photoreaction not only increased the yield to 90% but also drastically lowers the reaction time to 18 h (entry 9). Using K₂HPO₄ as the base did not have a great effect on the yield but also lowered the reaction time (entry 10). With these improved conditions the yield for *fac*-Ir(ppy)₃ (**49**) also rose to 57% and the reaction time decreased but the copper catalyst was still the best catalyst for this reaction. If the yields of **183** and the ATRA product **184** are determined again with the addition of Na₂CO₃ via

B Main Part

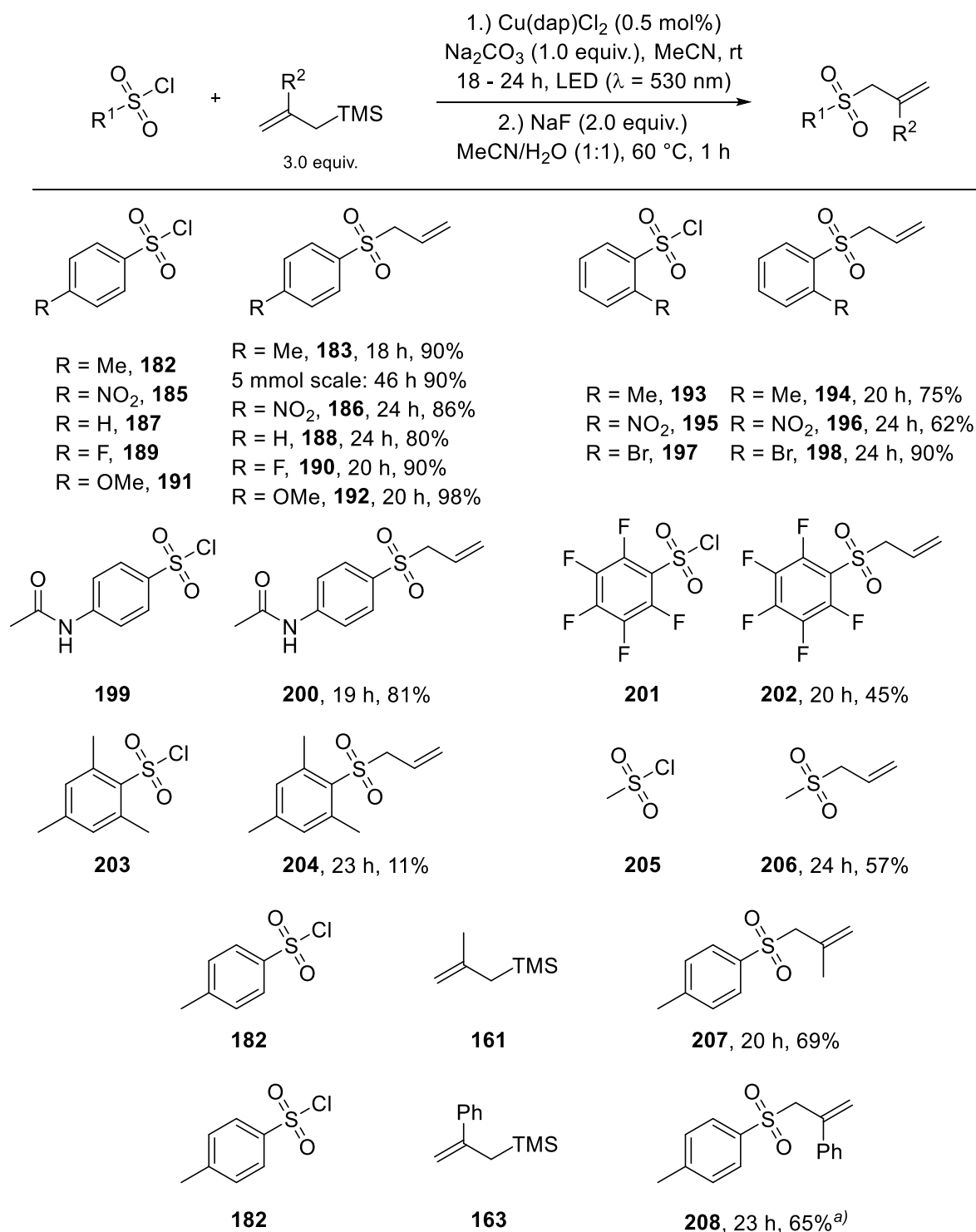
internal NMR standard, 29% of the allyl compound **183** and 63% of the ATRA product **184** were observed (entry 11). Comparing this to the reaction without the base shows that there is an overall much higher combined yield of 92% compared to 77% but also the ratio between both compounds is shifted to the allylation side, indicating that the base already partially facilitates the elimination (Scheme 36).



Scheme 36. Comparison of isolated yield of **183** with and without work-up with NaF; Observation of ATRA product **184** prior to work-up.

With the optimized conditions at hand, the scope of sulfonyl chlorides and allylsilanes was now explored (scheme 37). Several *para*-substituted aryl sulfonyl chlorides were tested with very good yields. As expected, electron-withdrawing substituents such as nitro- and fluoro-groups worked very well. More surprisingly, the sulfonyl chloride **191** with an electron-donating methoxy-group gave the best results with an almost quantitative yield of 98%. Going from *para*- to *ortho*-substitution of the methyl- and nitro-group, a rather big decline of yields from 90% to 75% and 86% to 62% is seen which might show that increased steric effects could hinder the reaction. This is even more the case for the reaction of 2-mesitylenesulfonyl chloride (**203**), which has two methyl-groups in *ortho*-position. The reaction of this compound only gave the product **204** in 11% yield. The same can be seen when the perfluorinated benzenesulfonyl chloride **201** was used which also only gave 45% of the product **202**. Methanesulfonyl chloride **205** can also be successfully applied demonstrating that the reaction is not limited to aryl sulfonyl chlorides but also works with alkyl sulfonyl chlorides.

B Main Part



Scheme 37. Substrate scope of different sulfonyl chlorides and allylsilanes; a) no work-up with NaF necessary.

Pleasingly, the substituted allyl sulfones **161** and **163** also gave good results even though the yields were noticeably lower than with **159**. Surprisingly, in the case of the phenyl substituted silane **163** no ATRA product was detected on TLC and in the crude NMR therefore the additional work-up with NaF was not necessary. In an attempt to test if this reaction could be scaled up, the allylation of tosyl chloride (**182**) was performed on a 5 mmol scale. All reagents and solvents were increased tenfold,

B Main Part

and the reaction carried out in a bigger flask (figure 3). Only the light source was the same as in the 0.5 mmol reaction. Probably due to that fact that the light intensity was not increased, irradiation for 46 h was necessary to achieve full conversion. The outcome of the reaction was equally successful as on small scale with 90% yield and 0.89 g of the product **183** obtained in a one-pot process.

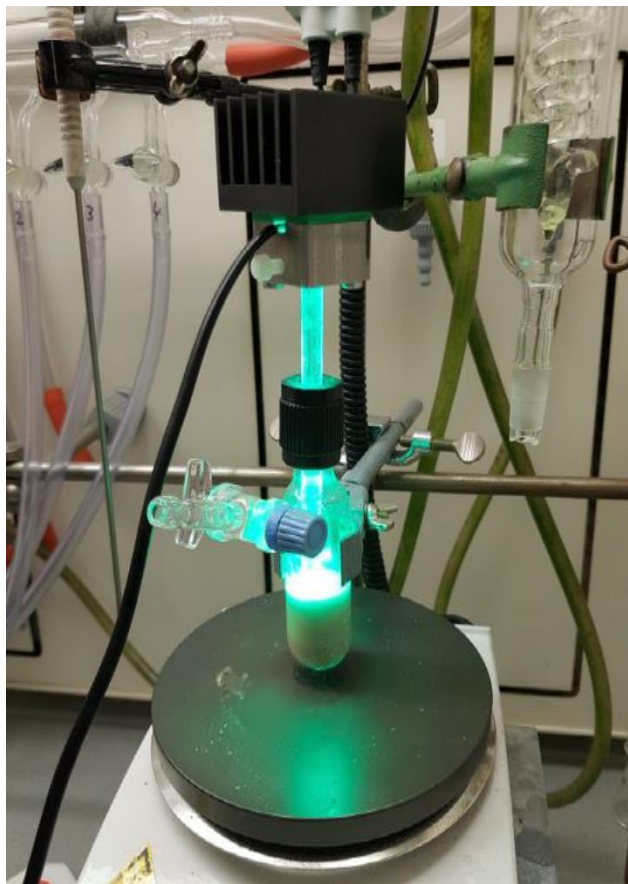
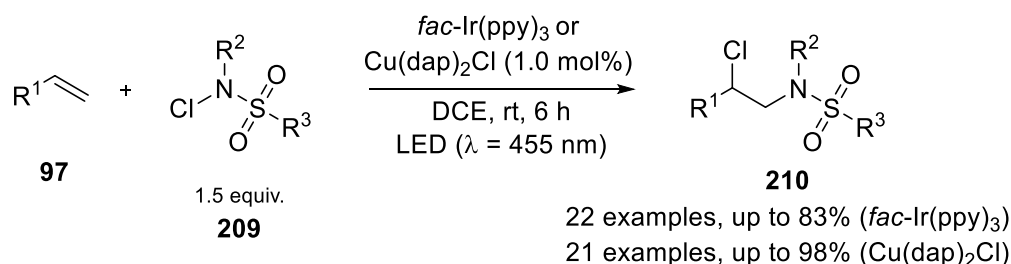


Figure 3. Photochemical big-scale set-up synthesis of 1-(allylsulfonyl)-4-methylbenzene (**183**).

B Main Part

1.4 Visible light mediated allylations of *N*-chloro-amines

In recent years, the generation of *N*-centered radicals has become a very powerful tool in photoredox-catalyzed synthesis.^[123] For example, protected *N*-chloro amines **209** can be used in ATRA processes to achieve *N*-chloroamination of vinyl arenes **97**.^[124] In the Reiser group, it was shown that these reactions can also even be outperformed with copper photocatalysts, especially for electron-deficient arenes^[125] (scheme 38).



Scheme 38. *N*-chloroamination of olefins **97** with *N*-chloro-amines **209** and *fac*-Ir(ppy)₃^[124] or Cu(dap)Cl₂.^[125]

These promising results initiated further research into whether *N*-centered radicals could also be used for a new mild approach towards the allylation of amines and amides. Studies began by investigating the reaction of *N*-chloro-*N*-methyl-4-nitrobenzenesulfonamide (**211**) (table 3).

Table 3. Optimization of the reaction of *N*-chloro-*N*-methyl-4-nitrobenzenesulfonamide (**211**) and allyltrimethylsilane (**159**).



Entry	Catalyst	Light	Time	Yield
1	Cu(dap)Cl ₂	530 nm	40 h	52%
2	<i>fac</i> -Ir(ppy) ₃	455 nm	40 h	50%
3^[a]	Cu(dap)Cl₂	530 nm	18 h	77%
4	-	455 nm	40 h	36%

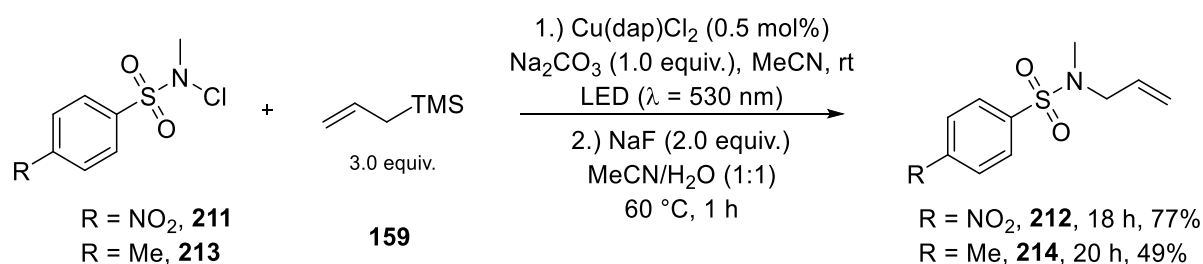
^[a] 1.0 equiv. of Na₂CO₃ was added; 2.0 equiv. of NaF in 1 mL of H₂O was added after irradiation and heated to 60 °C for 1 h.

Fortunately, allylation was achieved in moderate yields with both Cu(dap)Cl₂ (**102**) (entry 1) and *fac*-Ir(ppy)₃ (**49**) (entry 2) in 40 h. Applying the optimized reaction conditions from the reaction with sulfonyl chlorides and copper catalysts also improved the yield to 77% and decreased to reaction time

B Main Part

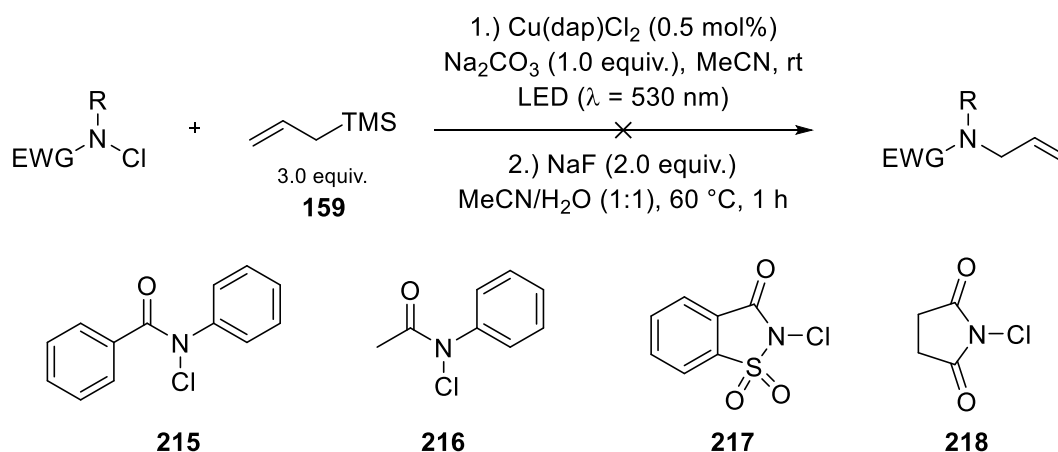
to 18 h in this case (entry 3). It is known that these compounds can already be activated by visible light^[124,125] so an according control experiment was performed as well. Under blue light irradiation ($\lambda = 455$ nm) without any catalyst for 40 h, the product **212** was obtained in 36% yield (entry 4).

With these conditions at hand, it was tested if the reaction also proceeds for different *N*-chloro amines. Going from the strong electron-withdrawing nosyl-group in **211** to the tosyl protected amine **213** there is already a yield drop to only 49% (scheme 39).



Scheme 39. allylation of two different *N*-chloro-amines **211** and **213** under optimized conditions.

To see if this method was really suited as an alternative approach towards the allylation of amines, a small selection of *N*-chloro amides was probed. In case of the *N*-chloro amides **215** and **216** no product formation was observed. Instead, only dehalogenation to the corresponding amides was seen. The same was the case for the chloro-derivative of the artificial sweetener saccharin **217**. As for *N*-chlorosuccinimide (**218**), the desired product was obtained but only in trace amounts (scheme 40).

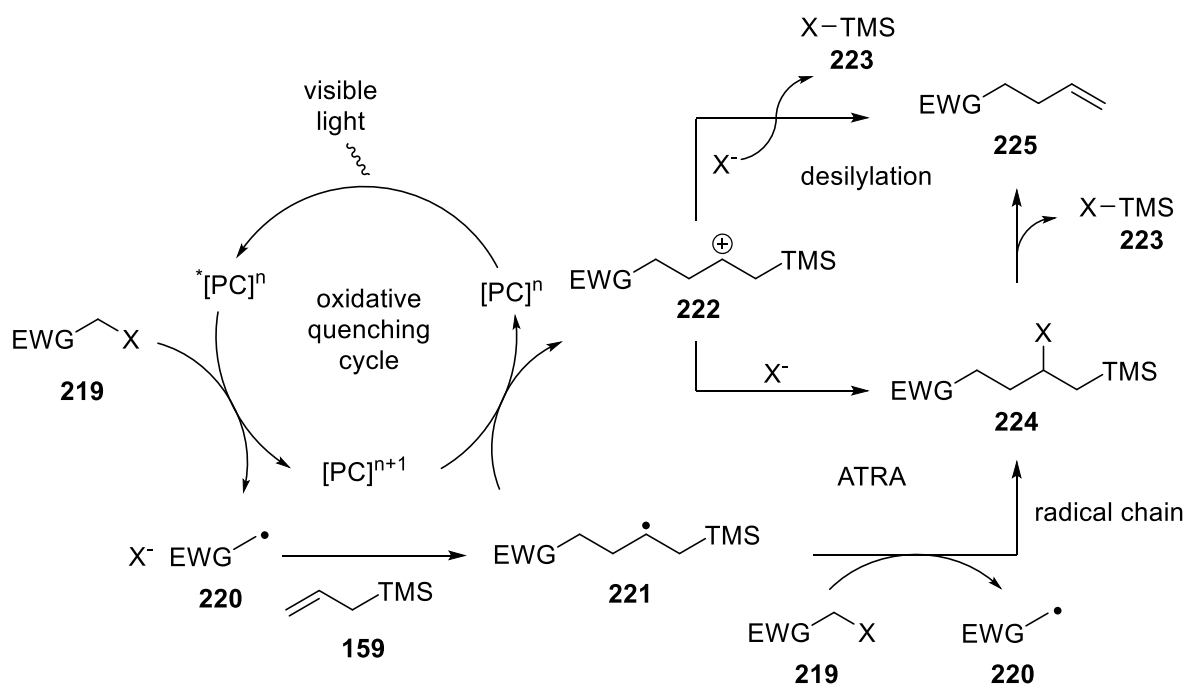


Scheme 40. Unsuccessful allylation of different *N*-chloro-amides.

Therefore, this method is not suited for the allylation of amides and amines and an alternative approach towards their synthesis could not be achieved.

1.5 Proposed mechanism

Regarding the mechanism of this reaction, the observation of the ATRA product in case of sulfonyl chlorides indicates that the reaction proceeds under a typical ATRA reaction mechanism (scheme 41). Initially, visible light is absorbed by the photocatalyst $[PC]^n$ which then undergoes SET to the radical precursor **219**. The radical **220** and a halide anion are formed, and the radical adds to the unactivated alkene, forming the intermediate **221**. The oxidized form of the catalyst $[PC]^{n+1}$ can now oxidize the radical intermediate **221** to the cationic species **222** while the catalyst $[PC]^n$ is regenerated, closing the oxidative quenching cycle. Two different pathways can now be considered for the cation **222**. The halide could trap the positive charge to form the rather unstable ATRA product **224** which can be transformed to the allyl product **225** by elimination of the halosilane $X-TMS$ **223**. This was the main pathway for the reaction of sulfonyl chlorides and was also observed in case of the *N*-chloro amines **211** and **213**. In the second possible pathway, the cationic intermediate **222** directly undergoes desilylation to the product **225**. In case of the α -halo carbonyl-compounds this seems to be the main pathway since the ATRA intermediate was not observed.

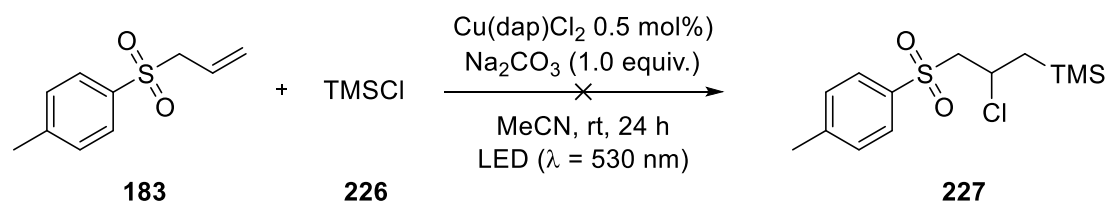


Scheme 41. Proposed reaction mechanism for the visible light mediated allylation reaction.

For this reaction it can also be assumed that a radical chain mechanism is feasible. Here, the radical intermediate **221** directly abstracts a halide radical from the starting material **219** to generate the ATRA product **224** and a new radical **220**, which then undergoes a radical chain. The ATRA product **224** is then again desilylated to the final allyl substrate **225** (scheme 41).

B Main Part

Another possible explanation for the formation of the ATRA intermediate **224** could be that the allylated product **225** could again react in an ATRA reaction with the halosilane X-TMS **223**. To rule out this possibility, a control experiment was performed in which the allylsulfone **183** was reacted with fresh TMSCl (**226**) under the standard reaction conditions. Fortunately, no reaction took place and the ATRA product **227** was not observed (scheme 42).



Scheme 42. Unsuccessful ATRA reaction between allylsulfone **183** and TMSCl (**226**).

1.6 Conclusion

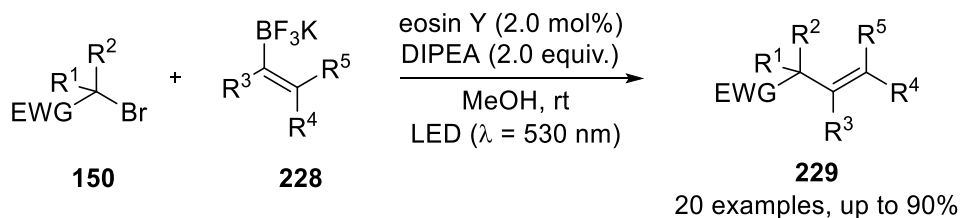
In summary, it was shown that allylsilanes can be applied in photoredox catalyzed allylations. They can be seen as a viable alternative to other commonly used reagents due to their bench stability and accessibility. Cu(dap)Cl₂ (**102**) was shown to be a potent catalyst for the photoredox catalyzed allylation of various sulfonyl chlorides whereas *fac*-Ir(ppy)₃ (**49**) was the best choice for the allylation of α-halo carbonyl-compounds. Two *N*-chloro-amines were used for this transformation as well, but a broad utilization of this compound class could not be established. During this investigation it was discovered that an ATRA product was formed during this reaction which was only observed in some cases due to its poor stability.

2. Visible light mediated ATRA reactions with vinylsilanes – Access to and utilization of α -haloalkylsilanes

2.1 Literature background and attempts towards photochemical vinylation

During the investigation of the photoredox-catalyzed allylations using allylsilanes (see chapter 1) the idea came up to use vinylsilanes in the same fashion to make vinyl sulfones or to generate substituted vinyl compounds *via* C-C bond formation. Vinyl sulfones and its derivatives are widely used in organic and medicinal chemistry as valuable building blocks.^[126] Furthermore, there are already some photoredox-catalyzed methods known to generate vinyl compounds.^[127]

For example, Leonori *et al.* reported the vinylation of electron-withdrawing halocarbon compounds like malonates or *p*-nitrobenzyl bromides with vinyl-BF₃K reagents using eosin Y (**51**) as the photocatalyst under visible light irradiation (scheme 43).^[115]

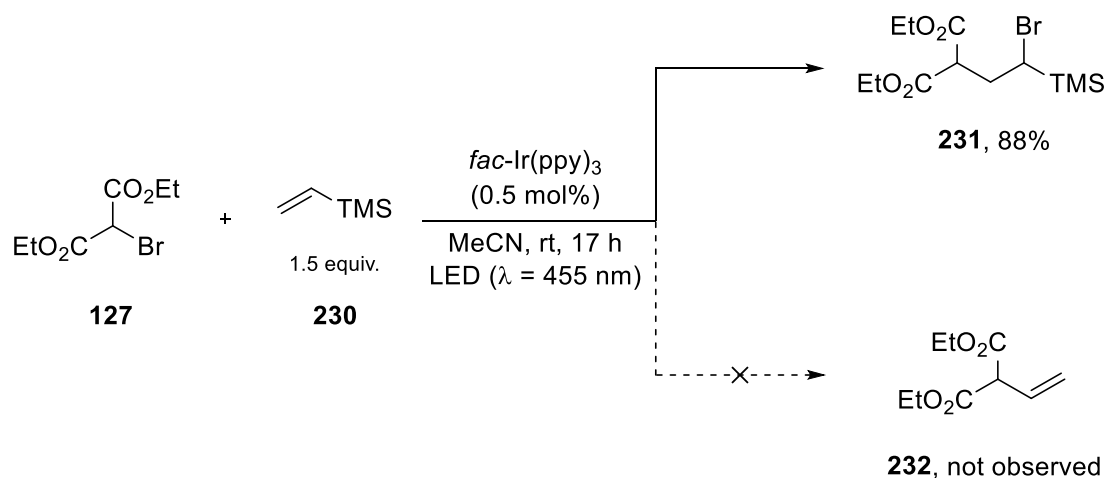


Scheme 43. Visible light mediated vinylation of electrophilic radicals.^[115]

The goal was to see if vinylsilanes could also be used as a cheap and chemically benign alternative for the photoredox-catalyzed vinylation of electrophilic radicals.

B Main Part

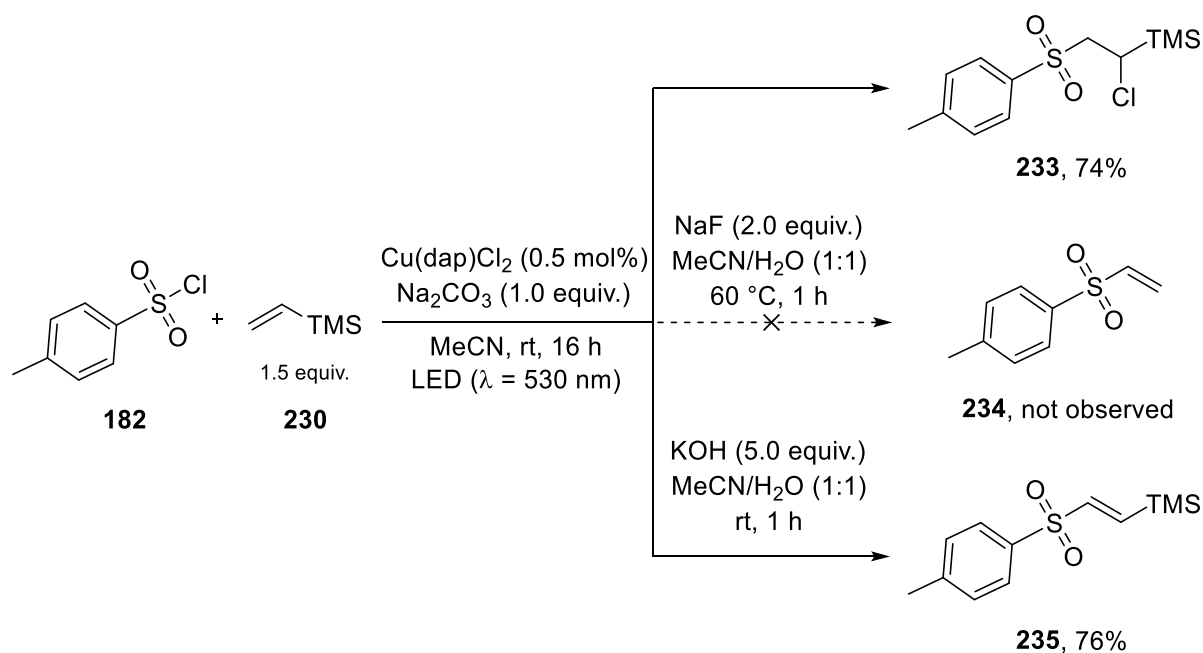
To start of the investigation, the reaction of bromomalonate **127** and vinyltrimethylsilane (**230**) using *fac*-Ir(ppy)₃ (**49**) under the established reaction conditions (see chapter 1.2) was performed.



Scheme 44. Visible light mediated ATRA reaction between diethyl bromomalonate (**127**) and vinyltrimethylsilane (**230**). Vinylation pathway not observed.

Surprisingly, the formation of the vinyl-substituted product **232** was not observed. Instead, only the ATRA product **231** was isolated in good yield of 88% (scheme 44). In the photoredox-catalyzed allylation discussed in chapter 1.3, the ATRA product was only seen as an unstable intermediate and in case of α-halocarbons was never observed. Therefore, it seems that for the reaction with vinyltrimethylsilane (**230**) the ATRA product is much more stable.

To test this, the vinyl silane **230** was also reacted with tosyl chloride (**182**) using Cu(dap)Cl₂ (**102**) as the catalyst under the established reaction conditions (chapter 1.3). Again, only the ATRA product **233** was isolated in 74% yield. The vinyl sulfone **234** was not observed (scheme 45). As previously discussed, for the photoredox-catalyzed allylation of sulfonyl chlorides, it was necessary to treat the reaction with NaF to perform elimination on the remaining ATRA product in order to obtain the allylated product in good yield.



Scheme 45. Visible light mediated ATRA reaction between tosyl chloride (**182**) and vinyltrimethylsilane (**230**) and elimination of HCl. Vinylation pathway not observed.

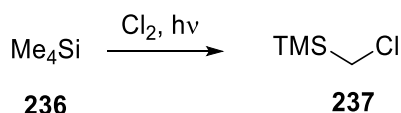
In the same fashion, the reaction mixture of the reaction here was also treated with an aqueous solution of NaF and stirred for an additional hour in a one-pot process. But no elimination to the vinyl sulfone **234** could be seen. Instead, the ATRA product **233** remained.

In case of the photochemical allylation of vinyl sulfones, KOH was also employed to eliminate the silyl-group. Therefore, it was also tried to achieve the desilylation of **233** by adding an aqueous solution of KOH after the photoreaction. But instead, HCl was eliminated and (*E*)-trimethyl(2-tosylvinyl)silane (**235**) was isolated in 76% yield (scheme 45).

So, it has been shown that a photochemical vinylation using vinyl silane is not feasible but instead it can be used for atom transfer radical additions (ATRA), leading to very interesting α -haloalkylsilanes.

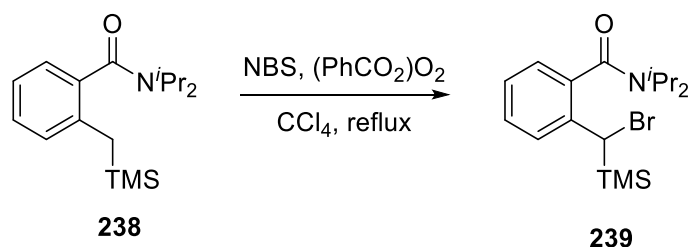
2.2 Common synthesis methods of α -haloalkylsilanes

There are various ways to access this group of compounds.^[128] The most common way to generate simple α -haloalkylsilanes is by direct radical halogenation of alkylsilanes. Probably the most important compound in this class, (chloromethyl)trimethylsilane (**237**), is produced from tetramethylsilane (**236**) and elemental chlorine (scheme 46).^[129]



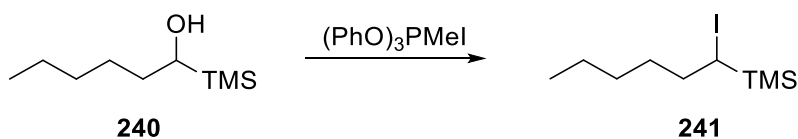
Scheme 46. Direct chlorination of tetramethylsilane (**236**).^[129]

Direct bromination is also feasible using elemental bromine or other bromine radical-sources such as NBS and radical starters (scheme 47).^[130]



Scheme 47. Direct bromination using NBS.^[130]

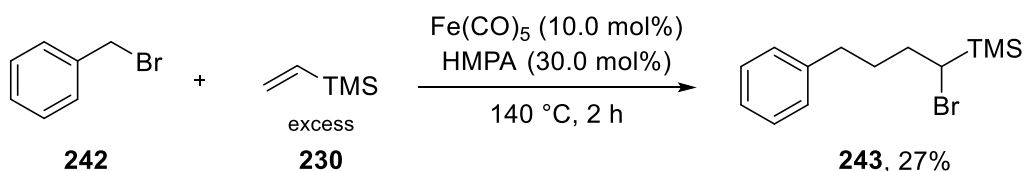
Only α -chloro- and α -bromoalkylsilanes can be accessed by this method. For the preparation of α -fluoro- or α -iodoalkylsilanes the best method is the substitution of α -hydroxyalkylsilanes like it is shown in the reaction of 1-(trimethylsilyl)hexan-1-ol (**240**) with methyl(triphenoxy)phosphonium iodide (scheme 48).^[131]



Scheme 48. Synthesis of α -iodoalkylsilanes.^[131]

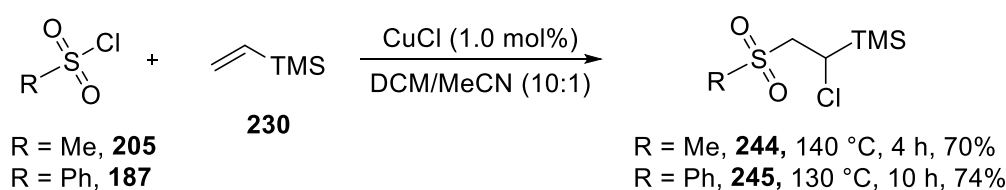
There are few reports on atom transfer radical additions onto vinylsilanes leading to the formation of α -haloalkylsilanes.^[132] For instance, the radical derived from benzyl bromide (**242**) can be added to vinyltrimethylsilane (**230**) through radical initiation by $\text{Fe}(\text{CO})_5$ and HMPA to give the product **243** in low yield of 27% at 140 °C (scheme 49).^[133]

B Main Part



Scheme 49. $\text{Fe}(\text{CO})_5$ -catalyzed ATRA reaction of benzyl bromide (**242**) and vinyltrimethylsilane (**230**).^[133]

In 1977 Calas *et al.* discovered that CuCl is also suitable for the ATRA reaction of methanesulfonyl chloride (**205**) and benzenesulfonyl chloride (**187**) with vinyltrimethylsilane (**230**) at high temperatures. The α -chlorosilanes **244** and **245** could be received in good yield of 70% and 74% (scheme 50).^[134]



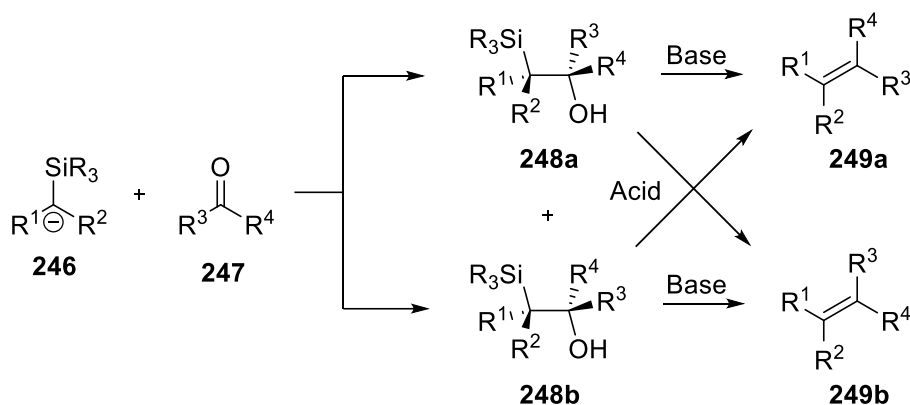
Scheme 50. CuCl catalyzed ATRA reaction of sulfonyl chlorides and vinyltrimethylsilane (**230**).^[134]

2.3 α -haloalkylsilanes in organic synthesis

The most common way α -haloalkylsilanes are used in organic synthesis is by their transformation into α -metalated silanes. These can then react with a variety of electrophiles. Probably the most important reaction using this methodology is the Peterson Olefination. In 1968 Peterson described for the first time that α -silyl carbanions can be reacted with ketones or aldehydes to access functionalized alkenes.^[135] Since then, the Peterson Olefination and related processes have become a strong tool for the synthesis of substituted alkenes.^[136,137]

The Peterson Olefination proceeds *via* the reaction of an α -silyl carbanion **246** with an aldehyde or ketone **247**. The carbanion is mostly generated from Grignard reagents or direct de-protonation.^[136] In the reaction, the β -hydroxysilyl intermediates **248a** and **248b** are formed. These can now be transformed either into the *cis*- or *trans*-alkenes **249a** or **249b** depending on whether the reaction is treated with acid or base (scheme 51).

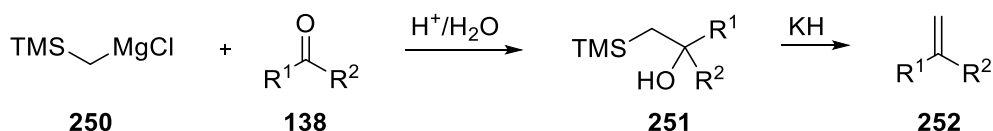
B Main Part



Scheme 51. General pathway of the Peterson olefination.^[137]

Therefore, it is possible to stereoselectively form both isomers in this reaction. When carbanion-stabilizing groups are present in **246**, the alkenes can be obtained directly. This stereoselectivity is one of the important features of the Peterson olefination making it a viable alternative for the Wittig reaction.^[138] Another advantage over the Wittig reaction is that the by-products of the Peterson olefination are mostly volatile disiloxanes which can be easily removed, in contrary to the triphenylphosphine oxide in the Wittig reaction.^[137]

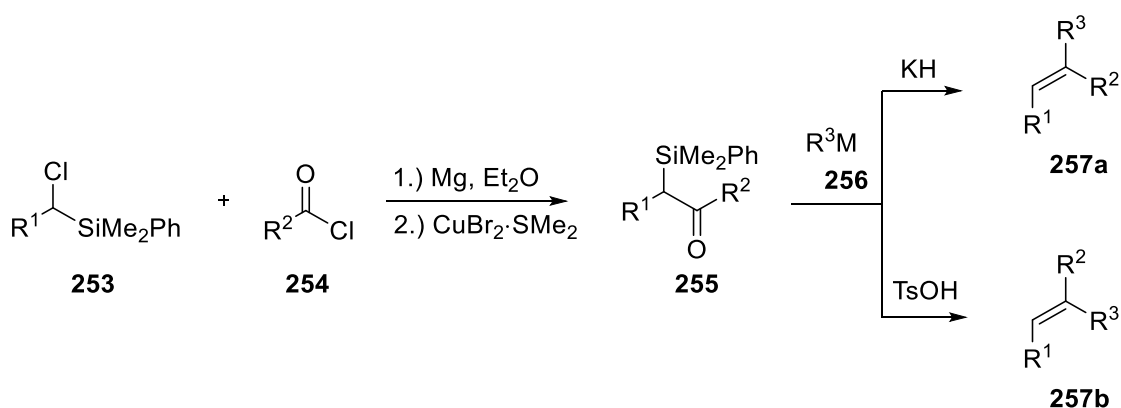
Probably the most important substrate in the Peterson olefination is the commercially available (trimethylsilyl)methylmagnesium chloride (**250**) which can be used to generate terminal alkenes **252** from aldehydes or ketones **138** after basic elimination of the β -hydroxyalkylsilane **251** (scheme 52).^[135]



Scheme 52. Peterson olefination of (trimethylsilyl)methylmagnesium chloride (**250**) with aldehydes and ketones **138**.^[135]

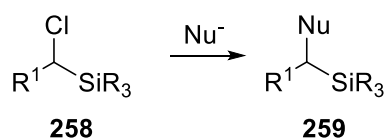
Grignard reagents derived from α -haloalkylsilanes **253** can also be reacted with acid chlorides **254**. The formed β -ketosilanes **255** are then again useful compounds for stereoselective Peterson alkenation reactions (scheme 53).^[139]

B Main Part



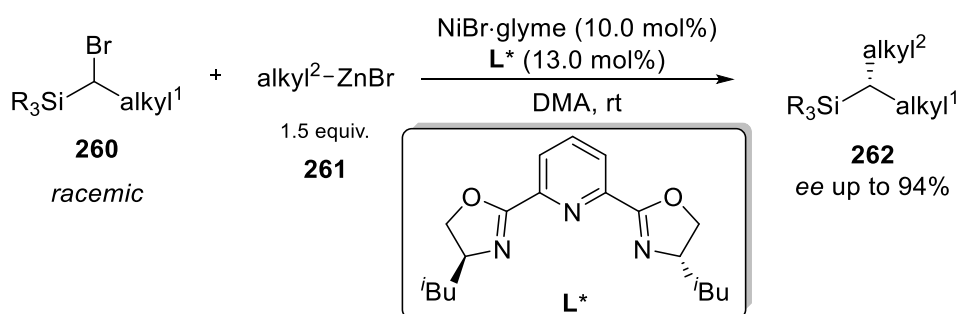
Scheme 53. Stereoselective Peterson alkenation of α -haloalkylsilanes **253**, acid chlorides **254** and organometallic compounds **256**.^[139]

Another important transformation of α -haloalkylsilanes **258** is the nucleophilic substitution of the halide (scheme 54). A wide variety of nucleophiles such as amines, azides, iodine, ammonia, phosphorus ylides or diethyl phosphonacetate are eligible.^[140]



Scheme 54. Nucleophilic halide substitution of α -haloalkylsilanes **258**.

More recently, Fu and co-workers described α -haloalkylsilanes **260** as a new class of electrophiles for the enantioconvergent substitution reaction of racemic alkyl electrophiles with carbon nucleophiles. They were able to perform enantioselective cross-coupling reactions between α -haloalkylsilanes **260** and alkylzinc reagents **261** using nickel and chiral pybox ligands L^* to provide chiral organosilanes **262** (scheme 55).^[141]

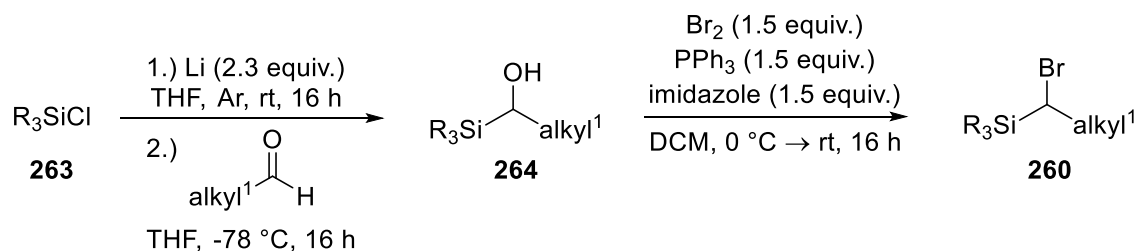


Scheme 55. Nickel-mediated enantioselective cross-coupling of α -haloalkylsilanes **260** and alkylzinc reagents **261**.^[141]

B Main Part

Chiral organosilanes are very interesting compounds in medicinal chemistry due to improved pharmacological properties such as lipophilicity or potency by replacement of carbon with silicon.^[142]

The α -halosilanes **260** were prepared by reaction of chlorosilanes **263** with elemental lithium and addition of aldehydes to form α -hydroxysilanes **264**, which were then treated with bromine in presence of PPh_3 and imidazole (scheme 56).^[141]



Scheme 56. Synthesis of α -halosilanes **260** via α -hydroxysilanes **264**.^[141]

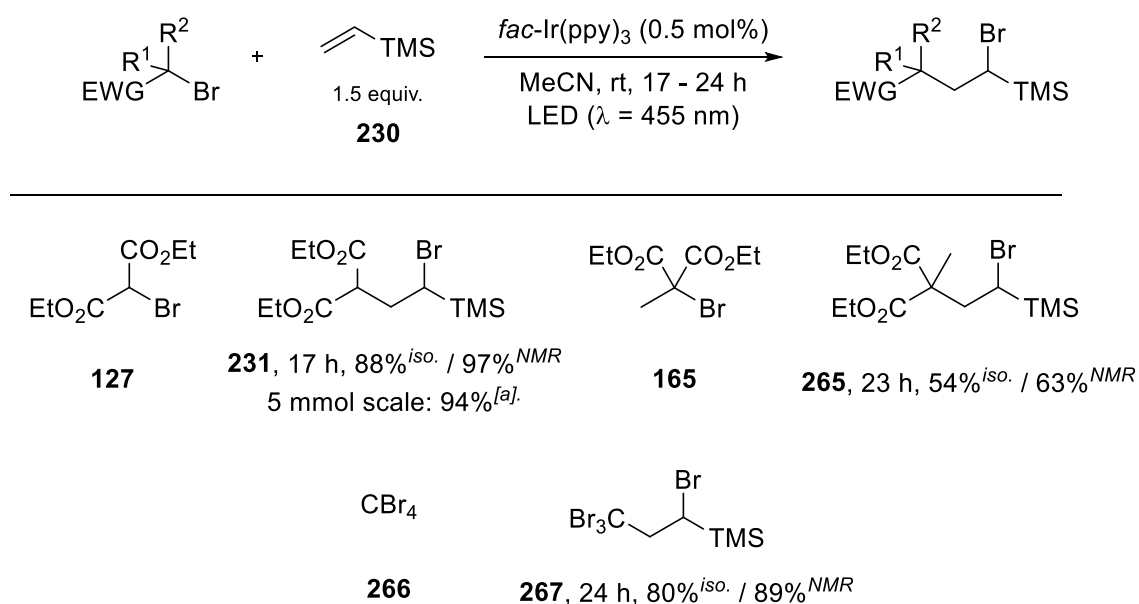
As stated above, α -haloalkylsilanes can be used for a variety of useful transformations. However, their application is limited by their complicated synthesis. The formation of α -haloalkylsilanes often involves highly reactive chemicals or very harsh reaction conditions. Therefore, mostly only simple molecules can be synthesized, and functional groups are often not tolerated.^[128]

B Main Part

2.4 Atom transfer radical additions with vinyltrimethylsilane

For those reasons, the establishment of the photoredox-catalyzed ATRA reaction of various electrophilic radicals with vinyltrimethylsilanes was studied, potentially leading to a new, synthetically useful method for the formation of α -haloalkylsilanes. Further investigation into the applications of these α -haloalkylsilanes was also conducted.

Investigation started for some more carbohalides bearing two or more electron-withdrawing groups (scheme 57).



Scheme 57. Visible light mediated ATRA reaction of α -halocarbons and vinyltrimethylsilane (**230**); [a] isolation *via* kugelrohr distillation.

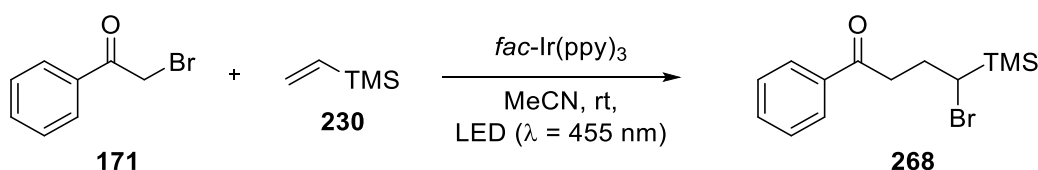
It was found that the isolated yields of these reactions were around 10% lower than the actual yield of the photoreaction as confirmed *via* NMR spectroscopy with 1,3,5-trimethoxybenzene as internal standard. It seems that during column chromatography, degradation of some product took place due to the fact that the compounds might still be somewhat unstable. Several attempts to change the chromatography conditions to different solvents and stationary phases such as aluminum oxide did not give better results. In case of the already discussed reaction of diethyl bromomalonate (**127**) with vinyltrimethylsilane (**230**), which initially gave 88% after irradiation with blue light for 17 h in presence of 0.5 mol% of *fac*-Ir(ppy)₃ (**49**), the yield determined *via* NMR standard was almost quantitative at 97%. This reaction could be performed at a 5 mmol scale and instead of purification by column chromatography, kugelrohr distillation was used to obtain the product in excellent yield of 94%, corresponding to about 1.6 g of pure product. The problem of product loss during purification therefore could be overcome by using distillation as purification method.

B Main Part

Changing the substrate to a compound with an additional methyl-group **165** at the radical center the yield dropped to 54% isolated yield and an observed NMR yield of 63%. This might be explained by the increased steric demand around the radical. Using tetrabromomethane (**266**) for the ATRA reaction gave good isolated yield of 80% with 89% determined by NMR prior to purification.

With this information at hand, it was switched to α -halo carbonyl compounds that only possess one electron-withdrawing group. As a model substrate, 2-bromoacetophenone (**171**) was chosen (table 4).

Table 4. Screening and optimization of the ATRA reaction between 2-bromoacetophenone (**171**) and vinyltrimethylsilane (**230**).



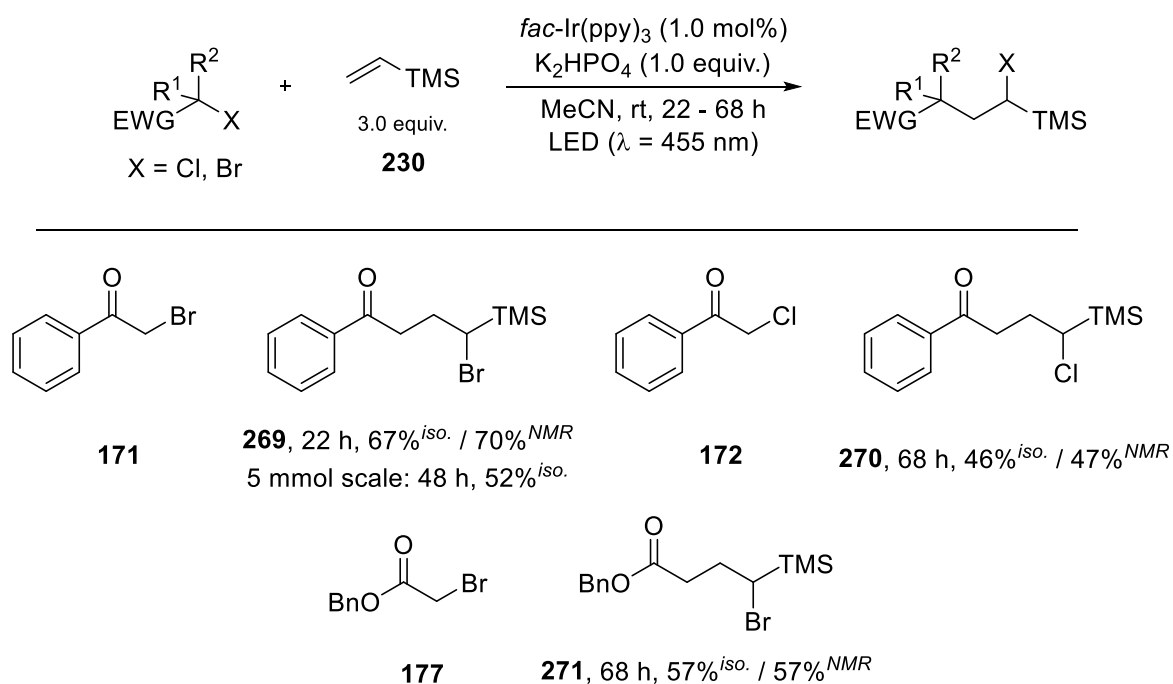
Entry	Catalyst-loading	Equivalents of 230	Additive	Time	Yield
1	0.5 mol%	1.5	-	48 h	Traces
2	1.0 mol%	1.5	-	48 h	8%
3	1.0 mol%	3.0	-	48 h	14% ^{NMR}
4	1.0 mol%	3.0	K ₂ HPO ₄ (1 equiv.)	22 h	67% / 70% ^{NMR}
5	1.0 mol%	1.5	K ₂ HPO ₄ (1 equiv.)	24 h	54% ^{NMR}
6	2.0 mol%	3.0	K ₂ HPO ₄ (1 equiv.)	22 h	69% ^{NMR}

However, under the conditions that were successful for diethyl bromomalonate (**127**), only traces of the product **268** were found (entry 1). Increasing the catalyst-loading to 1 mol% gave 8% isolated yield and the use of three equivalents of the vinylsilane **230** only 14% of the product according to NMR analysis. As it has previously been shown that the addition of inorganic bases helps to optimize similar reactions, one equivalent of K₂HPO₄ was added. This raised the yield to 67% while also reducing the reaction time to 22 h (entry 4). Interestingly, the yield determined by NMR analysis only differed slightly from the isolated yield. The excess of the vinylsilane **230** is still needed to get that amount of product (entry 5). An additional increase in catalyst-loading does not improve the reaction (entry 6). Unfortunately, the product **268** also contained some traces of its dehalogenated form which could not be removed by column chromatography.

B Main Part

Again, up-scaling was performed on this reaction on a 5 mmol scale. The reaction was performed twice and purified both by kugelrohr distillation and once by column chromatography. In both cases the product was obtained in 52% yield and both times impurities of the dehalogenated compound remained present.

A change to 2-chloroacetophenone (**172**) gave moderate yields of 46% and reaction times of 68 h were necessary to obtain the α -chlorosilane **270**. In case of benzyl 2-bromoacetate (**177**), moderate yield of 57% were obtained after 68 h. Interestingly, in all these cases no substantial difference between purified yields and determination *via* internal NMR standard were seen (scheme 58). This is in contrast to what was observed in the reaction of carbohalides bearing two or more electron-withdrawing groups (scheme 57), where degradation of products was observed during purification. It is possible that the higher electron-withdrawing character destabilizes these compounds.

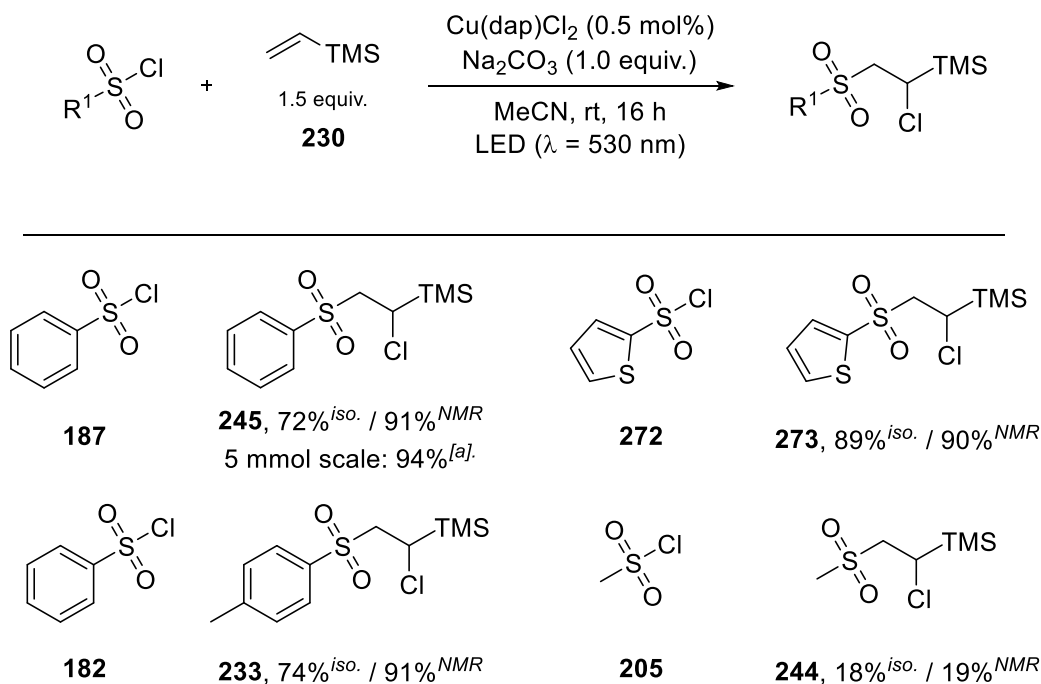


Scheme 58. Visible light mediated ATRA reaction of α -halo carbonyls and vinyltrimethylsilane (**230**).

Next, the approach towards sulfonyl chlorides that was established for the photocatalyzed allylation (see chapter 1.3) was tested for the ATRA reaction with vinyltrimethylsilane (**230**) as trapping reagent (scheme 59). Pleasingly, the reaction was successful from the get-go with a low catalyst-loading of 0.5 mol% of Cu(dap)Cl₂ (**102**) and addition of Na₂CO₃. In case of benzenesulfonyl chloride (**187**) and tosyl chloride (**182**) good yields of 72% and 74% were obtained and NMR studies showed that prior to purification even 91% of product were present. So again, there was a problem with degradation during column chromatography, but it was possible to overcome this by up-scaling the reaction of

B Main Part

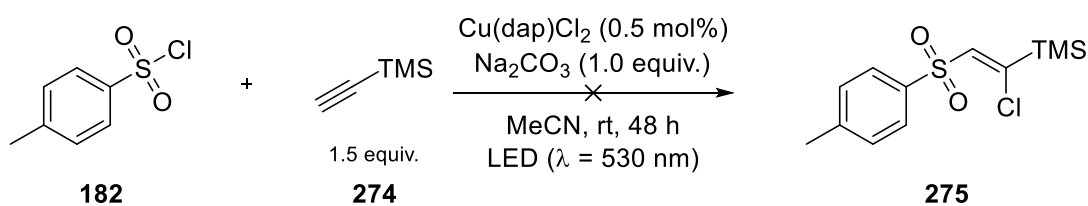
benzenesulfonyl chloride (**187**). On a 5 mmol scale the product **245** was purified by kugelrohr distillation and a yield of 94% was obtained, accounting for 1.3 g of pure product.



Scheme 59. Visible light mediated ATRA reaction of sulfonyl chlorides and vinyltrimethylsilane (**230**); [a] isolation *via* kugelrohr distillation.

Applying this method for the heterocyclic sulfonyl chloride **272** gave good yield of 89% and interestingly, the yield determined by NMR analysis did not show any discrepancy which implies a higher stability of the compound **273**. Same can be said about the reaction of methanesulfonyl chloride (**205**) where the isolated and NMR yield are also similar. However, the reaction only gave poor yield of 18%.

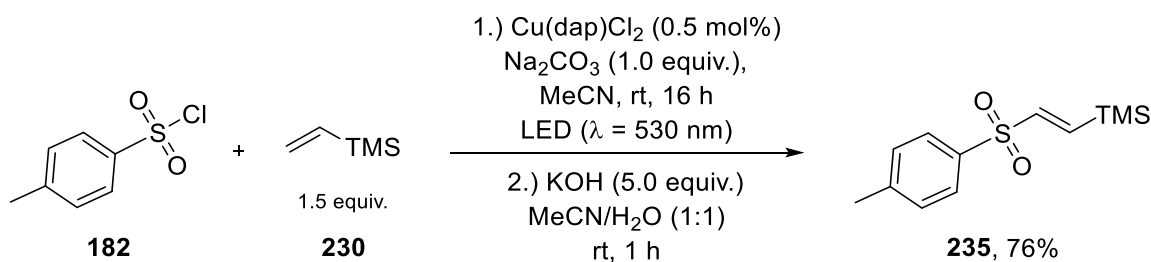
The next step was to try if this method is also suitable for the ATRA reaction of sulfonyl chlorides with ethynyltrimethylsilane (**274**). By this addition, the production of α -chloro-silylalkenes would be feasible which could be interesting compounds for cross-coupling reactions. The reaction of tosyl chloride (**182**) with ethynyltrimethylsilane (**274**) under the established Cu(dap)Cl₂-catalyzed conditions however did not give any reaction and no product **275** was found (scheme 60).



Scheme 60. Failed visible light mediated ATRA reaction of tosyl chloride (**182**) and ethynyltrimethylsilane (**274**).

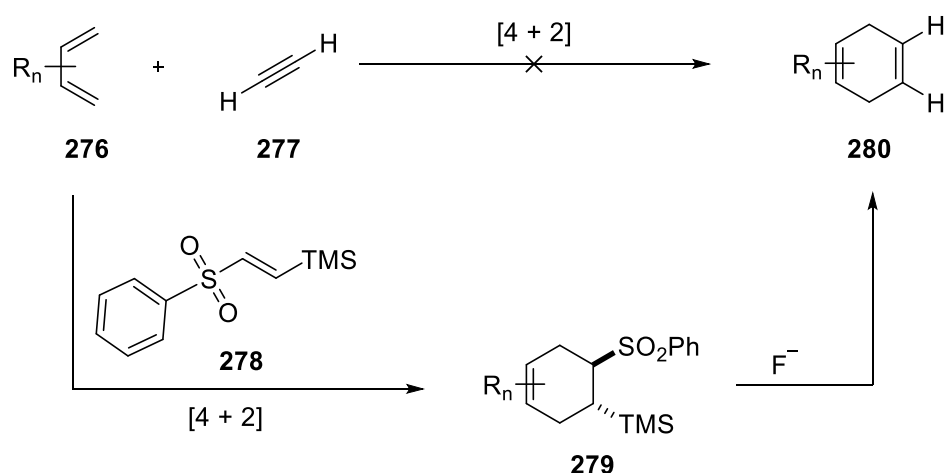
2.5 Applications of photoredox-catalytically formed α -haloalkylsilanes2.5.1 (*E*)-trimethyl(2-tosylvinyl)silane as synthon for acetylene in cycloaddition reactions

In the initial studies on this ATRA reaction it was found that if the product **233** is treated with KOH after the photoreaction, elimination of HCl takes place to form (*E*)-trimethyl(2-tosylvinyl)silane (**235**) (scheme 61).



Scheme 61. Visible light mediated ATRA reaction of tosyl chloride (**182**) and vinyltrimethylsilane (**230**) followed by elimination to the vinylsilane **235**.

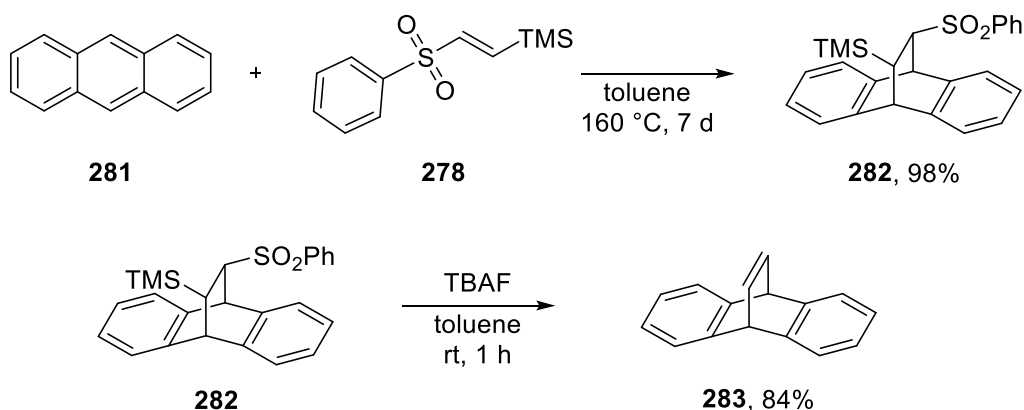
Similar compounds, and especially (*E*)-trimethyl(2-(phenylsulfonyl)vinyl)silane (**278**), are known in literature as potent synthons for acetylene (**277**) in cycloaddition reactions.^[143] Acetylene (**277**) is not suitable for most [4 + 2] cycloadditions due to its low dienophilic character and high explosive nature under high pressure. (*E*)-trimethyl(2-(phenylsulfonyl)vinyl)silane (**278**) is an elegant alternative for this since it combines the reactivities of vinylsilanes^[144] and vinylsulfones^[145] and is therefore well suited for [4 + 2] cycloadditions. Another advantage is that the double-bond can be reintroduced very easily by β -elimination of the adducts **279** with fluoride-anion sources under mild conditions. That way, formal cycloaddition products **280** of acetylene can be obtained. (scheme 62).^[146]



Scheme 62. (*E*)-trimethyl(2-(phenylsulfonyl)vinyl)silane (**278**) as synthon for the [4 + 2] cycloaddition of acetylene.

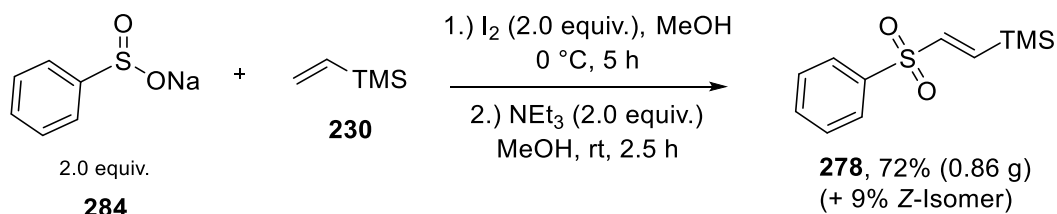
B Main Part

This method has been used in literature for example in the formal 9,10-addition of acetylene (**277**) to anthracene (**281**). (*E*)-trimethyl(2-(phenylsulfonyl)vinyl)silane (**278**) reacts with anthracene (**281**) to give the adduct **282** in excellent yield. This adduct **282** is then easily transformed into the formal acetylene addition product **283** by elimination with tetra-*n*-butylammonium fluoride (TBAF) (scheme 63).^[147]



Scheme 63. Cycloaddition of (*E*)-trimethyl(2-(phenylsulfonyl)vinyl)silane (**278**) with anthracene (**281**) followed by elimination with TBAF.^[147]

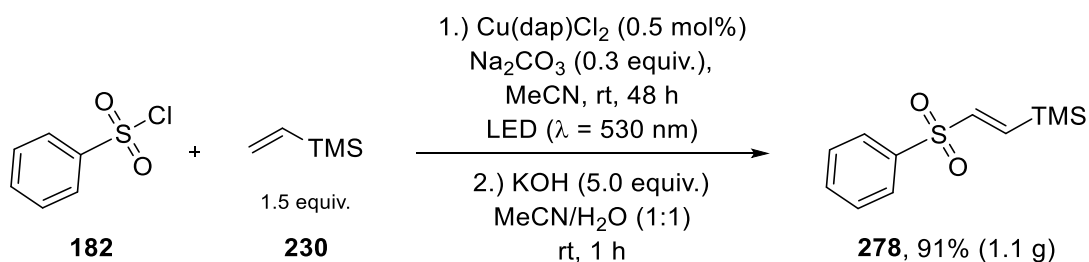
The best-known method to synthesize this compound **278** was published by Grigg *et al.* The synthesis starts with sodium benzenesulfinate (**284**), trimethylvinylsilane (**230**) and two equivalents of iodine at 0 °C followed by elimination with NEt₃ to yield 72% of the *E*-Isomer which can be separated from the also formed *Z*-Isomer by column chromatography (scheme 64).^[143]



Scheme 64. Synthesis of (*E*)-trimethyl(2-(phenylsulfonyl)vinyl)silane (**278**) by Grigg *et al.*^[143]

Using the new photoredox-catalyzed method, the reaction of benzenesulfonyl chloride (**187**) and trimethylvinylsilane (**230**) could be scaled up in presence of 0.5 mol% of Cu(dap)Cl₂ (**102**) and 0.3 equiv. of Na₂CO₃ to a 5 mmol scale (scheme 65).

B Main Part



Scheme 65. One-pot synthesis of (*E*)-trimethyl(2-(phenylsulfonyl)vinyl)silane (**278**) via photoredox-catalyzed ATRA reaction followed by elimination.

Irradiation with three green LEDs for 48 h (figure 4) followed by addition of an aqueous solution of KOH and one additional hour of stirring produced the desired compound **278** in very good yield of 91% in a one-pot synthesis. This strategy brings advantages because it is a catalyzed reaction at room temperature that does not require an excess of iodine and also gives better yield and diastereoselectivity compared to the method reported by Grigg *et al.*^[143]

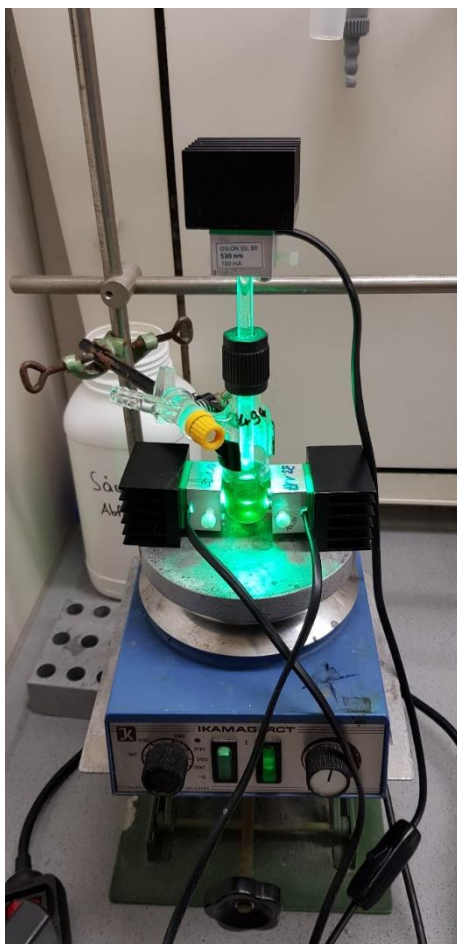
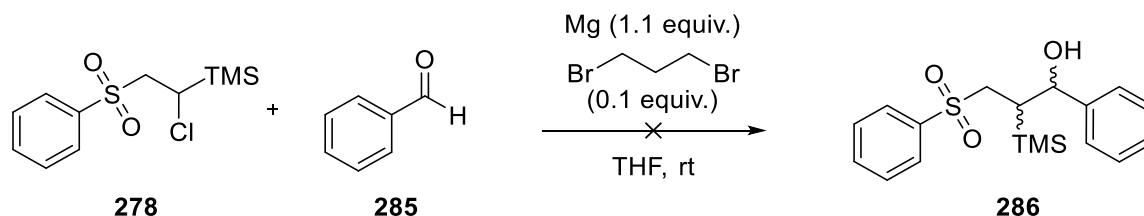


Figure 4. Big-scale set-up for the one-pot synthesis of (*E*)-trimethyl(2-(phenylsulfonyl)vinyl)silane (**278**).

B Main Part

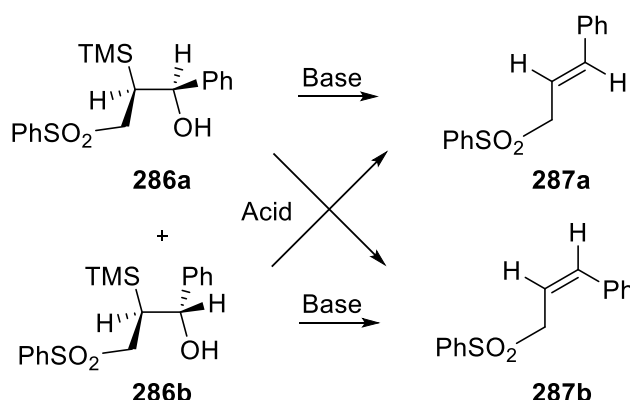
2.5.2 Peterson Olefination

Next up, it was examined if you could apply these α -haloalkylsilanes to Peterson olefination type chemistry. Therefore, the formation of the Grignard of the ATRA product **278** was tested by addition of magnesium followed by reaction with benzaldehyde (**285**) to get the mixture of two diastereomers of the α -hydroxysilane **286** (scheme 66).



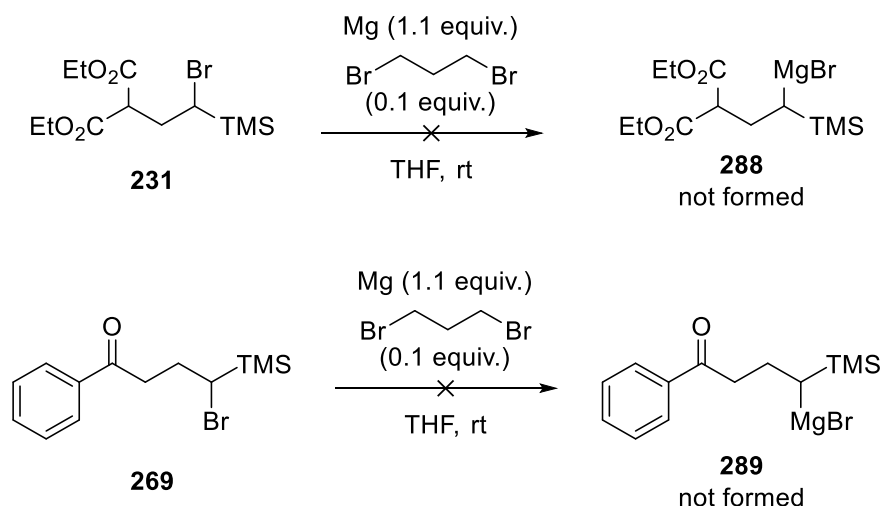
Scheme 66. Attempted Grignard formation of **278** and addition of benzaldehyde (**285**).

These isomers **286a** and **286b** then should be able to either be transferred into the *E*- or *Z*-Alkene **287a** and **287b** by addition of base or acid (scheme 67).



Scheme 67. Potential transformation of diastereomers **286a** and **286b** into *E*- and *Z*-Alkenes **287a** and **287b**.

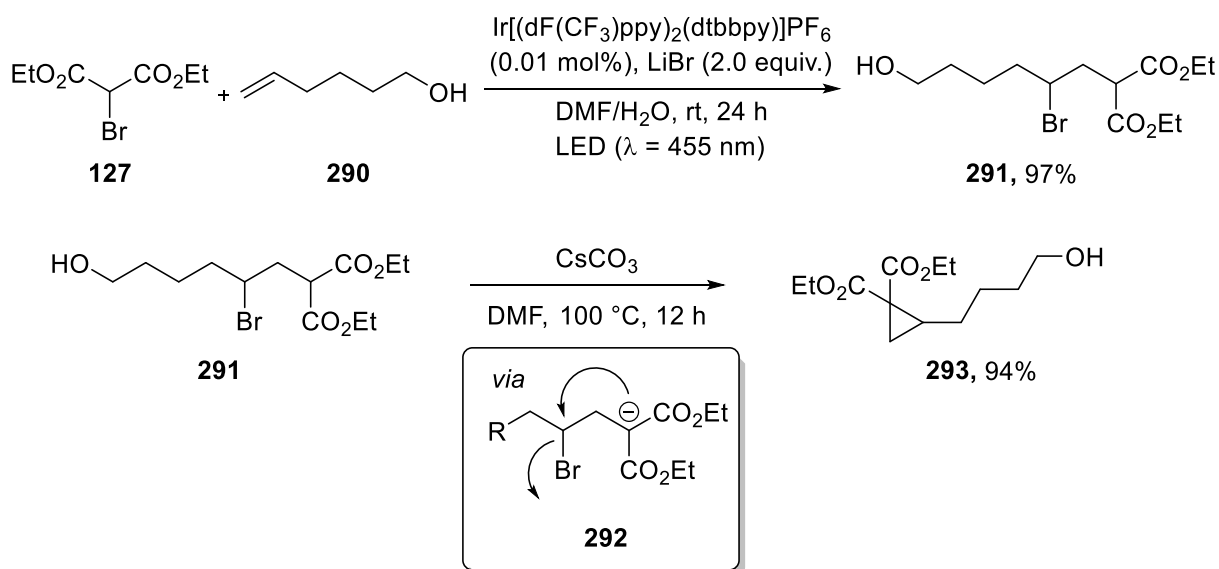
Addition of Mg in dry THF however did not lead to the formation of the Grignard. Activating the magnesium flakes in an ultrasonic bath and addition of 10 mol% of 1,3-dibromopropane did not give the desired reaction. Even heating the mixture at reflux conditions for several hours brought no consumption of the magnesium and the addition of Benzaldehyde (**285**) did not lead to any reaction. It was also tried to form the Grignard for the bromo compounds **231** and **269** (scheme 68). For those reagents it would also be possible to assume that intramolecular cyclization to form cyclobutanes could occur. However, again no formation of Grignard reagents **288** and **289** were observed when α -haloalkylsilanes **231** and **269** were treated with activated Mg in dry THF. No consumption of Mg took place and addition of benzaldehyde (**285**) did not result in any formation of new compounds (scheme 68).



Scheme 68. Unsuccessful formation of Grignard reagents **288** and **289**.

2.5.3 Formation of silyl-substituted cyclopropanes and steps towards their ring-opening

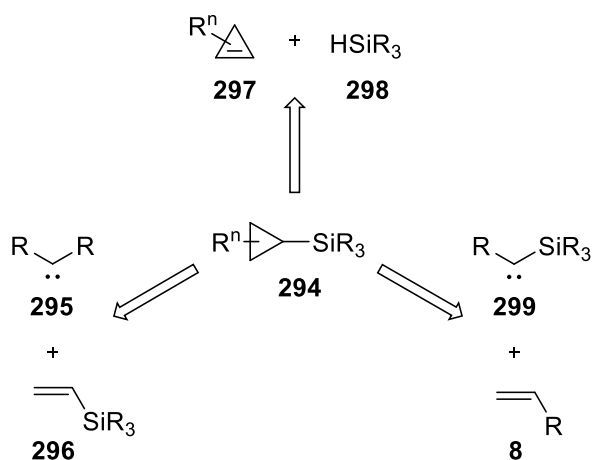
In 2012, Stephenson *et al.* published the photoredox-catalyzed ATRA reaction of various carbohalides to olefins. In this work they could also show that it is possible to transform the ATRA product **291** that is derived from diethyl bromomalonate (**127**) and hex-5-en-1-ol (**290**) into the cyclopropane **293**. This is possible since the malonate moiety has an acidic proton in α -position that can be deprotonated easily, and the carbanion **292** then undergoes intramolecular cyclization to form the cyclopropane **293** (scheme 69).^[73]



Scheme 69. ATRA reaction of diethyl bromomalonate (**127**) and hex-5-en-1-ol (**290**) followed by intramolecular cyclization.^[73]

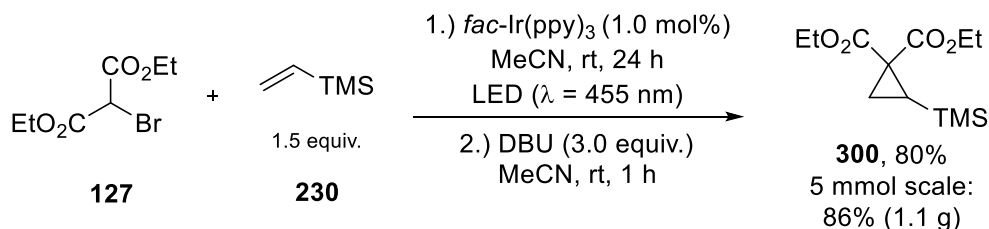
B Main Part

The vision was to transfer the ATRA products that possess an acidic proton in α -position into silylcyclopropanes in a similar approach. That way it could be possible to establish a new easy synthetic route to access this interesting compound class. Silylcyclopropanes **294** have gained interest in organic chemistry since the late 1970s^[148] and have since been used in a variety of useful synthetic transformations.^[149] The synthesis of silylcyclopropanes **294** usually involves the insertion of silyl-carbenes **299**, originating from compounds such as (trimethylsilyl)diazomethane (TMSCHN₂)^[150] or more complex diazo compounds,^[151] into olefins **8**. Other methods involve cyclopropanation of vinylsilanes **296**^[152] and more recently, the hydrosilylation of cyclopropenes **297** has also gathered some attention (scheme 70).^[153]



Scheme 70. Different synthetic pathways towards silylcyclopropanes **294**.

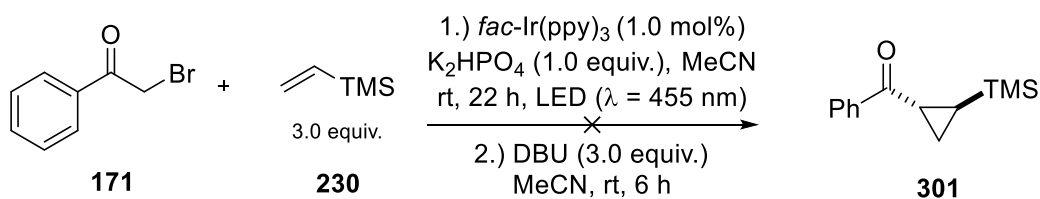
The investigation started with the ATRA reaction of diethyl bromomalonate (**127**) and vinyltrimethylsilane (**230**) and whether the resulting product could be transformed into the cyclopropane **300**. In this case, DBU was shown to be the suitable base for this transformation. The cyclopropane **300** could be synthesized in 80% yield *via* photoreaction followed by addition of DBU in a one-pot synthesis. Up-scaling was also successful and an even higher yield of 86% was achieved on a 5 mmol scale giving 1.1 g of the pure product **300** (scheme 71).



Scheme 71. One-pot synthesis of the cyclopropane **300** by photoredox-catalyzed ATRA reaction followed by base-induced cyclization.

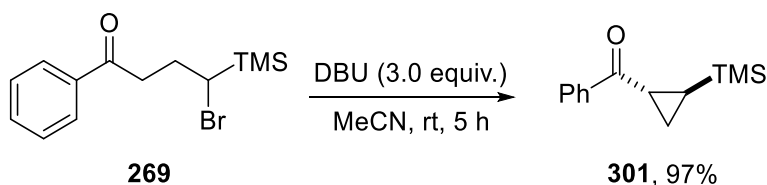
B Main Part

When trying to apply this one-pot synthesis with 2-bromoacetophenone (**171**), only formation of a complex reaction mixture was observed from which no cyclopropane **301** could be isolated (scheme 72).



Scheme 72. Unsuccessful one-pot synthesis of the cyclopropane **301**.

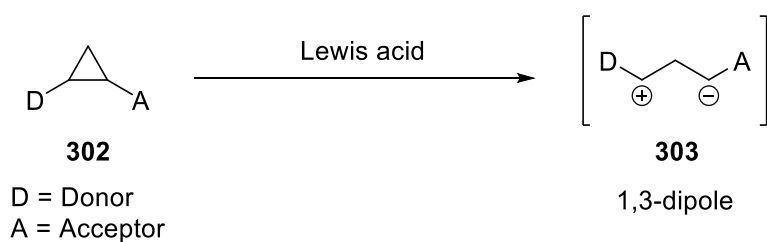
However, when the purified ATRA product **269** was treated with DBU, a clean reaction to form the cyclopropane **301** in 97% yield was observed. The reaction is diastereoselective and only the *trans*-isomer **301** was formed (scheme 73).



Scheme 73. Base-induced cyclization of **269** into the cyclopropane **301**.

This demonstrates that it is possible to form silylcyclopropanes starting from carbohalides that have an acidic proton on the same carbon atom as the halide.

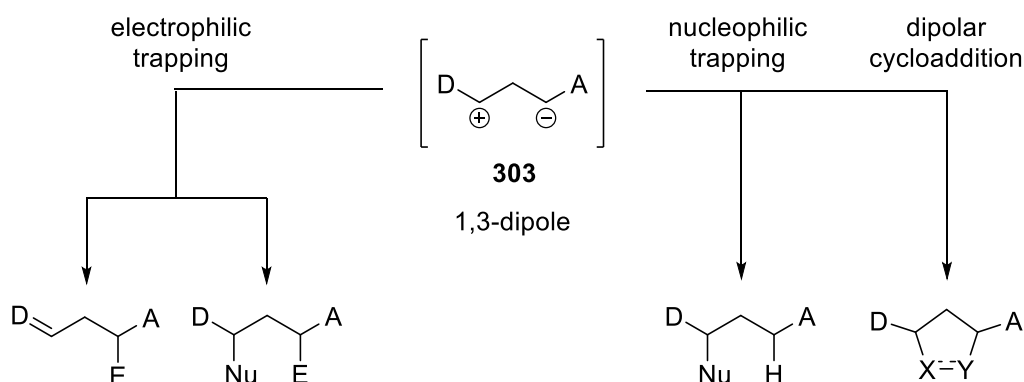
It was now time to study if these cyclopropanes can be used for further transformations. For a long time, chemists have used the ring-strain of cyclopropanes as an activation mode for organic transformations. Especially if cyclopropanes **302** contain functional groups that are electron-donating (D = Donor) and groups that are electron-withdrawing (A = Acceptor), the ring-opening leads to 1,3-dipole intermediates **303** which are stabilized. These cyclopropanes are called donor-acceptor cyclopropanes (DA-cyclopropanes) (scheme 74).^[154]



Scheme 74. Lewis acid induced ring-opening of DA-cyclopropane **303**.^[154]

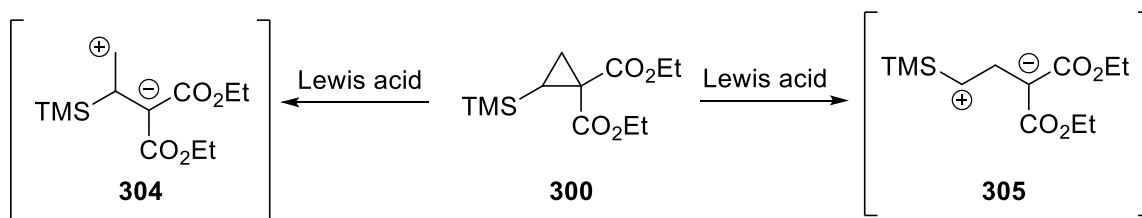
B Main Part

In recent years, these DA-cyclopropanes have been used in a plethora of transformations. The most common ones include the trapping of the 1,3-dipole with electrophiles, nucleophiles or in dipolar cycloadditions (scheme 75).^[154,155]



Scheme 75. Different reaction pathways for the opening of donor-acceptor cyclopropanes **303**.^[154]

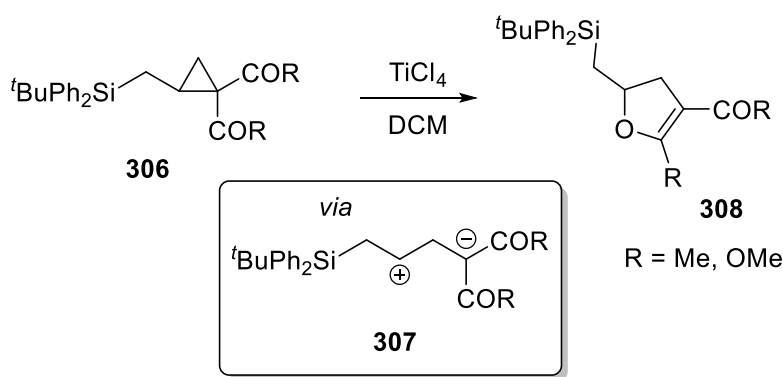
It was of interest to see if the cyclopropane **300**, synthesized through this new one-pot approach could also be used in similar fashion as DA-cyclopropane. With two ethyl esters, the cyclopropane **300** has the typical acceptor substituents already present. However, a silane cannot be described as a typical donor. But it could be possible that regular ring-opening occurs to form the 1,3-dipole intermediate **305**, nevertheless. On the other hand, it could also be assumed that the β -effect of the silicon atom could lead to ring-opening by cleavage of the other C-C bond to form the 1,3-dipole **304**. (scheme 76). The carbocation in this case would be primary but also stabilized by the β -effect.



Scheme 76. Different possible ring-opening pathways for cyclopropane **300**.

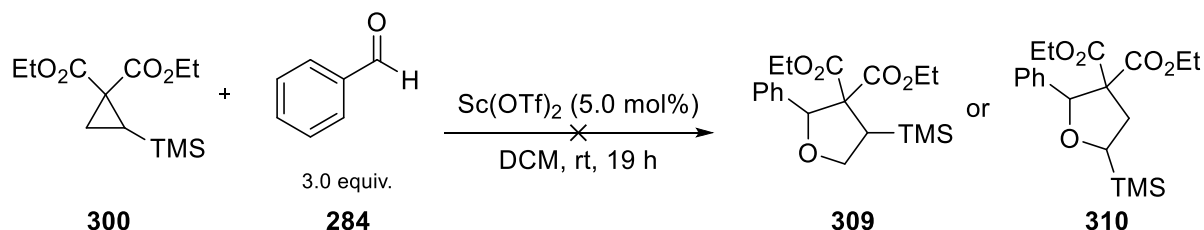
The β -effect of silicon has been used in various ring-opening transformations of silylmethyl-substituted cyclopropanes.^[156] For example the opening and rearrangement of cyclopropane **306** into dihydrofuran **308**. The secondary carbocation in the intermediate **307** is stabilized by the β -effect and thereby ring-opening favored (scheme 77).^[157]

B Main Part



Scheme 77. Lewis acid induced ring-opening and rearrangement of silylmethyl-substituted cyclopropane **306**.^[157]

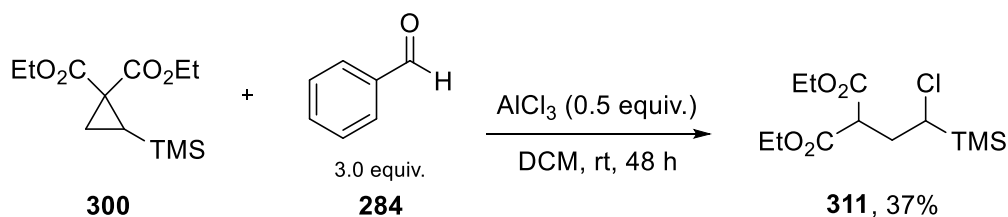
Investigation into the ring-opening of silylcyclopropanes was started with cyclopropane **300** as the model substrate. Opening the ring with $\text{Sc}(\text{OTf})_2$ as Lewis acid and trapping the resulting 1,3-dipole with benzaldehyde (**284**) would give a substituted tetrahydrofuran. Again, it could be assumed that two possible 1,3-dipole intermediates can be formed. If the β -effect of the silane is sufficient to stabilize the carbocation in intermediate **304** it should give the tetrahydrofuran **309** as product. In case of the intermediate **305**, the tetrahydrofuran **310** would be formed. Stirring the mixture in DCM with 5 mol% of $\text{Sc}(\text{OTf})_2$ as catalyst however did not lead to any product formation. No conversion of the cyclopropane **300** was observed (scheme 78).



Scheme 78. Unsuccessful Lewis acid-induced ring-opening of **300** and trapping with benzaldehyde (**284**).

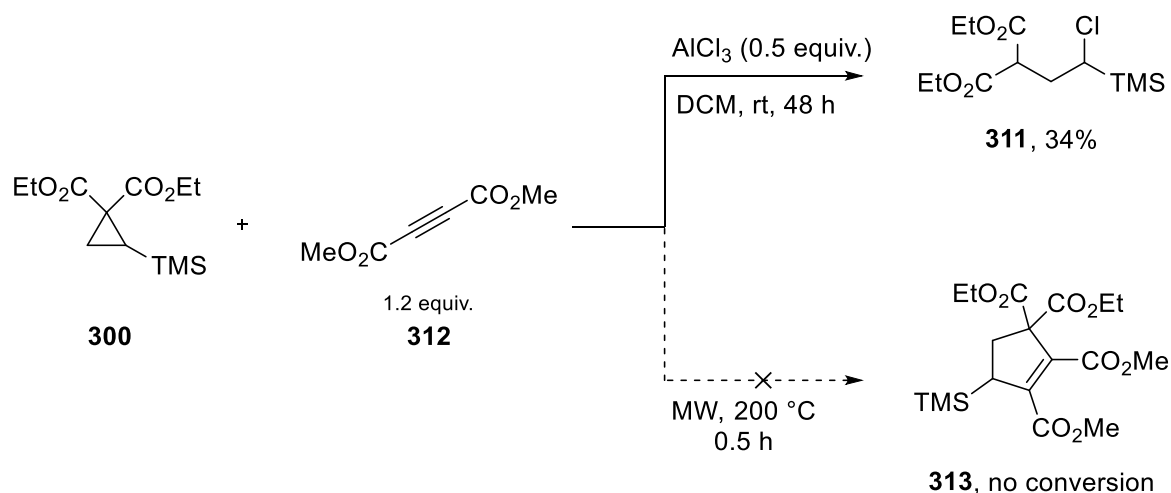
The next step was to try to open the ring with AlCl_3 as the Lewis acid at higher loading of 0.5 equiv. In this case, conversion of the cyclopropane **300** was observed but no reaction with benzaldehyde (**284**) occurred and formation of tetrahydrofuran derivatives was not seen. Instead, the ring-opened chlorine compound **311** was isolated in 37% yield (scheme 79). This indicates that the 1,3-dipole intermediate **305** is being formed and consecutively trapped with chloride from AlCl_3 . Accordingly, this suggests the β -effect of silicon is not strong enough to stabilize the primary carbocation and therefore form the 1,3-dipole **304**. It is not clear why the 1,3-dipole **305** does not undergo a reaction with benzaldehyde (**284**). Presumably, due to the unstable and short-lived nature of this intermediate **305**, reaction with the already bound AlCl_3 is preferred.

B Main Part



Scheme 79. Ring-opening of cyclopropane **300** with AlCl_3 .

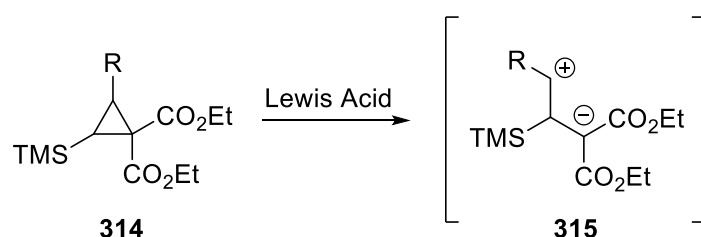
Apart from aldehydes, trapping of the 1,3-dipole intermediate **305** with dimethyl acetylenedicarboxylate (**312**) in a dipolar cycloaddition was also tested. This would give access to the highly substituted cyclopentene **313**. First, the reaction under microwave conditions at 200 °C for 30 min without any solvent was performed but no reaction was observed. Next, stirring in DCM with 0.5 equiv. of AlCl_3 gave the same result as before. No formation of the product **313** took place but instead, the ring-opened chlorine derivative **311** was isolated in 34% yield. Again, the intermediate 1,3-dipole **305** did not undergo reaction with the dienophile **312** and was instead rapidly trapped by Cl^- (scheme 80).



Scheme 80. Reaction of cyclopropane **300** with dimethyl acetylenedicarboxylate (**312**).

2.6 Conclusion and outlook

In summary, it was shown that, instead of a photochemical vinylation, vinyltrimethylsilane (**230**) undergoes atom transfer radical addition reactions with various radical precursors. With this, a new easy and convenient synthetic route for the formation of α -haloalkylsilanes was established. For sulfonyl chlorides the copper-complex Cu(dap)Cl₂ (**102**) was the photocatalyst of choice, whereas for carbohalides, *fac*-Ir(ppy)₃ (**49**) gave the best yields. It was also shown that some of these α -haloalkylsilanes can be easily transformed into silylcyclopropanes. It was not possible to utilize these silylcyclopropanes for transformations similar to those of donor-acceptor cyclopropanes yet. Further investigation into better reaction conditions need to be conducted. The introduction of additional substituents to the cyclopropane ring **314** could help to deliver better results by better stabilization of intermediates **315** making use of the β -effect of silanes (scheme 81).



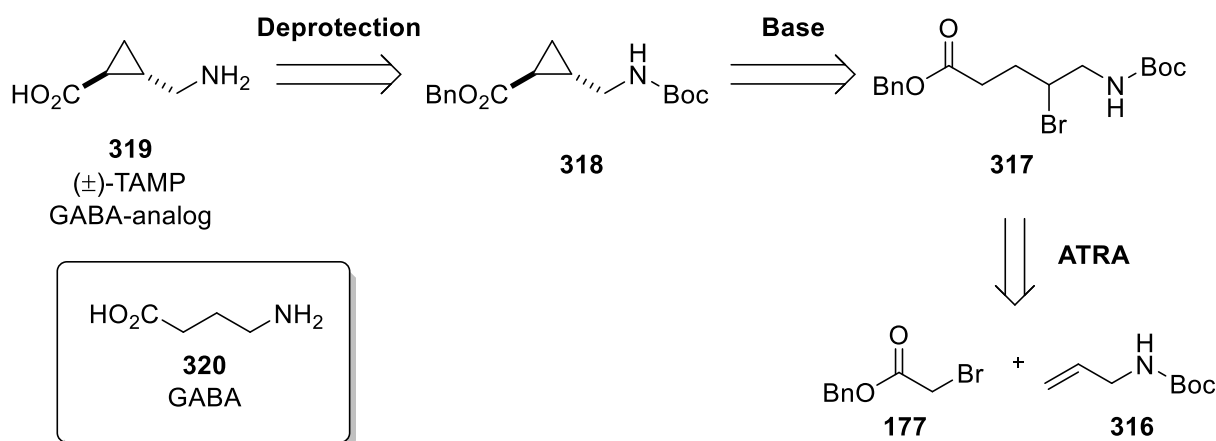
Scheme 81. Substituted cyclopropanes **314** could lead to more stable 1,3-dipole intermediates **315**.

In addition, it was shown that with this synthetic route, (*E*)-trimethyl(2-(phenylsulfonyl)vinyl)silane (**278**), a compound that can be used as a synthon for acetylene in various reactions, could be synthesized on a gram-scale in excellent yields.

3. Synthesis of cyclic γ -amino acids *via* visible light mediated ATRA reactions and cyclizations

3.1 Cyclic GABA-analogs

Inspired by the successful 1,3-cyclization of ATRA products to form silylcyclopropanes (see chapter 2.5.3), it was tested whether this strategy can also be applied towards the synthesis of other useful cyclopropanes. An easy retrosynthetic route towards the γ -amino acid and GABA-analog (\pm)-TAMP (**319**) was envisioned this way (scheme 82). The synthesis would start from benzyl 2-bromoacetate (**177**) and *tert*-butyl allylcarbamate (**316**), both of which have previously been used in ATRA reactions but never in combination. The resulting ATRA product **317** would then be diastereoselectively cyclized to form the cyclopropane **318**. Deprotection of the Boc-group and benzyl ester should be straight forward.^[158] By variation of α -halo esters and substituted allyl carbamates it could be possible to synthesize derivatives of these interesting cyclic γ -amino acids.

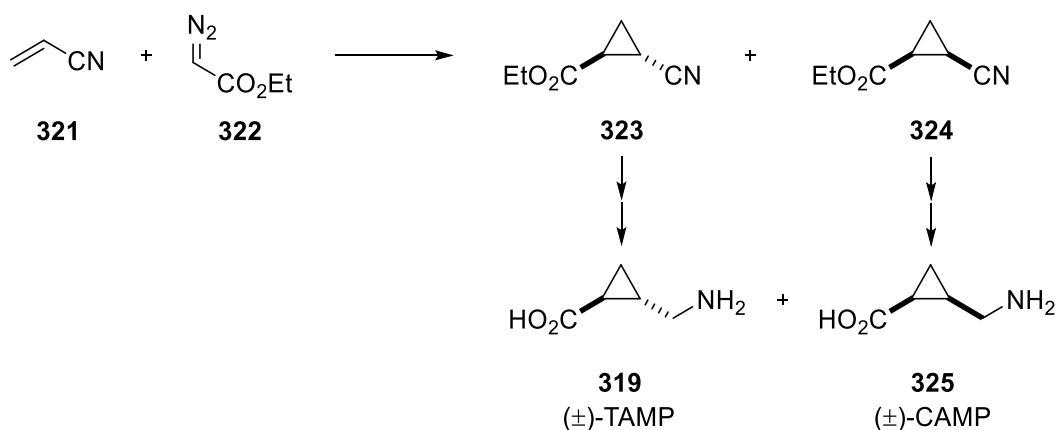


Scheme 82. Proposed retrosynthesis of the GABA-analog (\pm)-TAMP (**319**).

Aminobutyric acid (GABA) (**320**) is the most important inhibitory neurotransmitter in the central nervous systems of vertebrates. The two major classes of GABA receptors which are bound by GABA (**320**) are GABA_A and GABA_B receptors. GABA_A receptors are neurotransmitter gated ion channels that release Cl⁻ ions. GABA_B receptors belong to the family of G-protein coupled receptors and are connected to the release of K⁺ ions.^[159]

B Main Part

In 1972, the GABA-analog (\pm)-TAMP (**319**) was synthesized for the first time by Ivanskii and Maksimov *via* cyclopropanation of acrylonitrile (**321**) with ethyl 2-diazoacetate (**322**). The resulting *trans*- and *cis*-cyanoesters **323** and **324** were separated and then hydrogenated with Raney nickel followed by saponification of the ester to achieve (\pm)-TAMP (**319**) and the *cis*-isomer (\pm)-CAMP (**325**) (scheme 83).^[160]



Scheme 83. First synthesis of the GABA-analog (\pm)-TAMP (**319**).^[160]

Paulini and Reißig published an improved synthesis involving the cyclopropanation of *N*-silylated allylamines which also gives a mixture of both diastereomers.^[161] (\pm)-TAMP (**319**), (\pm)-CAMP (**325**) and other strained GABA-analogs have been developed to better understand and study GABA receptors and their potency to bind to those receptors have been well studied.^[162] It has been shown that (\pm)-TAMP (**319**) has much higher potency towards many GABA_A-rho receptors (a subclass of GABA_A receptors formerly classified as GABA_C receptors).^[163] Enantioselective synthesis of (+)-TAMP and (-)-TAMP have also been achieved, as well as chiral resolution of racemic (\pm)-TAMP (**319**)^[164] and their pharmacology at the GABA_A-rho receptor has been studied.^[165]

B Main Part

3.2 Visible light mediated ATRA reactions of *tert*-butyl allylcarbamate

Investigation started with the reaction of benzyl 2-bromoacetate (**177**) as radical precursor and *tert*-butyl allylcarbamate (**316**) as trapping reagent (table 5).

Table 5. Optimization of the ATRA reaction of benzyl 2-bromoacetate (**177**) and *tert*-butyl allylcarbamate (**316**).

Reaction scheme: Benzyl 2-bromoacetate (**177**, 2.0 equiv.) + *tert*-butyl allylcarbamate (**316**) $\xrightarrow[\text{solvent, rt}]{[\text{PC}]}$ Product (**317**).

Entry	Catalyst	Light	Additive	Solvent	Time	Yield
1	Cu(dap)Cl ₂ (1 mol%)	530 nm	-	MeCN	48 h	no conversion
2	Cu(dap)Cl ₂ (1 mol%)	530 nm	LiBr (2 equiv.)	MeCN	48 h	no conversion
3	<i>fac</i> -Ir(ppy) ₃ (1 mol%)	455 nm	-	MeCN	48 h	55%
4	<i>fac</i> -Ir(ppy) ₃ (1 mol%)	455 nm	K ₂ HPO ₄ (1 equiv.)	MeCN	18 h	73%
5	<i>fac</i> -Ir(ppy) ₃ (1 mol%)	455 nm	K ₂ HPO ₄ (1 equiv.)	DCM	16 h	72%
6	<i>fac</i>-Ir(ppy)₃ (1 mol%)	455 nm	K₂HPO₄ (1 equiv.)	DMF/H₂O (1:1)	16 h	80%
7	-	455 nm	K ₂ HPO ₄ (1 equiv.)	DMF/H ₂ O (1:1)	24 h	no conversion
8	<i>fac</i> -Ir(ppy) ₃ (1 mol%)	-	K ₂ HPO ₄ (1 equiv.)	DMF/H ₂ O (1:1)	24 h	no conversion
9 ^[a]	<i>fac</i> -Ir(ppy) ₃ (0.5 mol%)	455 nm	K ₂ HPO ₄ (0.5 equiv.)	DMF/H ₂ O (1:1)	24 h	56%

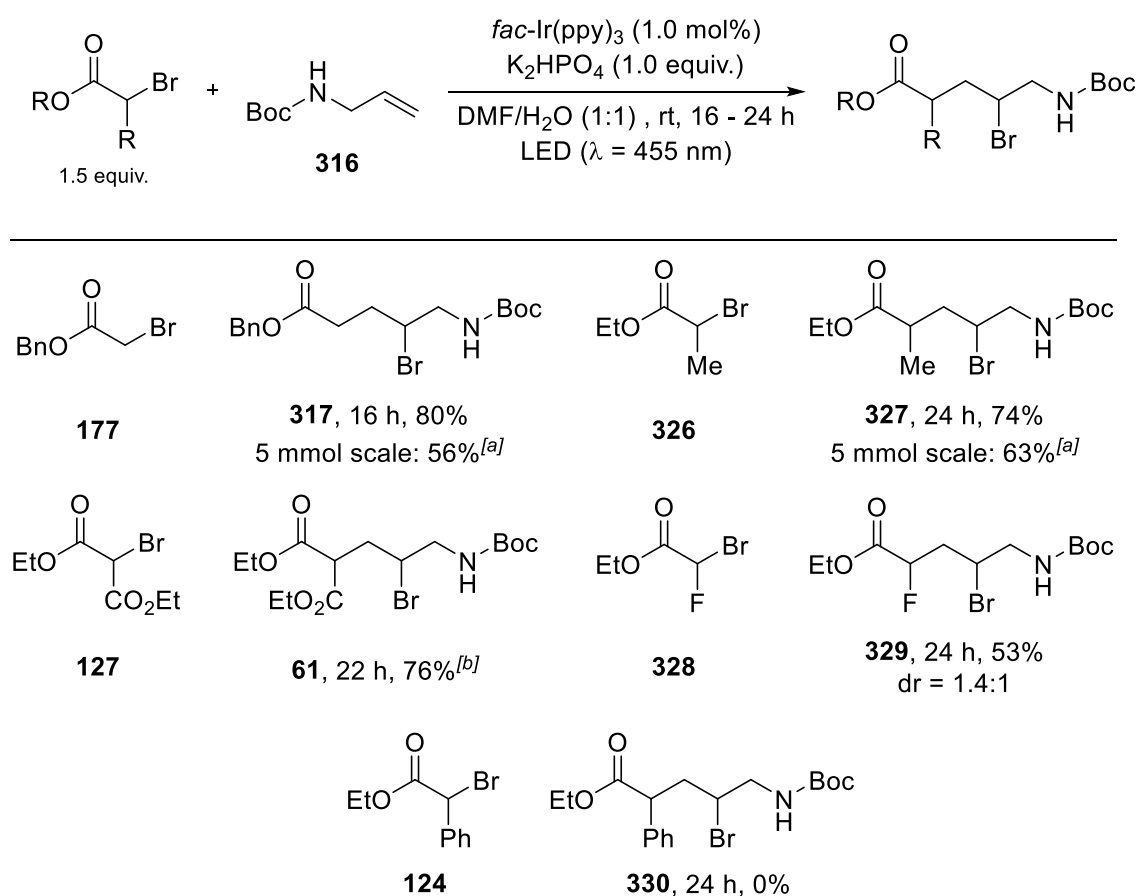
[a] 5 mmol scale

When Cu(dap)Cl₂ (**102**) was used as catalyst under green light irradiation in MeCN no reaction was observed (entry 1). Adding LiBr as weak Lewis acid for the activation of the carbonyl^[74] to facilitate radical formation of **317** was also not successful (entry 2). Switching to the iridium-based catalyst *fac*-Ir(ppy)₃ (**49**) and irradiation with blue light, the ATRA product **317** was received in 55% yield after 48 h (entry 3). As it was shown previously (chapter 1.2) the activation of α-halo carbonyl compounds

B Main Part

under these conditions can be improved by addition of the inorganic base K_2HPO_4 . With additional base the reaction time could be reduced to 18 h while the yield rose to 73% (entry 4). Changing the solvent to DCM did not improve the reaction further (entry 5). With a solvent mixture of DMF and water (1:1) the best results were achieved and product **317** was isolated in 80% after 16 h (entry 6). Control experiments showed that both catalyst and light are needed for this reaction (entry 7 & 8). It was again possible to up-scale the reaction to a 5 mmol scale with a reduced catalyst-loading of 0.5 mol% and reduced amount of the base to achieve a yield of 56% which gave more than 1 g of product (entry 9).

Inspired by these results, expansion of the scope to more α -bromo esters was tested (scheme 84).



Scheme 84. Substrate scope of α -halo esters in the ATRA reaction with *tert*-butyl allylcarbamate (**316**).

[a] 0.5 mol% of catalyst and 0.5 equiv. of K_2HPO_4 were used. [b] no K_2HPO_4 was used; reaction was performed in MeCN.

With ethyl 2-bromopropanoate (**326**), the product **327** was obtained in good yield of 74% after irradiation for 24 h. Since two stereocenters are formed in this reaction a mixture of two diastereomers was received but the diastereomeric ratio could not be determined. The reaction was also successfully up-scaled to 5 mmol and 63% of product **327** were isolated. In case of diethyl bromomalonate (**127**), no addition of K_2HPO_4 was needed and the best result of 76% was obtained in MeCN. In case of

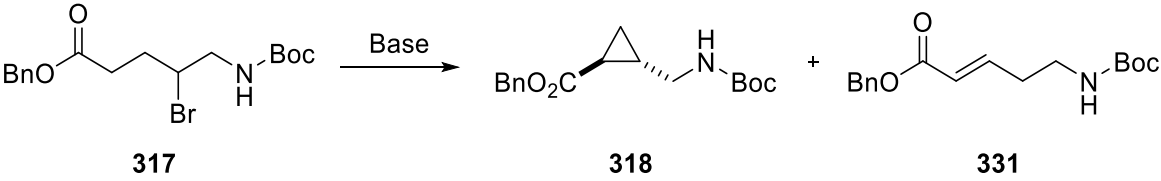
B Main Part

ethyl 2-bromo-2-fluoroacetate (**328**) a mixture of diastereomers was isolated in 53% yield and a diastereomeric ratio of 1.4:1 was determined. With ethyl 2-bromo-2-phenylacetate (**124**) no formation of the ATRA product **330** was seen, instead only decomposition of the starting material took place.

3.3 Cyclization reactions

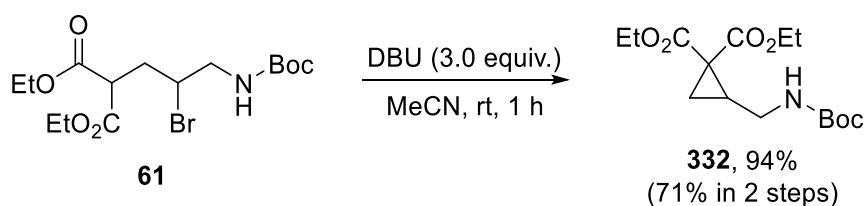
With these compounds at hand, the next step was to perform the base-induced 1,3-cyclization to form the cyclopropane moiety. Screening for some different bases and conditions for the ATRA adduct **317** was performed (table 6). Stirring the compound **317** in a mixture of MeCN and water for 20 h with 3 equiv. of KOH no formation of the cyclopropane **318** could be detected, instead partial cleavage of the ester takes place while the rest of the starting material decomposes (entry 1). In order to rule out water from being partially responsible for these side reactions the solvent system was changed to DMF, but the results remained unchanged (entry 2). Using DBU as base in MeCN the formation of α,β -unsaturated ester **331** was observed. The formation of this compounds can be explained by the elimination of HBr followed by isomerization of the double-bond (entry 3). With a weaker base like Cs_2CO_3 no conversion of the starting material could be seen. Same was the case for NEt_3 (entry 4 & 5).

Table 6. Base screening for the cyclization of ATRA product **317** into cyclopropane **318**.

				
Entry	Base	Solvent	Time	Yield
1	KOH (3 equiv.)	MeCN/H ₂ O (1:1)	20 h	Ester cleavage + decomposition
2	KOH (3 equiv.)	DMF	20 h	Ester cleavage + decomposition
3	DBU (3 equiv.)	MeCN	20 h	37% 331 + decomposition
4	Cs_2CO_3 (1.1 equiv.)	DMF	20 h	no conversion
5	NEt_3 (2 equiv.)	MeCN	20 h	no conversion
6	KO^tBu (3 equiv.)	THF	4 h	decomposition

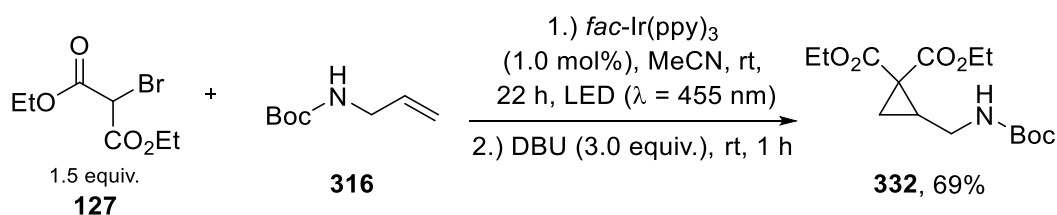
Pleasingly, in case of the compound **61** bearing two ester functionalities, addition of DBU lead to a clean transformation into the cyclopropane **332** after only 1 h in 94% yield (scheme 85). The deprotonation of the α -C-H seems to be strongly favored over the elimination of HBr making this reaction feasible.

B Main Part



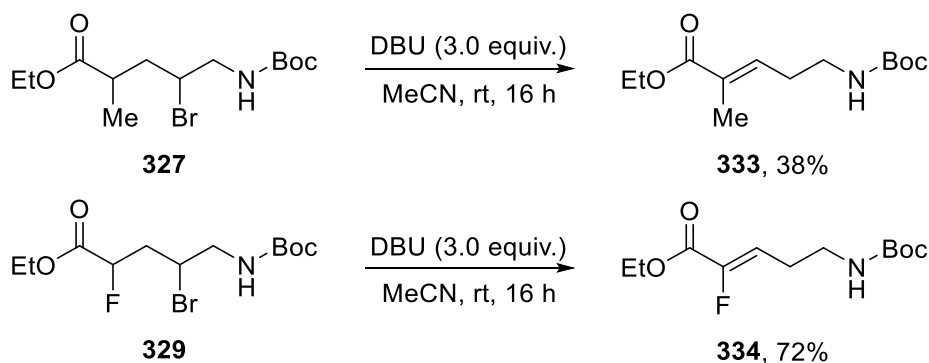
Scheme 85. Cyclization of **61** using DBU to form the cyclopropane **332**.

The reaction was also performed in a one-pot process where DBU was added after the photoreaction and the product was obtained in 69% yield (compared to 71% in 2 steps) and therefore making this process clearly favorable (scheme 86).



Scheme 86. One-pot ATRA reaction of **127** and **316** followed by cyclization with DBU to form the cyclopropane **332**.

It was assumed that the α -substituted esters **327** and **329** would also undergo ring-closure by deprotonation with DBU but again HBr elimination followed by isomerization was the only observed pathway. In case of the fluoro-substituted compound **329**, the alkene **334** was even isolated in good yield of 72% (scheme 87).



Scheme 87. Elimination of HBr from **327** and **329** followed by isomerization.

These results indicate that if only one electron-withdrawing ester group is present, the proton in α -position may not be acidic enough to undergo the desired cyclization. Instead, E_2 -type elimination of HBr is favored over cyclization in these cases.

3.4 Conclusion

In summary, it was shown that *tert*-butyl allylcarbamate (**316**) can be used in ATRA reactions with different α -bromo esters. *fac*-Ir(ppy)₃ (**49**) was the best catalyst for these transformations, allowing to perform some reactions on a 5 mmol scale. Successful cyclization of one of these compounds to generate a cyclic γ -amino acid derivative was achieved and even the development of a one-pot process for this reaction was feasible. Unfortunately, the target molecule (\pm)-TAMP (**319**) could not be synthesized using this method and only showed elimination followed by isomerization under these conditions. Similar results were observed for the other ATRA products. Further investigation is required to find suitable cyclization conditions for these substrates and the scope of these reactions needs to be explored in future studies.

4. Visible light mediated ATRA reactions with oxabicyclic alkenes

4.1 7-Oxanorbornane derivatives in nature and organic synthesis

The 7-oxabicyclo[2.2.1]heptane (7-oxanorbornane) ring system (**335**) and its derivatives are bicyclic structures bearing an oxygen bridgehead. This scaffold can be found in a large variety of natural products and biologically active systems such as 1,4-cineole (**336**). This compound with an odor similar to camphor is found in many plants and used in perfumes^[166] and is also one of the components of tequila.^[167] Or cantharidin (**337**)^[168] used in vesicants, the monoterpene 3',6'-epoxyaurapentene (**338**),^[169] the diterpenoid dactylomelol (**340**),^[170] the carotenoid pigment cucurbitaxanthin A (**339**) found in red paprika^[171] or even potential potent drugs for prostate cancer treatment such as BMS-641988 (**341**)^[172] just to name a few (figure 5).

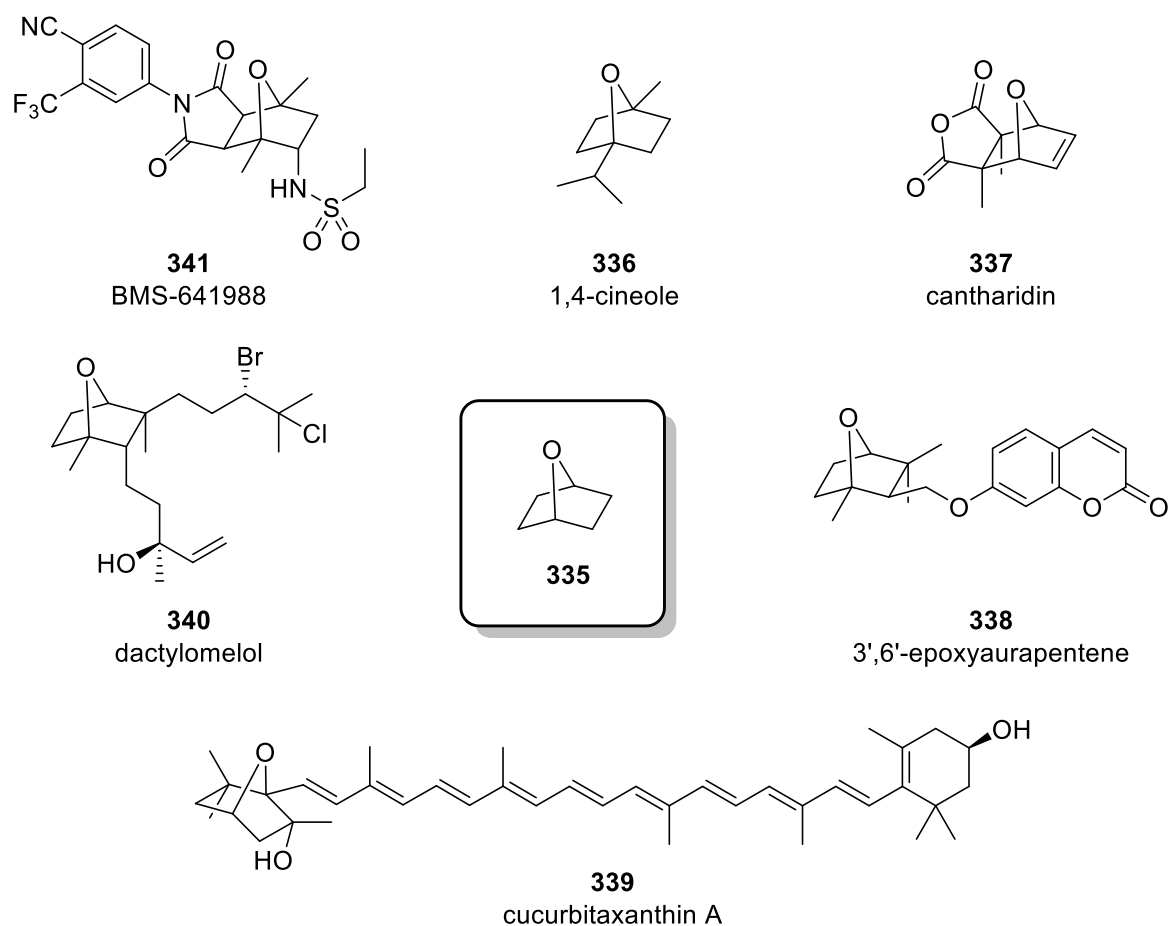
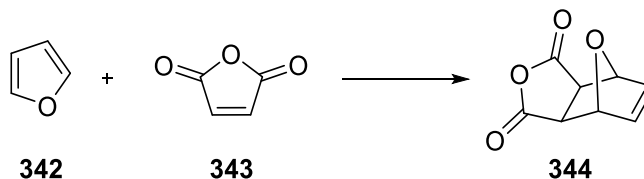


Figure 5. Selected examples of molecules containing the 7-oxabicyclo[2.2.1]heptane (**335**) subunit.

Over the years, numerous synthetic strategies have been developed for the synthesis of natural products bearing this subunit.^[173] One of the easiest ways to gain access to such molecules in the lab is through the Diels-Alder reaction (DA reaction) of furans and various dienophiles. In fact, one of the

B Main Part

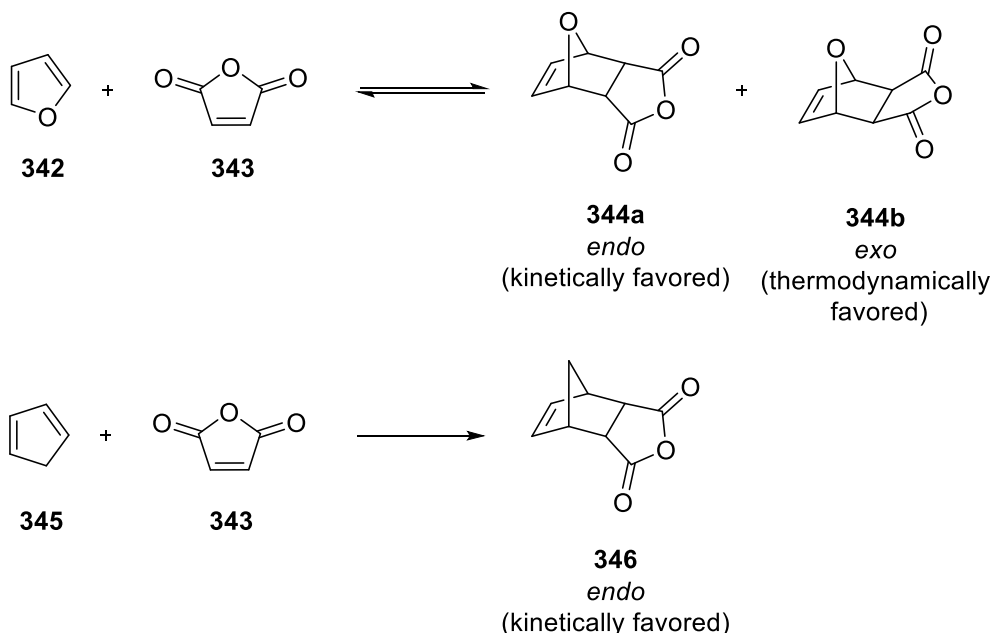
first examples that Diels and Alder published back in 1929 was the reaction of furan (**342**) with maleic anhydride (**343**) to generate the 7-oxanorbornene **344** (scheme 88).^[174]



Scheme 88. Diels-Alder reaction of furan (**342**) and maleic anhydride (**343**).^[174]

Its advantages lie in its ease of execution and high regio- and stereoselectivity and the intra- and inter-molecular DA reaction of furans has been widely used for the formation of 7-oxabicyclic systems and their further transformations.^[175]

In contrast to many other [4 + 2] cycloadditions with common dienes such as cyclopentadiene (**345**) where the *endo*-adduct **346** is usually the preferred product, the Diels-Alder reaction of furans often shows a strong preference for the *exo*-adduct **344b** (scheme 89). While the formation of the *endo*-adduct **344a** is slightly kinetically favored, its low thermodynamic stability leads to a rapid retro-DA reaction which in the end favors the formation of the thermodynamically more stable *exo*-adduct **344b**.^[176]



Scheme 89. Comparison of the DA reaction of furan (**342**) and cyclopentadiene (**345**) with maleic anhydride (**343**). Retro-DA reaction of **344a** leads to the formation of the *exo*-adduct **344b**.^[176]

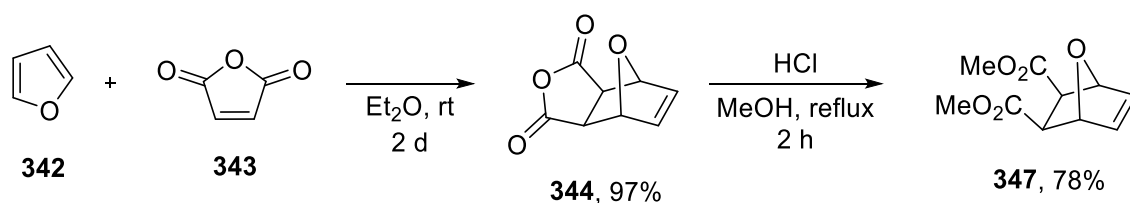
In addition to that, 7-oxanorbornane derivatives can also be widely used as synthetic intermediates and have been utilized for the synthesis of a plethora of highly functionalized molecules.^[177] These

B Main Part

transformations often involve the cleavage of the ethereal bridgehead either *via* Lewis acid induction,^[178] acid induced,^[179] under use of strong bases^[180] or reductive conditions.^[181] Furthermore, 7-oxanorbornenes have shown to be versatile building blocks for the synthesis of various polymers and macromolecules.^[182] It is also possible to obtain substances for this kind of chemistry from renewable bio-mass. Furan (**342**) and maleic anhydride (**343**) for example can be obtained from furfural^[183] and their Diels-Alder Adduct **344** was used for a renewable production of phthalic anhydride.^[184]

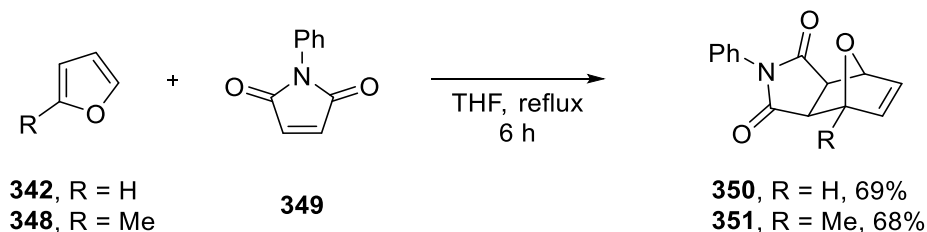
4.2 ATRA reactions with 7-oxanorbornenes

The main goal for this project was to see if simple 7-oxanorbornenes derived from renewable resources could serve as trapping reagents in photoredox-catalyzed ATRA reactions. Special attention was given to their stereo- and regio-selectivity and whether the highly functionalized resulting 7-oxanorbornanes could further be transformed *via* ring-opening strategies. Studies began with the synthesis of some simple oxabicyclohexenes. This class of compounds is easily accessible *via* the [4 + 2] cycloaddition of furans and dienophiles. The cycloaddition of furan (**342**) with maleic anhydride (**343**) proceeded smoothly at room temperature to afford the oxabicyclohexene **344** in almost quantitative yield which can then be easily transformed in the methyl ester **347** (scheme 90).^[185] Due to the reversibility of cycloadditions of furans the thermodynamically favored *exo*-adduct is formed exclusively.



Scheme 90. Diels-Alder reaction of furan (**342**) and maleic anhydride (**343**) followed by esterification with methanol.

The Diels-Alder reaction of furan (**342**) and 2-methylfuran (**348**) with *N*-phenylmaleimide (**349**) also proceeds smoothly to again exclusively give the *exo*-adducts **350** and **351** in good yield at elevated temperatures (scheme 91).^[186]

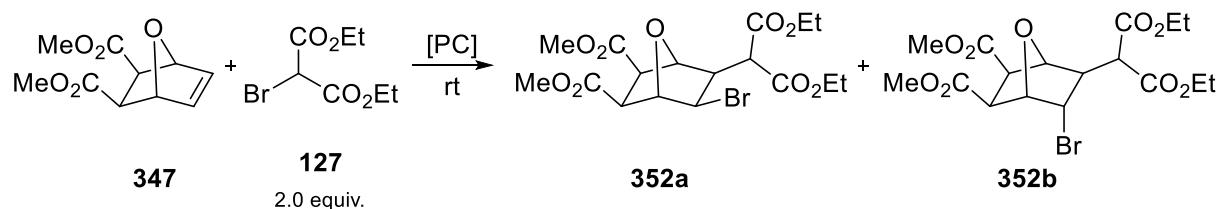


Scheme 91. Diels-Alder reaction of furan (**342**) and 2-methylfuran (**348**) with *N*-phenylmaleimide (**349**).

B Main Part

With these compounds at hand, the best reaction conditions for the ATRA reaction using diethyl 2-bromomalonate (**127**) and dimethyl-7-oxabicyclo[2.2.1]hept-5-ene-2,3-dicarboxylate (**347**) as model substrates were screened (table 7).

Table 7. Optimization of the reaction of diethyl 2-bromomalonate (**127**) and dimethyl-7-oxabicyclo[2.2.1]hept-5-ene-2,3-dicarboxylate (**347**).



Entry	Catalyst	Light	Solvent	Time	Yield	<i>dr</i> (352a : 352b)
1	Cu(dap) ₂ Cl (1 mol%)	530 nm	MeCN	48 h	54%	1.7:1
2	Cu(dap) ₂ Cl (1 mol%)	530 nm	DCM	48 h	33%	1.6:1
3	Cu(dap)₂Cl (1 mol%)	530 nm	DMF/H₂O (1:1)	24 h	73%	1.6:1
4 ^[a]	Cu(dap) ₂ Cl (1 mol%)	530 nm	DMF/H ₂ O (1:1)	24 h	62%	1.7:1
5	Cu(dap) ₂ Cl (2 mol%)	530 nm	DMF/H ₂ O (1:1)	24 h	71%	1.8:1
6	Ru(bpy) ₃ Cl ₂ (1 mol%)	455 nm	DMF/H ₂ O (1:1)	24 h	61%	1.7:1
7	<i>fac</i> -Ir(ppy) ₃ (1 mol%)	455 nm	DMF/H ₂ O (1:1)	24 h	68%	1.6:1
8	Cu(dap) ₂ Cl (1 mol%)	-	DMF/H ₂ O (1:1)	48 h	-	-
9	-	530 nm	DMF/H ₂ O (1:1)	48 h	-	-

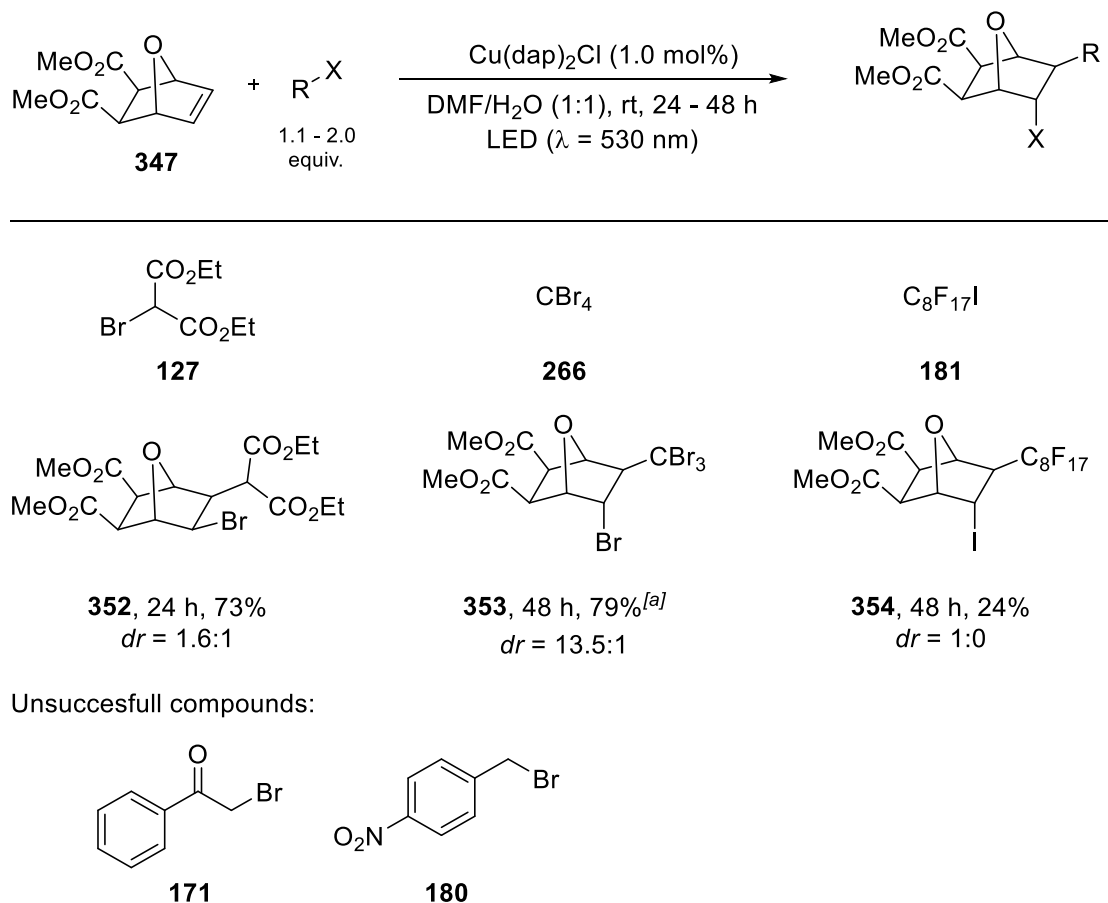
[a] 1.5 equiv. of **127** was used

With Cu(dap)₂Cl (**50**) as photocatalyst under green light irradiation in MeCN with two equivalents of diethyl 2-bromomalonate (**127**), a mixture of two diastereomers was formed in 54% yield after 48 hours (entry 1). The ratio of the two diastereomers was found to be 1.7:1 and the major diastereomer was identified as the isomer **352a** bearing both the malonate moiety as well as the bromine in *exo*-position. In the minor diastereomer **352b** the malonate is set in *exo*-position while the bromine is in *endo*-position. Using DCM as the solvent, the products were received in 33% in a diastereomeric ratio of 1:6:1 with the *exo-endo*-product being the major isomer again (entry 2). Changing to a very polar solvent mixture of DMF and water (1:1) reduced the reaction time to 24 h while increasing the yield to 73% while maintaining the diastereomeric ratio (entry 3). Reducing the equivalents of diethyl 2-bromomalonate (**127**) to 1.5 also reduced the obtained product to 62% (entry 4). An increased catalyst-loading of 2 mol% did not give better results (entry 5). Employing the ruthenium-based catalyst Ru(bpy)₃Cl₂ (**46**) and the iridium catalyst *fac*-Ir(ppy)₃ (**49**) under blue light irradiation also gave

B Main Part

the products in good yield of 61% and 68%, respectively, but could not match the best yields achieved with the copper-catalyst (entries 6 and 7). Control-experiments without light and without catalyst did not give any product formation (entries 8 and 9).

With the optimized conditions at hand, different radical precursors for the ATRA reaction of dimethyl-7-oxabicyclo[2.2.1]hept-5-ene-2,3-dicarboxylate (**347**) were tested (scheme 92).

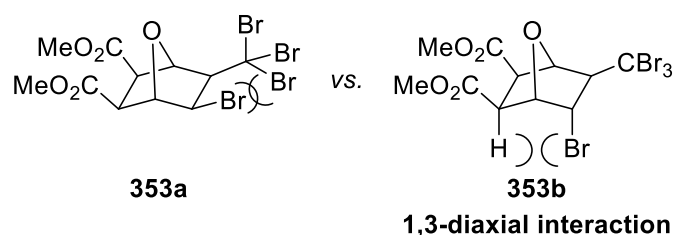


Scheme 92. ATRA reaction of different carbohalides and dimethyl-7-oxabicyclo[2.2.1]hept-5-ene-2,3-dicarboxylate (**347**). [a] reaction performed in DCM; 1.1 equiv. of **266** was used.

As already mentioned, the reaction of diethyl 2-bromomalonate (**127**) gave a mixture of two diastereomers in 73% yield with the *exo-exo*-isomer **352a** in slight excess. When tetrabromomethane (**266**) was used, a diastereomeric mixture of both isomers was received in 79% yield. Interestingly, the major diastereomer in this case was the *exo-endo*-compound **353b** which was obtained in a large excess over the *exo-exo*-isomer **353a** ($dr = 13.5:1$). This can be explained by the much bigger steric demand of the CBr_3 group compared to the malonate moiety in compound **352**. Generally, addition to the *exo*-position should be favored to avoid any 1,3-diaxial interaction (scheme 93). However, the CBr_3 group in *exo*-position is very bulky and the addition of bromine in *exo*-position would lead to even

B Main Part

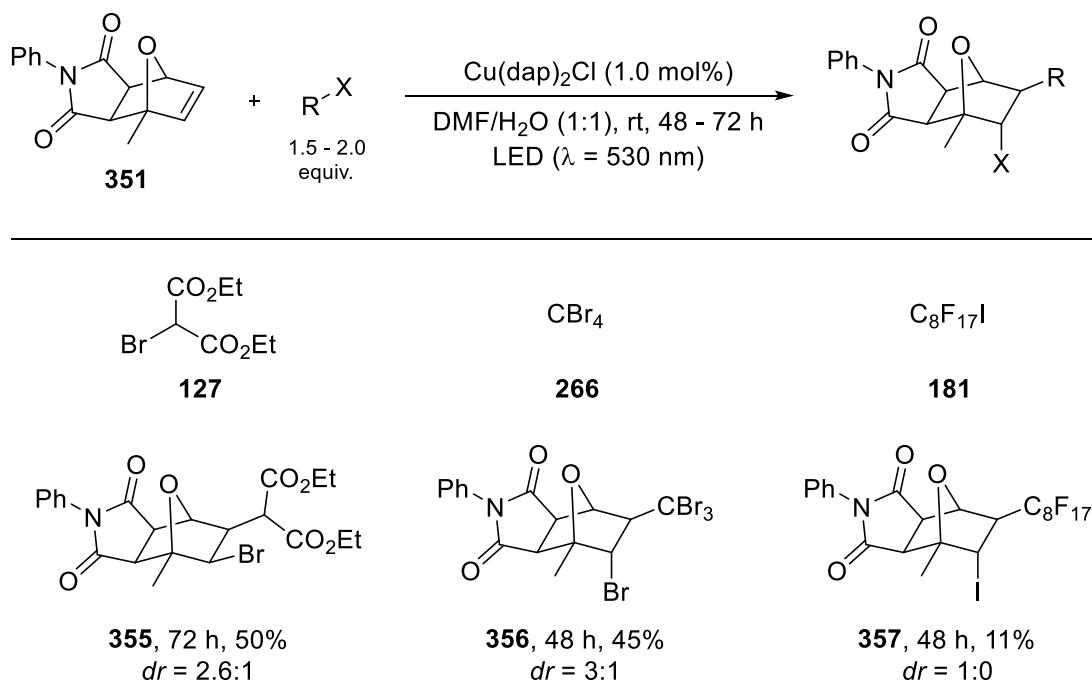
bigger strain and for that not favored. In case of **352a**, the two ester moieties can be turned away and therefore leave enough space for the addition of bromine making this the preferred addition. When the perfluorinated iodine $\text{C}_8\text{F}_{17}\text{I}$ (**181**) was used as radical precursor, only 24% of the product **354** were isolated but, in this case, only the *exo-endo*-isomer was observed. This can be explained by the much higher steric demand of iodine compared to bromine thus making an attack of iodine in *exo*-position impossible due to the high steric repulsion with the perfluorinated alkyl chain. It was also tried to achieve the ATRA reactions of 2-bromoacetophenone (**171**) and 4-nitrobenzyl bromide (**180**), both of which previously have been used in $\text{Cu}(\text{dap})_2\text{Cl}$ -catalyzed ATRA reactions^[74,118] but no formation of products was observed.



Scheme 93. 1,3-diaxial interaction and steric repulsion in the *exo-endo*- and *exo-exo*-isomer of **353**.

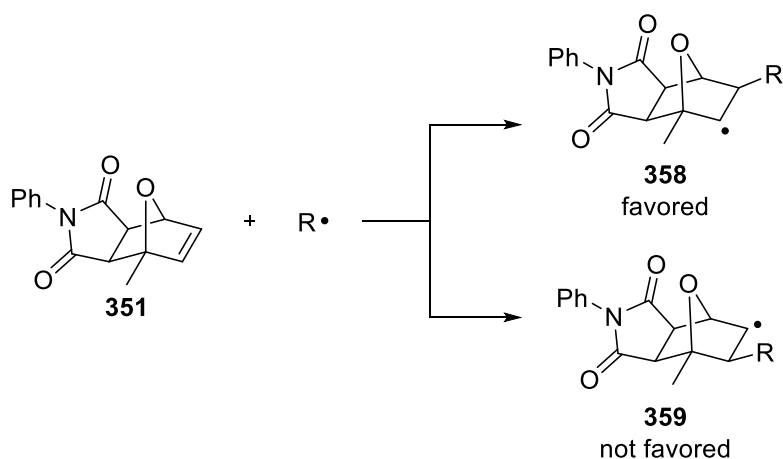
Encouraged by these results, the influence of substituents in the oxabicyclohexene on the regioselectivity of the addition of the radical and the influence on the *exo-endo*-addition was analyzed. Therefore, ATRA reactions were performed with 4-methyl-2-phenyl-3a,4,7,7a-tetrahydro-1H-4,7-epoxyisoindole-1,3(2H)-dione (**351**) originating from the Diels-Alder reaction of 2-methylfuran (**348**) and *N*-phenylmaleimide (**349**) to determine the influence the methyl-group has on these reactions (scheme 94).

B Main Part



Scheme 94. ATRA reaction of different carbohalides and 4-methyl-2-phenyl-3a,4,7,7a-tetrahydro-1H-4,7-epoxyisoindole-1,3(2H)-dione (**351**).

In the reaction of diethyl 2-bromomalonate (**127**) the products were isolated in 50% yield in a diastereomeric ratio of 2.6:1. Due to the lack of symmetry in this molecule, attack of the radical is possible at both carbons of the double bond of **351** giving potentially two different regio-isomers. Nevertheless, only addition on the carbon that is not in α -position to the methyl-group is observed. An explanation for this could be the lesser steric hinderance at that position but also the fact that the radical **358** that is formed is better stabilized by the hyperconjugation of the neighboring methyl-group (scheme 95).

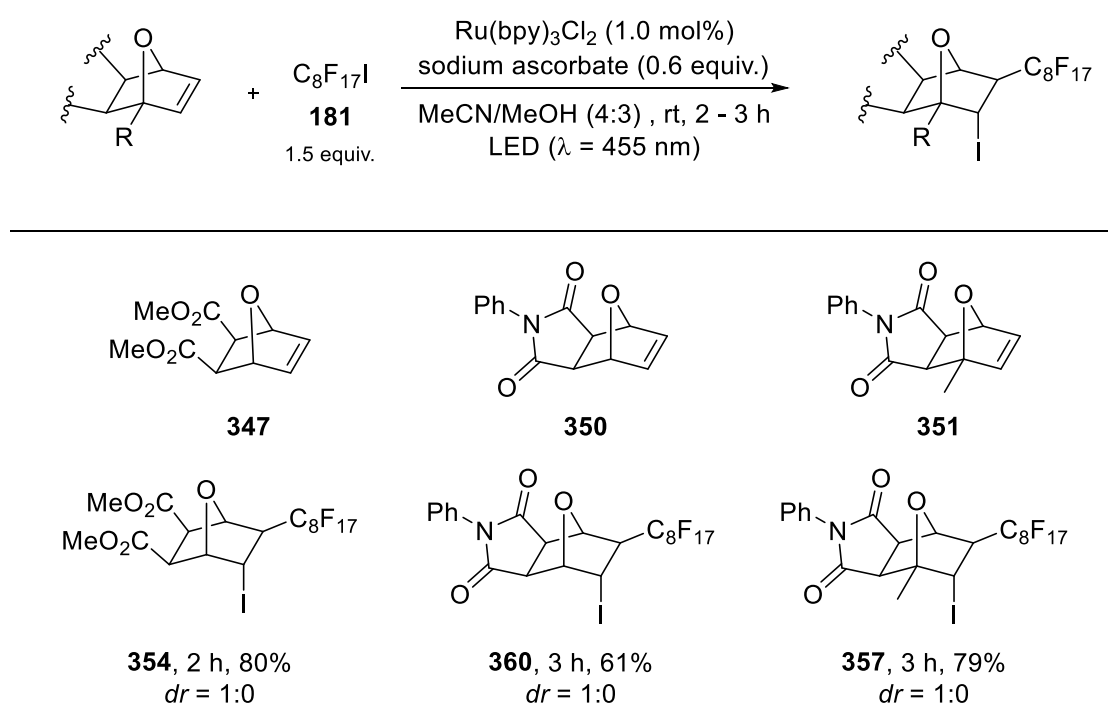


Scheme 95. Possible radical intermediates formed in the ATRA reaction of 4-methyl-2-phenyl-3a,4,7,7a-tetrahydro-1H-4,7-epoxyisoindole-1,3(2H)-dione (**351**).

B Main Part

Interestingly, the diastereomeric ratio is shifted even more towards the *exo-exo*-product. In case of the reaction with dimethyl-7-oxabicyclo[2.2.1]hept-5-ene-2,3-dicarboxylate (**347**) (scheme 92), a *dr* of 1.6:1 was observed whereas here it was 2.6:1 for product **355**. This indicates that the methyl-group is disfavoring the attack of the bromine in *endo*-position. Even stronger evidence for this can be seen in the reaction with tetrabromomethane (**266**) where a *dr* of 3:1 of **356** was isolated in 45% yield after 48 h. In comparison to the reaction with dimethyl-7-oxabicyclo[2.2.1]hept-5-ene-2,3-dicarboxylate (**347**) (scheme 92) the ratio is shifted from 13.5:1 to 3:1 making the attack on the *endo*-position still the favored one but not to an overwhelming degree anymore. In case of C₈F₁₇I (**181**) only a yield of 11% of **357** could be obtained but again exclusively one diastereomer was observed showing that even the blocking of the *endo*-position by the methyl-group cannot force the big iodine atom into the *exo*-position.

Since the reactions with the perfluorinated iodine **181** did not give satisfying results, different reaction conditions were looked into in order to achieve better yields. In 2012, Stephenson *et al.* published the ATRA reaction of perfluorinated iodines making use of the reductive quenching cycle of Ru(bpy)₃Cl₂ (**46**) with sodium ascorbate as reductant.^[90] Applying these conditions to the ATRA reaction of 7-oxanorbornenes improved the yields drastically (scheme 96).



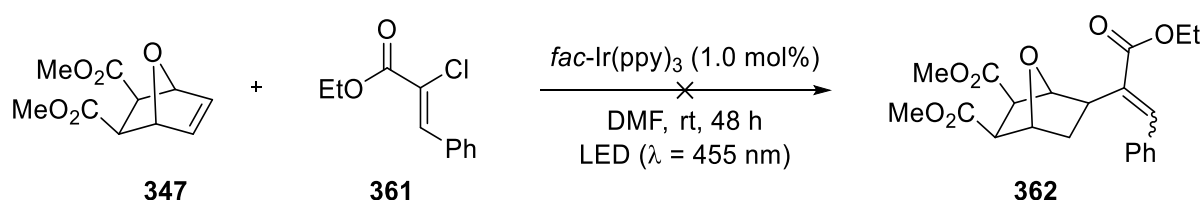
Scheme 96. ATRA reaction of perfluorooctyl iodide (**181**) and different oxabicyclohexenes using Ru(bpy)₃Cl₂.

When employing 1 mol% of Ru(bpy)₃Cl₂ (**46**) as the catalyst under blue light irradiation, sodium ascorbate (0.6 equiv.) as the sacrificial reductant and MeOH as co-solvent, 80% of **354** was generated from the reaction of dimethyl-7-oxabicyclo[2.2.1]hept-5-ene-2,3-dicarboxylate (**347**) in only 2 hours.

B Main Part

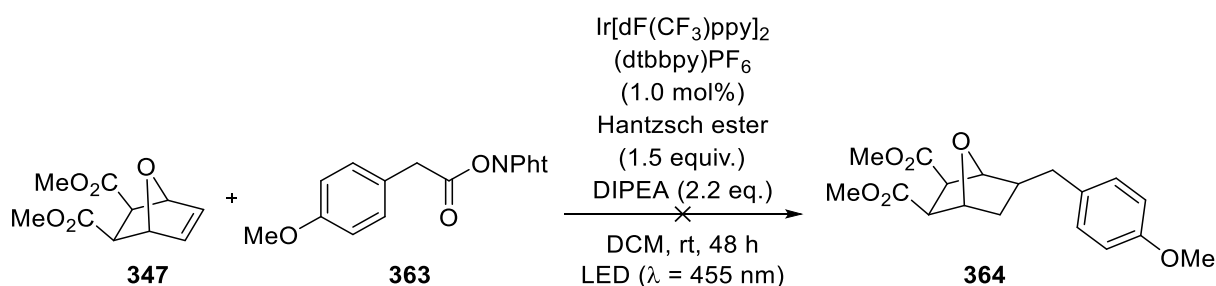
For the oxabicyclohexanes derived from the cycloaddition with *N*-phenylmaleimide (**349**), the products **360** and **357** were received in 61% and 79% after 3 hours. In all three cases only the *exo-endo*-isomers were observed. The very short reaction times are a strong indicator that a radical chain-propagation plays an important part in the reaction mechanism.

Inspired by these promising results, the use of oxabicyclohexenes as trapping reagents for different radicals in other photoredox-catalyzed reactions was tested. In the Reiser group it was discovered that α -chloro cinnamates can be used to generate vinyl radicals that can be trapped with enolates.^[187] Trying to use dimethyl-7-oxabicyclo[2.2.1]hept-5-ene-2,3-dicarboxylate (**347**) as a trapping reagent for the vinyl radical generated from ethyl (Z)-2-chloro-3-phenylacrylate (**361**) however did not lead to any formation of the product **362** and no conversion of the oxabicyclohexene **347** was observed (scheme 97).



Scheme 97. Attempted trapping of the vinyl radical generated from **361** with the oxabicyclohexene **347**.

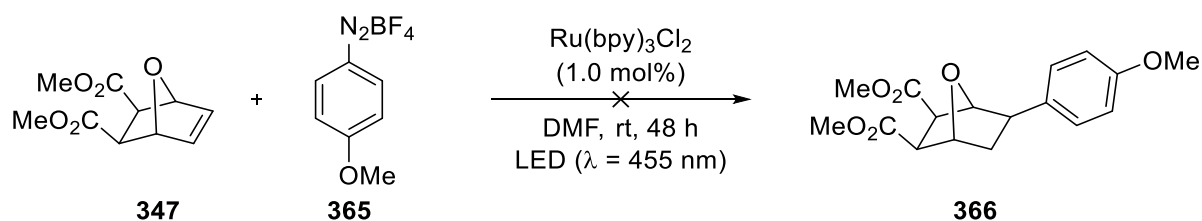
Another topic of interest explored by the Reiser Group is the decarboxylation of *N*-hydroxyphthalimide esters to generate and trap carbon radicals.^[188] It was attempted to generate a nucleophilic 4-methoxybenzyl radical from the redox-active ester **363** under reductive quenching conditions and trap it with oxabicyclohexene **347** but no product formation and starting material conversion was observed (scheme 98).



Scheme 98. Attempted trapping of the benzyl radical generated from **363** with the oxabicyclohexene **347**.

At last, a diazonium salt **365** was used to generate an aryl radical to see if trapping with the oxabicyclohexene **347** would occur but again no reaction took place (scheme 99).

B Main Part



Scheme 99. Attempted trapping of the aryl radical generated from **365** with the oxabicyclohexene **347**.

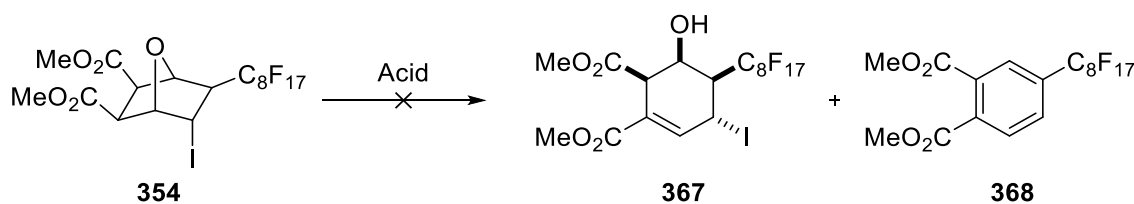
These experiments showed that trapping of rather nucleophilic radicals is not feasible with these oxabicyclohexenes. Nucleophilic radicals are typically trapped with electron-poor olefins while electrophilic radicals are usually trapped with electron-rich or un-activated olefins indicating that oxabicyclohexenes can be attributed to the latter of these classes.

4.3 Testing different ring-opening strategies

With several substituted oxabicyclohexanes at hand, further transformation of these compounds into interesting molecules was investigated. Especially the opening of the oxygen bridgehead was of interest since it could give access to a variety of highly substituted cyclohexenols or even aromatic compounds. The most common method to achieve this ethereal bridge opening is either acid- or Lewis acid-induced.^[189]

Investigation started with the perfluoro-tagged oxabicyclohexane **354**. Acid-induced bridge opening could potentially lead to a cyclohexanol akin to **367** but under these acidic conditions, further elimination of water and iodine could also be considered to generate the arene **368** (Table 8).

Table 8. Attempted ring-opening of 7-oxanorbornane **354** under acidic conditions.



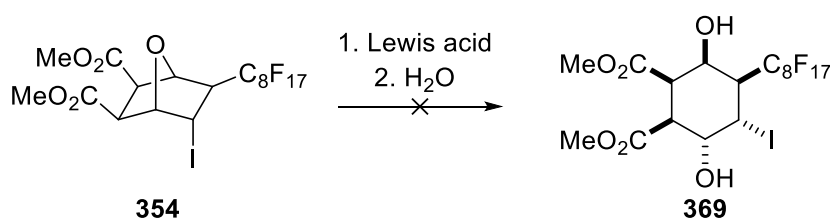
Entry	Acid	Solvent	Temperature	Time	Observation
1	HCl (0.5 M)	THF	rt	24 h	no conversion
2	TsOH (3 equiv.)	THF	rt	12 h	no conversion
3	TFA (7 equiv.)	DCM	rt	24 h	no conversion

B Main Part

However, when **354** was treated with diluted HCl in THF at rt for 24 h no conversion of the starting material was observed (entry 1). Changing to a strong acid such as *p*-toluenesulfonic acid (entry 2) or even a large excess of TFA (entry 3) did also not lead to any conversion of the oxabicyclohexane **354**.

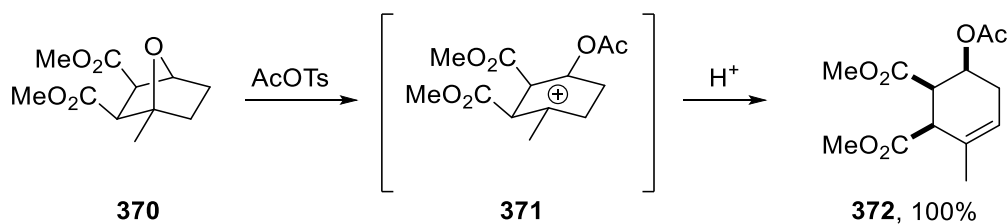
Next, the feasibility of ring-opening facilitated by Lewis acids followed by quenching with water to generate cyclohexanol **369** was tested (table 9). Using three equivalents of BF₃·OEt₂ in diethyl ether at – 78 °C for 1.5 h followed by quenching with water at 0 °C did not lead to any conversion of the perfluoro-tagged oxabicyclohexane **354** (entry 1). Stirring in DCM did also not give any reaction as well as performing the reaction at room temperature for 24 h (entry 3). Even applying the very strong Lewis acid AlCl₃ in an excess of 5 equivalents did not give the desired results.

Table 9. Attempted ring-opening of 7-oxanorbornane **354** with Lewis acids.



Entry	Lewis acid	Solvent	Temperature	Time	Observation
1	BF ₃ ·OEt ₂ (3 equiv.)	OEt ₂	- 78 °C → 0 °C	1.5 h	no conversion
2	BF ₃ ·OEt ₂ (3 equiv.)	DCM	- 78 °C → 0 °C	3 h	no conversion
3	BF ₃ ·OEt ₂ (3 equiv.)	DCM	rt	24 h	no conversion
4	AlCl ₃ (5 equiv.)	DCM	0 °C → rt	2.5 h	no conversion

When compared to literature, many of these acid- and Lewis acid-induced ring-openings involve oxabicyclic systems that bear substituents at the oxygen bridgehead. For example, Yamada *et al.* opened the 7-oxabicyclohexane **370**, having a methyl-substituent at the bridgehead, with AcOTs leading to cyclohexene **372** (scheme 100).^[190]



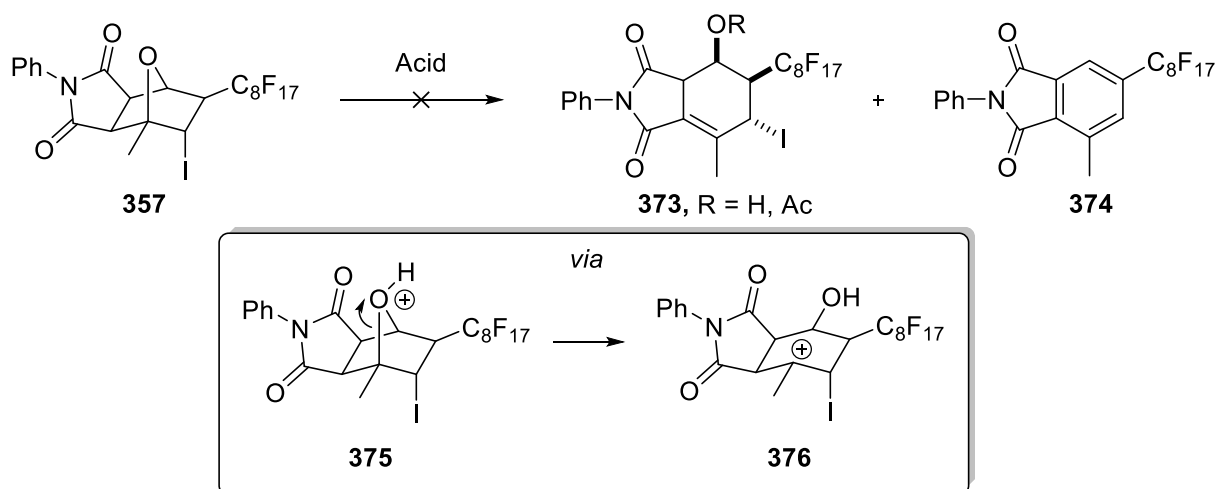
Scheme 100. Ring-opening of 7-oxanorbornane **370** after Yamada *et al.*^[190]

B Main Part

Since these reactions involve a cationic intermediate, having substituents at this position should favor the reaction. The methyl-group in the intermediate **371** stabilizes the positive charge whereas without its presence only a much less stable secondary cation would be present.

Therefore, it was investigated if one of the ATRA products that bears a methyl-substituent would be more prone to successfully undergo ring-opening. The oxabicyclic system **357** was chosen for this investigation to see if under acidic conditions or use of Lewis acids the product **373** or even the aromatic compound **374** could be obtained (table 10).

Table 10. Attempted ring-opening of 7-oxanorbornane **357** with acids and Lewis acids.

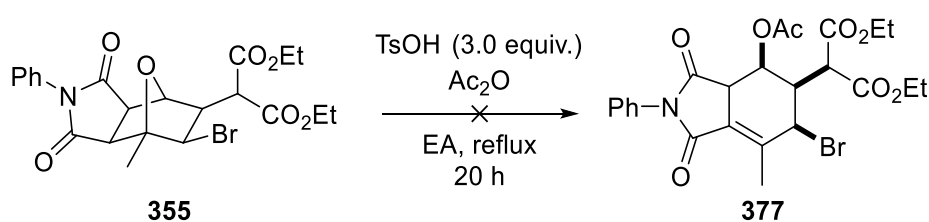


Entry	Acid	Solvent	Temperature	Time	Observation
1	TsOH (3 equiv.)	Ethyl acetate	rt	72 h	no conversion
2	TFA (20 equiv.)	Ethyl acetate	rt	72 h	no conversion
3	HCl (conc.)	Ethyl acetate	rt	72 h	no conversion
4	TsOH (3 equiv.)	THF	rt	72 h	no conversion
5	AcOH (90%) (48 equiv.)	-	rt	72 h	no conversion
6	TsOH (3 equiv.)	Ethyl acetate	77 °C	16 h	no conversion
7	HCl (10 equiv.)	<i>i</i> PrOH	82 °C	17 h	no conversion
8	Ac ₂ O, BF ₃ ·OEt ₂ (5 equiv.)	Toluene	0 °C	16 h	no conversion
9	TsOH (3 equiv.), Ac ₂ O (20 equiv.)	Ethyl acetate	77 °C	20 h	no conversion

B Main Part

The compound was stirred in ethyl acetate with TsOH, TFA and HCl, respectively, for 72 hours but even the use of large excess of acid did not lead to conversion (entries 1-3). The reaction also did not proceed in THF using TsOH as acid (entry 4) or even using acetic acid as the solvent (entry 5). Even under reflux conditions in ethyl acetate (entry 6 and 9) or *i*PrOH, the starting material did not react. Utilization of the Lewis acid $\text{BF}_3 \cdot \text{OEt}_2$ in combination with acetic anhydride was also unsuccessful (entry 8).

Finally, it was analyzed if the same results also apply to 7-oxanorbornanes without the perfluoro-tag to rule out any unwanted interactions. Therefore, the compound **355** was tested under reflux conditions in ethyl acetate with three equivalents of *p*-toluenesulfonic acid in presence of acetic anhydride but again no transformation of the starting material was observed (scheme 101).



Scheme 101. Attempted ring-opening of **355** with TsOH under reflux conditions.

These results show that under acidic conditions or the use of even strong Lewis acids, the ring-opening of the 7-oxabicyclic systems that were derivatized through photoredox-catalyzed ATRA reactions could not be achieved. Earlier studies on this topic (master thesis) to perform ring-opening using bases were also not successful.^[191] This may lead to the conclusion that these ring-systems generated *via* ATRA reactions seem to be way more stable than originally expected. One possible explanation for this could be that through the ATRA reaction even more electron-withdrawing groups are introduced into the molecule. The ring-opening under acidic conditions includes a cationic intermediate which could be disfavored by the various electron-withdrawing groups in the molecule. Another explanation could be the strong 1,3-diaxial interactions that might appear in the final products or the intermediates during these reactions.

4.4 Conclusion

In summary, it was shown that 7-oxanorbornenes can be used as trapping reagents in photoredox-catalyzed ATRA reactions. Cu(dap)₂Cl (**50**) was shown to be an effective catalyst for these transformations, whereas Ru(bpy)₃Cl₂ (**46**) was the best choice for perfluorinated iodines. It was shown that bulky radicals and halides prefer to add in *exo-endo*-configuration while smaller substrates favor *exo-exo*. Regio-selectivity can additionally be tuned by introduction of substituents into the 7-oxanorbornenes. However, ring-opening of these ATRA products could not be achieved and the reasons for their unexpected stability have yet to be determined.

C Summary

This thesis begins with a short overview over the development of atom transfer radical addition (ATRA) reactions and related processes as an important and atom efficient tool in organic synthesis. After a brief introduction into the history and photophysics of photoredox catalysis, the development of visible-light mediated ATRA processes over the last 15 years is discussed.

The chapter “Visible light mediated allylation reactions with allylsilanes” describes the use of benign and bench-stable allylsilanes as trapping reagents in photoredox-catalyzed allylation reactions. It was shown that *fac*-Ir(ppy)₃ (**49**) acts as an effective catalyst for the generation of carbon radicals from halocarbons and α -halo carbonyls and their utilization in allylations with allylsilanes. Using the copper(II)-complex Cu(dap)Cl₂ (**102**), the allylation of various sulfonyl chlorides and some *N*-chloro-amines was achieved. It was discovered that the generation of the ATRA side-product plays an important role in this reaction. After optimization by addition of Na₂CO₃ to protect the catalyst, and NaF to eliminate the ATRA side-product in a one-pot process, excellent yields could be achieved under mild reaction conditions even on a 5 mmol scale.

The chapter “Visible light mediated ATRA reactions with vinylsilanes – Access to and utilization of α -haloalkylsilanes” deals with the use of vinylsilane **230** as trapping reagent in photoredox-catalyzed ATRA reactions to generate interesting α -haloalkylsilanes. The general obstacles and limitations of the synthesis of α -haloalkylsilanes, as well as their applications are briefly discussed. Making use of the oxidative quenching cycle of *fac*-Ir(ppy)₃ (**49**), the synthesis of some α -haloalkylsilanes from halocarbons and vinylsilane **230** was achieved while Cu(dap)Cl₂ (**102**) was used for sulfonyl chlorides. These α -haloalkylsilanes were then utilized for a new improved synthesis of the important acetylene synthon (*E*)-trimethyl(2-tosylvinyl)silane (**278**) and a novel cyclization strategy to gain access to silyl-substituted cyclopropanes.

The following chapter “Synthesis of cyclic γ -amino acids *via* visible light mediated ATRA reactions and cyclizations” proposes a convenient and short synthesis for the GABA-analog (\pm)-TAMP (**319**) and derivatives by making use of photoredox-catalyzed ATRA reactions and base-induced cyclization. Several ATRA reactions using *tert*-butyl allylcarbamate (**316**) were achieved using *fac*-Ir(ppy)₃ (**49**) as photocatalyst. Cyclization was successful to generate a cyclic γ -amino acid in a one-pot synthesis while suitable reaction conditions were not found for (\pm)-TAMP (**319**) and other derivatives.

The final chapter “Visible light mediated ATRA reactions with oxabicyclic alkenes” continues previous work from my master thesis. The synthesis of easily available 7-oxanorbornene ring-systems and their

C Summary

use as trapping reagents in photoredox-catalyzed ATRA reactions is explored. Making use of $\text{Cu}(\text{dap})_2\text{Cl}$ (**50**) and the reductive quenching cycle of $\text{Ru}(\text{bpy})_3\text{Cl}_2$ (**46**), several halocarbons were successfully added to 7-oxanorbonenes. The regio- and diastereoselectivity of these reactions were briefly discussed and various ring-opening strategies were applied, however with no meaningful results.

D Zusammenfassung

D Zusammenfassung

Zu Beginn der vorliegenden Arbeit wird ein kurzer Überblick über die Entwicklung von Atom Transfer Radikal Addition (ATRA) Reaktionen und verwandter Prozesse als wichtige und atomeffiziente Methoden der organischen Synthese gegeben. Nach einer kurzen geschichtlichen und photophysikalischen Einführung in die Photoredoxkatalyse werden die Fortschritte in ATRA Prozessen mit sichtbarem Licht in den letzten 15 Jahren diskutiert.

Im Kapitel „Visible light mediated allylation reactions with allylsilanes“ wird die Verwendung von stabilen und ungefährlichen Allylsilanen als Abfangreagenzien in photoredoxkatalysierten Allylierungsreaktionen beschrieben. Es wurde gezeigt, dass *fac*-Ir(ppy)₃ (**49**) ein effizienter Katalysator für die Erzeugung von Kohlenstoffradikalen aus Halogenkohlenwasserstoffen und α -Halogen-Carbonylverbindungen und deren Verwendung für die Allylierung mit Allylsilanen ist. Indem man den Kupfer(II)-Komplex Cu(dap)Cl₂ (**102**) verwendete, konnte man die Allylierung vieler Sulfonylchloride und einiger weniger *N*-Chloramine durchführen. Man hat herausgefunden, dass die Erzeugung des ATRA Nebenprodukts eine wichtige Rolle bei dieser Reaktion spielt. Durch Zugabe von Na₂CO₃ konnte der Katalysator geschützt werden und mit NaF das ATRA Nebenprodukt eliminiert werden und somit die Reaktion optimiert. Dadurch konnten hervorragende Ausbeuten selbst in einem 5 mmol Maßstab in einer Eintopfreaktion unter milden Bedingungen erzielt werden.

Das Kapitel „Visible light mediated ATRA reactions with vinylsilanes – Access to and utilization of α -haloalkylsilanes“ beschäftigt sich mit der Verwendung von Vinylsilan **230** als Abfangreagenz in photoredoxkatalysierten ATRA Reaktionen und der dadurch ermöglichten Synthese interessanter α -Halogenalkylsilane. Zudem wird kurz auf die allgemeinen Schwierigkeiten und Hindernisse bei der Herstellung von α -Halogenalkylsilanen eingegangen, sowie deren Verwendung besprochen. Indem man den oxidativen Quenchzyklus von *fac*-Ir(ppy)₃ (**49**) verwendet, konnte man einige α -Halogenalkylsilane aus Halogenkohlenwasserstoffen und Vinylsilan **230** herstellen. Für Sulfonylchloride wurde hingegen erneut Cu(dap)Cl₂ (**102**) benutzt. Diese α -Halogenalkylsilane wurden anschließend in einer neuen, verbesserten Synthese des wichtigen Acetylen-Synthons (*E*)-trimethyl(2-tosylvinyl)silan (**278**) verwendet und durch eine neuartige Zyklisierungsstrategie konnten silyl-substituierte Cyclopropane erhalten werden.

Im folgenden Kapitel „Synthesis of cyclic γ -amino acids *via* visible light mediated ATRA reactions and cyclizations“ wird eine neue, kurze und zweckmäßige Syntheseroute für das GABA-Analog (\pm)-TAMP (**319**) und dessen Derivate vorgeschlagen. Dabei würde man sich die Kombination einer

D Zusammenfassung

photoredoxkatalysierten ATRA Reaktion gefolgt von einer baseninduzierten Zyklisierung zu Nutzen machen. Mehrere ATRA Reaktionen mit *tert*-butyl Allylcarbammat (**316**) und *fac*-Ir(ppy)₃ (**49**) als Photokatalysator waren erfolgreich. Die Zyklisierung zu einer zyklischen γ -Aminosäure konnte in einer Eintopfreaktion erzielt werden, wohingegen keine passenden Reaktionsbedingungen gefunden wurden um (\pm)-TAMP (**319**) und seine restlichen Derivate herzustellen.

Das letzte Kapitel „Visible light mediated ATRA reactions with oxabicyclic alkenes“ ist eine Fortführung meiner Masterarbeit. Die Synthese von leicht zugänglichen 7-Oxanorbornen-Ringsystemen und deren Verwendung als Abfangreagenzien in photoredoxkatalysierten ATRA Reaktionen wurde untersucht. Durch den Gebrauch von Cu(dap)₂Cl (**50**) und Ru(bpy)₃Cl₂ (**46**) in seinem reduktiven Quenchzyklus, konnten mehrere Halogenkohlenwasserstoffe an 7-Oxanorbornene addiert werden. Die Regio- und Diastereoselektivität dieser Reaktionen wurde kurz diskutiert und mehrere Ringöffnungsstrategien wurden angewendet, jedoch ohne bereits zufriedenstellende Ergebnisse zu liefern.

E Experimental part

E Experimental part

1. General information

All chemicals were used as received or purified according to Purification of Common Laboratory Chemicals.^[192] Glassware was dried in an oven at 90 °C or flame dried prior to use. All reactions under N₂-atmosphere were performed using Schlenk techniques. The blue light irradiation was performed using OSRAM Oslon SSI 80 LDCQ7P-1U3U LEDs (λ_{max} = 455 nm). Green light irradiation was performed using CREE XP-E LEDs (3 W, λ_{max} = 520 - 535 nm). Analytical thin layer chromatography was performed on Merck TLC aluminum sheets silica gel 60 F 254. Reactions were monitored by TLC and visualized by a short-wave UV lamp and stained with a solution of KMnO₃, vanillin or ninhydrin. Column flash chromatography was performed using Merck flash silica gel 60 (0.040 – 0.063 mm). The melting points were measured on an OptiMelt MPA 100 (uncorrected). IR spectroscopy measurements were performed on an Agilent Gary 630 FTIR spectrometer equipped with a Diamond Single Reflection Accessory. NMR spectra were recorded on Bruker Avance 300 and Bruker Avance 400 spectrometers. Chemical shifts for ¹H-NMR were reported as δ (parts per million) relative to the signal of CDCl₃ at 7.26 ppm. Chemical shifts for ¹³C-NMR were reported as δ (parts per million) relative to the center line signal of the CDCl₃ triplet at 77 ppm. Coupling constants J are given in Hertz (Hz). The following notations indicate the multiplicity of the signals: s = singlet, brs = broad singlet, d = doublet, dd = doublet of a doublet, ddd = doublet of a doublet of a doublet, ddt = doublet of a doublet of a triplet, dq = doublet of a quartet, dtd = doublet of a triplet of a doublet, t = triplet, td = triplet of a doublet, tt = triplet of a triplet, q = quartet, qd = quartet of a doublet, quint = quintet, sept = septet, and m = multiplet. Mass spectra were recorded at the Central Analytical Laboratory at the Department of Chemistry of the University of Regensburg on a Varian MAT 311A, Finnigan MAT 95, Thermoquest Finnigan TSQ 7000 or Agilent Technologies 6540 UHD AccurateMass Q-TOF LC/MS. The yields reported are referred to the isolated compounds unless otherwise stated. NMR yields were determined using 1,3,5-trimethoxybenzene as internal standard.

1.1 Synthesis of literature known compounds and reagents

The following compounds were synthesized according to the reported literature procedures. The spectral data were in agreement with the data reported: Cu(dap)₂Cl (**50**),^[74] Cu(dap)Cl₂ (**102**),^[87] Cu(binc)(dpp)BF₄,^[117] Ir[dF(CF₃)ppy]₂(dtbbpy)PF₆,^[193] 2-bromo-1,3-diphenylpropane-1,3-dione (**167**),^[194] 2-bromo-3,4-dihydronaphthalen-1(2*H*)-one (**174**),^[74] 2-chloro-3,4-dihydronaphthalen-1(2*H*)-one (**175**),^[74] trimethyl(2-phenylallyl)silane (**163**),^[195] *N*-chloro-*N*-methyl-4-nitrobenzenesulfonamide

E Experimental part

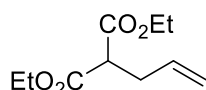
(**211**),^[124] *N*-chloro-*N*,4-dimethylbenzenesulfonamide (**213**),^[124] *N*-chloro-*N*-phenylbenzamide (**215**),^[196] *N*-chloro-*N*-phenylacetamide (**216**),^[196] *tert*-butyl allylcarbamate (**316**),^[197] dimethyl-7-oxabicyclo[2.2.1]hept-5-ene-2,3-dicarboxylate (**347**),^[185] 2-phenyl-3a,4,7,7a-tetrahydro-1*H*-4,7-epoxyisoindole-1,3(2*H*)-dione (**350**),^[198] 4-methyl-2-phenyl-3a,4,7,7a-tetrahydro-1*H*-4,7-epoxyisoindole-1,3(2*H*)-dione (**351**),^[186] ethyl (*Z*)-2-chloro-3-phenylacrylate (**361**),^[187] 1,3-dioxoisindolin-2-yl 2-(4-methoxyphenyl)acetate (**363**)^[199].

2. Visible-light mediated allylations of α -halo carbonyls

General procedure GP-A

A 5 mL flame-dried Schlenk tube equipped with a magnetic stirring bar was charged with the carbohalide (0.50 mmol, 1.0 equiv.), *fac*-Ir(ppy)₃ (**49**) (2.50 μ mol or 5.0 μ mol, 0.5 mol% or 1.0 mol%) and dry MeCN (1 mL). The flask was sealed with a plastic screw cap and the mixture degassed using the freeze-pump-thaw method (3 cycles). Under N₂ atmosphere, allyltrimethylsilane (**159**) (171.4 mg, 240.0 μ L, 1.50 mmol, 3.0 equiv.) was added and the plastic screw cap replaced by another screw cap with a Teflon sealed inlet for a quartz glass rod. A high-power LED (λ = 455 nm) was attached to the top of the quartz glass rod. After irradiation for 24 – 48 h the LED was removed, the solvent removed *in vacuo* and the residue was purified by column chromatography (silica, hexanes / EA).

Diethyl 2-allylmalonate (**160**)

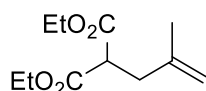


Following general procedure GP-A using diethyl 2-bromomalonate (**127**) (119.5 mg, 85.0 μ L, 0.50 mmol, 1.0 equiv.), allyltrimethylsilane (**159**) (171.4 mg, 240.0 μ L, 1.50 mmol, 3.0 equiv.), *fac*-Ir(ppy)₃ (**49**) (1.6 mg, 2.50 μ mol, 0.5 mol%) and dry MeCN (1 mL) after irradiation for 24 h gave **160** (92.9 mg, 0.46 mmol, 93%) as colorless liquid after flash chromatography purification (silica, hexanes / EA, 15:1).

R_f (hexanes / EA, 5:1): 0.53; **Staining**: KMnO₄ (UV active). **¹H-NMR** (400 MHz, CDCl₃): δ _H (ppm) = 5.78 (ddt, *J* = 17.0, 10.2, 6.8 Hz, 1H), 5.15 – 5.03 (m, 2H), 4.24 – 4.16 (m, 4H), 3.42 (dd, *J* = 9.6, 5.5 Hz, 1H), 2.64 (t, *J* = 7.2 Hz, 2H), 1.26 (t, *J* = 7.1 Hz, 6H). **¹³C-NMR** (101 MHz, CDCl₃): δ _C (ppm) = 168.93, 134.11, 117.51, 61.40, 51.68, 32.83, 14.09. **IR** (neat, ν /cm⁻¹): 2982, 2937, 1730, 1644, 1446, 1371, 1334, 1267, 1234, 1152, 1033, 921, 857. **HRMS** (ESI): exact mass calculated for C₁₀H₁₆O₄ [M+NH₄]⁺: *m/z* 218.1387, found: *m/z* 218.1382.

E Experimental part

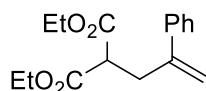
Diethyl 2-(2-methylallyl)malonate (**162**)



Following general procedure *GP-A* using diethyl 2-bromomalonate (**127**) (119.5 mg, 85.0 μ L, 0.50 mmol, 1.0 equiv.), trimethyl(2-methylallyl)silane (**161**) (192.4 mg, 260.0 μ L, 1.50 mmol, 3.0 equiv.), *fac*-Ir(ppy)₃ (**49**) (1.6 mg, 2.50 μ mol, 0.5 mol%) and dry MeCN (1 mL) after irradiation for 24 h gave **162** (83.4 mg, 0.39 mmol, 78%) as colorless liquid after flash chromatography purification (silica, hexanes / EA, 100:1).

R_f (hexanes / EA, 5:1): 0.56; **Staining**: KMnO₄ (UV active). **¹H-NMR** (300 MHz, CDCl₃): δ_{H} (ppm) = 4.74 (d, J = 17.9 Hz, 2H), 4.22 – 4.14 (m, 4H), 3.61 – 3.52 (m, 1H), 2.60 (d, J = 7.8 Hz, 2H), 1.74 (s, 3H), 1.25 (t, J = 7.1 Hz, 6H). **¹³C-NMR** (75 MHz, CDCl₃): δ_{C} (ppm) = 170.46, 143.03, 113.60, 62.74, 51.85, 37.81, 23.62, 15.40. **IR** (neat, ν/cm^{-1}): 2982, 2941, 1730, 1651, 1446, 1372, 1334, 1223, 1148, 1029, 895, 857, 693. **LRMS** (ESI): exact mass calculated for C₁₁H₁₈O₄ [M]⁺: m/z 215.1283, found: m/z 215.1338.

Diethyl 2-(2-phenylallyl)malonate (**164**)

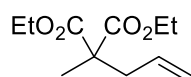


Following general procedure *GP-A* using diethyl 2-bromomalonate (**127**) (119.5 mg, 85.0 μ L, 0.50 mmol, 1.0 equiv.), trimethyl(2-phenylallyl)silane (**163**)^[195] (285.5 mg, 310.0 μ L, 1.50 mmol, 3.0 equiv.), *fac*-Ir(ppy)₃ (**49**) (1.6 mg, 2.50 μ mol, 0.5 mol%) and dry MeCN (1 mL) after irradiation for 24 h gave **164** (127.2 mg, 0.46 mmol, 92%) as yellow liquid after flash chromatography purification (silica, hexanes / EA, 20:1).

R_f (hexanes / EA, 5:1): 0.51; **Staining**: KMnO₄ (UV active). **¹H-NMR** (400 MHz, CDCl₃): δ_{H} (ppm) = 7.37 – 7.25 (m, 5H), 5.28 (d, J = 0.4 Hz, 1H), 5.11 (d, J = 1.1 Hz, 1H), 4.16 – 4.10 (m, 4H), 3.47 (dd, J = 9.7, 5.6 Hz, 1H), 3.10 (dd, J = 7.7, 0.8 Hz, 2H), 1.21 (t, J = 7.1 Hz, 6H). **¹³C-NMR** (101 MHz, CDCl₃): δ_{C} (ppm) = 169.01, 144.88, 140.05, 128.46, 127.80, 126.31, 114.81, 61.43, 50.98, 34.54, 14.08. **IR** (neat, ν/cm^{-1}): 3056, 2982, 1730, 1633, 1446, 1368, 1331, 1264, 1230, 1148, 1096, 1033, 906, 857, 779, 701. **HRMS** (ESI): exact mass calculated for C₁₆H₂₀O₄ [M+H]⁺: m/z 277.1434, found: m/z 277.1438.

E Experimental part

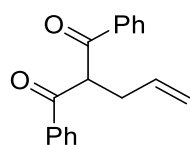
Diethyl 2-allyl-2-methylmalonate (**166**)



Following general procedure *GP-A* using diethyl 2-bromo-2-methylmalonate (**165**) (126.5 mg, 95.0 μ L, 0.50 mmol, 1.0 equiv.), allyltrimethylsilane (**159**) (171.4 mg, 240.0 μ L, 1.50 mmol, 3.0 equiv.), *fac*-Ir(ppy)₃ (**49**) (3.3 mg, 5.0 μ mol, 1.0 mol%) and dry MeCN (1 mL) after irradiation for 24 h gave **166** (76.9 mg, 0.36 mmol, 72%) as colorless liquid after flash chromatography purification (silica, hexanes / EA, 10:1).

R_f (hexanes / EA, 5:1): 0.67; **Staining**: KMnO₄ (UV active). **¹H-NMR** (300 MHz, CDCl₃): δ_{H} (ppm) = 5.76 – 5.57 (m, 1H), 5.12 – 5.07 (m, 1H), 5.05 (s, 1H), 4.19 – 4.12 (m, 4H), 2.58 (dd, J = 7.4, 1.0 Hz, 2H), 1.36 (s, 3H), 1.22 (dd, J = 9.9, 4.3 Hz, 6H). **¹³C-NMR** (75 MHz, CDCl₃): δ_{C} (ppm) = 170.91, 131.64, 118.05, 60.21, 52.40, 39.01, 18.69, 13.04. **IR** (neat, ν/cm^{-1}): 2982, 2941, 1730, 1640, 1450, 1379, 1293, 1241, 1204, 1148, 1107, 1021, 921, 861. **HRMS** (ESI): exact mass calculated for C₁₁H₁₈O₄ [M+H]⁺: m/z 215.1278, found: m/z 215.1277.

2-allyl-1,3-diphenylpropane-1,3-dione (**168**)

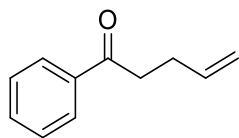


Following general procedure *GP-A* using 2-bromo-1,3-diphenylpropane-1,3-dione (**167**)^[194] (151.6 mg, 0.50 mmol, 1.0 equiv.), allyltrimethylsilane (**159**) (171.4 mg, 240.0 μ L, 1.50 mmol, 3.0 equiv.), *fac*-Ir(ppy)₃ (**49**) (3.3 mg, 5.0 μ mol, 1.0 mol%) and dry MeCN (1 mL) after irradiation for 44 h gave **168** (55.9 mg, 0.21 mmol, 42%) as yellow solid after flash chromatography purification (silica, hexanes / EA, 40:1).

R_f (hexanes / EA, 5:1): 0.44; **Staining**: vanillin (UV active). **¹H-NMR** (300 MHz, CDCl₃): δ_{H} (ppm) = 7.99 – 7.92 (m, 4H), 7.60 – 7.53 (m, 2H), 7.49 – 7.41 (m, 4H), 5.87 (ddt, J = 17.0, 10.1, 6.9 Hz, 1H), 5.29 (t, J = 6.7 Hz, 1H), 5.10 (dq, J = 17.1, 1.5 Hz, 1H), 5.02 (ddd, J = 10.1, 2.6, 1.1 Hz, 1H), 2.87 (tt, J = 6.8, 1.2 Hz, 2H). **¹³C-NMR** (75 MHz, CDCl₃): δ_{C} (ppm) = 195.54, 136.03, 135.11, 133.57, 128.92, 128.63, 117.27, 56.84, 33.58. **IR** (neat, ν/cm^{-1}): 3064, 2974, 2915, 1692, 1666, 1595, 1446, 1331, 1271, 1234, 1208, 1003, 924, 846, 801, 760, 686. **HRMS** (ESI): exact mass calculated for C₁₈H₁₆O₂ [M+H]⁺: m/z 265.1223, found: m/z 265.1229.

E Experimental part

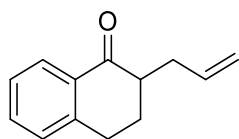
1-phenylpent-4-en-1-one (**173**)



Following general procedure *GP-A* using 2-chloroacetophenone (**172**) (77.3 mg, 0.50 mmol, 1.0 equiv.), allyltrimethylsilane (**159**) (171.4 mg, 240.0 μ L, 1.50 mmol, 3.0 equiv.), *fac*-Ir(ppy)₃ (**49**) (3.3 mg, 5.0 μ mol, 1.0 mol%) and dry MeCN (1 mL) after irradiation for 48 h gave **173** (57.3 mg, 0.36 mmol, 72%) as colorless liquid after flash chromatography purification (silica, hexanes / EA, 100:1).

R_f (hexanes / EA, 5:1): 0.71; **Staining**: vanillin (UV active). **¹H-NMR** (300 MHz, CDCl₃): δ_{H} (ppm) = 8.04 – 7.98 (m, 2H), 7.64 – 7.57 (m, 1H), 7.54 – 7.47 (m, 2H), 5.95 (ddt, J = 16.8, 10.2, 6.5 Hz, 1H), 5.13 (dq, J = 17.1, 1.6 Hz, 1H), 5.08 – 5.03 (m, 1H), 3.15 – 3.09 (m, 2H), 2.59 – 2.50 (m, 2H). **¹³C-NMR** (75 MHz, CDCl₃): δ_{C} (ppm) = 199.48, 137.34, 136.95, 133.05, 128.62, 128.06, 115.32, 37.76, 28.17. **IR** (neat, ν/cm^{-1}): 3068, 2978, 2919, 1685, 1595, 1446, 1413, 1361, 1249, 1208, 999, 910, 746, 690. **HRMS** (ESI): exact mass calculated for C₁₁H₁₂O [M+H]⁺: m/z 161.0961, found: m/z 161.0960.

2-allyl-3,4-dihydronaphthalen-1(2H)-one (**176**)

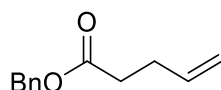


Following general procedure *GP-A* using 2-bromo-3,4-dihydronaphthalen-1(2H)-one (**174**)^[74] (112.5 mg, 0.50 mmol, 1.0 equiv.), allyltrimethylsilane (**159**) (171.4 mg, 240 μ L, 1.50 mmol, 3.0 equiv.), *fac*-Ir(ppy)₃ (**49**) (3.3 mg, 5.0 μ mol, 1.0 mol%) and dry MeCN (1 mL) after irradiation for 44 h gave **176** (59.6 mg, 0.32 mmol, 64%) as colorless liquid after flash chromatography purification (silica, hexanes / EA, 50:1).

R_f (hexanes / EA, 9:1): 0.53; **Staining**: vanillin (UV active). **¹H-NMR** (400 MHz, CDCl₃): δ_{H} (ppm) = 8.05 (dd, J = 7.8, 1.0 Hz, 1H), 7.47 (td, J = 7.5, 1.4 Hz, 1H), 7.31 (t, J = 7.6 Hz, 1H), 7.25 (d, J = 7.7 Hz, 1H), 5.92 – 5.80 (m, 1H), 5.11 (ddd, J = 11.1, 2.5, 1.3 Hz, 2H), 3.01 (dd, J = 7.7, 4.6 Hz, 2H), 2.77 (dddd, J = 10.9, 6.1, 2.9, 1.3 Hz, 1H), 2.56 (ddd, J = 12.8, 8.7, 4.5 Hz, 1H), 2.33 – 2.22 (m, 2H), 1.88 (ddt, J = 13.4, 11.8, 7.8 Hz, 1H). **¹³C-NMR** (101 MHz, CDCl₃): δ_{C} (ppm) = 199.48, 144.09, 136.25, 133.22, 132.55, 128.73, 127.50, 126.61, 116.85, 47.21, 34.07, 28.64, 27.98. **IR** (neat, ν/cm^{-1}): 3071, 2930, 2863, 1681, 1599, 1484, 1357, 1279, 1219, 1165, 995, 910, 775, 742. **HRMS** (EI): exact mass calculated for C₁₃H₁₄O [M]⁺: m/z 186.1039, found: m/z 186.1039.

E Experimental part

Benzyl pent-4-enoate (**178**)



Following general procedure *GP-A* using benzyl 2-bromoacetate (**177**) (114.5 mg, 0.50 mmol, 1.0 equiv.), allyltrimethylsilane (**159**) (171.4 mg, 240 μ L, 1.50 mmol, 3.0 equiv.), *fac*-Ir(ppy)₃ (**49**) (3.3 mg, 5.0 μ mol, 1.0 mol%) and dry MeCN (1 mL) after irradiation for 44 h gave **178** (72.6 mg, 0.38 mmol, 76%) as colorless liquid after flash chromatography purification (silica, hexanes / EA, 40:1).

R_f (hexanes / EA, 5:1): 0.64; **Staining**: vanillin (UV active). **¹H-NMR** (300 MHz, CDCl₃): δ_{H} (ppm) = 7.41 – 7.33 (m, 5H), 5.84 (ddt, J = 16.4, 10.3, 6.2 Hz, 1H), 5.14 (s, 2H), 5.11 – 4.99 (m, 2H), 2.52 – 2.39 (m, 4H). **¹³C-NMR** (75 MHz, CDCl₃): δ_{C} (ppm) = 172.91, 136.61, 136.00, 128.58, 128.25, 115.60, 66.25, 33.56, 28.87. **IR** (neat, ν/cm^{-1}): 3034, 3071, 2922, 1733, 1640, 1498, 1545, 1349, 1238, 1215, 1156, 992, 913, 842, 738, 697. **HRMS** (EI): exact mass calculated for C₁₂H₁₄O₂ [M]⁺: m/z 190.0988, found: m/z 190.0992.

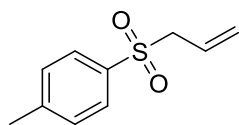
3. Visible-light mediated allylations of sulfonyl chlorides

General procedure *GP-B*

A 5 mL flame-dried Schlenk tube equipped with a magnetic stirring bar was charged with the sulfonyl chloride or *N*-chloroamine (0.50 mmol, 1.0 equiv.), Na₂CO₃ (53.0 mg, 0.50 mmol, 1.0 equiv.), Cu(dap)Cl₂ (**102**) (1.3 mg, 2.50 μ mol, 0.5 mol%) and dry MeCN (1 mL). The flask was sealed with a plastic screw cap and the mixture degassed using the freeze-pump-thaw method (3 cycles). Under N₂ atmosphere, allyltrimethylsilane (**159**) (171.4 mg, 240.0 μ L, 1.50 mmol, 3.0 equiv.) was added and the plastic screw cap replaced by another screw cap with a Teflon sealed inlet for a quartz glass rod. A high-power LED (λ = 530 nm) was attached to the top of the quartz glass rod. After irradiation for 18 – 24 h the LED was removed, and a solution of NaF (42.0 mg, 1.0 mmol, 2.0 equiv.) in H₂O (1 mL) was added and stirred for 1 h at 60 °C. The solution was transferred to a separating funnel and extracted with DCM (3 x 40 mL) and washed with H₂O (30 mL). The combined organic layers were dried over MgSO₄, the solvent removed *in vacuo* and the residue was purified by column chromatography (silica, hexanes / EA).

E Experimental part

1-(allylsulfonyl)-4-methylbenzene (**183**)



Following general procedure *GP-B* using tosyl chloride (**182**) (95.3 mg, 0.50 mmol, 1.0 equiv.), allyltrimethylsilane (**159**) (171.4 mg, 240.0 μ L, 1.50 mmol, 3.0 equiv.), Na_2CO_3 (53.0 mg, 0.50 mmol, 1.0 equiv.), NaF (42.0 mg, 1.0 mmol, 2.0 equiv.), $\text{Cu}(\text{dap})\text{Cl}_2$ (**102**) (1.3 mg, 2.50 μ mol, 0.5 mol%) and dry MeCN (1 mL) after irradiation for 18 h gave **183** (88.4 mg, 0.45 mmol, 90%) as a colorless liquid after flash chromatography purification (silica, hexanes / EA, 15:1).

R_f (hexanes / EA, 5:1): 0.22; **Staining**: KMnO_4 (UV active). $^1\text{H-NMR}$ (300 MHz, CDCl_3): δ_{H} (ppm) = 7.78 – 7.72 (m, 2H), 7.34 (d, J = 8.0 Hz, 2H), 5.79 (ddt, J = 17.5, 10.2, 7.4 Hz, 1H), 5.32 (dd, J = 10.1, 0.9 Hz, 1H), 5.15 (dq, J = 17.1, 1.2 Hz, 1H), 3.79 (dd, J = 7.4, 0.8 Hz, 2H), 2.44 (s, 3H). $^{13}\text{C-NMR}$ (75 MHz, CDCl_3): δ_{C} (ppm) = 144.77, 135.35, 129.70, 128.51, 124.80, 124.61, 60.95, 21.66. **IR** (neat, v/cm^{-1}): 2974, 2919, 1595, 1495, 1424, 1316, 1286, 1241, 1200, 1141, 1081, 992, 939, 872, 809, 708. **HRMS** (EI): exact mass calculated for $\text{C}_{10}\text{H}_{12}\text{O}_2\text{S}$ $[\text{M}]^+$: m/z 196.0553, found: m/z 196.0558.

Big scale

A 20 mL flame-dried Schlenk tube equipped with a magnetic stirring bar was charged with tosyl chloride (**182**) (953.2 mg, 5.0 mmol, 1.0 equiv.), Na_2CO_3 (529.9 mg, 5.0 mmol, 1.0 equiv.), $\text{Cu}(\text{dap})\text{Cl}_2$ (**102**) (13.2 mg, 25.0 μ mol, 0.5 mol%) and dry MeCN (10 mL). The flask was sealed with a plastic screw cap and the mixture degassed using the freeze-pump-thaw method (3 cycles). Under N_2 atmosphere, allyltrimethylsilane (**159**) (1.71 g, 2.40 mL, 15.0 mmol, 3.0 equiv.) was added and the plastic screw cap replaced by another screw cap with a Teflon sealed inlet for a quartz glass rod. A high-power LED (λ = 530 nm) was attached to the top of the quartz glass rod (see figure 6). After irradiation for 46 h the LED was removed, and a solution of NaF (420.0 mg, 10.0 mmol, 2.0 equiv.) in H_2O (10 mL) was added and stirred for 1 h at 60 $^\circ\text{C}$. The solution was transferred to a separating funnel and extracted with DCM (4 x 60 mL) and washed with H_2O (60 mL) and brine (60 mL). The combined organic layers were dried over MgSO_4 , the solvent removed *in vacuo* and the residue was purified by column chromatography (silica, hexanes / EA, 7:1) to obtain **183** (887.4 mg, 4.52 mmol, 90%) as a colorless oil.

E Experimental part

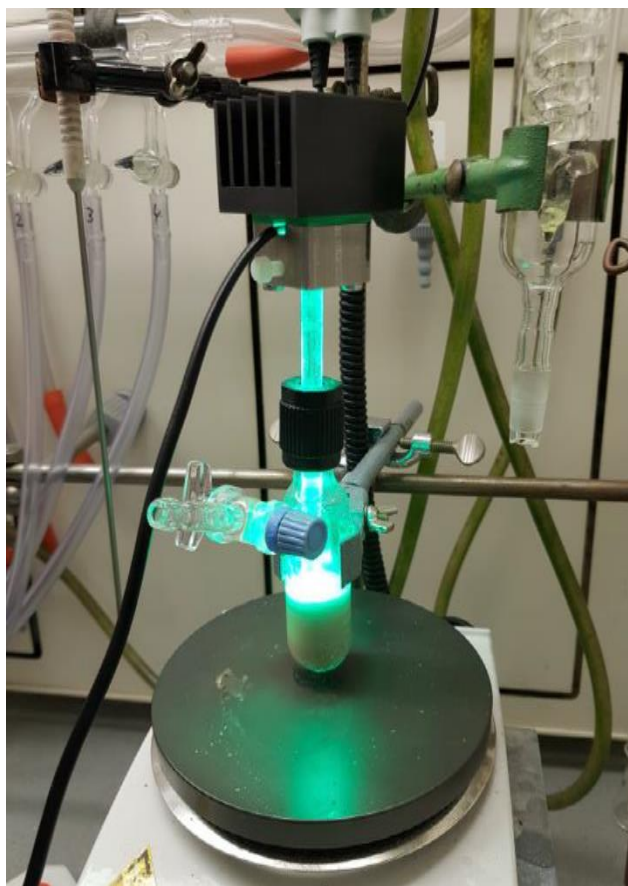
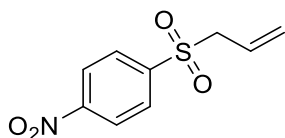


Figure 6. Big-scale set-up for the synthesis of 1-(allylsulfonyl)-4-methylbenzene (**183**).

1-(allylsulfonyl)-4-nitrobenzene (**186**)

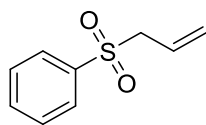


Following general procedure *GP-B* using 4-nitrobenzenesulfonyl chloride (**185**) (110.8 mg, 0.50 mmol, 1.0 equiv.), allyltrimethylsilane (**159**) (171.4 mg, 240.0 μ L, 1.50 mmol, 3.0 equiv.), Na_2CO_3 (53.0 mg, 0.50 mmol, 1.0 equiv.), NaF (42.0 mg, 1.0 mmol, 2.0 equiv.), $\text{Cu}(\text{dap})\text{Cl}_2$ (**102**) (1.3 mg, 2.50 μ mol, 0.5 mol%) and dry MeCN (1 mL) after irradiation for 24 h gave **186** (97.5 mg, 0.43 mmol, 86%) as a yellow solid after flash chromatography purification (silica, hexanes / EA, 6:1).

R_f (hexanes / EA, 3:1): 0.31; **Staining**: KMnO_4 (UV active). **¹H-NMR** (300 MHz, CDCl_3): δ_{H} (ppm) = 8.41 – 8.32 (m, 2H), 8.09 – 7.99 (m, 2H), 5.77 (ddt, J = 17.4, 10.1, 7.4 Hz, 1H), 5.34 (dd, J = 10.1, 0.7 Hz, 1H), 5.12 (dd, J = 17.1, 1.0 Hz, 1H), 3.84 (d, J = 7.4 Hz, 2H). **¹³C-NMR** (75 MHz, CDCl_3): δ_{C} (ppm) = 150.90, 143.62, 130.13, 125.72, 124.26, 123.97, 60.78. **IR** (neat, v/cm^{-1}): 3112, 3038, 2967, 2919, 2866, 1607, 1528, 1402, 1349, 1293, 1241, 1200, 1140, 1084, 1006, 951, 876, 727, 678. **HRMS** (ESI): exact mass calculated for $\text{C}_9\text{H}_9\text{NO}_4\text{S}$ [$\text{M}+\text{H}$]⁺: m/z 228.0325, found: m/z 228.0327.

E Experimental part

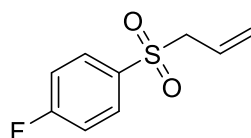
(Allylsulfonyl)benzene (**188**)



Following general procedure *GP-B* using benzenesulfonyl chloride (**187**) (88.3 mg, 64.0 μ L, 0.50 mmol, 1.0 equiv.), allyltrimethylsilane (**159**) (171.4 mg, 240.0 μ L, 1.50 mmol, 3.0 equiv.), Na_2CO_3 (53.0 mg, 0.50 mmol, 1.0 equiv.), NaF (42.0 mg, 1.0 mmol, 2.0 equiv.), $\text{Cu}(\text{dap})\text{Cl}_2$ (**102**) (1.3 mg, 2.50 μ mol, 0.5 mol%) and dry MeCN (1 mL) after irradiation for 24 h gave **188** (72.8 mg, 0.40 mmol, 80%) as a colorless liquid after flash chromatography purification (silica, hexanes / EA, 10:1).

R_f (hexanes / EA, 5:1): 0.26; **Staining**: KMnO_4 (UV active). $^1\text{H-NMR}$ (300 MHz, CDCl_3): δ_{H} (ppm) = 7.91 – 7.83 (m, 2H), 7.69 – 7.61 (m, 1H), 7.60 – 7.50 (m, 2H), 5.79 (ddt, J = 17.3, 10.1, 7.4 Hz, 1H), 5.33 (dd, J = 10.1, 0.8 Hz, 1H), 5.14 (dq, J = 17.1, 1.1 Hz, 1H), 3.81 (dd, J = 7.4, 0.9 Hz, 2H). $^{13}\text{C-NMR}$ (75 MHz, CDCl_3): δ_{C} (ppm) = 138.26, 133.79, 129.08, 128.51, 124.78, 124.63, 60.89. **IR** (neat, v/cm^{-1}): 3064, 2974, 2922, 1640, 1584, 1480, 1446, 1398, 1308, 1241, 1141, 1085, 992, 936, 872, 790, 686. **HRMS** (EI): exact mass calculated for $\text{C}_9\text{H}_{10}\text{O}_2\text{S}$ $[\text{M}]^+$: m/z 182.0396, found: m/z 182.0395.

1-(allylsulfonyl)-4-fluorobenzene (**190**)

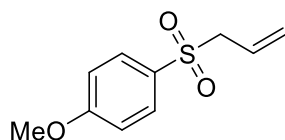


Following general procedure *GP-B* using 4-fluorobenzenesulfonyl chloride (**189**) (97.3 mg, 0.50 mmol, 1.0 equiv.), allyltrimethylsilane (**159**) (171.4 mg, 240.0 μ L, 1.50 mmol, 3.0 equiv.), Na_2CO_3 (53.0 mg, 0.50 mmol, 1.0 equiv.), NaF (42.0 mg, 1.0 mmol, 2.0 equiv.), $\text{Cu}(\text{dap})\text{Cl}_2$ (**102**) (1.3 mg, 2.50 μ mol, 0.5 mol%) and dry MeCN (1 mL) after irradiation for 20 h gave **190** (92.6 mg, 0.46 mmol, 90%) as a colorless liquid after flash chromatography purification (silica, hexanes / EA, 7:1).

R_f (hexanes / EA, 5:1): 0.22; **Staining**: KMnO_4 (UV active). $^1\text{H-NMR}$ (400 MHz, CDCl_3): δ_{H} (ppm) = 7.87 (ddd, J = 8.0, 5.0, 2.5 Hz, 2H), 7.25 – 7.20 (m, 2H), 5.78 (ddt, J = 17.5, 10.1, 7.4 Hz, 1H), 5.34 (dd, J = 10.2, 0.7 Hz, 1H), 5.14 (dd, J = 17.1, 1.1 Hz, 1H), 3.80 (d, J = 7.4 Hz, 2H). $^{13}\text{C-NMR}$ (101 MHz, CDCl_3): δ_{C} (ppm) = 131.52, 131.39, 124.99, 124.60, 116.57, 116.27, 61.04. $^{19}\text{F-NMR}$ (376 MHz, CDCl_3): δ_{F} (ppm) = -103.86. **IR** (neat, v/cm^{-1}): 3105, 3079, 2979, 2922, 1588, 1495, 1405, 1320, 1230, 1141, 1085, 936, 839, 682. **HRMS** (ESI): exact mass calculated for $\text{C}_9\text{H}_9\text{FO}_2\text{S}$ $[\text{M}+\text{H}]^+$: m/z 201.0386, found: m/z 201.0383.

E Experimental part

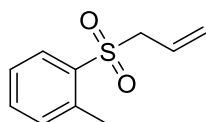
1-(allylsulfonyl)-4-methoxybenzene (**192**)



Following general procedure *GP-B* using 4-methoxybenzenesulfonyl chloride (**191**) (103.3 mg, 0.50 mmol, 1.0 equiv.), allyltrimethylsilane (**159**) (171.4 mg, 240.0 μ L, 1.50 mmol, 3.0 equiv.), Na_2CO_3 (53.0 mg, 0.50 mmol, 1.0 equiv.), NaF (42.0 mg, 1.0 mmol, 2.0 equiv.), $\text{Cu}(\text{dap})\text{Cl}_2$ (**102**) (1.3 mg, 2.50 μ mol, 0.5 mol%) and dry MeCN (1 mL) after irradiation for 20 h gave **192** (103.6 mg, 0.49 mmol, 98%) as a colorless liquid after flash chromatography purification (silica, hexanes / EA, 7:1).

R_f (hexanes / EA, 3:1): 0.31; **Staining**: KMnO_4 (UV active). $^1\text{H-NMR}$ (300 MHz, CDCl_3): δ_{H} (ppm) = 7.82 – 7.74 (m, 2H), 7.02 – 6.96 (m, 2H), 5.78 (ddt, J = 17.5, 10.1, 7.4 Hz, 1H), 5.31 (dd, J = 10.2, 1.0 Hz, 1H), 5.14 (dq, J = 17.1, 1.2 Hz, 1H), 3.87 (s, 3H), 3.80 – 3.75 (m, 2H). $^{13}\text{C-NMR}$ (75 MHz, CDCl_3): δ_{C} (ppm) = 163.76, 130.68, 129.90, 124.99, 124.49, 114.22, 61.15, 55.69. **IR** (neat, v/cm^{-1}): 3079, 3015, 2974, 2844, 1595, 1498, 1461, 1293, 1260, 1133, 1088, 1021, 872, 835, 682. **HRMS** (ESI): exact mass calculated for $\text{C}_{10}\text{H}_{12}\text{O}_3\text{S}$ $[\text{M}+\text{H}]^+$: m/z 213.0585, found: m/z 213.0584.

1-(allylsulfonyl)-2-methylbenzene (**194**)

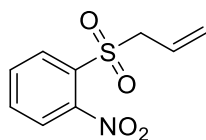


Following general procedure *GP-B* using 2-methylbenzenesulfonyl chloride (**193**) (95.3 mg, 0.50 mmol, 1.0 equiv.), allyltrimethylsilane (**159**) (171.4 mg, 240.0 μ L, 1.50 mmol, 3.0 equiv.), Na_2CO_3 (53.0 mg, 0.50 mmol, 1.0 equiv.), NaF (42.0 mg, 1.0 mmol, 2.0 equiv.), $\text{Cu}(\text{dap})\text{Cl}_2$ (**102**) (1.3 mg, 2.50 μ mol, 0.5 mol%) and dry MeCN (1 mL) after irradiation for 20 h gave **194** (73.9 mg, 0.37 mmol, 75%) as a colorless liquid after flash chromatography purification (silica, hexanes / EA, 7:1).

R_f (hexanes / EA, 5:1): 0.28; **Staining**: KMnO_4 (UV active). $^1\text{H-NMR}$ (300 MHz, CDCl_3): δ_{H} (ppm) = 7.92 (d, J = 7.9 Hz, 1H), 7.49 (td, J = 7.5, 1.3 Hz, 1H), 7.33 (ddd, J = 5.4, 3.1, 1.2 Hz, 2H), 5.83 – 5.66 (m, 1H), 5.33 – 5.11 (m, 2H), 3.84 (d, J = 7.4 Hz, 2H), 2.69 (s, 3H). $^{13}\text{C-NMR}$ (75 MHz, CDCl_3): δ_{C} (ppm) = 138.07, 136.47, 133.77, 132.65, 130.78, 126.47, 124.62, 124.48, 60.07, 20.57. **IR** (neat, v/cm^{-1}): 3064, 3023, 2982, 2922, 1640, 1454, 1312, 1238, 1148, 1059, 992, 936, 872, 805, 757, 708. **HRMS** (ESI): exact mass calculated for $\text{C}_{10}\text{H}_{13}\text{O}_2\text{S}$ $[\text{M}+\text{H}]^+$: m/z 197.0631, found: m/z 197.0633.

E Experimental part

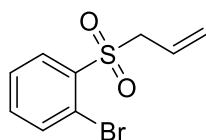
1-(allylsulfonyl)-2-nitrobenzene (**196**)



Following general procedure *GP-B* using 2-nitrobenzenesulfonyl chloride (**195**) (110.8 mg, 0.50 mmol, 1.0 equiv.), allyltrimethylsilane (**159**) (171.4 mg, 240.0 μ L, 1.50 mmol, 3.0 equiv.), Na_2CO_3 (53.0 mg, 0.50 mmol, 1.0 equiv.), NaF (42.0 mg, 1.0 mmol, 2.0 equiv.), $\text{Cu}(\text{dap})\text{Cl}_2$ (**102**) (1.3 mg, 2.50 μ mol, 0.5 mol%) and dry MeCN (1 mL) after irradiation for 24 h gave **196** (70.8 mg, 0.31 mmol, 62%) as a yellow solid after flash chromatography purification (silica, hexanes / EA, 5:1).

R_f (hexanes / EA, 3:1): 0.20; **Staining**: KMnO_4 (UV active). $^1\text{H-NMR}$ (300 MHz, CDCl_3): δ_{H} (ppm) = 8.08 – 8.02 (m, 1H), 7.84 – 7.69 (m, 3H), 5.83 (ddt, J = 17.5, 10.1, 7.5 Hz, 1H), 5.41 – 5.28 (m, 2H), 4.31 – 4.25 (m, 2H). $^{13}\text{C-NMR}$ (75 MHz, CDCl_3): δ_{C} (ppm) = 134.87, 133.02, 132.28, 132.01, 125.87, 124.88, 124.07, 61.06. **IR** (neat, v/cm^{-1}): 3093, 3019, 2993, 2914, 1595, 1536, 1420, 1357, 1320, 1241, 1141, 1085, 992, 783, 697. **HRMS** (ESI): exact mass calculated for $\text{C}_9\text{H}_9\text{NO}_4\text{S}$ $[\text{M}+\text{H}]^+$: m/z 228.0325, found: m/z 228.0328.

1-(allylsulfonyl)-2-bromobenzene (**198**)

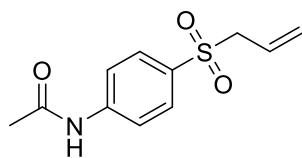


Following general procedure *GP-B* using 2-bromobenzenesulfonyl chloride (**197**) (127.7 mg, 0.50 mmol, 1.0 equiv.), allyltrimethylsilane (**159**) (171.4 mg, 240.0 μ L, 1.50 mmol, 3.0 equiv.), Na_2CO_3 (53.0 mg, 0.50 mmol, 1.0 equiv.), NaF (42.0 mg, 1.0 mmol, 2.0 equiv.), $\text{Cu}(\text{dap})\text{Cl}_2$ (**102**) (1.3 mg, 2.50 μ mol, 0.5 mol%) and dry MeCN (1 mL) after irradiation for 24 h gave **198** (117.6 mg, 0.45 mmol, 90%) as a colorless oil after flash chromatography purification (silica, hexanes / EA, 8:1).

R_f (hexanes / EA, 5:1): 0.22; **Staining**: KMnO_4 (UV active). $^1\text{H-NMR}$ (400 MHz, CDCl_3): δ_{H} (ppm) = 8.07 (dd, J = 7.6, 2.0 Hz, 1H), 7.73 (dd, J = 7.6, 1.5 Hz, 1H), 7.49 – 7.41 (m, 2H), 5.72 (ddt, J = 17.5, 10.2, 7.4 Hz, 1H), 5.28 – 5.19 (m, 2H), 4.16 (d, J = 7.4 Hz, 2H). $^{13}\text{C-NMR}$ (101 MHz, CDCl_3): δ_{C} (ppm) = 137.47, 135.32, 134.79, 132.64, 127.88, 125.04, 124.17, 120.75, 58.16. **IR** (neat, v/cm^{-1}): 3086, 2982, 2922, 1640, 1573, 1424, 1252, 1316, 1144, 1021, 936, 872, 757. **HRMS** (ESI): exact mass calculated for $\text{C}_9\text{H}_9\text{BrO}_2\text{S}$ $[\text{M}+\text{H}]^+$: m/z 260.9579, found: m/z 260.9579.

E Experimental part

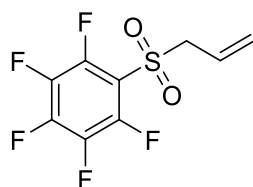
N-(4-(allylsulfonyl)phenyl)acetamide (**200**)



Following general procedure *GP-B* using 4-acetamidobenzenesulfonyl chloride (**199**) (116.8 mg, 0.50 mmol, 1.0 equiv.), allyltrimethylsilane (**159**) (171.4 mg, 240.0 μ L, 1.50 mmol, 3.0 equiv.), Na_2CO_3 (53.0 mg, 0.50 mmol, 1.0 equiv.), NaF (42.0 mg, 1.0 mmol, 2.0 equiv.), $\text{Cu}(\text{dap})\text{Cl}_2$ (**102**) (1.3 mg, 2.50 μ mol, 0.5 mol%) and dry MeCN (1 mL) after irradiation for 19 h gave **200** (96.9 mg, 0.41 mmol, 81%) as a white solid after flash chromatography purification (silica, hexanes / EA, 2:1).

R_f (hexanes / EA, 1:2): 0.31; **Staining**: KMnO_4 (UV active). $^1\text{H-NMR}$ (400 MHz, CDCl_3): δ_{H} (ppm) = 7.79 – 7.75 (m, 2H), 7.72 (s, 1H), 7.69 (d, J = 8.8 Hz, 2H), 5.77 (ddt, J = 17.5, 10.1, 7.4 Hz, 1H), 5.32 (dd, J = 10.2, 0.7 Hz, 1H), 5.14 (dd, J = 17.1, 1.1 Hz, 1H), 3.78 (d, J = 7.4 Hz, 2H), 2.20 (d, J = 3.0 Hz, 3H). $^{13}\text{C-NMR}$ (101 MHz, CDCl_3): δ_{C} (ppm) = 168.84, 143.04, 132.75, 129.84, 124.87, 124.63, 119.19, 61.05, 24.77. **IR** (neat, v/cm^{-1}): 3358, 3317, 3272, 3191, 3116, 3056, 2922, 1677, 1588, 1323, 1260, 1137, 1085, 872, 787, 708. **HRMS** (ESI): exact mass calculated for $\text{C}_{11}\text{H}_{13}\text{NO}_3\text{S}$ $[\text{M}+\text{H}]^+$: m/z 240.0689, found: m/z 240.0695.

1-(allylsulfonyl)-2,3,4,5,6-pentafluorobenzene (**202**)



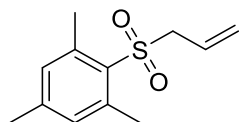
Following general procedure *GP-B* using 2,3,4,5,6-pentafluorobenzenesulfonyl chloride (**201**) (133.3 mg, 0.50 mmol, 1.0 equiv.), allyltrimethylsilane (**159**) (171.4 mg, 240.0 μ L, 1.50 mmol, 3.0 equiv.), Na_2CO_3 (53.0 mg, 0.50 mmol, 1.0 equiv.), NaF (42.0 mg, 1.0 mmol, 2.0 equiv.), $\text{Cu}(\text{dap})\text{Cl}_2$ (**102**) (1.3 mg, 2.50 μ mol, 0.5 mol%) and dry MeCN (1 mL) after irradiation for 20 h gave **202** (61.66 mg, 0.23 mmol, 45%) as a white solid after flash chromatography purification (silica, hexanes / EA, 10:1).

R_f (hexanes / EA, 5:1): 0.27; **Staining**: KMnO_4 (UV active). $^1\text{H-NMR}$ (300 MHz, CDCl_3): δ_{H} (ppm) = 5.89 (ddt, J = 17.5, 10.1, 7.4 Hz, 1H), 5.44 (dd, J = 10.1, 0.8 Hz, 1H), 5.30 (dd, J = 17.0, 1.0 Hz, 1H), 4.03 (d, J = 7.2 Hz, 2H). $^{13}\text{C-NMR}$ (75 MHz, CDCl_3): δ_{C} (ppm) = 126.36, 123.40, 62.13 (aromatic carbons not visible). $^{19}\text{F-NMR}$ (282 MHz, CDCl_3): δ_{F} (ppm) = -135.42 – -135.65 (m), -143.13 (tt, J = 21.1,

E Experimental part

7.5 Hz), -158.04 – -158.49 (m). **IR** (neat, ν/cm^{-1}): 2978, 2922, 1640, 1495, 1398, 1353, 1293, 1245, 1148, 1088, 984, 950, 883, 813, 842, 779, 726. **HRMS** (ESI): exact mass calculated for $\text{C}_9\text{H}_5\text{F}_5\text{O}_2\text{S}$ $[\text{M}+\text{H}]^+$: m/z 273.0003, found: m/z 273.0003.

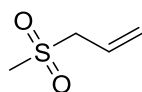
2-(allylsulfonyl)-1,3,5-trimethylbenzene (**204**)



Following general procedure *GP-B* using 1,3,5-trimethylbenzenesulfonyl chloride (**203**) (109.4 mg, 0.50 mmol, 1.0 equiv.), allyltrimethylsilane (**159**) (171.4 mg, 240.0 μL , 1.50 mmol, 3.0 equiv.), Na_2CO_3 (53.0 mg, 0.50 mmol, 1.0 equiv.), NaF (42.0 mg, 1.0 mmol, 2.0 equiv.), $\text{Cu}(\text{dap})\text{Cl}_2$ (**102**) (1.3 mg, 2.50 μmol , 0.5 mol%) and dry MeCN (1 mL) after irradiation for 23 h gave **204** (12.6 mg, 0.06 mmol, 11%) as a white solid after flash chromatography purification (silica, hexanes / EA, 10:1).

R_f (hexanes / EA, 5:1): 0.40; **Staining**: KMnO_4 (UV active). **$^1\text{H-NMR}$** (300 MHz, CDCl_3): δ_{H} (ppm) = 6.95 (s, 2H), 5.81 (ddt, J = 17.5, 10.1, 7.4 Hz, 1H), 5.32 (d, J = 10.1 Hz, 1H), 5.19 (dd, J = 17.0, 1.2 Hz, 1H), 3.81 (d, J = 7.4 Hz, 2H), 2.65 (s, 6H), 2.30 (s, 3H). **$^{13}\text{C-NMR}$** (75 MHz, CDCl_3): δ_{C} (ppm) = 142.30, 139.23, 131.34, 131.11, 123.55, 123.47, 59.70, 22.05, 19.99. **IR** (neat, ν/cm^{-1}): 2963, 2922, 2855, 1733, 1602, 1562, 1439, 1398, 1308, 1260, 1141, 1081, 1033, 943, 850, 783. **HRMS** (ESI): exact mass calculated for $\text{C}_{12}\text{H}_{16}\text{O}_2\text{S}$ $[\text{M}+\text{H}]^+$: m/z 225.0944, found: m/z 225.0949.

3-(methylsulfonyl)prop-1-ene (**206**)

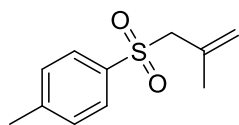


Following general procedure *GP-B* using methylsulfonyl chloride (**205**) (57.3 mg, 39.0 μL , 0.50 mmol, 1.0 equiv.), allyltrimethylsilane (**159**) (171.4 mg, 240.0 μL , 1.50 mmol, 3.0 equiv.), Na_2CO_3 (53.0 mg, 0.50 mmol, 1.0 equiv.), NaF (42.0 mg, 1.0 mmol, 2.0 equiv.), $\text{Cu}(\text{dap})\text{Cl}_2$ (**102**) (1.3 mg, 2.50 μmol , 0.5 mol%) and dry MeCN (1 mL) after irradiation for 24 h gave **206** (30.4 mg, 0.28 mmol, 57%) as a colorless liquid after flash chromatography purification (silica, hexanes / EA, 4:1).

R_f (hexanes / EA, 3:1): 0.11; **Staining**: KMnO_4 . **$^1\text{H-NMR}$** (300 MHz, CDCl_3): δ_{H} (ppm) = 5.99 (ddt, J = 17.6, 10.2, 7.4 Hz, 1H), 5.57 – 5.44 (m, 2H), 3.78 – 3.72 (m, 2H), 2.89 (t, J = 0.7 Hz, 3H). **$^{13}\text{C-NMR}$** (75 MHz, CDCl_3): δ_{C} (ppm) = 126.22, 125.61, 60.35, 39.88. **IR** (neat, ν/cm^{-1}): 3019, 2930, 1640, 1423, 1290, 1245, 1200, 1129, 1081, 995, 939, 880, 738. **HRMS** (ESI): exact mass calculated for $\text{C}_4\text{H}_8\text{O}_2\text{S}$ $[\text{M}+\text{NH}_4]^+$: m/z 138.0583, found: m/z 138.0583.

E Experimental part

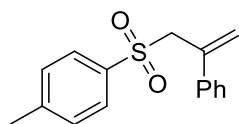
1-methyl-4-((2-methylallyl)sulfonyl)benzene (**207**)



Following general procedure *GP-B* using tosyl chloride (**182**) (95.3 mg, 0.50 mmol, 1.0 equiv.), trimethyl(2-methylallyl)silane (**161**) (192.4 mg, 260.0 μ L, 1.5 mmol, 3.0 equiv.), Na_2CO_3 (53.0 mg, 0.50 mmol, 1.0 equiv.), NaF (42.0 mg, 1.0 mmol, 2.0 equiv.), $\text{Cu}(\text{dap})\text{Cl}_2$ (**102**) (1.3 mg, 2.50 μ mol, 0.5 mol%) and dry MeCN (1 mL) after irradiation for 20 h gave **207** (72.2 mg, 0.34 mmol, 69%) as a colorless liquid after flash chromatography purification (silica, hexanes / EA, 10:1).

R_f (hexanes / EA, 5:1): 0.29; **Staining**: KMnO_4 (UV active). $^1\text{H-NMR}$ (400 MHz, CDCl_3): δ_{H} (ppm) = 7.75 (d, J = 8.2 Hz, 2H), 7.33 (d, J = 8.0 Hz, 2H), 5.04 – 5.00 (m, 1H), 4.69 (s, 1H), 3.74 (s, 2H), 2.44 (s, 3H), 1.86 (s, 3H). $^{13}\text{C-NMR}$ (101 MHz, CDCl_3): δ_{C} (ppm) = 144.64, 135.52, 133.55, 129.62, 128.53, 120.66, 64.54, 22.73, 21.66. **IR** (neat, v/cm^{-1}): 2960, 2915, 1759, 1730, 1439, 1282, 1197, 1144, 1085, 1036, 913, 839, 708, 682. **HRMS** (EI): exact mass calculated for $\text{C}_{11}\text{H}_{14}\text{O}_2\text{S}$ $[\text{M}]^+$: m/z 210.0709, found: m/z 210.0707.

1-methyl-4-((2-phenylallyl)sulfonyl)benzene (**208**)



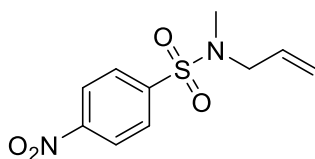
Following general procedure *GP-B* using tosyl chloride (**182**) (95.3 mg, 0.50 mmol, 1.0 equiv.), trimethyl(2-phenylallyl)silane (**163**)^[195] (285.5 mg, 310.0 μ L, 1.50 mmol, 3.0 equiv.), Na_2CO_3 (53.0 mg, 0.50 mmol, 1.0 equiv.), $\text{Cu}(\text{dap})\text{Cl}_2$ (**102**) (1.3 mg, 2.50 μ mol, 0.5 mol%) and dry MeCN (1 mL) after irradiation for 23 h gave **208** (88.0 mg, 0.32 mmol, 65%) as a white solid after flash chromatography purification (silica, hexanes / EA, 10:1).

R_f (hexanes / EA, 5:1): 0.27; **Staining**: KMnO_4 (UV active). $^1\text{H-NMR}$ (400 MHz, CDCl_3): δ_{H} (ppm) = 7.66 (d, J = 8.2 Hz, 2H), 7.25 (dt, J = 6.9, 4.5 Hz, 7H), 5.59 (s, 1H), 5.22 (s, 1H), 4.25 (s, 2H), 2.39 (s, 3H). $^{13}\text{C-NMR}$ (101 MHz, CDCl_3): δ_{C} (ppm) = 144.61, 138.92, 136.64, 135.51, 129.52, 128.71, 128.38, 127.95, 126.26, 121.75, 62.19, 21.60. **IR** (neat, v/cm^{-1}): 3027, 2933, 1625, 1495, 1446, 1402, 1312, 1245, 1133, 1174, 1085, 898, 809, 772, 697. **HRMS** (ESI): exact mass calculated for $\text{C}_{16}\text{H}_{16}\text{O}_2\text{S}$ $[\text{M}+\text{H}]^+$: m/z 273.0944, found: m/z 273.0944.

E Experimental part

4. Visible-light mediated allylations of *N*-chloro-amines

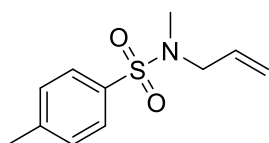
N-allyl-*N*-methyl-4-nitrobenzenesulfonamide (**212**)



Following general procedure *GP-B* using *N*-chloro-*N*-methyl-4-nitrobenzenesulfonamide (**211**)^[124] (125.3 mg, 0.50 mmol, 1.0 equiv.), allyltrimethylsilane (**159**) (171.4 mg, 240.0 μ L, 1.50 mmol, 3.0 equiv.), Na₂CO₃ (53.0 mg, 0.50 mmol, 1.0 equiv.), NaF (42.0 mg, 1.0 mmol, 2.0 equiv.), Cu(dap)Cl₂ (**102**) (1.3 mg, 2.50 μ mol, 0.5 mol%) and dry MeCN (1 mL) after irradiation for 18 h gave **212** (98.6 mg, 0.38 mmol, 77%) as yellow solid after flash chromatography purification (silica, hexanes / EA, 7:1).

R_f (hexanes / EA, 5:1): 0.29; **Staining**: KMnO₄ (UV active). **¹H-NMR** (300 MHz, CDCl₃): δ_{H} (ppm) = 8.37 – 8.30 (m, 2H), 7.97 – 7.91 (m, 2H), 5.71 – 5.57 (m, 1H), 5.22 – 5.13 (m, 2H), 3.67 (d, J = 6.3 Hz, 2H), 2.71 (s, 3H). **¹³C-NMR** (75 MHz, CDCl₃): δ_{C} (ppm) = 150.07, 143.81, 131.65, 128.56, 124.42, 119.89, 52.99, 34.20. **IR** (neat, ν/cm^{-1}): 3120, 2956, 2922, 2851, 1644, 1607, 1528, 1446, 1398, 1342, 1305, 1208, 1163, 1126, 1062, 984, 936, 854, 828, 760, 682. **HRMS** (ESI): exact mass calculated for C₁₀H₁₂N₂O₄S [M+H]⁺: m/z 247.0591, found: m/z 257.0593.

N-allyl-*N*,4-dimethylbenzenesulfonamide (**214**)



Following general procedure *GP-B* using *N*-chloro-*N*,4-dimethylbenzenesulfonamide (**213**)^[124] (109.8 mg, 0.50 mmol, 1.0 equiv.), allyltrimethylsilane (**159**) (171.4 mg, 240.0 μ L, 1.50 mmol, 3.0 equiv.), Na₂CO₃ (53.0 mg, 0.50 mmol, 1.0 equiv.), NaF (42.0 mg, 1.0 mmol, 2.0 equiv.), Cu(dap)Cl₂ (**102**) (1.3 mg, 2.50 μ mol, 0.5 mol%) and dry MeCN (1 mL) after irradiation for 20 h gave **214** (55.3 mg, 0.25 mmol, 49%) as yellow solid after flash chromatography purification (silica, hexanes / EA, 10:1).

R_f (hexanes / EA, 5:1): 0.49; **Staining**: KMnO₄ (UV active). **¹H-NMR** (400 MHz, CDCl₃): δ_{H} (ppm) = 7.67 (d, J = 8.2 Hz, 2H), 7.32 (d, J = 8.0 Hz, 2H), 5.71 (ddt, J = 16.2, 9.8, 6.3 Hz, 1H), 5.19 (ddd, J = 12.5, 3.1, 1.4 Hz, 2H), 3.62 (d, J = 6.3 Hz, 2H), 2.66 (s, 3H), 2.43 (s, 3H). **¹³C-NMR** (101 MHz, CDCl₃): δ_{C} (ppm) = 143.40, 134.52, 132.65, 129.70, 127.52, 119.11, 53.08, 34.22, 21.53. **IR** (neat, ν/cm^{-1}): 3068,

E Experimental part

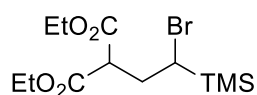
3015, 2967, 2922, 1644, 1599, 1495 1454, 1334, 1204, 1156, 1089, 984, 913, 816, 753. **HRMS** (ESI): exact mass calculated for $C_{11}H_{15}NO_2S$ $[M+H]^+$: m/z 226.0896, found: m/z 226.0898.

5. Atom transfer radical additions with vinyltrimethylsilane

General procedure GP-C

A 5 mL flame-dried Schlenk tube equipped with a magnetic stirring bar was charged with the carbohalide (0.50 mmol, 1.0 equiv.), *fac*-Ir(ppy)₃ (**49**) (1.6 mg, 2.50 μ mol, 0.5 mol%) and dry MeCN (1 mL). The flask was sealed with a plastic screw cap and the mixture degassed using the freeze-pump-thaw method (3 cycles). Under N₂ atmosphere, vinyltrimethylsilane (**230**) (75.2 mg, 110.0 μ L, 0.75 mmol, 1.5 equiv.) was added and the plastic screw cap replaced by another screw cap with a Teflon sealed inlet for a quartz glass rod. A high-power LED (λ = 455 nm) was attached to the top of the quartz glass rod. After irradiation for 17 – 24 h the LED was removed, and the solvent evaporated *in vacuo*. The residue was purified by column chromatography (silica, hexanes / EA).

Diethyl 2-(2-bromo-2-(trimethylsilyl)ethyl)malonate (**231**)



Following general procedure GP-C using diethyl 2-bromomalonate (**127**) (119.5 mg, 0.50 mmol, 1.0 equiv.), vinyltrimethylsilane (**230**) (75.2 mg, 110.0 μ L, 0.75 mmol, 1.5 equiv.), *fac*-Ir(ppy)₃ (**49**) (1.6 mg, 2.50 μ mol, 0.5 mol%) and dry MeCN (1 mL) after irradiation for 17 h gave **231** (149.7 mg, 0.44 mmol, 88%) as a colorless liquid after flash chromatography purification (silica, hexanes / EA, 10:1).

R_f (hexanes / EA, 5:1): 0.56, **Staining**: KMnO₄ (UV active). **¹H-NMR** (400 MHz, CDCl₃): δ_H (ppm) = 4.28 – 4.17 (m, 4H), 3.88 (dd, J = 11.0, 3.3 Hz, 1H), 3.21 (dd, J = 13.1, 2.1 Hz, 1H), 2.47 (ddd, J = 15.0, 11.0, 2.1 Hz, 1H), 2.11 (ddd, J = 15.0, 13.2, 3.3 Hz, 1H), 1.28 (td, J = 7.1, 5.1 Hz, 6H), 0.16 (s, 9H). **¹³C-NMR** (101 MHz, CDCl₃): δ_C (ppm) = 169.37, 168.83, 61.65, 61.49, 51.17, 41.26, 32.59, 14.11, 14.05, -3.23. **IR** (neat, ν/cm^{-1}): 2982, 2907, 1730, 1372, 1338, 1252, 1178, 1148, 1033, 839, 753. **HRMS** (ESI): exact mass calculated for $C_{12}H_{23}BrO_4Si$ $[M+Na]^+$: m/z 361.0441, found: m/z 361.0444.

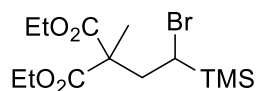
Big scale

A 20 mL flame-dried Schlenk tube equipped with a magnetic stirring bar was charged with diethyl 2-bromomalonate (**127**) (1.2 g, 850.0 μ L, 5.0 mmol, 1.0 equiv.), *fac*-Ir(ppy)₃ (**49**) (16.4 mg, 25.0 μ mol, 0.5 mol%) and dry MeCN (10 mL). The flask was sealed with a plastic screw cap and the mixture degassed using the freeze-pump-thaw method (3 cycles). Under N₂ atmosphere, vinyltrimethylsilane

E Experimental part

(230) (751.7 mg, 1.10 mL, 7.5 mmol, 1.5 equiv.) was added and the plastic screw cap replaced by another screw cap with a Teflon sealed inlet for a quartz glass rod. A high-power LED ($\lambda = 455$ nm) was attached to the top of the quartz glass rod and two additional LEDs were placed next to the flask. After irradiation for 24 h the LEDs were removed, and the solvent evaporated *in vacuo*. The residue was purified by Kugelrohr distillation (1.4 mbar, 95 °C) to obtain **231** (1.6 g, 4.7 mmol, 94%) as colorless liquid.

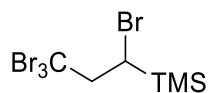
Diethyl 2-(2-bromo-2-(trimethylsilyl)ethyl)-2-methylmalonate (**265**)



Following general procedure *GP-C* using diethyl 2-bromo-2-methylmalonate (**165**) (126.5 mg, 0.50 mmol, 1.0 equiv.), vinyltrimethylsilane (**230**) (75.2 mg, 110.0 μ L, 0.75 mmol, 1.5 equiv.), *fac*-Ir(ppy)₃ (**49**) (1.6 mg, 2.50 μ mol, 0.5 mol%) and dry MeCN (1 mL) after irradiation for 23 h gave **265** (95.6 mg, 0.27 mmol, 54%) as a colorless oil after flash chromatography purification (silica, hexanes / EA, 30:1).

R_f (hexanes / EA, 5:1): 0.58, **Staining**: KMnO₄ (UV active). **¹H-NMR** (300 MHz, CDCl₃): δ_H (ppm) = 4.19 (qd, $J = 7.2, 2.3$ Hz, 4H), 3.28 (dd, $J = 10.5, 2.4$ Hz, 1H), 2.54 (dd, $J = 16.1, 2.5$ Hz, 1H), 2.44 (dd, $J = 16.1, 10.5$ Hz, 1H), 1.52 (s, 3H), 1.26 (td, $J = 7.1, 2.9$ Hz, 6H), 0.16 (s, 9H). **¹³C-NMR** (75 MHz, CDCl₃): δ_C (ppm) = 172.11, 172.01, 61.61, 61.38, 53.77, 38.66, 37.08, 19.75, 13.99, 13.94, -3.19. **IR** (neat, ν/cm^{-1}): 2982, 2907, 1730, 1446, 1379, 1305, 1252, 1185, 1103, 1023, 943, 839, 753, 716. **HRMS** (ESI): exact mass calculated for C₁₃H₂₅BrO₄Si [M+H]⁺: m/z 353.0778, found: m/z 353.0781.

Trimethyl(1,3,3,3-tetrabromopropyl)silane (**267**)



Following general procedure *GP-C* using tetrabromomethane (**266**) (165.8 mg, 0.50 mmol, 1.0 equiv.), vinyltrimethylsilane (**230**) (75.2 mg, 110.0 μ L, 0.75 mmol, 1.5 equiv.), *fac*-Ir(ppy)₃ (**49**) (1.6 mg, 2.50 μ mol, 0.5 mol%) and dry MeCN (1 mL) after irradiation for 24 h gave **267** (172.5 mg, 0.40 mmol, 80%) as a colorless liquid after flash chromatography purification (silica, hexanes).

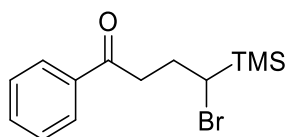
R_f (hexanes / EA, 5:1): 0.64, **Staining**: KMnO₄ (UV active). **¹H-NMR** (300 MHz, CDCl₃): δ_H (ppm) = 3.50 (d, $J = 4.7$ Hz, 2H), 3.33 (t, $J = 4.8$ Hz, 1H), 0.20 (s, 9H). **¹³C-NMR** (75 MHz, CDCl₃): δ_C (ppm) = 62.01, 40.24, 37.29, -2.82. **IR** (neat, ν/cm^{-1}): 2956, 2900, 1409, 1252, 1185, 1085, 984, 939, 835, 731, 678. **HRMS** (LIFDI): exact mass calculated for C₆H₁₂Br₄Si [M-CH₃-HBr]⁺: m/z 332.7940, found: m/z 332.7940.

E Experimental part

General procedure *GP-D*

A 5 mL flame-dried Schlenk tube equipped with a magnetic stirring bar was charged with the carbohalide (0.5 mmol, 1.0 equiv.), K_2HPO_4 (87.1 mg, 0.5 mmol, 1.0 equiv.), *fac*-Ir(ppy)₃ (**49**) (3.3 mg, 5.0 μ mol, 1.0 mol%) and dry MeCN (1 mL). The flask was sealed with a plastic screw cap and the mixture degassed using the freeze-pump-thaw method (3 cycles). Under N₂ atmosphere, vinyltrimethylsilane (**230**) (150.3 mg, 220.0 μ L, 1.5 mmol, 3.0 equiv.) was added and the plastic screw cap replaced by another screw cap with a Teflon sealed inlet for a quartz glass rod. A high-power LED (λ = 455 nm) was attached to the top of the quartz glass rod. After irradiation for 17 – 48 h the LED was removed, and the reaction suspension was filtered through a Büchner funnel and the solvent evaporated *in vacuo*. The residue was purified by column chromatography (silica, hexanes / EA).

4-bromo-1-phenyl-4-(trimethylsilyl)butan-1-one (**269**)



Following general procedure *GP-D* using 2-bromoacetophenone (**171**) (99.5 mg, 0.50 mmol, 1.0 equiv.), K_2HPO_4 (87.1 mg, 0.50 mmol, 1.0 equiv.), vinyltrimethylsilane (**230**) (150.3 mg, 220.0 μ L, 1.50 mmol, 3.0 equiv.), *fac*-Ir(ppy)₃ (**49**) (3.3 mg, 5.0 μ mol, 1.0 mol%) and dry MeCN (1 mL) after irradiation for 22 h gave **269** (99.8 mg, 0.33 mmol, 67%) as a yellow liquid after flash chromatography purification (silica, hexanes / EA, 20:1).

R_f (hexanes / EA, 5:1): 0.71, **Staining**: vanillin (UV active). **¹H-NMR** (300 MHz, CDCl₃): δ_H (ppm) = 8.03 – 7.97 (m, 2H), 7.60 – 7.54 (m, 1H), 7.50 – 7.44 (m, 2H), 3.45 – 3.30 (m, 2H), 3.21 (ddd, J = 17.7, 8.1, 6.8 Hz, 1H), 2.38 (dddd, J = 15.0, 8.1, 6.8, 2.4 Hz, 1H), 2.02 (dddd, J = 14.0, 11.7, 7.6, 4.2 Hz, 1H), 0.17 (s, 9H). **¹³C-NMR** (75 MHz, CDCl₃): δ_C (ppm) = 199.66, 136.91, 133.18, 128.66, 128.06, 44.99, 38.25, 27.74, -3.02. **IR** (neat, ν/cm^{-1}): 2956, 2900, 1685, 1599, 1446, 1410, 1364, 1320, 1249, 1163, 1111, 999, 928, 835, 742, 690. **HRMS** (ESI): exact mass calculated for C₁₃H₁₉BrOSi [M+H]⁺: m/z 299.0461, found: m/z 299.0466.

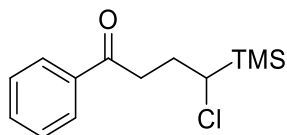
Big scale

A 20 mL flame-dried Schlenk tube equipped with a magnetic stirring bar was charged with 2-bromoacetophenone (**171**) (996.0 mg, 5.00 mmol, 1.0 equiv.), K_2HPO_4 (435.1 mg, 2.50 mmol, 0.5 equiv.), *fac*-Ir(ppy)₃ (**49**) (32.7 mg, 50.0 μ mol, 1.0 mol%), and dry MeCN (10 mL). The flask was sealed with a plastic screw cap and the mixture degassed using the freeze-pump-thaw method (3 cycles). Under N₂ atmosphere, vinyltrimethylsilane (**230**) (1.5 g, 2.20 mL, 15.0 mmol, 3.0 equiv.) was

E Experimental part

added and the plastic screw cap replaced by another screw cap with a Teflon sealed inlet for a quartz glass rod. A high-power LED ($\lambda = 455$ nm) was attached to the top of the quartz glass rod and two additional LEDs were placed next to the flask. After irradiation for 48 h the LEDs were removed, and the solvent evaporated *in vacuo*. The residue was purified by Kugelrohr distillation (28.0 mbar, 108 °C) to obtain **269** (779.6 mg, 2.60 mmol, 52%) as yellow liquid.

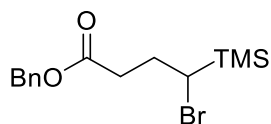
4-chloro-1-phenyl-4-(trimethylsilyl)butan-1-one (270)



Following general procedure *GP-D* using 2-chloroacetophenone (**172**) (77.3 mg, 0.50 mmol, 1.0 equiv.), K_2HPO_4 (87.1 mg, 0.50 mmol, 1.0 equiv.), vinyltrimethylsilane (**230**) (150.3 mg, 220.0 μ L, 1.50 mmol, 3.0 equiv.), *fac*-Ir(ppy)₃ (**49**) (3.3 mg, 5.0 μ mol, 1.0 mol%) and dry MeCN (1 mL) after irradiation for 68 h gave **270** (58.3 mg, 0.23 mmol, 46%) as a colorless liquid after flash chromatography purification (silica, hexanes / EA, 100:1).

R_f (hexanes / EA, 5:1): 0.71, **Staining**: vanillin (UV active). **¹H-NMR** (300 MHz, CDCl₃): δ_H (ppm) = 8.03 – 7.96 (m, 2H), 7.61 – 7.54 (m, 1H), 7.51 – 7.44 (m, 2H), 3.43 – 3.30 (m, 2H), 3.19 (ddd, $J = 17.6, 8.1, 6.8$ Hz, 1H), 2.33 (dddd, $J = 15.0, 8.2, 6.8, 2.4$ Hz, 1H), 1.95 (dddd, $J = 14.8, 12.7, 8.1, 4.8$ Hz, 1H), 0.15 (s, 9H). **¹³C-NMR** (75 MHz, CDCl₃): δ_C (ppm) = 199.80, 136.97, 133.14, 128.65, 128.06, 51.59, 36.74, 27.64, -3.58. **IR** (neat, ν/cm^{-1}): 2956, 2900, 1685, 1599, 1446, 1409, 1364, 1319, 1249, 1204, 1148, 835, 746, 690. **HRMS** (ESI): exact mass calculated for C₁₃H₁₉ClOSi [M+NH₄]⁺: m/z 272.1232, found: m/z 272.1235.

Benzyl 4-bromo-4-(trimethylsilyl)butanoate (271)



Following general procedure *GP-D* using benzyl 2-bromoacetate (**177**) (114.5 mg, 0.50 mmol, 1.0 equiv.), K_2HPO_4 (87.1 mg, 0.50 mmol, 1.0 equiv.), vinyltrimethylsilane (**230**) (150.3 mg, 220.0 μ L, 1.50 mmol, 3.0 equiv.), *fac*-Ir(ppy)₃ (**49**) (3.3 mg, 5.0 μ mol, 1.0 mol%) and dry MeCN (1 mL) after irradiation for 68 h gave **271** (93.3 mg, 0.28 mmol, 57%) as a colorless liquid after flash chromatography purification (silica, hexanes / EA, 100:1).

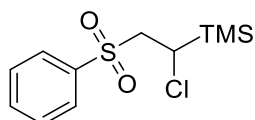
E Experimental part

R_f (hexanes / EA, 5:1): 0.73, **Staining**: vanillin (UV active). **¹H-NMR** (400 MHz, CDCl₃): δ_{H} (ppm) = 7.39 – 7.33 (m, 5H), 5.14 (d, J = 1.4 Hz, 2H), 3.24 (dd, J = 12.4, 2.5 Hz, 1H), 2.77 (ddd, J = 16.5, 8.3, 4.9 Hz, 1H), 2.62 – 2.53 (m, 1H), 2.27 – 2.18 (m, 1H), 2.00 – 1.90 (m, 1H), 0.14 (s, 9H). **¹³C-NMR** (101 MHz, CDCl₃): δ_{C} (ppm) = 174.87, 137.83, 130.51, 130.20, 130.18, 68.25, 45.78, 35.81, 30.45, -1.18. **IR** (neat, ν/cm^{-1}): 3034, 2956, 1733, 1454, 1416, 1383, 1312, 1249, 1149, 1029, 977, 835, 749, 693. **HRMS** (ESI): exact mass calculated for C₁₄H₂₁BrO₂Si [M+Na]⁺: m/z 351.0386, found: m/z 351.0387.

General procedure GP-E

A 5 mL flame-dried Schlenk tube equipped with a magnetic stirring bar was charged with the sulfonyl chloride (0.50 mmol, 1.0 equiv.), Na₂CO₃ (53.0 mg, 0.50 mmol, 1.0 equiv.), Cu(dap)Cl₂ (**102**) (1.3 mg, 2.50 μmol , 0.5 mol%) and dry MeCN (1 mL). The flask was sealed with a plastic screw cap and the mixture degassed using the freeze-pump-thaw method (3 cycles). Under N₂ atmosphere, vinyltrimethylsilane (**230**) (75.2 mg, 110.0 μL , 0.75 mmol, 1.5 equiv.) was added and the plastic screw cap replaced by another screw cap with a Teflon sealed inlet for a quartz glass rod. A high-power LED (λ = 530 nm) was attached to the top of the quartz glass rod. After irradiation for 16 h the LED was removed, and the reaction suspension was filtered through a Büchner funnel and the solvent evaporated *in vacuo*. The residue was purified by column chromatography (silica, hexanes / EA).

(1-chloro-2-(phenylsulfonyl)ethyl)trimethylsilane (**245**)



Following general procedure GP-E using benzenesulfonyl chloride (**187**) (88.3 mg, 64.0 μL , 0.50 mmol, 1.0 equiv.), vinyltrimethylsilane (**230**) (75.2 mg, 110.0 μL , 0.75 mmol, 1.5 equiv.), Na₂CO₃ (53.0 mg, 0.50 mmol, 1.0 equiv.), Cu(dap)Cl₂ (**102**) (1.3 mg, 2.50 μmol , 0.5 mol%) and dry MeCN (1 mL) after irradiation for 16 h gave **245** (100.2 mg, 0.36 mmol, 72%) as a colorless liquid after flash chromatography purification (silica, hexanes / EA, 5:1).

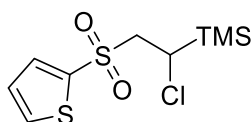
R_f (hexanes / EA, 5:1): 0.40 (UV active). **¹H-NMR** (300 MHz, CDCl₃): δ_{H} (ppm) = 7.99 – 7.94 (m, 2H), 7.70 – 7.63 (m, 1H), 7.60 – 7.54 (m, 2H), 3.70 – 3.64 (m, 1H), 3.47 (dd, J = 15.2, 10.8 Hz, 1H), 3.36 (dd, J = 15.2, 2.2 Hz, 1H), 0.13 – 0.10 (s, 9H). **¹³C-NMR** (75 MHz, CDCl₃): δ_{C} (ppm) = 139.80, 133.92, 129.25, 128.51, 60.30, 41.05, -3.86. **IR** (neat, ν/cm^{-1}): 3064, 2960, 1588, 1446, 1387, 1323, 1252, 1137, 1085, 1025, 891, 839, 790, 731, 686. **HRMS** (ESI): exact mass calculated for C₁₁H₁₇ClO₂SSi [M+Na]⁺: m/z 299.0299, found: m/z 299.0301.

E Experimental part

Big scale

A 20 mL flame-dried Schlenk tube equipped with a magnetic stirring bar was charged with benzenesulfonyl chloride (**187**) (883.1 mg, 640.0 μL , 5.0 mmol, 1.0 equiv.), Na_2CO_3 (265.0 mg, 2.50 mmol, 0.5 equiv.), $\text{Cu}(\text{dap})\text{Cl}_2$ (**102**) (13.2 mg, 25.0 μmol , 0.5 mol%) and dry MeCN (10 mL). The flask was sealed with a plastic screw cap and the mixture degassed using the freeze-pump-thaw method (3 cycles). Under N_2 atmosphere, vinyltrimethylsilane (**230**) (751.7 mg, 1.10 mL, 7.50 mmol, 1.5 equiv.) was added and the plastic screw cap replaced by another screw cap with a Teflon sealed inlet for a quartz glass rod. A high-power LED ($\lambda = 530 \text{ nm}$) was attached to the top of the quartz glass rod and two additional LEDs were placed next to the flask. After irradiation for 24 h the LEDs were removed, and the reaction suspension was filtered through a Büchner funnel and the solvent evaporated *in vacuo*. The residue was purified by Kugelrohr distillation (1.2 – 0.8 mbar, 115 – 120 $^\circ\text{C}$) to obtain **245** (1.3 g, 4.70 mmol, 94%) as colorless liquid.

(1-chloro-2-(thiophen-2-ylsulfonyl)ethyl)trimethylsilane (**273**)

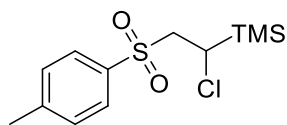


Following general procedure *GP-E* using thiophene-2-sulfonyl chloride (**272**) (91.3 mg, 0.50 mmol, 1.0 equiv.), vinyltrimethylsilane (**230**) (75.2 mg, 110.0 μL , 0.75 mmol, 1.5 equiv.), Na_2CO_3 (53.0 mg, 0.50 mmol, 1.0 equiv.), $\text{Cu}(\text{dap})\text{Cl}_2$ (**102**) (1.3 mg, 2.50 μmol , 0.5 mol%) and dry MeCN (1 mL) after irradiation for 16 h gave **273** (125.1 mg, 0.44 mmol, 89%) as a white solid after flash chromatography purification (silica, hexanes / EA, 5:1).

R_f (hexanes / EA, 5:1): 0.40 (UV active). mp: 67 $^\circ\text{C}$. $^1\text{H-NMR}$ (300 MHz, CDCl_3): δ_{H} (ppm) = 7.73 (dq, $J = 4.0, 1.4 \text{ Hz}$, 2H), 7.16 – 7.11 (m, 1H), 3.64 (dd, $J = 10.2, 2.3 \text{ Hz}$, 1H), 3.57 – 3.48 (m, 1H), 3.44 (dd, $J = 14.9, 2.3 \text{ Hz}$, 1H), 0.12 – 0.08 (s, 9H). $^{13}\text{C-NMR}$ (75 MHz, CDCl_3): δ_{C} (ppm) = 140.30, 135.01, 134.64, 128.07, 61.61, 41.17, -3.83. IR (neat, v/cm^{-1}): 3112, 2960, 1402, 1320, 1290, 1256, 1133, 1014, 883, 839, 783, 731. HRMS (ESI): exact mass calculated for $\text{C}_9\text{H}_{15}\text{ClO}_2\text{S}_2\text{Si}$ $[\text{M}+\text{H}]^+$: m/z 283.0044, found: m/z 283.0043.

E Experimental part

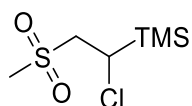
(1-chloro-2-tosylethyl)trimethylsilane (**233**)



Following general procedure *GP-E* using tosyl chloride (**182**) (95.3 mg, 0.50 mmol, 1.0 equiv.), vinyltrimethylsilane (**230**) (75.2 mg, 110.0 μ L, 0.75 mmol, 1.5 equiv.), Na_2CO_3 (53.0 mg, 0.50 mmol, 1.0 equiv.), $\text{Cu}(\text{dap})\text{Cl}_2$ (**102**) (1.3 mg, 2.50 μ mol, 0.5 mol%) and dry MeCN (1 mL) after irradiation for 16 h gave **233** (107.9 mg, 0.37 mmol, 74%) as a white solid after flash chromatography purification (silica, hexanes / EA, 8:1).

R_f (hexanes / EA, 5:1): 0.42 (UV active). mp: 60 °C. $^1\text{H-NMR}$ (400 MHz, CDCl_3): δ_{H} (ppm) = 7.87 (d, J = 8.3 Hz, 2H), 7.39 (d, J = 8.0 Hz, 2H), 3.69 (dd, J = 10.9, 2.1 Hz, 1H), 3.48 (dd, J = 15.2, 10.9 Hz, 1H), 3.39 (dd, J = 15.2, 2.1 Hz, 1H), 2.49 (s, 3H), 0.16 – 0.14 (s, 9H). $^{13}\text{C-NMR}$ (101 MHz, CDCl_3): δ_{C} (ppm) = 144.95, 136.83, 129.89, 128.53, 60.32, 41.15, 21.71, -3.84. IR (neat, v/cm^{-1}): 2960, 2922, 1595, 1320, 1290, 1249, 1167, 1129, 1036, 883, 842, 719. HRMS (ESI): exact mass calculated for $\text{C}_{12}\text{H}_{19}\text{ClO}_2\text{Si}$ $[\text{M}+\text{H}]^+$: m/z 291.0636, found: m/z 291.0641.

(1-chloro-2-(methanesulfonyl)ethyl)trimethylsilane (**244**)

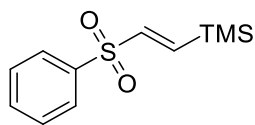


Following general procedure *GP-E* using methanesulfonyl chloride (**205**) (57.3 mg, 0.50 mmol, 1.0 equiv.), vinyltrimethylsilane (**230**) (75.2 mg, 110.0 μ L, 0.75 mmol, 1.5 equiv.), Na_2CO_3 (53.0 mg, 0.50 mmol, 1.0 equiv.), $\text{Cu}(\text{dap})\text{Cl}_2$ (**102**) (1.3 mg, 2.50 μ mol, 0.5 mol%) and dry MeCN (1 mL) after irradiation for 16 h gave **244** (19.0 mg, 0.09 mmol, 18%) as a colorless liquid after flash chromatography purification (silica, hexanes / EA, 4:1).

R_f (hexanes / EA, 5:1): 0.13, **Staining**: KMnO_4 . $^1\text{H-NMR}$ (300 MHz, CDCl_3): δ_{H} (ppm) = 3.79 (dd, J = 11.6, 1.7 Hz, 1H), 3.40 (dd, J = 15.6, 11.6 Hz, 1H), 3.25 – 3.18 (m, 1H), 3.12 (d, J = 1.0 Hz, 3H), 0.22 – 0.18 (s, 9H). $^{13}\text{C-NMR}$ (75 MHz, CDCl_3): δ_{C} (ppm) = 59.32, 43.78, 42.26, -3.80. IR (neat, v/cm^{-1}): 3015, 2960, 1413, 1316, 1252, 1126, 1033, 969, 891, 839, 453, 701. HRMS (ESI): exact mass calculated for $\text{C}_6\text{H}_{15}\text{ClO}_2\text{Si}$ $[\text{M}+\text{H}]^+$: m/z 215.0323, found: m/z 215.0323.

E Experimental part

(*E*)-trimethyl(2-(phenylsulfonyl)vinyl)silane (**278**)



A 20 mL flame-dried Schlenk tube equipped with a magnetic stirring bar was charged with benzenesulfonyl chloride (**187**) (883.1 mg, 640.0 mL, 5.0 mmol, 1.0 equiv.), Na₂CO₃ (265.0 mg, 2.50 mmol, 0.5 equiv.), Cu(dap)Cl₂ (**102**) (13.2 mg, 25.0 μmol, 0.5 mol%) and dry MeCN (10 mL). The flask was sealed with a plastic screw cap and the mixture degassed using the freeze-pump-thaw method (3 cycles). Under N₂ atmosphere, vinyltrimethylsilane (**230**) (751.7 mg, 1.10 mL, 7.50 mmol, 1.5 equiv.) was added and the plastic screw cap replaced by another screw cap with a Teflon sealed inlet for a quartz glass rod. A high-power LED (λ = 530 nm) was attached to the top of the quartz glass rod and two additional LEDs were placed next to the flask (see figure 7). After irradiation for 24 h the LEDs were removed, and a solution of KOH (1.40 g, 25.0 mmol, 5.0 equiv.) in H₂O (10 mL) was added and stirred for 1 h. The solution was transferred to a separating funnel and extracted with DCM (3 x 60 mL) and washed with H₂O (50 mL) and brine (50 mL). The combined organic layers were dried over MgSO₄, the solvent removed *in vacuo* and the residue was purified by column chromatography (silica, hexanes / EA, 20:1) to obtain **278** (1.1 g, 4.57 mmol, 91%) as a colorless oil.

R_f (hexanes / EA, 5:1): 0.51, **Staining**: KMnO₄ (UV active). **¹H-NMR** (300 MHz, CDCl₃): δ_H (ppm) = 7.87 (ddd, *J* = 6.9, 3.6, 1.9 Hz, 2H), 7.65 – 7.59 (m, 1H), 7.57 – 7.51 (m, 2H), 7.23 (d, *J* = 17.9 Hz, 1H), 6.62 (d, *J* = 17.9 Hz, 1H), 0.13 (s, *J* = 3.4 Hz, 9H). **¹³C-NMR** (75 MHz, CDCl₃): δ_C (ppm) = 145.54, 141.67, 139.76, 133.50, 129.33, 127.93, -1.99. **IR** (neat, ν/cm⁻¹): 3064, 2960, 2900, 1584, 1446, 1308, 1252, 1144, 1085, 977, 842, 801, 731, 686. **HRMS** (ESI): exact mass calculated for C₁₁H₁₆O₂SSi [M+H]⁺: *m/z* 241.0713, found: *m/z* 241.0718.

E Experimental part

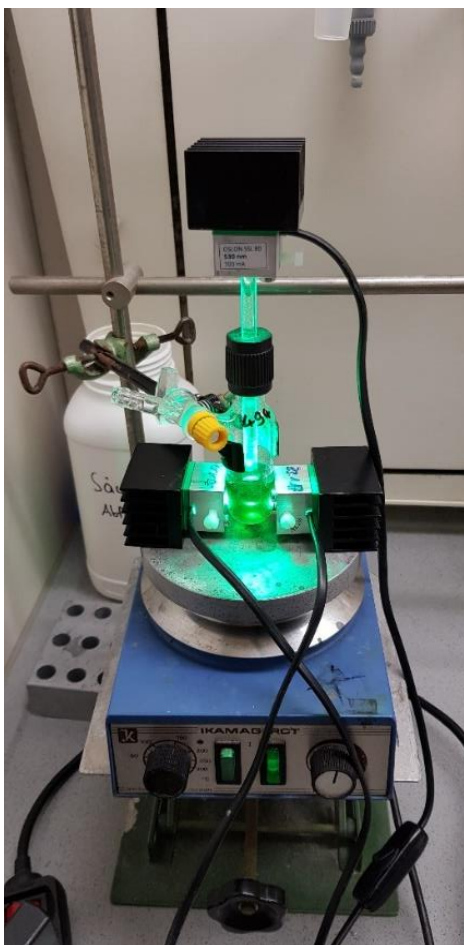
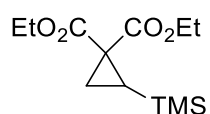


Figure 7. Big-scale set-up for the synthesis of (*E*)-trimethyl(2-(phenylsulfonyl)vinyl)silane (**278**).

6. Formation of silyl-substituted cyclopropanes

Diethyl 2-(trimethylsilyl)cyclopropane-1,1-dicarboxylate (**300**)



A 5 mL flame-dried Schlenk tube equipped with a magnetic stirring bar was charged with diethyl 2-bromomalonate (**127**) (119.5 mg, 85.0 μ L, 0.50 mmol, 1.0 equiv.), *fac*-Ir(ppy)₃ (**49**) (1.6 mg, 2.50 μ mol, 0.5 mol%) and dry MeCN (1 mL). The flask was sealed with a plastic screw cap and the mixture degassed using the freeze-pump-thaw method (3 cycles). Under N₂ atmosphere, vinyltrimethylsilane (**230**) (75.2 mg, 110.0 μ L, 0.75 mmol, 1.5 equiv.) was added and the plastic screw cap replaced by another screw cap with a Teflon sealed inlet for a quartz glass rod. A high-power LED (λ = 455 nm) was attached to the top of the quartz glass rod. After irradiation for 24 h the LED was removed, and DBU (228.4 mg, 220.0 μ L, 1.50 mmol, 3.0 equiv.) was added and the reaction stirred for

E Experimental part

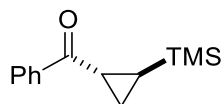
an additional hour. The solution was transferred to a separating funnel and extracted with DCM (3 x 40 mL) and washed with H₂O (50 mL) and brine (50 mL). The combined organic layers were dried over MgSO₄, the solvent removed *in vacuo* and the residue was purified by column chromatography (silica, hexanes / EA, 10:1) to obtain **300** (104.0 mg, 0.4 mmol, 80%) as a colorless oil.

R_f(hexanes 5:1): 0.64, **Staining**: KMnO₄. **¹H-NMR** (400 MHz, CDCl₃): δ_H (ppm) = 4.22 – 4.08 (m, 4H), 1.41 (dd, *J* = 11.1, 3.5 Hz, 1H), 1.25 (dt, *J* = 10.5, 7.1 Hz, 6H), 1.28 (dd, *J* = 8.9, 3.4 Hz, 1H), 0.86 (dd, *J* = 11.1, 9.6 Hz, 1H), 0.00 (s, 9H). **¹³C-NMR** (101 MHz, CDCl₃): δ_C (ppm) = 171.30, 169.42, 61.56, 61.24, 33.19, 18.34, 16.37, 14.06, 14.01, -1.79. **IR** (neat, ν/cm⁻¹): 2982, 2960, 2904, 1722, 1446, 1372, 1241, 1197, 1133, 1074, 1029, 969, 835, 753, 693. **HRMS** (ESI): exact mass calculated for C₁₂H₂₂O₄Si [M+H]⁺: *m/z* 259.1366, found: *m/z* 259.1363.

Big scale

A 20 mL flame-dried Schlenk tube equipped with a magnetic stirring bar was charged with diethyl 2-bromomalonate (**127**) (1.19 mg, 850.0 μL, 5.0 mmol, 1.0 equiv.), *fac*-Ir(ppy)₃ (**49**) (16.4 mg, 25.0 μmol, 0.5 mol%) and dry MeCN (10 mL). The flask was sealed with a plastic screw cap and the mixture degassed using the freeze-pump-thaw method (3 cycles). Under N₂ atmosphere, vinyltrimethylsilane (**230**) (752.0 mg, 7.50 mmol, 1.5 equiv.) was added and the plastic screw cap replaced by another screw cap with a Teflon sealed inlet for a quartz glass rod. A high-power LED (λ = 455 nm) was attached to the top of the quartz glass rod and two additional LEDs were placed next to the flask. After irradiation for 25 h the LED was removed, and DBU (2.28 g, 2.20 mL, 15.0 mmol, 3.0 equiv.) was added and the reaction stirred for 30 min. The solution was transferred to a separating funnel and extracted with DCM (3 x 60 mL) and washed with KH₂PO₄ (1 M) solution (50 mL) and brine (50 mL). The combined organic layers were dried over MgSO₄, the solvent removed *in vacuo* and the residue was purified by column chromatography (silica, hexanes / EA, 10:1) to obtain **300** (1.1 g, 4.32 mmol, 86%) as a colorless oil.

Phenyl-2-(trimethylsilyl)cyclopropyl)methanone (**301**)



A 5 mL pressure-tube equipped with a magnetic stirring bar was charged with 4-bromo-1-phenyl-4-(trimethylsilyl)butan-1-one (**269**) (149.6 mg, 0.50 mmol, 1.0 equiv.), DBU (228.4 mg, 220.0 μL, 1.50 mmol, 3.0 equiv.) and MeCN (1 mL). The flask was sealed with a plastic screw cap and the mixture stirred at room temperature for 5 h. The solution was transferred to a separating funnel and extracted with DCM (3 x 40 mL) and washed with KH₂PO₄ (1 M) solution (30 mL) and brine (30 mL). The combined

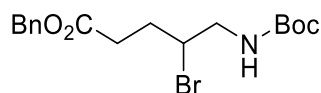
E Experimental part

organic layers were dried over MgSO_4 , the solvent removed *in vacuo* and the residue was purified by column chromatography (silica, hexanes) to obtain **301** (107.5 mg, 0.49 mmol, 97%) as a colorless oil.

R_f (hexanes 10:1): 0.63, **Staining**: vanillin (UV active). $^1\text{H-NMR}$ (300 MHz, CDCl_3): δ_{H} (ppm) = 7.95 (dd, J = 5.3, 3.3 Hz, 2H), 7.56 – 7.49 (m, 1H), 7.48 – 7.40 (m, 2H), 2.47 (ddd, J = 7.1, 5.9, 4.1 Hz, 1H), 1.44 (ddd, J = 10.6, 4.0, 2.8 Hz, 1H), 0.92 (ddd, J = 8.4, 7.2, 2.8 Hz, 1H), 0.67 (ddd, J = 10.6, 8.4, 5.9 Hz, 1H), 0.00 (s, 9H). $^{13}\text{C-NMR}$ (75 MHz, CDCl_3): δ_{C} (ppm) = 200.65, 138.24, 132.66, 128.53, 127.96, 21.18, 15.38, 13.60, -2.42. **IR** (neat, v/cm^{-1}): 3064, 2997, 2952, 2896, 1670, 1599, 1450, 1383, 1249, 1219, 1178, 1055, 1014, 977, 831, 746, 712. **HRMS** (ESI): exact mass calculated for $\text{C}_{13}\text{H}_{18}\text{OSi}$ $[\text{M}+\text{H}]^+$: m/z 219.1205, found: m/z 219.1202.

7. Atom transfer radical additions with *tert*-butyl allylcarbamate

Benzyl 4-bromo-5-((*tert*-butoxycarbonyl)amino)pentanoate (**317**)



A 5 mL Schlenk tube equipped with a magnetic stirring bar was charged with benzyl 2-bromoacetate (**177**) (229.1 mg, 157.0 μL , 1.0 mmol, 2.0 equiv.), K_2HPO_4 (87.1 mg, 0.50 mmol, 1.0 equiv.), *fac*- $\text{Ir}(\text{ppy})_3$ (**49**) (3.3 mg, 5.0 μmol , 1.0 mol%), *tert*-butyl allylcarbamate (**316**)^[197] (78.6 mg, 0.50 mmol, 1.0 equiv.), H_2O (0.5 mL) and DMF (0.5 mL). The flask was sealed with a plastic screw cap with a Teflon sealed inlet for a quartz glass rod and the mixture degassed using the freeze-pump-thaw method (3 cycles). A high-power LED (λ = 455 nm) was attached to the top of the quartz glass rod. After irradiation for 16 h the LED was removed, the solution was transferred to a separating funnel and extracted with DCM (3 x 40 mL) and washed with H_2O (30 mL). The combined organic layers were dried over MgSO_4 , the solvent removed *in vacuo* to give **317** (154.8 mg, 0.40 mmol, 80%) as a white solid after flash chromatography purification (silica, hexanes / EA, 20:1).

R_f (hexanes / EA, 5:1): 0.29, **Staining**: ninhydrin (UV active). **mp**: 150 $^\circ\text{C}$. $^1\text{H-NMR}$ (400 MHz, CDCl_3): δ_{H} (ppm) = 7.41 – 7.30 (m, 5H), 5.13 (s, 2H), 4.97 (s, 1H), 4.13 (s, J = 33.8 Hz, 1H), 3.56 (dd, J = 12.6, 7.0 Hz, 1H), 3.46 – 3.38 (m, 1H), 2.67 (ddd, J = 16.7, 8.4, 5.7 Hz, 1H), 2.60 – 2.51 (m, 1H), 2.23 (dddd, J = 15.2, 8.4, 6.9, 3.9 Hz, 1H), 2.06 (dtd, J = 14.8, 8.9, 5.8 Hz, 1H), 1.45 (s, 9H). $^{13}\text{C-NMR}$ (101 MHz, CDCl_3): δ_{C} (ppm) = 172.39, 155.71, 135.79, 128.64, 128.35, 128.28, 79.89, 66.53, 55.53, 47.29, 32.09, 30.91, 28.38. **IR** (neat, v/cm^{-1}): 3377, 2971, 2926, 1730, 1689, 1521, 1446, 1390, 1327, 1249, 1211, 1152, 1051, 954, 910, 865, 824, 749, 697. **HRMS** (ESI): exact mass calculated for $\text{C}_{17}\text{H}_{24}\text{BrNO}_4$ $[\text{M}+\text{Na}]^+$: m/z 408.0781, found: m/z 408.0782.

E Experimental part

Big scale

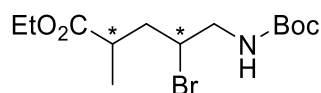
A 20 mL Schlenk tube equipped with a magnetic stirring bar was charged with benzyl 2-bromoacetate (**177**) (1.72 g, 1.18 mL, 7.50 mmol, 1.5 equiv.), K_2HPO_4 (435.5 mg, 2.50 mmol, 0.5 equiv.), *fac*-Ir(ppy)₃ (**49**) (16.4 mg, 25.0 μ mol, 0.5 mol%), *tert*-butyl allylcarbamate (**316**)^[197] (786.1 mg, 5.0 mmol, 1.0 equiv.), H₂O (5.0 mL) and DMF (5.0 mL). The flask was sealed with a plastic screw cap with a Teflon sealed inlet for a quartz glass rod and the mixture degassed using the freeze-pump-thaw method (3 cycles). A high-power LED ($\lambda = 455$ nm) was attached to the top of the quartz glass rod and two additional LEDs were placed next to the flask (see Figure 8). After irradiation for 20 h the LEDs were removed, the solution was transferred to a separating funnel and extracted with DCM (3 x 60 mL) and washed with H₂O (50 mL) and brine (50 mL). The combined organic layers were dried over MgSO₄, the solvent removed *in vacuo* to give **317** (1.09 g, 2.82 mmol, 56%) as a white solid after flash chromatography purification (silica, hexanes / EA, 10:1).



Figure 8. Big-scale set-up for the synthesis of benzyl 4-bromo-5-((*tert*-butoxycarbonyl)amino)pentanoate (**317**).

E Experimental part

Ethyl 4-bromo-5-((*tert*-butoxycarbonyl)amino)-2-methylpentanoate (**327**)



A 5 mL Schlenk tube equipped with a magnetic stirring bar was charged with ethyl 2-bromopropanoate (**326**) (135.8 mg, 98.4 μ L, 0.75 mmol, 1.5 equiv.), K₂HPO₄ (87.1 mg, 0.50 mmol, 1.0 equiv.), *fac*-Ir(ppy)₃ (**49**) (3.3 mg, 5.0 μ mol, 1.0 mol%), *tert*-butyl allylcarbamate (**316**)^[197] (78.6 mg, 0.50 mmol, 1.0 equiv.), H₂O (0.5 mL) and DMF (0.5 mL). The flask was sealed with a plastic screw cap with a Teflon sealed inlet for a quartz glass rod and the mixture degassed using the freeze-pump-thaw method (3 cycles). A high-power LED (λ = 455 nm) was attached to the top of the quartz glass rod. After irradiation for 24 h the LED was removed, the solution was transferred to a separating funnel and extracted with DCM (3 x 40 mL) and washed with H₂O (30 mL). The combined organic layers were dried over MgSO₄, the solvent removed *in vacuo* to give **327** (126.0 mg, 0.37 mmol, 74%) as a colorless liquid after flash chromatography purification (silica, hexanes / EA, 15:1).

R_f (hexanes / EA, 5:1): 0.33, **Staining**: ninhydrin (UV active). **¹H-NMR** (300 MHz, CDCl₃): δ_{H} (ppm) = 4.98 (d, J = 22.2 Hz, 1H), 4.13 (m, J = 7.1, 1.3 Hz, 2H + 1H), 3.65 – 3.32 (m, 2H), 2.87 – 2.68 (m, 1H), 2.27 – 2.13 (m, 1H), 1.90 – 1.71 (m, 1H), 1.44 (s, 9H), 1.25 (t, J = 7.1 Hz, 3H), 1.18 (dd, J = 14.2, 7.1 Hz, 3H). (Peak splitting due to diastereomers) **¹³C-NMR** (75 MHz, CDCl₃): δ_{C} (ppm) = 175.87, 175.54, 155.69, 79.85, 60.68, 60.61, 54.90, 54.03, 47.53, 47.26, 39.82, 38.77, 37.84, 37.54, 28.35, 18.02, 16.27, 14.22. (Peak splitting due to diastereomers) **IR** (neat, ν/cm^{-1}): 3355, 2978, 2937, 1715, 1513, 1457, 1368, 1249, 1163, 1081, 1021, 857, 768. **HRMS** (ESI): exact mass calculated for C₁₃H₂₄BrNO₄ [M+Na]⁺: m/z 360.0781, found: m/z 360.0780.

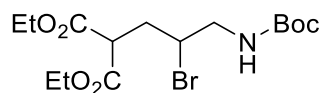
Big scale

A 20 mL Schlenk tube equipped with a magnetic stirring bar was charged with ethyl 2-bromopropanoate (**326**) (1.36 g, 1.38 mL, 7.50 mmol, 1.5 equiv.), K₂HPO₄ (435.5 mg, 2.50 mmol, 0.5 equiv.), *fac*-Ir(ppy)₃ (**49**) (16.4 mg, 25.0 μ mol, 0.5 mol%), *tert*-butyl allylcarbamate (**316**)^[197] (786.1 mg, 5.0 mmol, 1.0 equiv.), H₂O (5.0 mL) and DMF (5.0 mL). The flask was sealed with a plastic screw cap with a Teflon sealed inlet for a quartz glass rod and the mixture degassed using the freeze-pump-thaw method (3 cycles). A high-power LED (λ = 455 nm) was attached to the top of the quartz glass rod and two additional LEDs were placed next to the flask. After irradiation for 42 h the LEDs were removed, the solution was transferred to a separating funnel and extracted with DCM (3 x 60 mL) and washed with H₂O (50 mL) and brine (50 mL). The combined organic layers were dried

E Experimental part

over MgSO_4 , the solvent removed *in vacuo* to give **327** (1.07 g, 3.15 mmol, 63%) as a colorless liquid after flash chromatography purification (silica, hexanes / EA, 15:1).

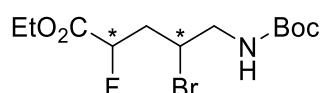
Diethyl 2-(2-bromo-3-((*tert*-butoxycarbonyl)amino)propyl)malonate (**61**)



A 5 mL flame-dried Schlenk tube equipped with a magnetic stirring bar was charged with diethyl 2-bromomalonate (**127**) (179.3 mg, 128.0 μL , 0.75 mmol, 1.5 equiv.), *fac*-Ir(ppy)₃ (**49**) (3.3 mg, 5.0 μmol , 1.0 mol%), *tert*-butyl allylcarbamate (**316**)^[197] (78.6 mg, 0.50 mmol, 1.0 equiv.), and dry MeCN (1.0 mL). The flask was sealed with a plastic screw cap with a Teflon sealed inlet for a quartz glass rod and the mixture degassed using the freeze-pump-thaw method (3 cycles). A high-power LED ($\lambda = 455 \text{ nm}$) was attached to the top of the quartz glass rod. After irradiation for 22 h the LED was removed, the solvent removed *in vacuo* to give **61** (151.4 mg, 0.38 mmol, 76%) as a colorless liquid after flash chromatography purification (silica, hexanes / EA, 10:1).

R_f (hexanes / EA, 5:1): 0.27, **Staining**: ninhydrin (UV active). **¹H-NMR** (300 MHz, CDCl_3): δ_{H} (ppm) = 4.98 (s, 1H), 4.25 – 4.08 (m, 4H + 1H), 3.77 – 3.70 (m, 1H), 3.60 – 3.42 (m, 2H), 2.47 (ddd, $J = 14.8, 9.5, 3.8 \text{ Hz}$, 1H), 2.33 – 2.19 (m, 1H), 1.44 (s, $J = 7.3 \text{ Hz}$, 9H), 1.27 (td, $J = 7.1, 1.7 \text{ Hz}$, 6H). **¹³C-NMR** (101 MHz, CDCl_3): δ_{C} (ppm) = 168.86, 168.50, 155.61, 79.90, 61.83, 61.76, 53.28, 50.16, 47.12, 34.63, 28.33, 14.06, 14.03. **IR** (neat, v/cm^{-1}): 3386, 2982, 2937, 1718, 1510, 1450, 1368, 1338, 1245, 1148, 1025, 965, 857, 783. **HRMS** (ESI): exact mass calculated for $\text{C}_{15}\text{H}_{26}\text{BrNO}_6$ $[\text{M}+\text{NH}_4]^+$: m/z 413.1282, found: m/z 413.1287.

Ethyl 4-bromo-5-((*tert*-butoxycarbonyl)amino)-2-fluoropentanoate (**329**)



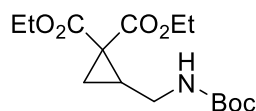
A 5 mL Schlenk tube equipped with a magnetic stirring bar was charged with ethyl 2-bromo-2-fluoroacetate (**328**) (138.7 mg, 0.75 mmol, 1.5 equiv.), K_2HPO_4 (87.1 mg, 0.50 mmol, 1.0 equiv.), *fac*-Ir(ppy)₃ (**49**) (3.3 mg, 5.0 μmol , 1.0 mol%), *tert*-butyl allylcarbamate (**316**)^[197] (78.6 mg, 0.50 mmol, 1.0 equiv.), H_2O (0.5 mL) and DMF (0.5 mL). The flask was sealed with a plastic screw cap with a Teflon sealed inlet for a quartz glass rod and the mixture degassed using the freeze-pump-thaw method (3 cycles). A high-power LED ($\lambda = 455 \text{ nm}$) was attached to the top of the quartz glass rod. After irradiation for 24 h the LED was removed, the solution was transferred to a separating funnel and extracted with DCM (3 x 40 mL) and washed with H_2O (30 mL). The combined organic layers were dried over MgSO_4 , the solvent removed *in vacuo* to give **329** (86.6 mg, 0.26 mmol, 53%) as a colorless liquid

E Experimental part

as a mixture of two diastereomers (*dr* = 1.4:1) after flash chromatography purification (silica, hexanes / EA, 20:1).

R_f (hexanes / EA, 5:1): 0.31, **Staining**: ninhydrin (UV active). **¹H-NMR** (400 MHz, CDCl₃): δ_{H} (ppm) = 5.29 – 5.07 (m, 1H), 5.07 – 4.82 (m, 1H), 4.35 – 4.22 (m, 2H + 1H), 3.68 – 3.54 (m, 1H), 3.54 – 3.45 (m, 1H), 2.54 – 2.16 (m, 2H), 1.44 (s, 9H), 1.30 (t, *J* = 7.1 Hz, 3H). (Peak splitting due to diastereomers) **¹³C-NMR** (101 MHz, CDCl₃): δ_{C} (ppm) = 169.23, 169.01, 155.68, 87.91, 87.66, 86.07, 85.83, 80.03, 61.90, 50.96, 49.61, 47.32, 46.24, 38.79, 38.59, 38.13, 37.92, 28.31, 14.10, 14.08. (Peak splitting due to diastereomers) **¹⁹F-NMR** (376 MHz, CDCl₃): δ_{F} (ppm) = -191.60, -194.97. **IR** (neat, ν/cm^{-1}): 3370, 2982, 2937, 1759, 1700, 1510, 1453, 1368, 1249, 1215, 1163, 1096, 1021, 857, 779. **LRMS** (ESI): exact mass calculated for C₁₂H₂₁BrFNO₄ [M+H]⁺: *m/z* 342.0716, found: *m/z* 342.0189.

Diethyl 2-(((*tert*-butoxycarbonyl)amino)methyl)cyclopropane-1,1-dicarboxylate (**332**)



A 5 mL flame-dried Schlenk tube equipped with a magnetic stirring bar was charged with diethyl 2-bromomalonate (**127**) (179.3 mg, 128.0 μL , 0.75 mmol, 1.5 equiv.), *fac*-Ir(ppy)₃ (**49**) (3.3 mg, 5.0 μmol , 1.0 mol%), *tert*-butyl allylcarbamate (**316**)^[197] (78.6 mg, 0.50 mmol, 1.0 equiv.), and dry MeCN (1.0 mL). The flask was sealed with a plastic screw cap with a Teflon sealed inlet for a quartz glass rod and the mixture degassed using the freeze-pump-thaw method (3 cycles). A high-power LED (λ = 455 nm) was attached to the top of the quartz glass rod. After irradiation for 22 h the LED was removed and DBU (228.4 mg, 220.0 mL, 1.50 mmol, 3.0 equiv.) was added. The mixture was stirred at room temperature for 1 h and then the solution was transferred to a separating funnel and extracted with DCM (3 x 40 mL) and washed with H₂O (40 mL) and brine (40 mL). The combined organic layers were dried over MgSO₄, the solvent removed *in vacuo* to give **332** (108.6 mg, 0.34 mmol, 69%) as a colorless liquid after flash chromatography purification (silica, hexanes / EA, 5:1).

R_f (hexanes / EA, 5:1): 0.27, **Staining**: ninhydrin (UV active). **¹H-NMR** (400 MHz, CDCl₃): δ_{H} (ppm) = 4.75 (d, *J* = 119.0 Hz, 1H), 4.28 – 4.15 (m, 4H), 3.69 – 3.43 (m, 1H), 2.82 – 2.70 (m, 1H), 2.06 (tdd, *J* = 9.0, 7.4, 5.6 Hz, 1H), 1.44 (s, 9H), 1.28 (dt, *J* = 16.6, 7.1 Hz, 6H). **¹³C-NMR** (101 MHz, CDCl₃): δ_{C} (ppm) = 169.85, 168.06, 155.61, 79.45, 61.80, 61.72, 40.45, 33.79, 28.41, 27.65, 18.87, 14.08, 14.05. **IR** (neat, ν/cm^{-1}): 3380, 2982, 2937, 1715, 1510, 1454, 1368, 1320, 1252, 1204, 1163, 1133, 1018, 943, 861, 708. **HRMS** (ESI): exact mass calculated for C₁₅H₂₅NO₆ [M+H]⁺: *m/z* 316.1755, found: *m/z* 316.1756.

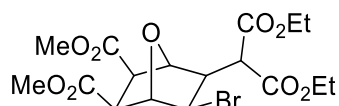
E Experimental part

8. Atom transfer radical additions with oxabicyclohexenes

General procedure *GP-E*

A 5 mL Schlenk tube equipped with a magnetic stirring bar was charged with the oxabicyclohexene (0.50 mmol, 1.0 equiv.), the carbo halide (1.0 mmol, 2.0 equiv.), Cu(dap)₂Cl (**50**) (4.4 mg, 5.0 μmol, 1.0 mol%), DMF (1 mL) and H₂O (1 mL). The flask was sealed with a plastic screw cap with a Teflon sealed inlet for a quartz glass rod and the mixture degassed using the freeze-pump-thaw method (3 cycles). A high-power LED (λ = 530 nm) was attached to the top of the quartz glass rod. After irradiation for 24 – 72 h the LED was removed, the solution was transferred to a separating funnel and extracted with DCM (3 x 40 mL) and washed with H₂O (30 mL). The combined organic layers were dried over MgSO₄, the solvent removed *in vacuo* and the residue was purified by column chromatography (silica, hexanes / EA).

Dimethyl-(-5-bromo-6-(1-ethoxy-3-(ethylperoxy)-1-oxo-3λ²-propan-2-yl)-7-oxabicyclo[2.2.1]heptane-2,3-dicarboxylate (**352**)

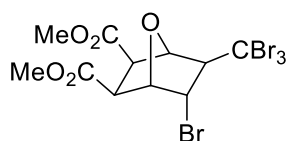


Following general procedure *GP-E* using dimethyl-7-oxabicyclo[2.2.1]hept-5-ene-2,3-dicarboxylate (**347**)^[185] (106.1 mg, 0.50 mmol, 1.0 equiv.), diethyl 2-bromomalonate (**127**) (239.0 mg, 170.0 μL, 1.0 mmol, 2.0 equiv.), Cu(dap)₂Cl (**50**) (4.4 mg, 5.0 μmol, 1.0 mol%), DMF (1 mL) and H₂O (1 mL) after irradiation for 24 h gave **352** (168.1 mg, 0.37 mmol, 73%) as a yellow solid as two diastereomers (*dr* = 1.6:1) after flash chromatography purification (silica, hexanes / EA, 4:1).

Major diastereomer: *R_f*(hexanes / EA, 3:1): 0.26, **Staining**: KMnO₄ (UV active). **mp**: 94 °C. **¹H-NMR** (400 MHz, CDCl₃): δ_H (ppm) = 5.01 (s, 1H), 4.68 (s, 1H), 4.37 (d, *J* = 7.2 Hz, 1H), 4.27 – 4.18 (m, 4H), 3.77 (d, *J* = 11.9 Hz, 1H), 3.69 (s, 3H), 3.66 (s, 3H), 3.09 (dd, *J* = 25.3, 9.4 Hz, 2H), 2.82 (dd, *J* = 11.9, 7.2 Hz, 1H), 1.31 – 1.26 (m, 6H). **¹³C-NMR** (101 MHz, CDCl₃): δ_C (ppm) = 170.16, 170.10, 168.26, 167.97, 86.20, 81.22, 62.26, 62.12, 55.99, 53.87, 52.45, 52.37, 51.98, 49.12, 47.05, 14.06, 13.92. **IR** (neat, ν/cm⁻¹): 2989, 2952, 2848, 1730, 1439, 1379, 1350, 1320, 1264, 1193, 1163, 1029, 857, 813, 468, 712. **HRMS** (ESI): exact mass calculated for C₁₇H₂₃BrO₉ [M+H]⁺: *m/z* 541.0598, found: *m/z* 451.0590.

E Experimental part

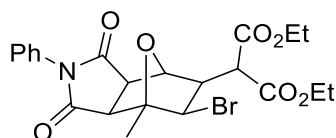
Dimethyl-(-5-bromo-6-(tribromomethyl)-7-oxabicyclo[2.2.1]heptane-2,3-dicarboxylate (353)



A 5 mL flame-dried Schlenk tube equipped with a magnetic stirring bar was charged with dimethyl-7-oxabicyclo[2.2.1]hept-5-ene-2,3-dicarboxylate (**347**)^[185] (318.3 mg, 1.50 mmol, 1.0 equiv.), tetrabromomethane (**266**) (547.0 mg, 1.65 mmol, 1.1 equiv.), Cu(dap)₂Cl (**50**) (9.9 mg, 11.25 μmol, 0.75 mol%) and dry DCM (1.5 mL). The flask was sealed with a plastic screw cap with a Teflon sealed inlet for a quartz glass rod and the mixture degassed using the freeze-pump-thaw method (3 cycles). A high-power LED (λ = 530 nm) was attached to the top of the quartz glass rod. After irradiation for 48 h the LED was removed to give **253** (646.7 mg, 1.19 mmol, 79%) as a colorless oil as two diastereomers (*dr* = 13.5:1) after flash chromatography purification (silica, hexanes / EA, 8:1).

Major diastereomer: *R_f* (hexanes / EA, 3:1): 0.41, **Staining**: KMnO₄ (UV active). **¹H-NMR** (400 MHz, CDCl₃): δ_H (ppm) = 5.11 (d, *J* = 4.8 Hz, 1H), 4.98 (s, 1H), 4.05 (t, *J* = 5.0 Hz, 1H), 4.01 (d, *J* = 9.6 Hz, 1H), 3.73 (d, *J* = 1.8 Hz, 6H), 3.19 (dd, *J* = 9.0, 7.4 Hz, 2H). **¹³C-NMR** (101 MHz, CDCl₃): δ_C (ppm) = 170.52, 169.84, 83.34, 82.73, 73.36, 52.62, 52.53, 51.17, 48.24, 47.67, 39.31. **IR** (neat, ν/cm⁻¹): 1783, 1719, 1600, 1487, 1375, 1330, 1201, 1144, 975, 887, 795, 699. **HRMS** (ESI): exact mass calculated for C₁₁H₁₂Br₄O₅ [M+NH₄]⁺: *m/z* 561.7721, found: *m/z* 561.7724.

Ethyl-2-(6-bromo-7-methyl-1,3-dioxo-2-phenyloctahydro-1H-4,7-epoxyisoindol-5-yl)-3-(ethylperoxy)-3λ²-propanoate (355)



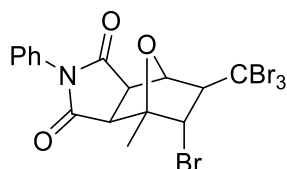
Following general procedure *GP-E* using 4-methyl-2-phenyl-3a,4,7,7a-tetrahydro-1H-4,7-epoxyisoindole-1,3(2H)-dione (**351**)^[186] (127.6 mg, 0.50 mmol, 1.0 equiv.), diethyl 2-bromomalonate (**127**) (239.0 mg, 170.0 μL, 1.0 mmol, 2.0 equiv.), Cu(dap)₂Cl (**50**) (4.4 mg, 5.0 μmol, 1.0 mol%), DMF (1 mL) and H₂O (1 mL) after irradiation for 72 h gave **255** (123.0 mg, 0.25 mmol, 50%) as a yellow solid as two diastereomers (*dr* = 2.6:1) after flash chromatography purification (silica, hexanes / EA, 4:1).

Major diastereomer: *R_f* (hexanes / EA, 3:1): 0.35, **Staining**: KMnO₄ (UV active). **mp**: 130 °C. **¹H-NMR** (400 MHz, CDCl₃): δ_H (ppm) = 7.45 – 7.40 (m, 2H), 7.38 – 7.33 (m, 1H), 7.20 (s, 2H), 4.71 (s, 1H), 4.26 – 4.18 (m, 4H), 3.82 (d, *J* = 7.3 Hz, 1H), 3.79 (d, *J* = 4.7 Hz, 1H), 3.40 (d, *J* = 9.2 Hz, 1H), 3.30 (d, *J* = 7.3 Hz, 1H), 2.69 (dd, *J* = 9.2, 4.7 Hz, 1H), 1.59 (d, *J* = 4.9 Hz, 3H), 1.27 (dt, *J* = 9.7, 7.1 Hz, 6H).

E Experimental part

¹³C-NMR (101 MHz, CDCl₃): δ_c (ppm) = 174.87, 174.83, 167.36, 167.13, 131.71, 129.21, 128.85, 126.46, 89.60, 81.55, 62.27, 62.19, 54.03, 53.71, 52.73, 50.73, 47.52, 15.63, 14.08, 14.06. **IR** (neat, ν/cm^{-1}): 2974, 1782, 1707, 1599, 1454, 1495, 1390, 1297, 1241, 1193, 1156, 1096, 1021, 973, 872, 846, 734, 693. **HRMS** (ESI): exact mass calculated for C₂₂H₂₄BrNO₇ [M+H]⁺: m/z 494.0809, found: m/z 494.0808.

5-bromo-4-methyl-2-phenyl-6-(tribromomethyl)hexahydro-1H-4,7-epoxyisoindole-1,3(2H)-dione (356)



A 5 mL Schlenk tube equipped with a magnetic stirring bar was charged with 4-methyl-2-phenyl-3a,4,7,7a-tetrahydro-1H-4,7-epoxyisoindole-1,3(2H)-dione (**351**)^[186] (127.6 mg, 0.50 mmol, 1.0 equiv.), tetrabromomethane (**266**) (248.7 mg, 0.75 mmol, 1.5 equiv.), Cu(dap)₂Cl (**50**) (4.4 mg, 5.0 μmol , 1.0 mol%), DMF (1 mL) and H₂O (1 mL). The flask was sealed with a plastic screw cap with a Teflon sealed inlet for a quartz glass rod and the mixture degassed using the freeze-pump-thaw method (3 cycles). A high-power LED (λ = 530 nm) was attached to the top of the quartz glass rod. After irradiation for 48 h the LED was removed, the solution was transferred to a separating funnel and extracted with DCM (3 x 40 mL) and washed with H₂O (30 mL). The combined organic layers were dried over MgSO₄, the solvent removed *in vacuo* to give **356** (132.2 mg, 0.23 mmol, 45%) as a colorless oil as two diastereomers (*dr* = 3:1) after flash chromatography purification (silica, hexanes / EA, 8:1).

Major diastereomer: **R_f** (hexanes / EA, 3:1): 0.45, **Staining**: KMnO₄ (UV active). **¹H-NMR** (400 MHz, CDCl₃): δ_H (ppm) = 7.51 – 7.47 (m, 2H), 7.44 – 7.40 (m, 1H), 7.26 (d, J = 5.1 Hz, 2H), 5.07 (s, 1H), 3.96 (d, J = 7.2 Hz, 1H), 3.88 (d, J = 5.1 Hz, 1H), 3.41 (d, J = 5.1 Hz, 1H), 3.30 (d, J = 7.2 Hz, 1H), 1.73 (d, J = 4.1 Hz, 3H). **¹³C-NMR** (101 MHz, CDCl₃): δ_c (ppm) = 175.29, 174.18, 131.55, 129.32, 129.06, 126.47, 90.87, 82.17, 73.91, 55.61, 50.62, 48.10, 39.06, 15.67. **IR** (neat, ν/cm^{-1}): 1777, 1708, 1495, 1390, 1340, 1247, 1192, 1139, 1111, 950, 876, 858, 703. **HRMS** (ESI): exact mass calculated for C₁₆H₁₃Br₄NO₃ [M+H]⁺: m/z 587.7666, found: m/z 587.7663.

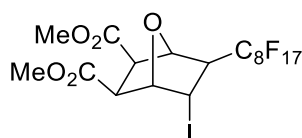
General procedure GP-F

A 5 mL flame-dried Schlenk tube equipped with a magnetic stirring bar was charged with the oxabicyclohexene (0.50 mmol, 1.0 equiv.), sodium ascorbate (59.4 mg, 0.30 mmol, 0.6 equiv.), Ru(bpy)₃Cl₂·6H₂O (**46**) (3.74 mg, 5.0 μmol , 1.0 mol%), MeCN (1 mL), MeOH (0.75 mL) and C₈F₁₇I (**181**) (409.5 mg, 200.0 μL , 0.75 mmol, 1.5 equiv.). The flask was sealed with a plastic screw cap with a Teflon sealed inlet for a quartz glass rod and the mixture degassed using the freeze-pump-thaw method

E Experimental part

(3 cycles). A high-power LED ($\lambda = 455$ nm) was attached to the top of the quartz glass rod. After irradiation for 2 – 3 h the LED was removed, the solution was transferred to a separating funnel and extracted with DCM (3 x 40 mL) and washed with H₂O (30 mL). The combined organic layers were dried over MgSO₄, the solvent removed *in vacuo* and the residue was purified by column chromatography (silica, hexanes / EA).

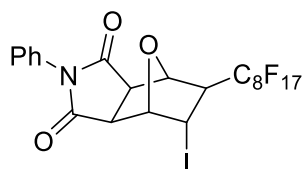
Dimethyl-(-5-iodo-6-(perfluorooctyl)-7-oxabicyclo[2.2.1]heptane-2,3-dicarboxylate (**354**)



Following general procedure *GP-F* using dimethyl-7-oxabicyclo[2.2.1]hept-5-ene-2,3-dicarboxylate (**347**)^[185] (106.1 mg, 0.50 mmol, 1.0 equiv.), sodium ascorbate (59.4 mg, 0.30 mmol, 0.6 equiv.), Ru(bpy)₃Cl₂*6H₂O (**46**) (3.74 mg, 5.0 μ mol, 1.0 mol%), MeCN (1 mL), MeOH (0.75 mL) and C₈F₁₇I (**181**) (409.5 mg, 200.0 μ L, 0.75 mmol, 1.5 equiv.) after irradiation for 2 h gave **354** (302.7 mg, 0.40 mmol, 80%) as a white solid after flash chromatography purification (silica, hexanes / EA, 3:1).

R_f (hexanes / EA, 3:1): 0.58, **Staining**: KMnO₄ (UV active). **mp**: 195 °C. **¹H-NMR** (400 MHz, CDCl₃): δ_{H} (ppm) = 5.01 (s, 1H), 4.94 (d, $J = 4.7$ Hz, 1H), 4.13 (t, $J = 5.3$ Hz, 1H), 3.97 (d, $J = 9.5$ Hz, 1H), 3.71 (dd, $J = 5.9, 2.6$ Hz, 6H), 3.06 (d, $J = 9.5$ Hz, 1H), 2.58 (td, $J = 14.6, 5.7$ Hz, 1H). **¹³C-NMR** (101 MHz, CDCl₃): δ_{C} (ppm) = 170.42, 169.64, 82.16, 78.62, 55.99, 55.78, 55.56, 52.59, 52.56, 51.63, 49.71, 15.27. (perfluorinated carbons not visible) **¹⁹F NMR** (376 MHz, CDCl₃): δ_{F} (ppm) = -81.23 (t, $J = 9.9$ Hz, 3F), -117.68 (s, 2F), -121.21 (s, 2F), -122.04 (s, 2F), -122.28 (s, 4F), -123.16 (s, 2F), -126.57 (s, 2F). **IR** (neat, ν/cm^{-1}): 1782, 1718, 1599, 1498, 1394, 1368, 1331, 1197, 1144, 973, 850, 790, 768, 697. **HRMS** (ESI): exact mass calculated for C₁₈H₁₂F₁₇IO₅ [M+H]⁺: m/z 758.9531, found: m/z 758.9533.

5-iodo-6-(perfluorooctyl)-2-phenylhexahydro-1H-4,7-epoxyisoindole-1,3(2H)-dione (**360**)

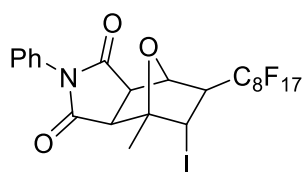


Following general procedure *GP-F* using 2-phenyl-3a,4,7,7a-tetrahydro-1H-4,7-epoxyisoindole-1,3(2H)-dione (**350**)^[198] (120.6 mg, 0.50 mmol, 1.0 equiv.), sodium ascorbate (59.4 mg, 0.30 mmol, 0.6 equiv.), Ru(bpy)₃Cl₂*6H₂O (**46**) (3.74 mg, 5.0 μ mol, 1.0 mol%), MeCN (1 mL), MeOH (0.75 mL) and C₈F₁₇I (**181**) (409.5 mg, 200.0 μ L, 0.75 mmol, 1.5 equiv.) after irradiation for 3 h gave **360** (240.1 mg, 0.31 mmol, 61%) as a white solid after flash chromatography purification (silica, hexanes / EA, 3:1).

E Experimental part

R_f (hexanes / EA, 3:1): 0.56, **Staining**: KMnO₄ (UV active). **mp**: 93 °C. **¹H-NMR** (400 MHz, CDCl₃): δ_{H} (ppm) = 7.48 (d, J = 7.8 Hz, 2H), 7.45 – 7.39 (m, 1H), 7.24 (s, 2H), 5.15 (s, 1H), 5.05 – 4.99 (m, 1H), 4.27 – 4.21 (m, 1H), 4.09 (d, J = 7.2 Hz, 1H), 3.16 (d, J = 7.2 Hz, 1H), 2.80 – 2.69 (m, 1H). **¹³C-NMR** (101 MHz, CDCl₃): δ_{C} (ppm) = 175.17, 173.83, 131.45, 129.36, 129.16, 126.39, 83.37, 79.15, 55.79, 55.57, 49.28, 48.56, 13.96. (perfluorinated carbons not visible) **¹⁹F NMR** (376 MHz, CDCl₃): δ_{F} (ppm) = -81.20 (s, 3F), -117.37 – -117.56 (m, 2F), -120.90 – -121.16 (m, 2F), -121.90 – -122.13 (m, 1F), -122.22 – -122.42 (m, 5F), -123.15 (s, 2F), -126.58 (s, 2F). **IR** (neat, ν/cm^{-1}): 2960, 1759, 1730, 1439, 1368, 1327, 1282, 1197, 1144, 1036, 1006, 951, 913, 813, 708. **HRMS** (ESI): exact mass calculated for C₂₂H₁₂F₁₇INO₃ [M+H]⁺: m/z 787.9590, found: m/z 787.9585.

5-iodo-4-methyl-6-(perfluorooctyl)-2-phenylhexahydro-1*H*-4,7-epoxyisoindole-1,3(2*H*)-dione (**357**)



Following general procedure *GP-F* using 4-methyl-2-phenyl-3a,4,7,7a-tetrahydro-1*H*-4,7-epoxyisoindole-1,3(2*H*)-dione (**351**)^[186] (127.6 mg, 0.5 mmol, 1.0 equiv.), sodium ascorbate (59.4 mg, 0.30 mmol, 0.6 equiv.), Ru(bpy)₃Cl₂·6H₂O (**46**) (3.74 mg, 5.0 μmol , 1.0 mol%), MeCN (1 mL), MeOH (0.75 mL) and C₈F₁₇I (**181**) (409.5 mg, 200.0 μL , 0.75 mmol, 1.5 equiv.) after irradiation for 3 h gave **357** (315.8 mg, 0.39 mmol, 79%) as a white solid after flash chromatography purification (silica, hexanes / EA, 4:1).

R_f (hexanes / EA, 3:1): 0.56, **Staining**: KMnO₄ (UV active). **mp**: 162 °C. **¹H-NMR** (400 MHz, CDCl₃): δ_{H} (ppm) = δ 7.46 – 7.42 (m, 2H), 7.40 – 7.35 (m, 1H), 7.19 (s, 2H), 5.05 (s, 1H), 3.97 (d, J = 5.8 Hz, 1H), 3.90 (d, J = 7.2 Hz, 1H), 3.16 (d, J = 7.2 Hz, 1H), 2.76 (td, J = 14.5, 5.8 Hz, 1H), 1.66 (s, 3H). **¹³C-NMR** (101 MHz, CDCl₃): δ_{C} (ppm) = 174.23, 174.00, 131.48, 129.32, 129.09, 126.40, 89.98, 56.86, 50.93, 49.83, 23.74, 15.15. (perfluorinated carbons not visible) **¹⁹F NMR** (376 MHz, CDCl₃): δ_{F} (ppm) = -81.21 (t, J = 9.9 Hz, 3F), -117.65 (s, 2F), -121.04 (s, 2F), -122.00 (s, 2F), -122.26 (s, 4F), -123.13 (s, 2F), -126.55 (s, 2F). **IR** (neat, ν/cm^{-1}): 1778, 1707, 1502, 1383, 1331, 1230, 1192, 1152, 1115, 1014, 876, 850, 693. **HRMS** (ESI): exact mass calculated for C₂₃H₁₃F₁₇INO₃ [M+H]⁺: m/z 801.9741, found: m/z 801.9748.

F References

F References

- [1] B. M. Trost, *Science*, **1983**, 219, 245.
- [2] B. M. Trost, *Science*, **1991**, 254, 1471.
- [3] B. M. Trost, *Angew. Chem. Int. Ed.* **1995**, 34, 259.
- [4] (a) R. A. Sheldon, *Chem. Ind. (London)* **1992**, 903; (b) R. A. Sheldon, *Green. Chem.* **2007**, 9, 1273.
- [5] P. Anastas, J. C. Warner, *Green Chemistry: Theory and Practice*, eds., Oxford University Press, Oxford, **1998**.
- [6] B. M. Trost, *Acc. Chem. Res.* **2002**, 35, 695.
- [7] M. S. Kharasch, H. Engelmann, F. R. Mayo, *J. Org. Chem.* **1937**, 2, 288.
- [8] M. S. Kharasch, E. V. Jensen, W. H. Urry, *Science* **1945**, 102, 128.
- [9] M. S. Kharasch, E. V. Jensen, W. H. Urry, *J. Am. Chem. Soc.* **1945**, 67, 1626.
- [10] M. De Malde, F. Minisci, U. Pallini, E. Volterra, A. Quilico, *Chim. Ind.* **1956**, 38, 371.
- [11] F. Minisci, *Gazz. Chim. Ital.* **1961**, 91, 386.
- [12] (a) M. Asscher, D. Vofsi, *J. Chem. Soc.* **1963**, 1887; (b) M. Asscher, D. Vofsi, *J. Chem. Soc.* **1963**, 3921.
- [13] (a) Z.-Y. Yang, D. J. Burton, *J. Org. Chem.* **1991**, 56, 5125; (b) J. O. Metzger, R. Mahler, *Angew. Chem. Int. Ed.* **1995**, 34, 902; (c) J. M. Munoz-Molina, A. Caballero, M. M. Diaz-Requejo, S. Trofimenko, T. R. Belderrain, P. J. Perez, *Inorg. Chem.* **2007**, 46, 7725.
- [14] (a) L. Forti, F. Ghelfi, E. Libertini, U. M. Pagnoni, E. Soragni, *Tetrahedron* **1997**, 53, 17761; (b) Z. Liu, J. Wang, Y. Zhao, B. Zhuo, *Adv. Synth. Catal.* **2009**, 351, 371.
- [15] B. C. Gilbert, W. Kalz, C. I. Lindsay, P. T. McGrail, A. F. Parsons, D. T. Whittaker, *J. Chem. Soc., Perkin Trans 1* **2000**, 1187.
- [16] T. Lübbers, H. J. Schäfer, *Synlett* **1991**, 12, 861.
- [17] (a) H. Matsumoto, T. Nakano, Y. Nagai, *Tetrahedron Lett.* **1973**, 14, 5147; (b) D. M. Grove, G. Van Koten, A. H. Verschuuren, *J. Mol. Catal.* **1988**, 45, 169.
- [18] (a) P. Renaud, C. Ollivier, P. Panchaud, *Angew. Chem. Int. Ed.* **2002**, 41, 3460; (b) P. Panchaud, C. Ollivier, P. Renaud, S. Zigmantas, *J. Org. Chem.* **2004**, 69, 2755; (c) L. Chabaud, Y. Landais, P. Renaud, *Org. Lett.* **2005**, 7, 2587.
- [19] (a) H. Yorimitsu, T. Nakamura, H. Shinokubo, K. Oshima, *J. Org. Chem.* **1998**, 63, 8604; (b) H. Yorimitsu, H. Shinokubo, S. Matsubara, K. Oshima, K. Omoto, H. Fujimoto, *J. Org. Chem.* **2001**, 66, 7776.
- [20] H. Matsumoto, T. Nakano, Y. Nagai, *Tetrahedron Lett.* **1973**, 14, 5147.

F References

- [21] L. Delaude, A. Demonceau, A. F. Noels, *Top. Organomet. Chem.* **2004**, *11*, 155.
- [22] F. Simal, L. Wlodarczyk, A. Demonceau, A. F. Noels, *Eur. J. Org. Chem.* **2001**, *39*, 2689.
- [23] (a) F. Simal, A. Demonceau, A. F. Noels, *Tetrahedron Lett.* **1999**, *40*, 5689; (b) B. De Clercq, F. Verpoort, *J. Organomet. Chem.* **2003**, *672*, 11.
- [24] R. Sugise, N. Sonoda, S. Murai, *Angew. Chem. Int. Ed.* **1981**, *20*, 475.
- [25] B. Cheng, C. Fang, P. Liu, J. M. Ready, *Angew. Chem. Int. Ed.* **2017**, *56*, 8780.
- [26] A. J. Cresswell, S. T. Eey, S. E. Denmark, *Angew. Chem. Int. Ed.* **2015**, *54*, 15642.
- [27] W. R. Bowman, C. F. Bridge, P. Brookes, *J. Chem. Soc., Perkin Trans. 1* **2000**, *1*.
- [28] D. P. Curran, C.-T. Chang, *Tetrahedron Lett.* **1987**, *28*, 2477.
- [29] A. J. Clark, *Chem. Soc. Rev.* **2002**, *31*, 1.
- [30] H. Nagashim, K. Seji, N. Ozaki, H. Wakamatsu, K. Itoh, Y. Tomo, J. Tsuji, *J. Org. Chem.* **1990**, *55*, 986.
- [31] (a) M. Kato, M. Kamigaito, M. Sawamoto, T. Higashimura, *Macromolecules* **1995**, *28*, 1721; (b) J.-S. Wang, K. Matyjaszewski, *J. Am. Chem. Soc.* **1995**, *117*, 5614.
- [32] K. Matyjaszewski, J. Xia, *Chem. Rev.* **2001**, *101*, 2921.
- [33] N. V. Tsarevsky, K. Matyjaszewski, *Chem. Rev.* **2007**, *107*, 2270.
- [34] E. V. Jensen, W. H. Urry, M. S. Kharasch, *J. Am. Chem. Soc.*, **1947**, *69*, 1100.
- [35] Z.-M. Qiu, D. J. Burton, *J. Org. Chem.*, **1995**, *60*, 3465.
- [36] M. Mitani, M. Nakayama, K. Koyama, *Tetrahedron Lett.* **1980**, *21*, 4457.
- [37] M. Mitani, I. Kato, K. Koyama, *J. Am. Chem. Soc.* **1983**, *105*, 6719.
- [38] J. M. Munoz-Molina, T. R. Belderrain, P. J. Perez, *Eur. J. Inorg. Chem.* **2011**, 3155.
- [39] G. Ciamician, *Science* **1912**, *36*, 385.
- [40] G. Ciamician, P. Silber, *Ber. Dtsch. Chem. Ges.* **1886**, *19*, 2899.
- [41] A. Studer, D. P. Curran, *Angew. Chem. Int. Ed.* **2016**, *55*, 58.
- [42] (a) M. P. Thekaekara, *Solar Energy* **1976**, *18*, 309; (b) D. M. Schultz, T. P. Yoon, *Science* **2014**, *343*, 1239176.
- [43] M. Fagnoni, D. Dondi, D. Ravelli, A. Albini, *Chem. Rev.* **2007**, *107*, 2725.
- [44] (a) D. M. Hedstrand, W. H. Kruizinga, R. M. Kellogg, *Tetrahedron Lett.* **1978**, *19*, 1255; (b) T. J. Van Bergen, D. M. Hedstrand, W. H. Kruizinga, R. M. Kellogg, *J. Org. Chem.* **1979**, *44*, 4953.
- [45] H. Cano-Yelo, A. Deronzier, *Tetrahedron Lett.* **1984**, *25*, 5517.

F References

- [46] K. Okada, K. Okamoto, N. Morita, K. Okubo, M. Oda, *J. Am. Chem. Soc.* **1991**, *113*, 9401.
- [47] J.-M. Kern, J.-P. Sauvage, *J. Chem. Soc. Chem. Commun.* **1987**, 546.
- [48] (a) K. Hironaka, S. Fukuzumi, T. Tonaka, *J. Chem. Soc., Perkin Trans. 2* **1984**, 1705; (b) C. Pac, M. Ihama, M. Yasuda, Y. Miyauchi, H. Sakurai, *J. Am. Chem. Soc.* **1981**, *103*, 6495; (c) O. Ishitani, C. Pac, H. Sakurai, *J. Org. Chem.* **1983**, *48*, 2941.
- [49] K. Kalyanasundaram, M. Grätzel, *Coord. Chem. Rev.* **1998**, *177*, 347.
- [50] H. Takeda, O. Ishitani, *Coord. Chem. Rev.* **2010**, *254*, 346.
- [51] M. Grätzel, *Acc. Chem. Rev.* **1981**, *14*, 376.
- [52] M. A. Ischay, M. E. Anzovino, J. Du, T. P. Yoon, *J. Am. Chem. Soc.* **2008**, *130*, 12886.
- [53] D. A. Nicewicz, D. W. MacMillan, *Science* **2008**, *322*, 77.
- [54] J. M. Narayanam, J. W. Tucker, C. R. Stephenson, *J. Am. Chem. Soc.* **2009**, *131*, 8756.
- [55] (a) F. H. Burstall, *J. Chem. Soc.* **1936**, 173; (b) J. P. Paris, W. W. Brandt, *J. Am. Chem. Soc.* **1959**, *81*, 5001; (c) A. Juris, V. Balzani, F. Barigelletti, S. Campagna, P. Belser, A. Von Zelewsky, *Coord. Chem. Rev.* **1988**, *84*, 85.
- [56] C. K. Prier, D. A. Rankic, D. W. MacMillan, *Chem. Rev.* **2013**, *113*, 5322.
- [57] (a) K. Kalyanasundaram, *Coord. Chem. Rev.* **1982**, *46*, 159; (b) J. K. McCusker, *Acc. Chem. Rev.* **2003**, *36*, 876.
- [58] D. M. Arias-Rotondo, J. K. McCusker, *Chem. Soc. Rev.* **2016**, *45*, 5803.
- [59] R. C. McAtee, E. J. McClain, C. R. Stephenson, *Trends Chem.* **2019**, *1*, 111.
- [60] (a) F. Scandola, M. T. Indelli, C. Chiorboli, C. A. Bignozzi, *Photoinduced Electron Transfer II*; (Ed. J. Mattay), Springer, Berlin, Heidelberg, **1990**; (b) G. D. Scholes, *Annu. Rev. Phys. Chem.* **2003**, *54*, 57.
- [61] F. Strieth-Kalthoff, M. J. James, M. Teders, L. Pitzer, F. Glorius, *Chem. Soc. Rev.* **2018**, *47*, 7190.
- [62] A. Hossain, A. Bhattacharyya, O. Reiser, *Science*, **2019**, *364*, 450.
- [63] D. P. Hari, B. König, *Chem. Commun.* **2014**, *50*, 6688.
- [64] L. Marzo, S. K. Pagire, O. Reiser, B. König, *Angew. Chem. Int. Ed.* **2018**, *57*, 10034.
- [65] J. Twilton, C. Le, P. Zhang, M. H. Shaw, R. W. Evans, D. W. MacMillan, *Nat. Rev. Chem.* **2017**, *0052*, 1.
- [66] C. Jiang, W. Chen, W.-H. Zheng, H. Lu, *Org. Biomol. Chem.* **2019**, *17*, 8673.
- [67] Z. C. Litman, Y. Wang, H. Zhao, J. F. Hartwig, *Nature* **2018**, *560*, 355.
- [68] J. P. Barham, B. König, *Angew. Chem. Int. Ed.* **2020**, *59*, 11732.
- [69] Q. Zhu, E. C. Gentry, R. R. Knowles, *Angew. Chem. Int. Ed.* **2016**, *55*, 9969.

F References

- [70] (a) Q.-Y. Meng, T. E. Schirmer, A. L. Berger, K. Donabauer, B. König, *J. Am. Chem. Soc.* **2019**, *141*, 11393; (b) L. Pitzer, J. L. Schwarz, F. Glorius, *Chem. Sci.* **2019**, *10*, 8285.
- [71] J. P. Phelan, S. B. Lang, J. S. Compton, C. B. Kelly, R. Dykstra, O. Gutierrez, G. A. Molander, *J. Am. Chem. Soc.* **2018**, *140*, 8037.
- [72] D. H. Barton, M. A. Csiba J. C. Jaszberenyi, *Tetrahedron Lett.* **1994**, *35*, 2869.
- [73] J. D. Nguyen, J. W. Tucker, M. D. Konieczynska, C. R. Stephenson, *J. Am. Chem. Soc.* **2011**, *133*, 4160.
- [74] M. Pirtsch, S. Paria, T. Matsuno, H. Isobe, O. Reiser, *Chem. Eur. J.* **2012**, *18*, 7336.
- [75] E. Arceo, E. Montroni, P. Melchiorre, *Angew. Chem. Int. Ed.* **2014**, *53*, 12064.
- [76] E. Zhu, X.-X. Liu, A.-J. Wang, T. Mao, L. Zhao, X. Zhang, C.-Y. He, *Chem. Commun.* **2019**, *55*, 12259.
- [77] G. Magagano, A. Gualandi, M. Machini, L. Mengozzi, P. Ceroni, P. G. Cozzi, *Chem. Commun.* **2017**, *53*, 1591.
- [78] N. F. Nikitas, E. Voutyritsa, P. L. Gkizis, C. G. Kokotos, *Eur. J. Org. Chem.* **2021**, 96.
- [79] C. Rosso, G. Filippini, P. G. Cozzi, A. Gaulandi, M. Prato, *ChemPhotoChem* **2019**, *3*, 193.
- [80] P. Riente, M. A. Pericas, *ChemSusChem* **2015**, *8*, 1841.
- [81] T. Koike, M. Akita, *Acc. Chem. Res.* **2016**, *49*, 1937.
- [82] S. H. Oh, Y. R. Malpani, N. Ha, Y.-S. Jung, S. B. Han, *Org. Lett.* **2014**, *16*, 1310.
- [83] X.-J. Tang, W. R. Dolbier, *Angew. Chem. Int. Ed.* **2015**, *54*, 4246.
- [84] D. B. Bagal, G. Kachkovskyi, M. Knorn, T. Rawner, B. M. Bhanage, O. Reiser, *Angew. Chem. Int. Ed.* **2015**, *54*, 6999.
- [85] T. Rawner, M. Knorn, E. Lutsker, A. Hossain, O. Reiser, *J. Org. Chem.* **2016**, *81*, 7139.
- [86] P. Ehrnsberger, O. Reiser, *Science of Synthesis: Photocatalysis in Organic Synthesis* (Ed. B. König), Thieme, Stuttgart, **2019**, 271.
- [87] A. Hossain, A. Vidyasagar, C. Eichinger, C. Lankes, J. Phan, J. Rehbein, O. Reiser, *Angew. Chem. Int. Ed.* **2018**, *57*, 8288.
- [88] S. Engl, O. Reiser, *Eur. J. Org. Chem.* **2020**, 2020, 1523.
- [89] J. K. Kochi, *J. Am. Chem. Soc.* **1962**, *84*, 2121.
- [90] C.-J. Wallentin, J. D. Nguyen, P. Finkbeiner, C. R. Stephenson, *J. Am. Chem. Soc.* **2012**, *134*, 8875.
- [91] C. Rosso, G. Filippini, P. G. Cozzi, A. Gaulandi, M. Prato, *ChemPhotoChem* **2019**, *3*, 193.
- [92] T. Rawner, E. Lutsker, C. A. Kaiser, O. Reiser, *ACS Catal.* **2018**, *8*, 3950.
- [93] A. Hossain, S. Engl, E. Lutsker, O. Reiser, *ACS Catal.* **2019**, *9*, 1103.

F References

- [94] S. Engl, O. Reiser, *ACS Catal.* **2020**, *10*, 9899.
- [95] R. Fayad, S. Engl, E. O. Danilov, C. E. Hauke, O. Reiser, F. N. Castellano, *J. Phys. Chem. Lett.* **2020**, *11*, 5345.
- [96] T. M. Williams, C. R. Stephenson, *Visible Light Photocatalysis in Organic Chemistry* (Ed. T. P. Yoon, D. W. MacMillan, C. R. Stephenson), Wiley-VCH, Weinheim, **2018**, 73.
- [97] T. Courant, G. Masson, *J. Org. Chem.* **2016**, *81*, 6945.
- [98] X. Gu, X. Li, Y. Qu, P. Li, Y. Yao, *Chem. Eur. J.* **2013**, *19*, 11878.
- [99] (a) X. Gu, P. Lu, W. Fan, P. Li, Y. Yao, *Org. Biomol. Chem.* **2013**, *11*, 7088; (b) Y. Shen, J. Cornella, F. Julia-Hernandez, R. Martin, *ACS Catal.* **2017**, *7*, 409; (c) W.-Z. Weng, H. Liang, R.-Z. Hao, Y.-X. Ji, B. Zhang, *Org. Lett.* **2019**, *21*, 5586.
- [100] B. P. Fors, C. J. Hawker, *Angew. Chem. Int. Ed.* **2012**, *51*, 8850.
- [101] T. Courant, G. Masson, *Chem. Eur. J.* **2012**, *18*, 423.
- [102] Y. Yasu, T. Koike, M. Akita, *Angew. Chem. Int. Ed.* **2012**, *51*, 9567.
- [103] A. Carboni, G. Dagousset, E. Magnier, G. Masson, *Org. Lett.* **2014**, *16*, 1240.
- [104] L. Li, M. Huang, C. Liu, J.-C. Xiao, Q.-Y. Chen, Y. Guo, Z.-G. Zhao, *Org. Lett.* **2015**, *17*, 4714.
- [105] (a) S. Mizuta, S. Verhoog, K. M. Engle, T. Khotavivattana, M. O'Duill, K. Wheelhouse, G. Rassias, M. Medebielle, V. Gouverneur, *J. Am. Chem. Soc.* **2013**, *135*, 2505; (b) D. J. Wilger, N. J. Gesmundo, D. A. Nicewicz, *Chem. Sci.* **2013**, *4*, 3160; (c) Q. Lefebvre, N. Hoffmann, M. Rueping, *Chem. Commun.* **2016**, *52*, 2493.
- [106] (a) Y. Yasu, T. Koike, M. Akita, *Org. Lett.* **2013**, *15*, 2136; (b) G. Dagousset, A. Carboni, E. Magnier, G. Masson, *Org. Lett.* **2014**, *16*, 4340.
- [107] A. Carboni, G. Dagousset, E. Magnier, G. Masson, *Chem. Commun.* **2014**, *50*, 14197.
- [108] G. Levitre, G. Dagousset, E. Anselmi, B. Tuccio, E. Magnier, G. Masson, *Org. Lett.* **2019**, *21*, 6005.
- [109] (a) G. E. Keck, E. J. Enholm, J. B. Yates, M. R. Wiley, *Tetrahedron* **1985**, *41*, 4079; (b) J. Grignon, M. Pereyre, *J. Organomet. Chem.* **1973**, *61*, 33.
- [110] (a) J. Podlech, T. C. Maier, *Synthesis* **2003**, 633; (b) P. Cintas, *Synlett* **1995**, 1087; (c) Y. Okude, S. Hirano, T. Hiyama, H. Nozaki, *J. Am. Chem. Soc.* **1977**, *99*, 3179; (d) M. Bandini, P. G. Cozzi, P. Melchiorre, A. Umani-Ronchi, *Angew. Chem. Int. Ed.* **1999**, *38*, 3357; (e) P. Cintas, *Synlett* **1995**, 1087.
- [111] (a) X. Li, X. Liu, Y. Fu, L. Wang, L. Zhou, X. Feng, *Chem. Eur. J.* **2008**, *14*, 4796; (b) D. G. Hall, *Synlett* **2007**, 1644; (c) V. Rauniyar, D. G. Hall, *J. Am. Chem. Soc.* **2004**, *126*, 4518.
- [112] (a) V. Hornillos, M. Perez, M. Fananas-Mastral, B. L. Feringa, *J. Am. Chem. Soc.* **2013**, *135*, 2140; (b) J. Nokami, K. Nomiyama, S. M. Shafi, K. Kataoka, *Org. Lett.* **2004**, *6*, 1261.

F References

- [113] (a) M. Kosugi, H. Arai, A. Yoshino, T. Migaita, *Chem. Lett.* **1978**, 795; (b) D. P. Curran, W. Shen, J. Zhang, T. A. Heffner, *J. Am. Chem. Soc.* **1990**, *112*, 6738; (c) L. de Quadras, J. Stahl, F. Zhuravlev, J. A. Gladysz, *J. Organomet. Chem.* **2007**, *692*, 1859.
- [114] (a) A. Dossena, S. Sampaolesi, A. Palmieri, S. Protti, M. Fagnoni, *J. Org. Chem.* **2017**, *82*, 10687; (b) G. Pandey, K. S. Rani, G. Lakshmaiah, *Tetrahedron Lett.* **1992**, *33*, 5107; (c) L. Möhlmann, S. Blechert, *Adv. Synth. Catal.* **2014**, *356*, 2825; (d) M.-H. Larraufie, R. Pellet. L. Fensterbank, J.-P. Goddard, E. Lacote, M. Malacria, C. Ollivier, *Angew. Chem. Int. Ed.* **2011**, *50*, 4463; (e) S. Milanesi, M. Fagnoni, A. Albini, *J. Org. Chem.* **2005**, *70*, 603.
- [115] D. F. Reina, A. Ruffoni, Y. S. Al-Faiyz, J. J. Douglas, N. S. Sheikh, D. Leonori, *ACS Catal.* **2017**, *7*, 4126.
- [116] S. Mizuta, K. M. Engle, S. Verhoog, O. Galicia-Lopez, M. O'Duill, M. Medebielle, K. Wheelhouse, G. Rassias, A. L. Thompson, V. Gouverneur, *Org. Lett.* **2013**, *15*, 1250.
- [117] M. Knorn, T. Rawner, R. Czerwieniec, O. Reiser, *ACS Catal.* **2015**, *5*, 5186.
- [118] S. Paria, M. Pirtsch, V. Kais, O. Reiser, *Synthesis* **2013**, *45*, 2689.
- [119] (a) A. Wimmer, B. König, *Beilstein J. Org. Chem.* **2018**, *14*, 54; (b) A. U. Meyer, A. Wimmer, B. König, *Angew. Chem. Int. Ed.* **2017**, *56*, 409; (c) Y. Zheng, Y. You, Q. Shen, J. Zhang, L. Liu, X.-D. Duan, *Org. Chem. Front.* **2020**, *7*, 2069; (d) M. S. Santos, H. L. Betim, C. M. Kisukuri, J. A. Campos Delgado, A. G. Correa, M. W. Paixao, *Org. Lett.* **2020**, *22*, 4266; (e) V. V. Levin, A. D. Dilman, *J. Org. Chem.* **2019**, *84*, 8337.
- [120] S. K. Pagire, A. Hossain, O. Reiser, *Org. Lett.* **2018**, *20*, 648.
- [121] (a) D. C. Meadows, J. Gervay-Hague, *Med. Res. Rev.* **2006**, *26*, 793; (b) S. Y. Woo, J. H. Kim, K. M. Moon, S.-H. Han, S. K. Yeon, J. W. Choi, B. K. Jang, H. J. Song, Y. G. Kang, J. W. Kim, J. Lee, D. J. Kim, O. Hwang, K. D. Park, *J. Med. Chem.* **2014**, *57*, 1473; (c) E. N. Prilezhaeva, *Russ. Chem. Rev.* **2000**, *66*, 367.
- [122] (a) K. Anczkiewicz, M. Krolikiewicz, Z. Wrobel, K. Wojciechowski, *Tetrahedron* **2015**, *71*, 3924; (b) X. Huang, S. Lou, O. Burghaus, R. D. Webster, K. Harms, E. Meggers, *Chem. Sci.* **2017**, *8*, 7126; (c) L. Cui, H. Chen, C. Liu, C. Li, *Org. Lett.* **2016**, *18*, 2188; (d) G. Le Duc, E. Bernoud, G. Prestat, S. Cacchi, G. Fabrizi, A. Iazzetti, D. Madec, G. Poli, *Synlett* **2011**, *20*, 2943.
- [123] (a) S. Z. Zard, *Chem. Soc. Rev.* **2008**, *37*, 1603; (b) M. D. Kärkäs, *ACS Catal.* **2017**, *7*, 4999; (c) L. N. S. Crespín, A. Greb, D. C. Blakemore, S. V. Ley, *J. Org. Chem.* **2017**, *82*, 13093; (d) Q. Qin, S. Yu, *Org. Lett.* **2015**, *17*, 1894.
- [124] Q. Qin, D. Ren, S. Yu, *Org. Biomol. Chem.* **2015**, *13*, 10295.
- [125] C. Lankes, *Photoredox catalysis Using Copper Complexes*. Dissertation, Universität Regensburg, **2017**.
- [126] (a) A.-N. Alba, X. Companyo, R. Rios, *Chem. Soc. Rev.* **2010**, *39*, 2018; (b) D. C. Meadows, J. Gervay-Hague, *Med. Res. Rev.* **2006**, *26*, 793.
- [127] (a) H. Chen, L. Guo, S. Yu, *Org. Lett.* **2018**, *20*, 6255; (b) N. Iqbal, J. Jung, S. Park, E. Cho, *Angew. Chem. Int. Ed.* **2014**, *53*, 539; (c) W. J. Choi, S. Choi, K. Ohkubo, S. Fukuzumi, E. Choi, Y. You, *Chem. Sci.* **2015**, *6*, 1454.

F References

- [128] N. J. Lawrence, *Science of Synthesis, Houben-Weyl, Methods of Molecular Transformations* (Ed. I. Fleming), Thieme, Stuttgart, **2002**, 1(4), 579.
- [129] K. Tamao, M. Kumada, *J. Organomet. Chem.* **1971**, 30, 339.
- [130] C.-W. Chen, P. Beak, *J. Org. Chem.* **1986**, 52, 3325.
- [131] A. G. Barret, J. A. Flygare, *J. Org. Chem.* **1991**, 56, 638.
- [132] (a) J. P. Pillot, J. Dunogues, R. Calas, *Synthesis* **1977**, 7, 469; (b) J. Gonzalez, C. J. Foti, S. Elsheimer, *J. Org. Chem.* **1991**, 56, 4322; (c) P. G. Janson, I. Ghoneim, N. O. Ilchenko, K. J. Szabo, *Org. Lett.* **2012**, 14, 2882.
- [133] (a) T. T. Vasil'eva, S. I. Gapusenko, S. V. Vitt, A. B. Terent'ev, *Izv. Akad. Nauk. Ser. Khim.* **1992**, 2347; (b) T. T. Vasil'eva, S. I. Gapusenko, A. B. Terent'ev, V. V. Pinyaskin, I. V. Sankevich, A. L. Chistyakov, E. I. Mysov, *Russ. Chem. Bull.* **1993**, 42, 840.
- [134] J. P. Pillot, J. Dunogues, R. Calas, *Synthesis* **1977**, 7, 469.
- [135] D. J. Peterson, *J. Org. Chem.* **1968**, 33, 780.
- [136] D. J. Ager, *Org. Reactions* **1990**, 38, 1.
- [137] L. F. van Staden, D. Gravestock, D. J. Ager, *Chem. Soc. Rev.*, **2002**, 31, 195.
- [138] C. Palomo, J. M. Aizpurua, J. M. Garcia, L. Ganboa, F. P. Cossio, B. Lecea, C. Lopez, *J. Org. Chem.* **1990**, 55, 2498.
- [139] A. G. Barret, J. A. Flygare, J. M. Hill, E. M. Wallace, *Org. Synth.* **1996**, 73, 50.
- [140] (a) B. Kirschleger, R. Queignec, *Synthesis* **1986**, 926; (b) I. Fleming, I. Paterson, *Synthesis* **1979**, 446; (c) S. Ambasht, S. K. Chiu, P. E. Peterson, J. Queen, *Synthesis* **1980**, 318; (d) K. Nishiyama, N. Tanaka, *J. Chem. Soc., Chem. Commun.* **1983**, 318; (e) N. Shirai, Y. Sato, *J. Org. Chem.* **1988**, 53, 194; (f) H. Yoshioka, M. Shimizu, F. Yagihashi, T. Takahata, A. Yamamoto, (*Jpn. Kokai Tokkyo Koho*), JP 02 290,885, [90 290,885], **1990**.
- [141] G. M. Schwarzwald, C. D. Matier, G. C. Fu, *Angew. Chem. Int. Ed.* **2019**, 58, 3571.
- [142] (a) R. Ramesh, D. S. Reddy, *J. Med. Chem.* **2018**, 61, 3779; (b) S. Fuiji, Y. Hasimoto, *Future Med. Chem.* **2017**, 9, 485.
- [143] R. Grigg, C. Najera, J. M. Sansano, M. Yus, *Synth. Commun.* **2006**, 27, 1111.
- [144] D. J. Ager, *Chem. Soc. Rev.* **1982**, 11, 493.
- [145] N. S. Simpkins, *Sulphones in Organic Synthesis*, Pergamon Press, Oxford, **1993**.
- [146] P. J. Kocienski, *Tetrahedron Lett.* **1979**, 2649.
- [147] R. C. Carr, R. V. Williams, L. A. Paquette, *J. Org. Chem.* **1983**, 48, 4976.
- [148] L. A. Paquette, *Isr. J. Chem.* **1981**, 21, 128.

F References

- [149] (a) L. A. Paquette, *Chemical Reviews*, **1986**, 86, 733; (b) G. J. Wells, T.-H. Yan, L. A. Paquette, *J. Org. Chem.* **1984**, 49, 3604.
- [150] V. B. Sharma, S. L. Jain, B. Sain, *Catal. Commun.* **2006**, 7, 454.
- [151] G. Maas, *Organometallics* **2001**, 20, 4607.
- [152] M. Lautens, P. M. Delanghe, *J. Org. Chem.* **1992**, 57, 798.
- [153] (a) H. Wang, G. Zhang, Q. Zhang, Y. Wang, Y. Li, T. Xiong, Q. Zhang, *Chem. Commun.* **2020**, 56, 1819; (b) Z.-Y. Zhao, Y.-X. Nie, R.-H. Tang, G.-W. Yin, J. Cao, Z. Xu, Y.-M. Cui, Z.-J. Zheng, L.-W. Xu, *ACS Catal.* **2019**, 9, 9110.
- [154] N. R. O'Connor, J. L. Wood, B. M. Stoltz, *Isr. J. Chem.* **2016**, 56, 431.
- [155] (a) T. F. Schneider, J. Kaschel, D. B. Werz, *Angew. Chem. Int. Ed.* **2014**, 53, 5504; (b) H. K. Grover, M. R. Emmett, M. A. Kerr, *Org. Biomol. Chem.* **2015**, 13, 655; (c) H.-U. Reissig, R. Zimmer, *Chem. Rev.* **2003**, 103, 1151.
- [156] D. C. Braddock, D. M. Badine, T. Gottschalk, *Synlett* **2001**, 1909.
- [157] K. V. Yadav, R. Balamurugan, *Org. Lett.* **2001**, 3, 2717.
- [158] P. G. Wuts, T. W. Greene, *Greene's Protective Groups in Organic Synthesis*, John Wiley & Sons, Inc, Hoboken, NJ, USA, **2006**.
- [159] G. A. Johnston, *Pharmacol. Ther.* **1996**, 69, 173.
- [160] V. I. Ivanskii, V. N. Maksimov, *Zh. Org. Khim.* **1972**, 8, 52.
- [161] K. Paulini, H.-U. Reissig, *Liebigs Ann. Chem.* **1991**, 5, 455.
- [162] (a) R. D. Allan, G. A. Johnston, *Med. Res. Rev.* **1983**, 3, 91; (b) P. D. Kennwell, S. S. Matharu, J. B. Taylor, R. Westwood, P. G. Sammes, *J. Chem. Soc., Perkin Trans. 1.* **1982**, 2563; (c) C. R. Gardner, C. J. Roberts, R. J. Walker, L. Chidley, S. Clements-Jewery, *Neuropharmacology* **1982**, 21, 197.
- [163] (a) R. D. Allan, D. R. Curtis, P. M. Headley, G. A. Johnston, D. Lodge, B. Twitchin, *J. Neurochem.* **1980**, 34, 652; (b) T. Kasuma, T.-L. Wang, W. B. Guggino, G. R. Cutting, G. R. Uhl, *Eur. J. Pharmacol.* **1993**, 245, 83; (c) J. Vien, R. K. Duke, K. N. Mewett, G. A. Johnston, R. Shingai, M. Chebib, *Br. J. Pharmacol.* **2002**, 135, 883.
- [164] (a) T. Morikawa, H. Sasaki, R. Hanai, A. Shibuya, T. Taguchi, *J. Org. Chem.* **1994**, 59, 97; (b) R. Gelazzi, G. Mobbili, M. Orena, *Tetrahedron: Asymmetry* **1997**, 8, 133; (c) R. K. Duke, R. D. Allan, M. Chebib, J. R. Greenwood, G. A. Johnston, *Tetrahedron: Asymmetry* **1998**, 9, 2533.
- [165] R. K. Duke, M. Chebib, V. J. Balcar, R. D. Allan, K. N. Mewett, G. A. Johnston, *J. Neurochem.* **2000**, 75, 2602.
- [166] (a) O. Wallach, *Justus Liebigs. Ann. Chem.* **1907**, 356, 197; (b) Y.-R. Naves, P. Ardizio, *Bull. Soc. Chim. Fr.* **1950**, 673.
- [167] M. Benn, T. L. Peppard, *J. Agric. Food Chem.* **1996**, 44, 557.

F References

- [168] M. Robiquet, *Ann. Chim.* **1810**, 76, 302.
- [169] F. Bohlmann, C. Zdero, H. Kapteyn, *Liebigs. Ann. Chem.* **1968**, 717, 186.
- [170] D. M. Estrada, J. L. Ravelo, C. Ruiz-Perez, J. Martin, *Tetrahedron Lett.* **1989**, 30, 6219.
- [171] K. E. Parkes, G. Pattenden, *Tetrahedron Lett.* **1986**, 27, 2535.
- [172] C. A. Rizzo, L. Schweizer, T. E. Spires, J. S. Platero, M. Obermeier, W. Shan, M. E. Salvati, W. R. Foster, J. Dinchuk, S.-J. Chen, G. Vite, R. Kramer, M. M. Gottardis, *Cancer Res.* **2009**, 69, 652.
- [173] S. Roscales, J. Plumet, *Heterocycles*, **2015**, 90, 741.
- [174] O. Diels, K. Alder, *Ber. Dtsch. Chem. Ges.* **1929**, 62, 554.
- [175] C. O. Kappe, S. S. Murphree, A. Padwa, *Tetrahedron*, **1997**, 53, 14179.
- [176] L. Rulisek, P. Sebek, Z. Havlas, R. Hrabal, P. Capek, A. Svatos, *J. Org. Chem.* **2005**, 70, 6295.
- [177] J. Cossy, J. Plumet, O. Arjona, P. Vogel, *Tetrahedron*, **1999**, 55, 3521.
- [178] (a) V. P. Zaytsev, D. F. Mersalov, L. V. Chervyakova, G. Krishna, F. I. Zubkov, P. V. Dorovatovskii, V. N. Khrustalev, V. V. Zarubaev, *Tetrahedron Letters*, **2019**, 60, 151204; (b) A. Baran, C. Kazaz, H. Secen, Y. Sutbeyaz, *Tetrahedron*, **2003**, 59, 3643; (c) N. Jotterand, P. Vogel, K. Schenk, *Helv. Chim. Acta.* **1999**, 82, 821; (d) Y. Kitahara, T. Kato, O. Noboru, A. Inoue, H. Izumi, *J. Chem. Soc. C*, **1968**, 20, 2508.
- [179] (a) J. T. Maynard, *J. Org. Chem.* **1963**, 28, 112; (b) L. C. Garver, E. E. Van Tamelen, *J. Am. Chem. Soc.* **1982**, 104, 867; (c) H. Takayama, K. Hayashi, T. Koizumi, *Tetrahedron Lett.* **1986**, 27, 5509; (d) T. Kato, T. Suzuki, N. Ototani, H. Maeda, K. Yamada, *J. Chem. Soc., Perkin Trans. 1*, **1977**, 206.
- [180] (a) I. B. Masesane, P. G. Steel, *Synlett*, **2003**, 5, 735; (b) F. Brion, *Tetrahedron Lett.* **1982**, 23, 5299.
- [181] (a) A. Padwa, E. A. Curtis, V. P. Sandanakaya, *J. Org. Chem.* **1997**, 62, 1317; (b) M. Lautens, S. Ma, R. K. Belter, P. Chiu, A. Leschziner, *J. Org. Chem.* **1992**, 57, 4065; (c) R. J. Moss, B. Rickborn, *J. Org. Chem.* **1985**, 50, 1381.
- [182] A. Gandini, *Prog. Polym. Sci.* **2013**, 38, 1.
- [183] (a) H. Singh, M. Prasad, R. D. Srivastava, *J. Chem. Technol. Biotechnol.* **1980**, 30, 293; (b) W. Zhang, Y. L. Zhu, S. Niu, Y. W. Li, *J. Mol. Catal. A: Chem.* **2011**, 335, 71; (b) N. Alonso-Fagundez, M. L. Granados, R. Mariscal, M. Ojeda, *ChemSusChem*, **2012**, 5, 1984.
- [184] E. Mahmoud, D. A. Watson, R. F. Lobo, *Green. Chem.* **2014**, 16, 167.
- [185] T. Earl, L. Alty, M. France, *J. Chem. Educ.* **1999**, 76, 659.
- [186] C. S. Daeffler, R. H. Grubbs, *Macromolecules*, **2013**, 46, 3288.
- [187] T. Föll, J. Rehbein, O. Reiser, *Org. Lett.* **2018**, 20, 5794.
- [188] (a) C. Faderl, S. Budde, G. Kachkovskyi, D. Rackl, O. Reiser, *J. Org. Chem.* **2018**, 83, 12192; (b) G. Kachkovskyi, C. Faderl, O. Reiser, *Adv. Synth. Catal.* **2013**, 355, 2240.

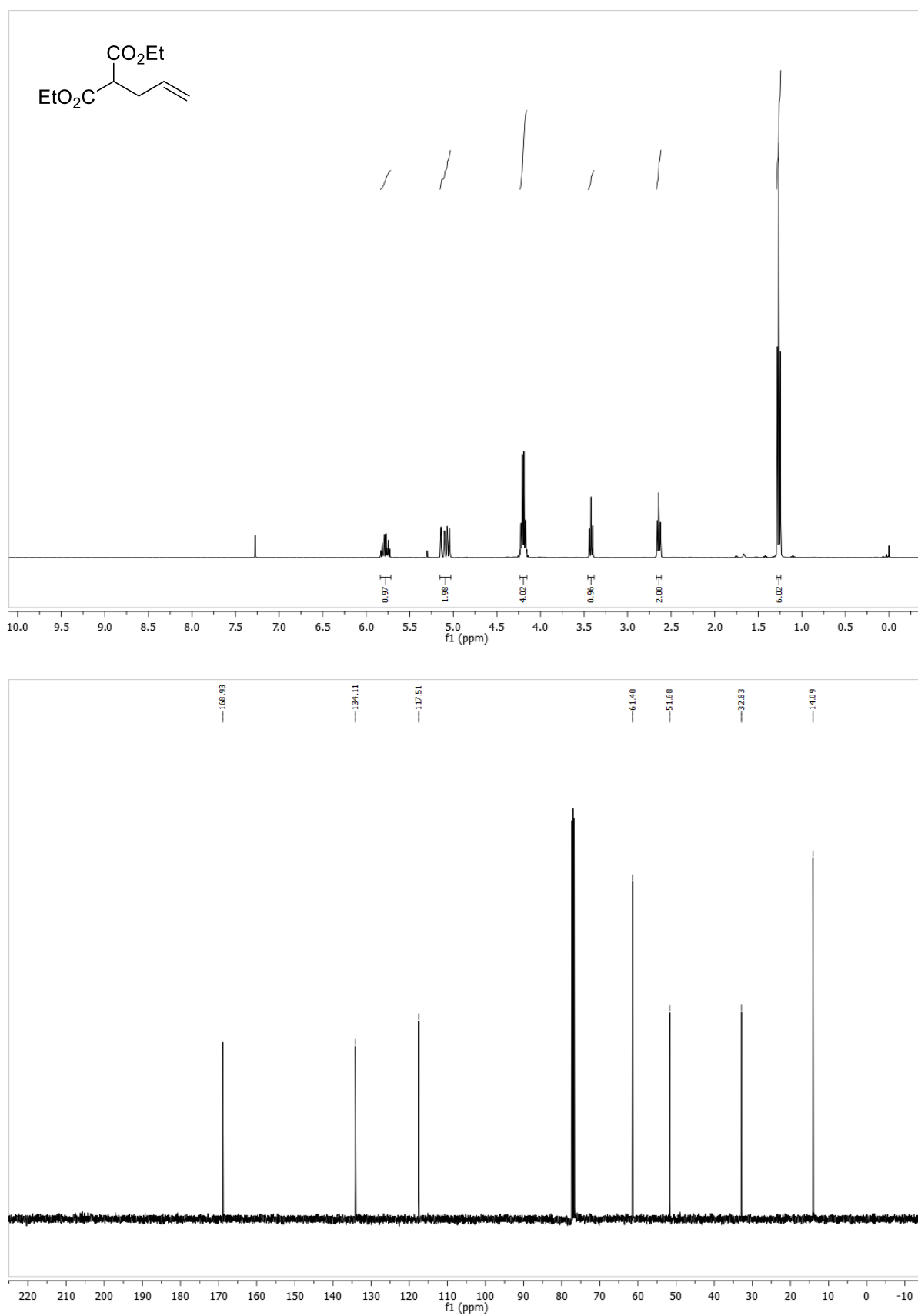
F References

- [189] (a) H. A. Carless, O. Z. Oak, *Chem. Soc., Chem. Commun.* **1991**, 61; (b) J. T. Maynard, *J. Org. Chem.* **1963**, 28, 112; (c) S. Ogawa, Y. Iwasawa, T. Nose, T. Suami, S. Ohba, M. Ito, Y. Saito, *J. Chem. Soc., Perkin Trans. 1* **1985**, 903; (d) W. M. Best, D. Wege, *Tetrahedron Lett.* **1981**, 22, 4877; (e) E. A. Curtis, V. P. Sandanayaka, A. Padwa, *Tetrahedron Lett.* **1995**, 36, 1989; (f) N. Jotterand, P. Vogel, *Helv. Chim. Acta* **1999**, 82, 821.
- [190] T. Kato, T. Suzuki, N. Ototani, H. Maeda, K. Yamada, *J. Chem. Soc., Perkin Trans. 1*, **1977**, 206.
- [191] P. Ehrnsberger, *Master Thesis*, University of Regensburg, **2016**.
- [192] W. L. Armarego, C. L. Chai, *Purification of Laboratory Chemicals*, 6th ed. Butterworth Heinemann: Oxford, **2009**.
- [193] M. Lee, S. Neukirchen, C. Cabrele, O. Reiser, *J. Pept. Sci.* **2017**, 23, 556.
- [194] A. Podgorsek, S. Stavber, M. Zupan, J. Iskra, *Green Chem.* **2007**, 9, 1212.
- [195] M. Mahlau, P. Garcia-Garcia, B. List, *Chem. Eur. J.* **2012**, 18, 16283.
- [196] V. Percec, C. Grigoras, *J. Polym. Sci. A Polym. Chem.* **2005**, 43, 5283.
- [197] O. Pavlyuk, H. Teller, M. C. McMills, *Tetrahedron Lett.* **2009**, 50, 2716.
- [198] M. V. Gil, V. Luque-Agudo, E. Roman, J. A. Serrano, *Synlett* **2014**, 25, 2179.
- [199] C. Faderl, *Photoinduced Decarboxylation of N-Acyloxyphthalimides*. Dissertation, Universität Regensburg, **2017**.

G Appendix

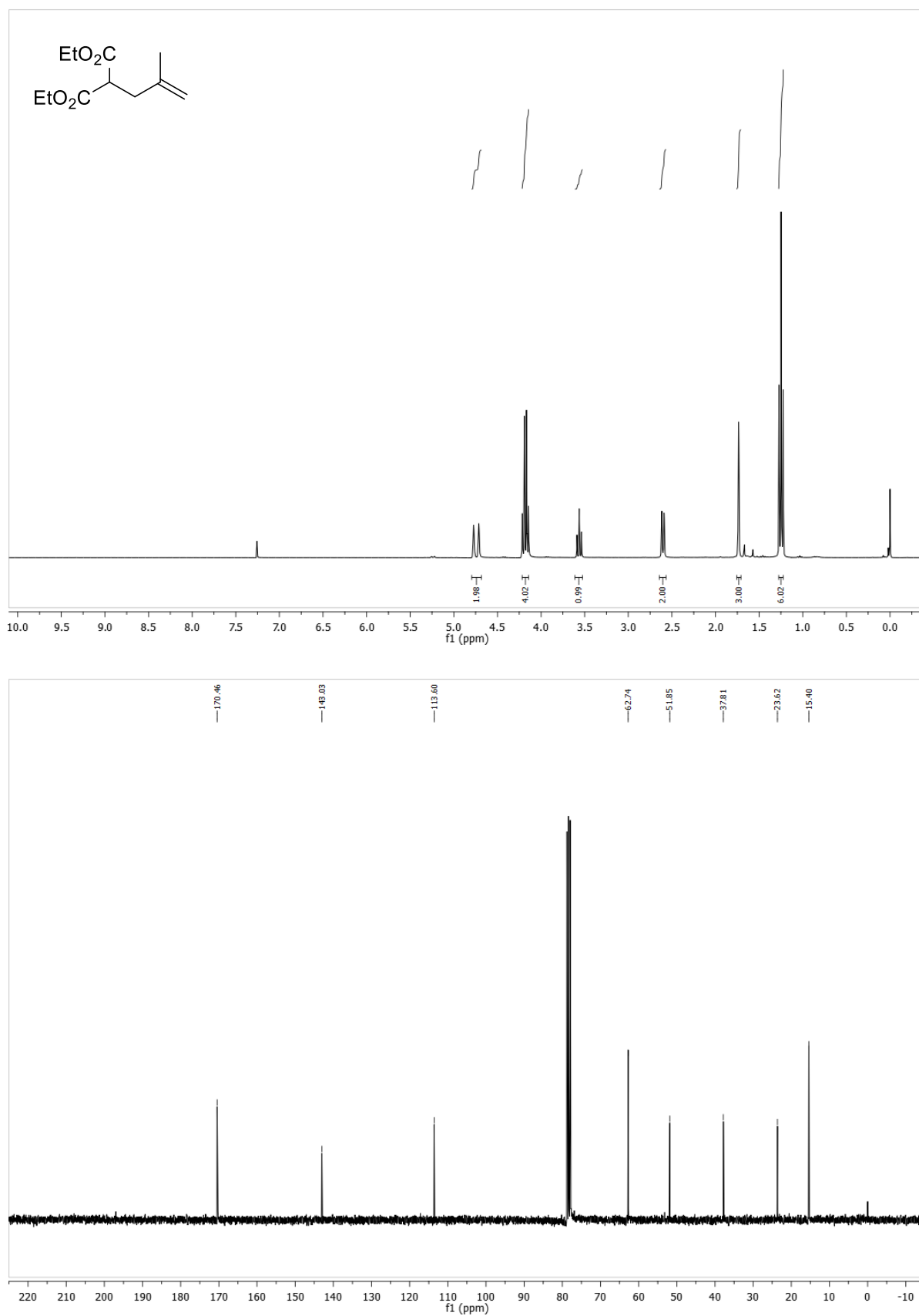
G Appendix

Diethyl 2-allylmalonate (160)



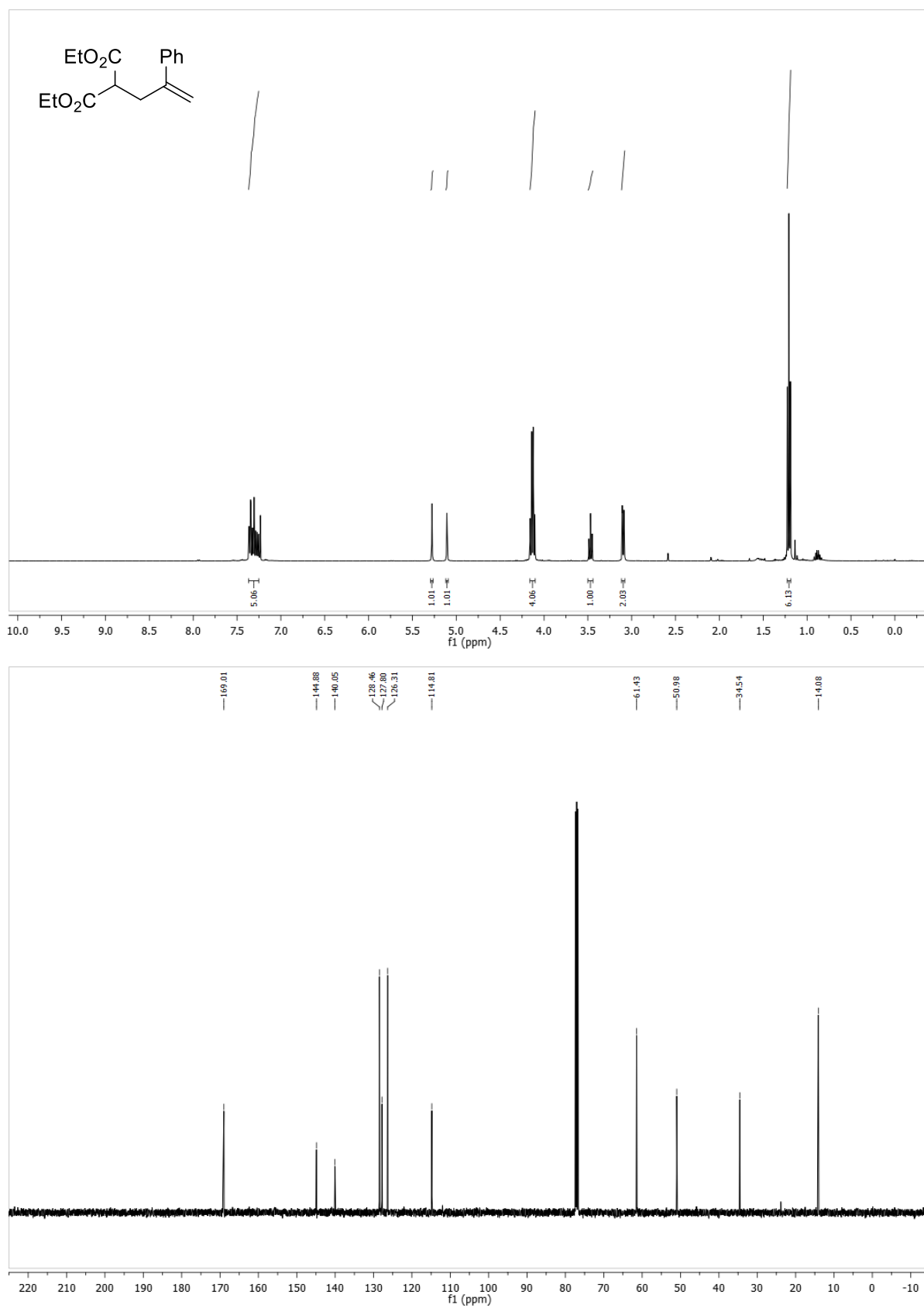
G Appendix

Diethyl 2-(2-methylallyl)malonate (162)



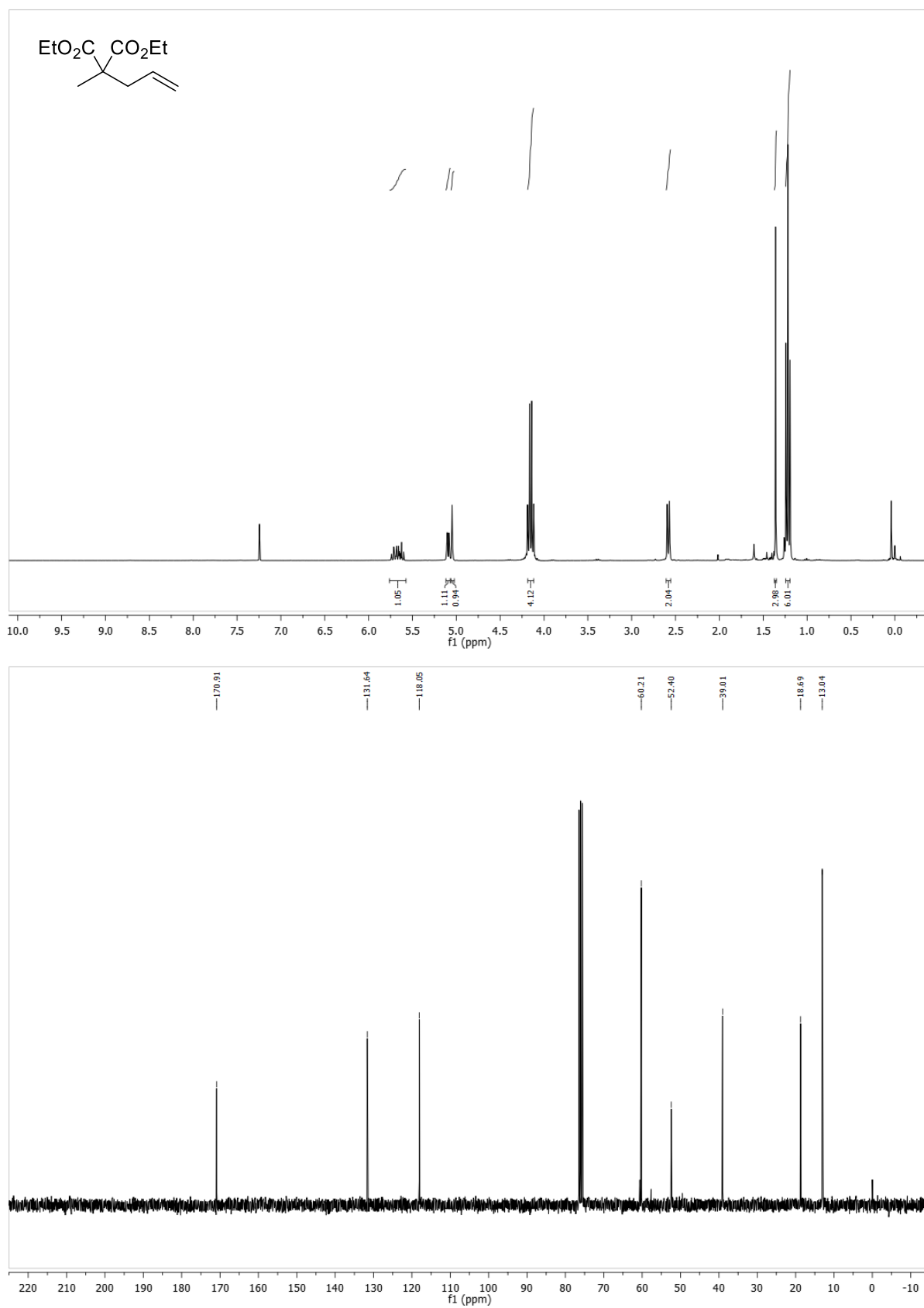
G Appendix

Diethyl 2-(2-phenylallyl)malonate (164)



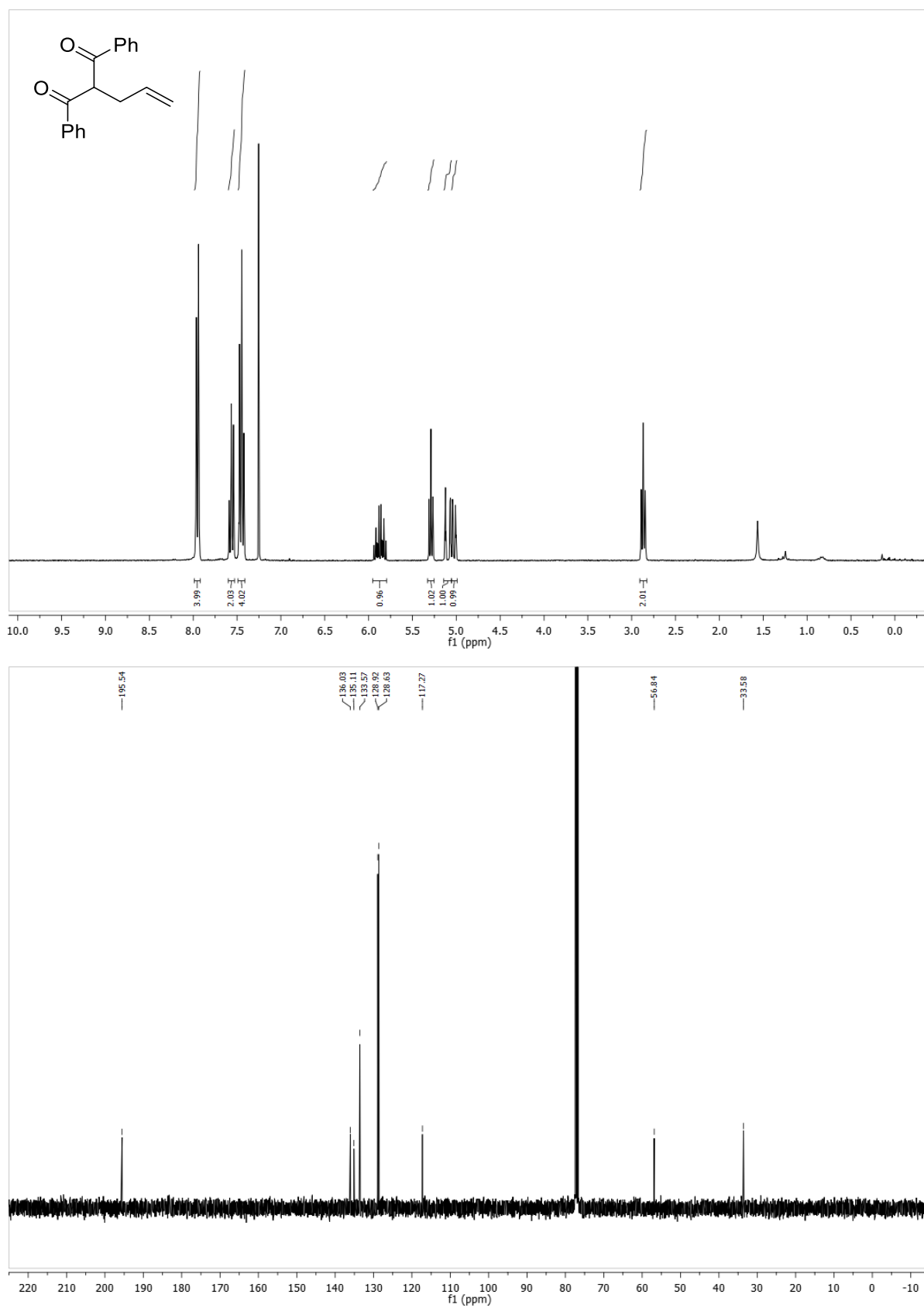
G Appendix

Diethyl 2-allyl-2-methylmalonate (166)



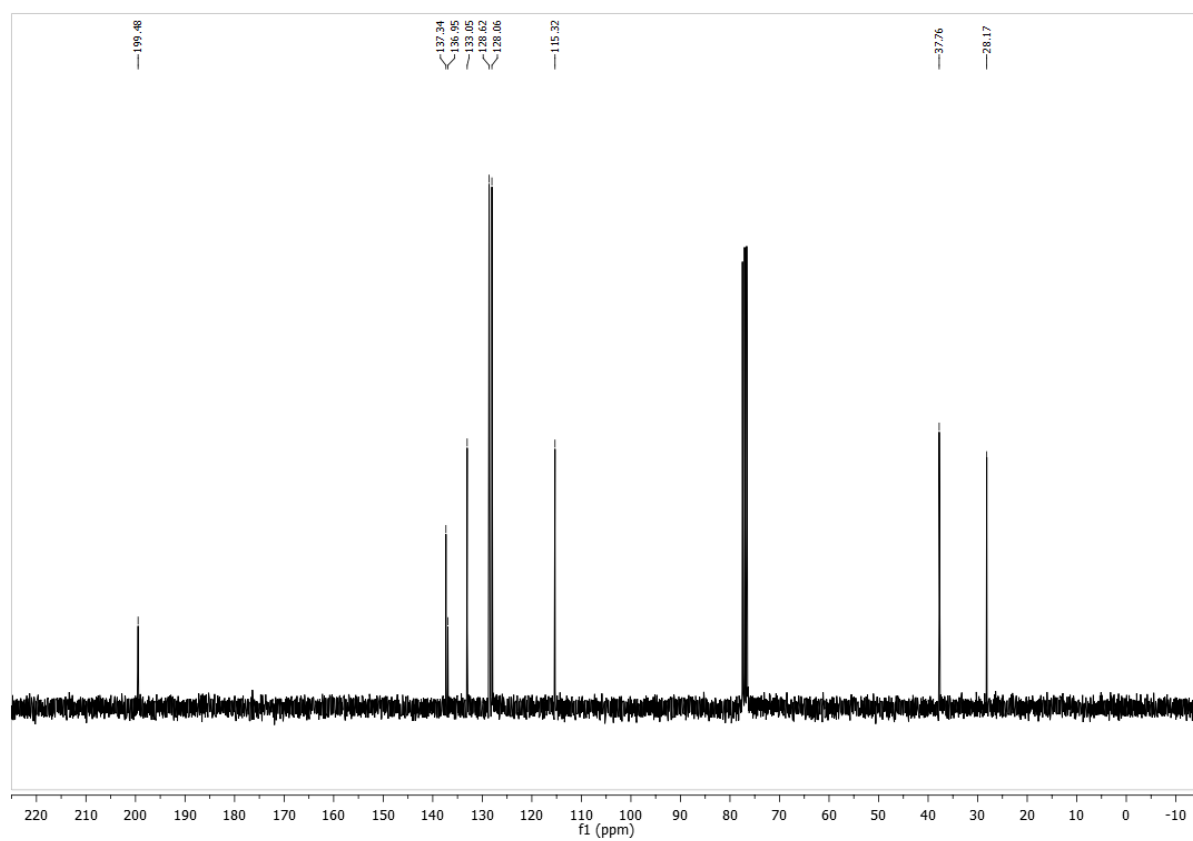
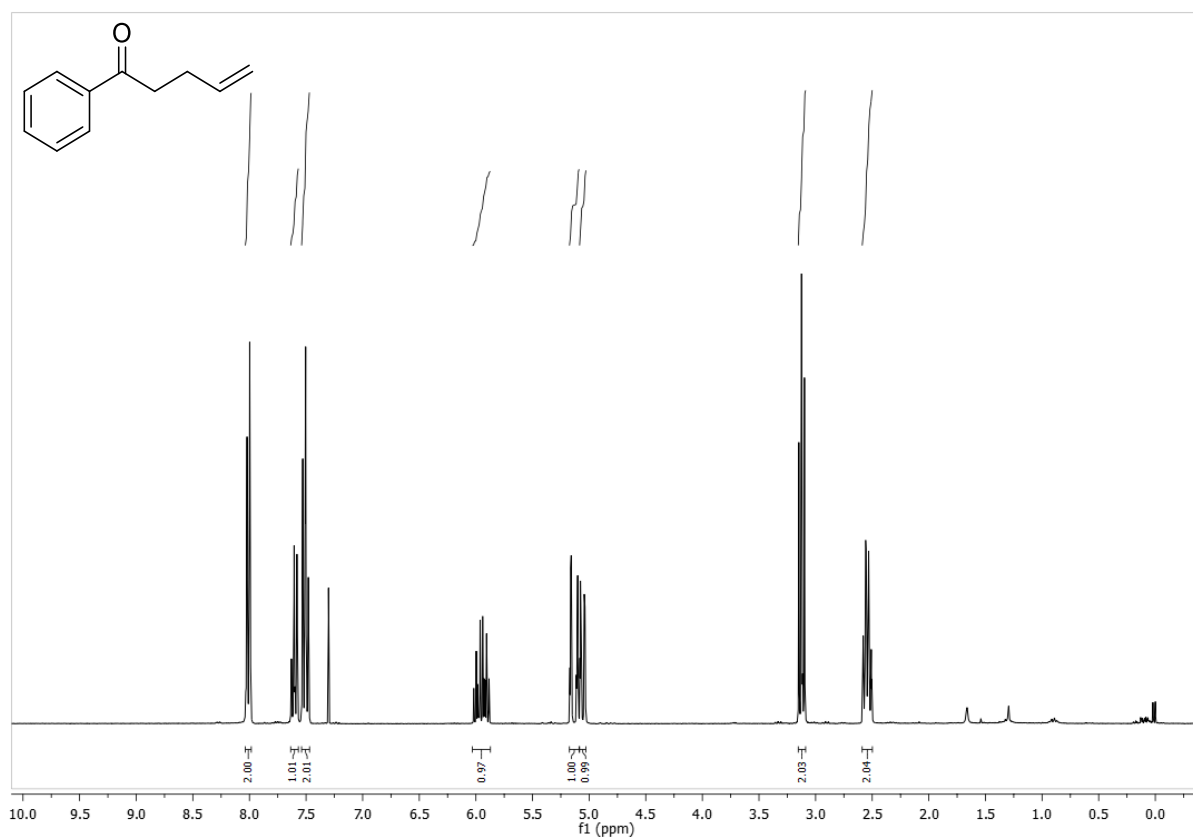
G Appendix

2-allyl-1,3-diphenylpropane-1,3-dione (168)



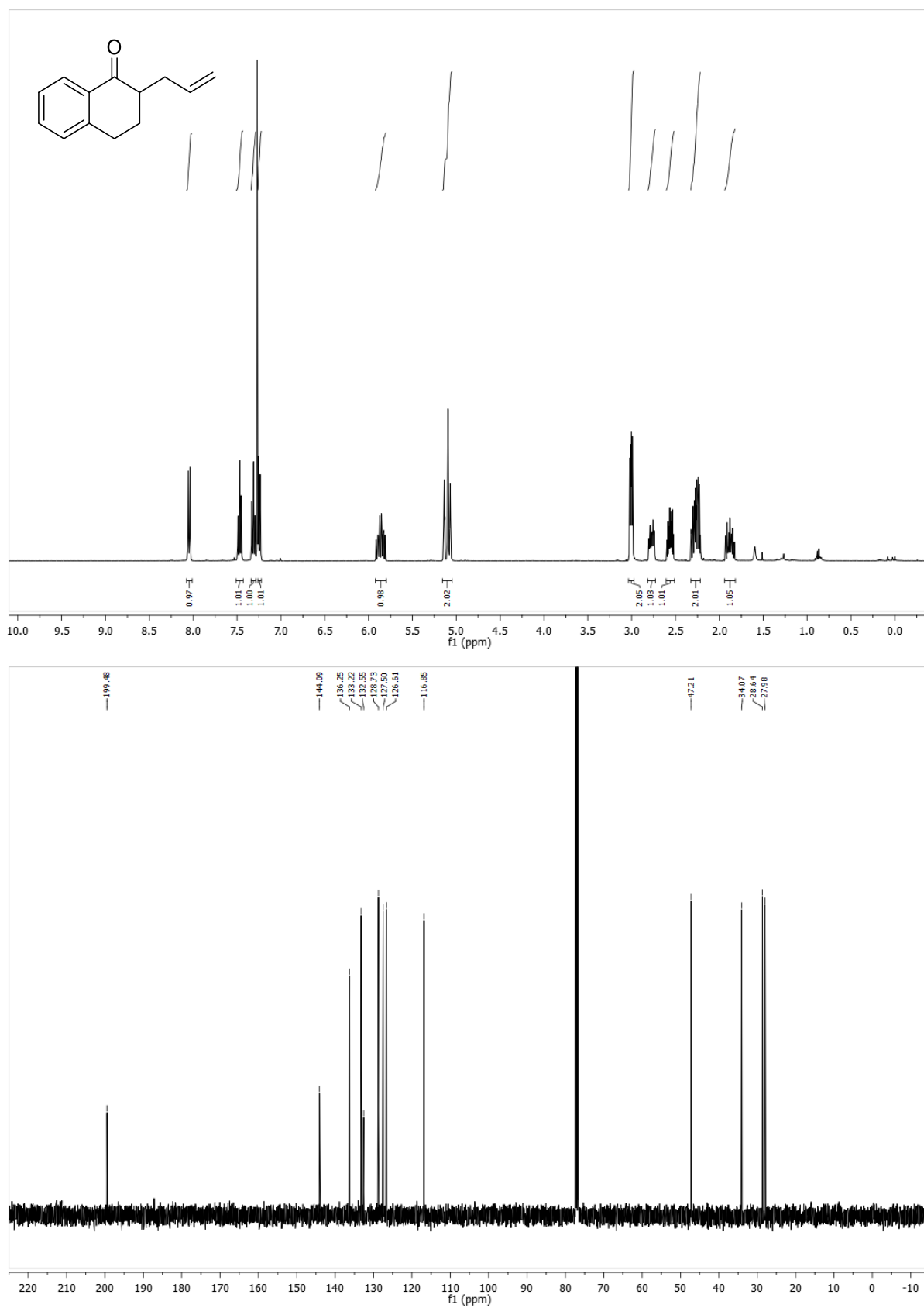
G Appendix

1-phenylpent-4-en-1-one (173)



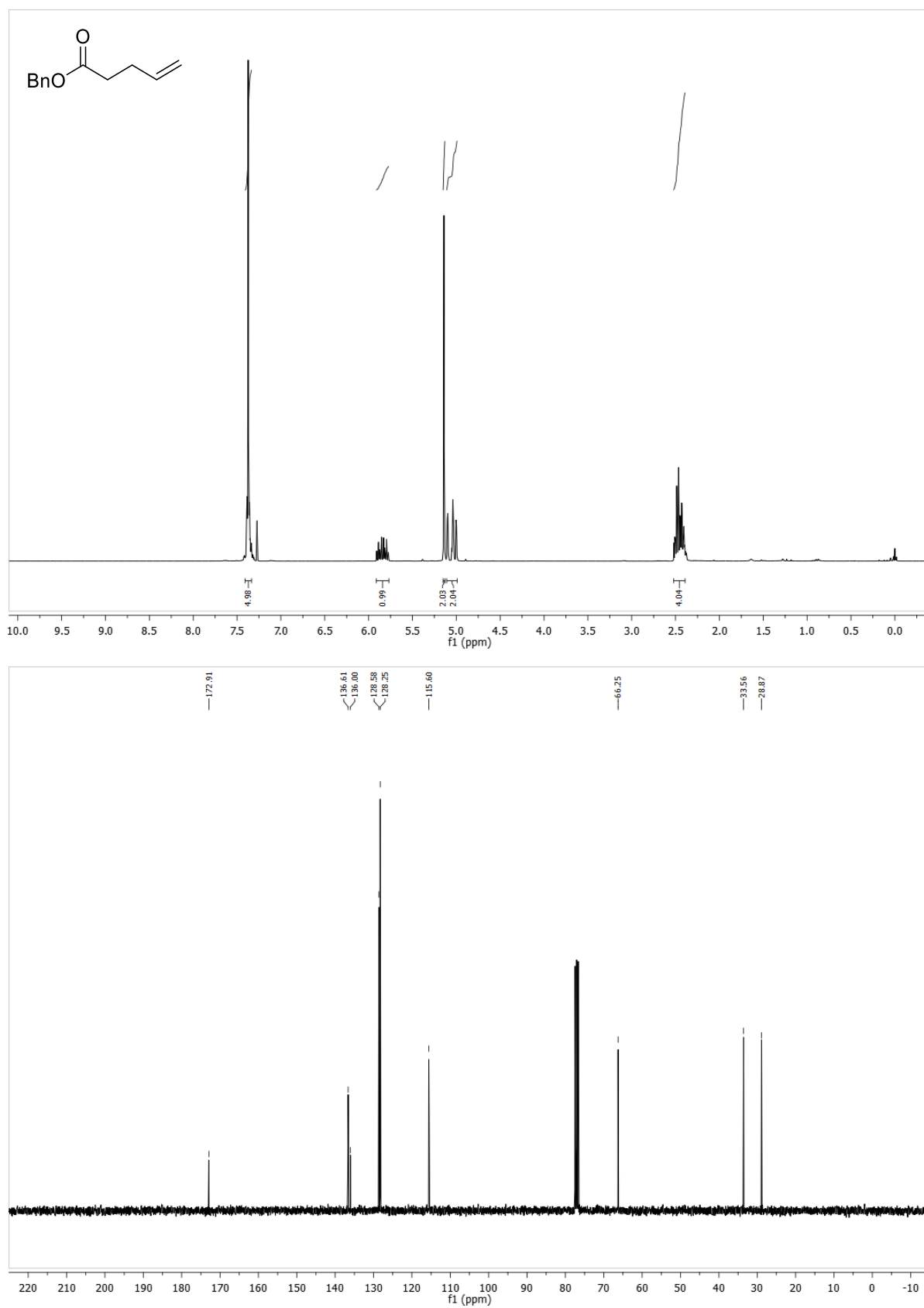
G Appendix

2-allyl-3,4-dihydronaphthalen-1(2H)-one (176)



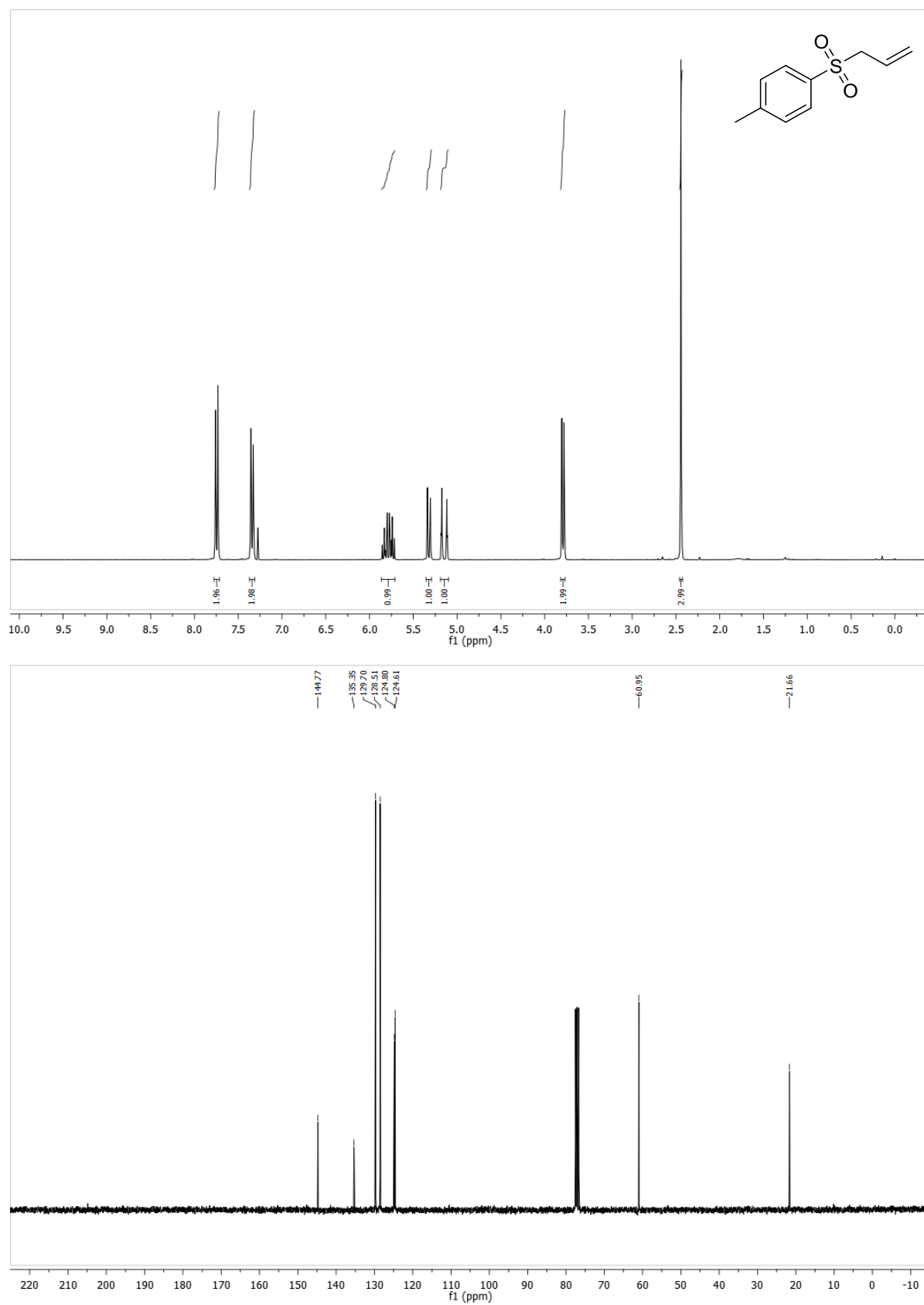
G Appendix

Benzyl pent-4-enoate (178)



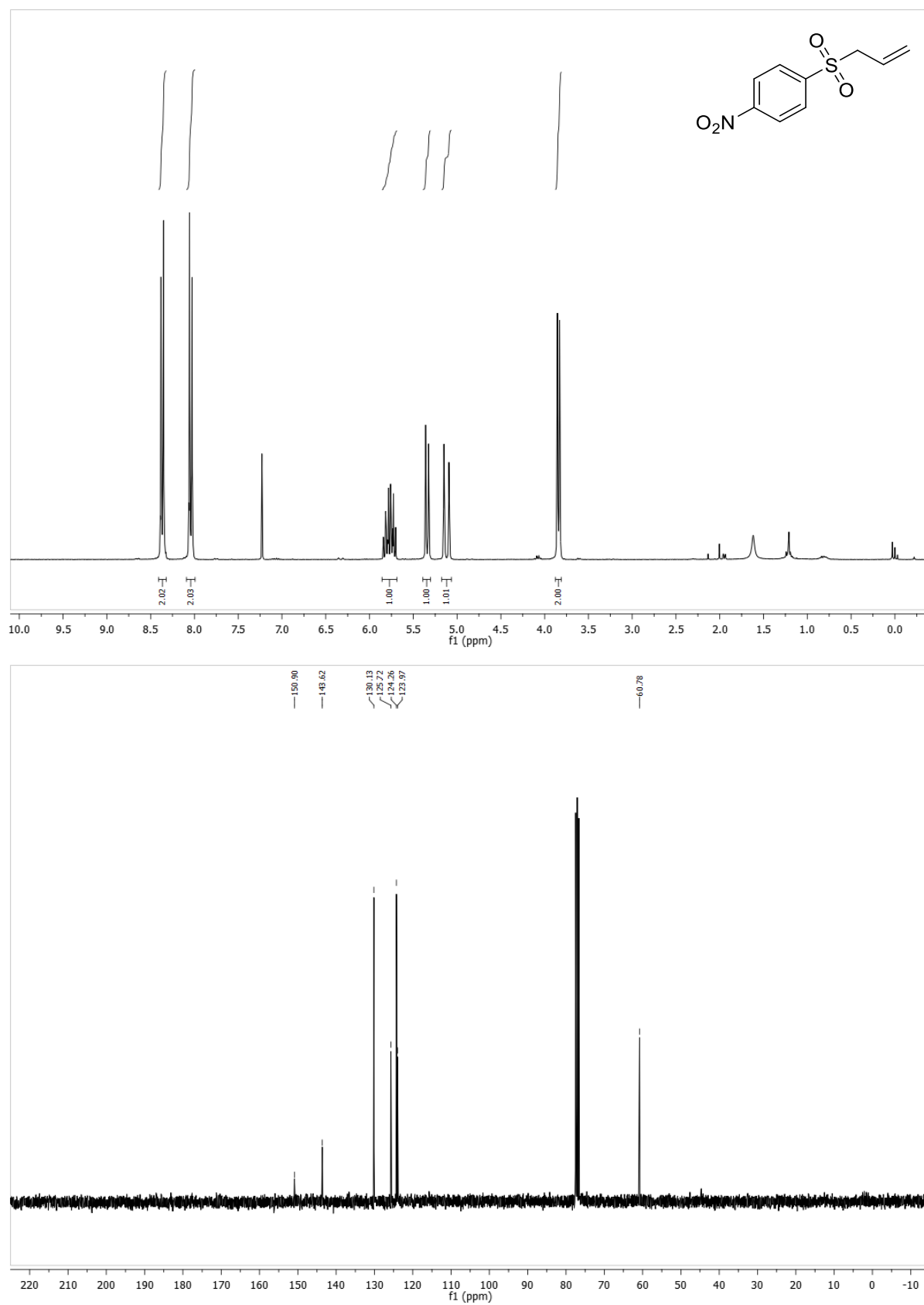
G Appendix

1-(allylsulfonyl)-4-methylbenzene (183)



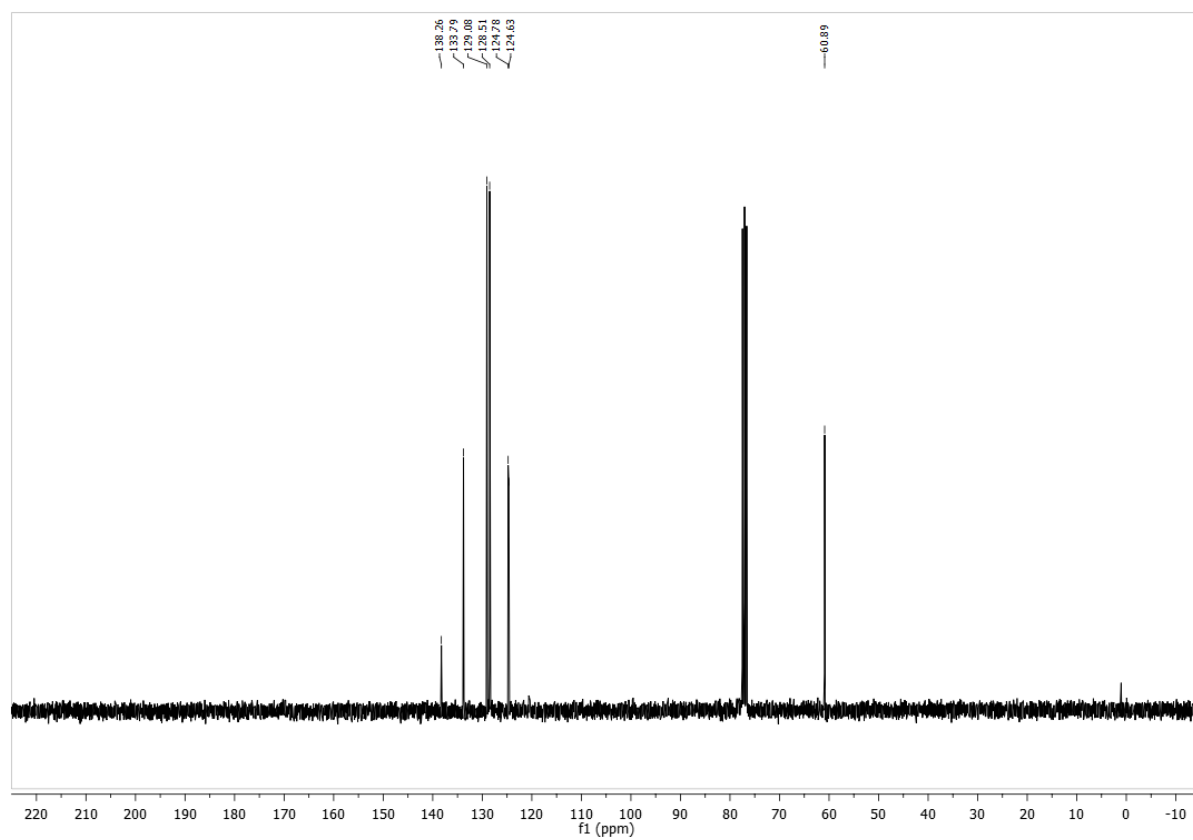
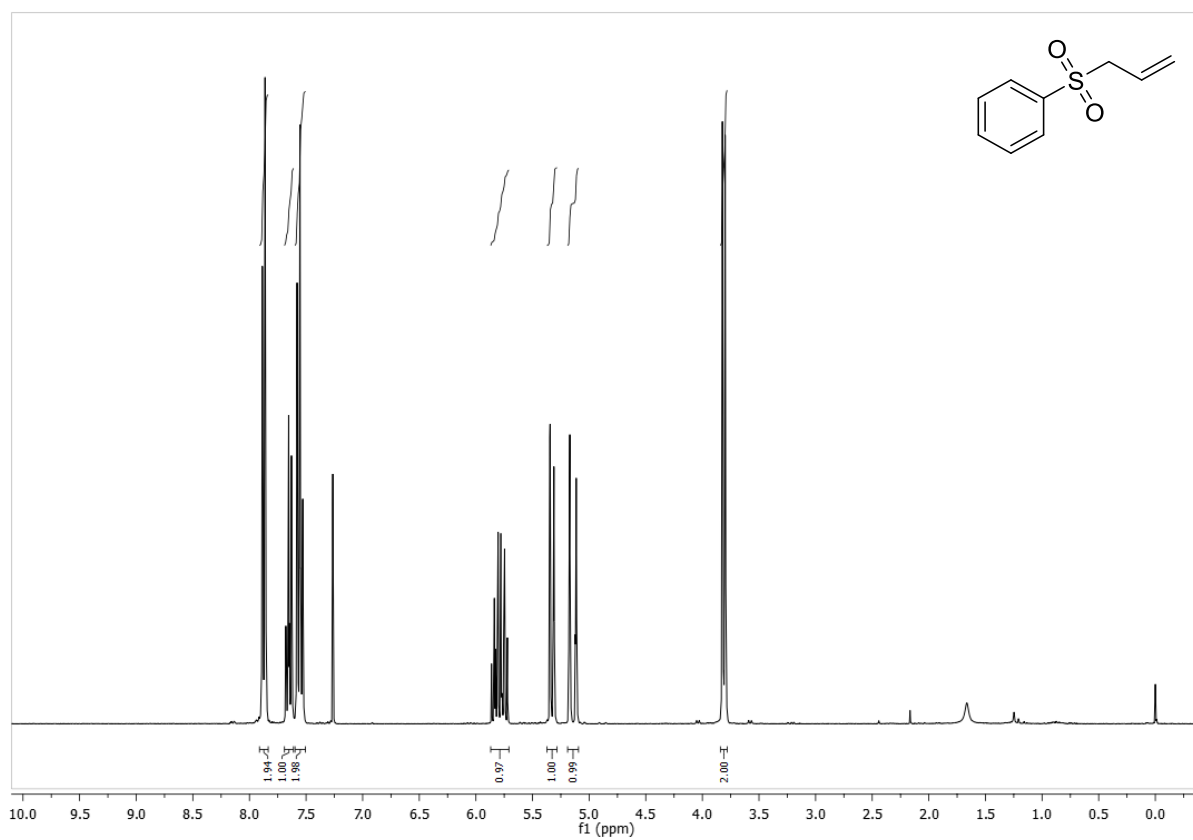
G Appendix

1-(allylsulfonyl)-4-nitrobenzene (186)



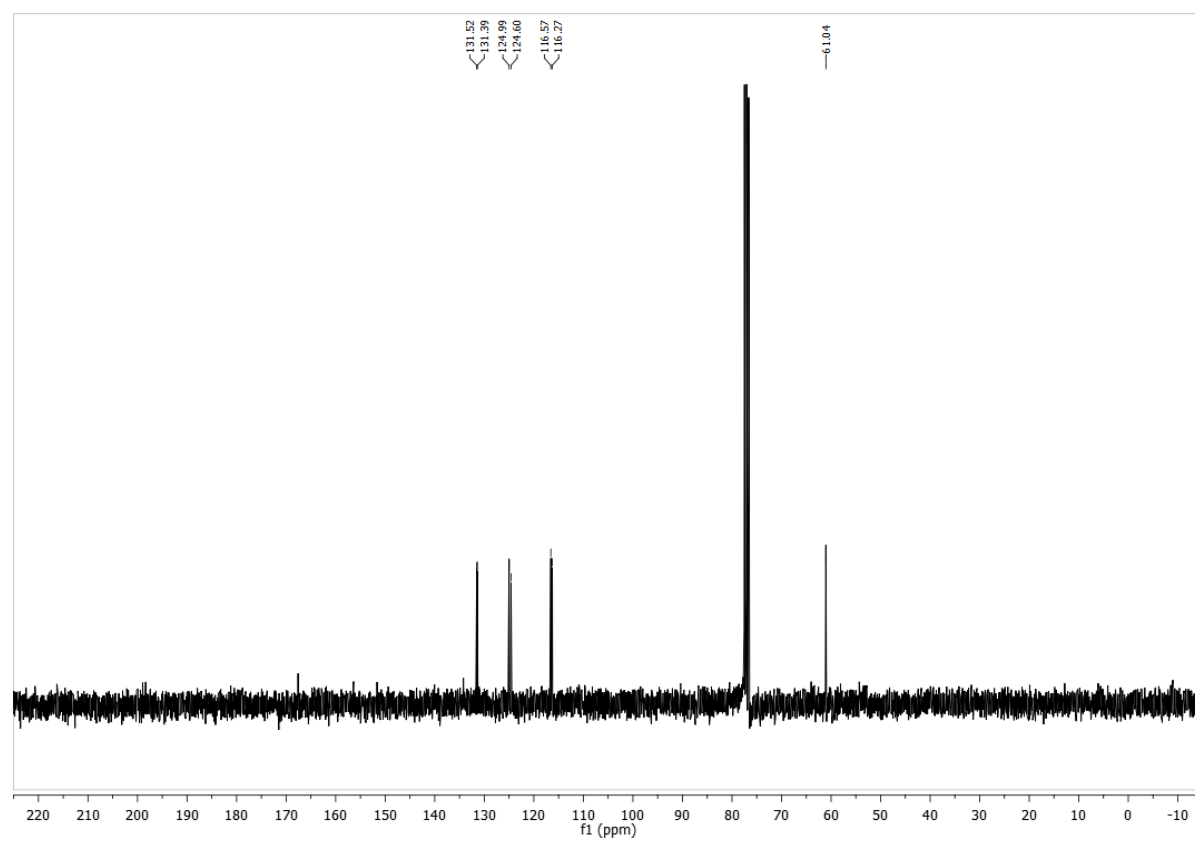
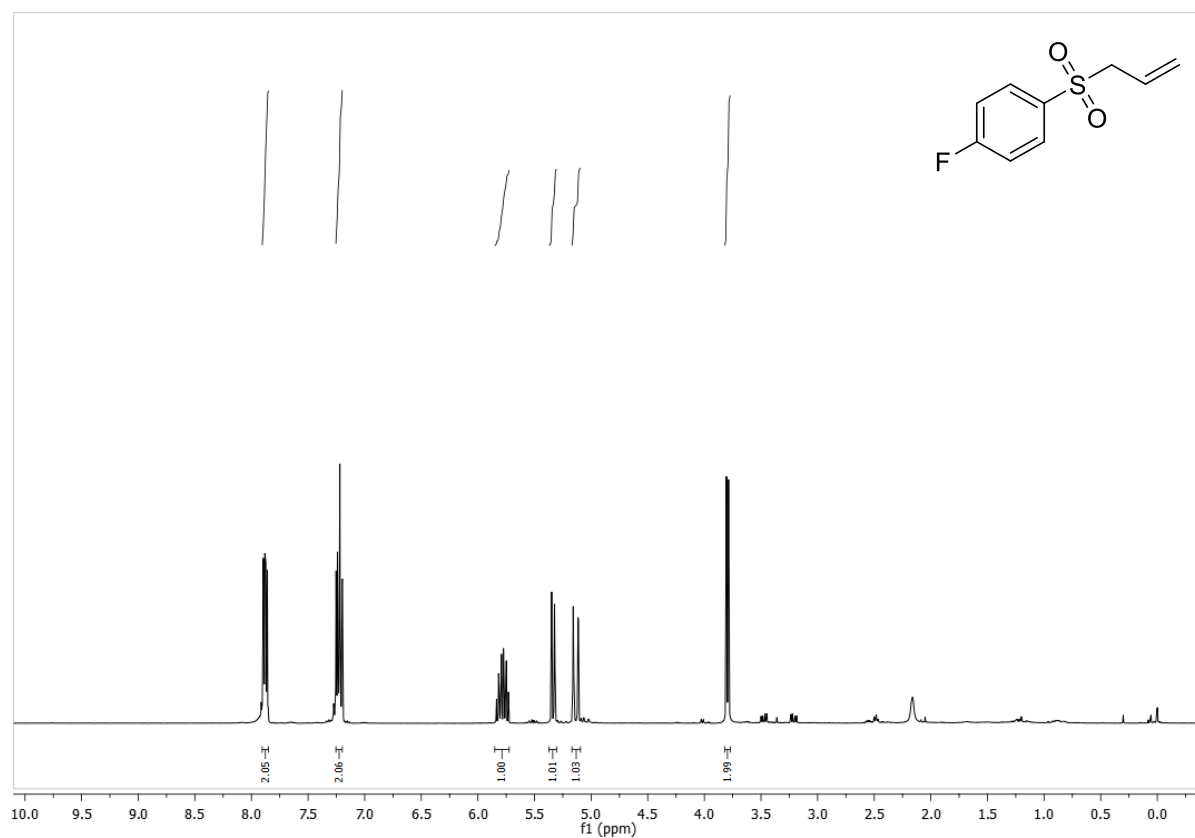
G Appendix

(Allylsulfonyl)benzene (188)

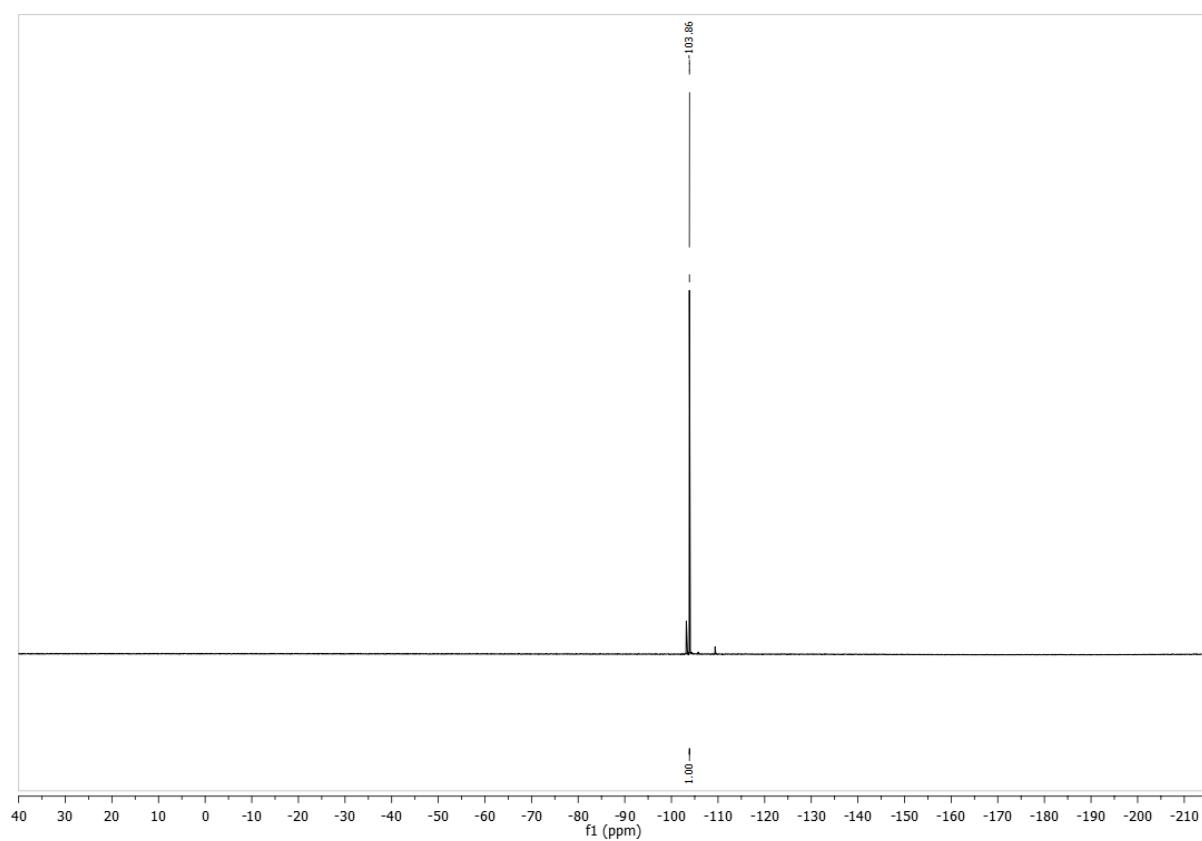


G Appendix

1-(allylsulfonyl)-4-fluorobenzene (190)

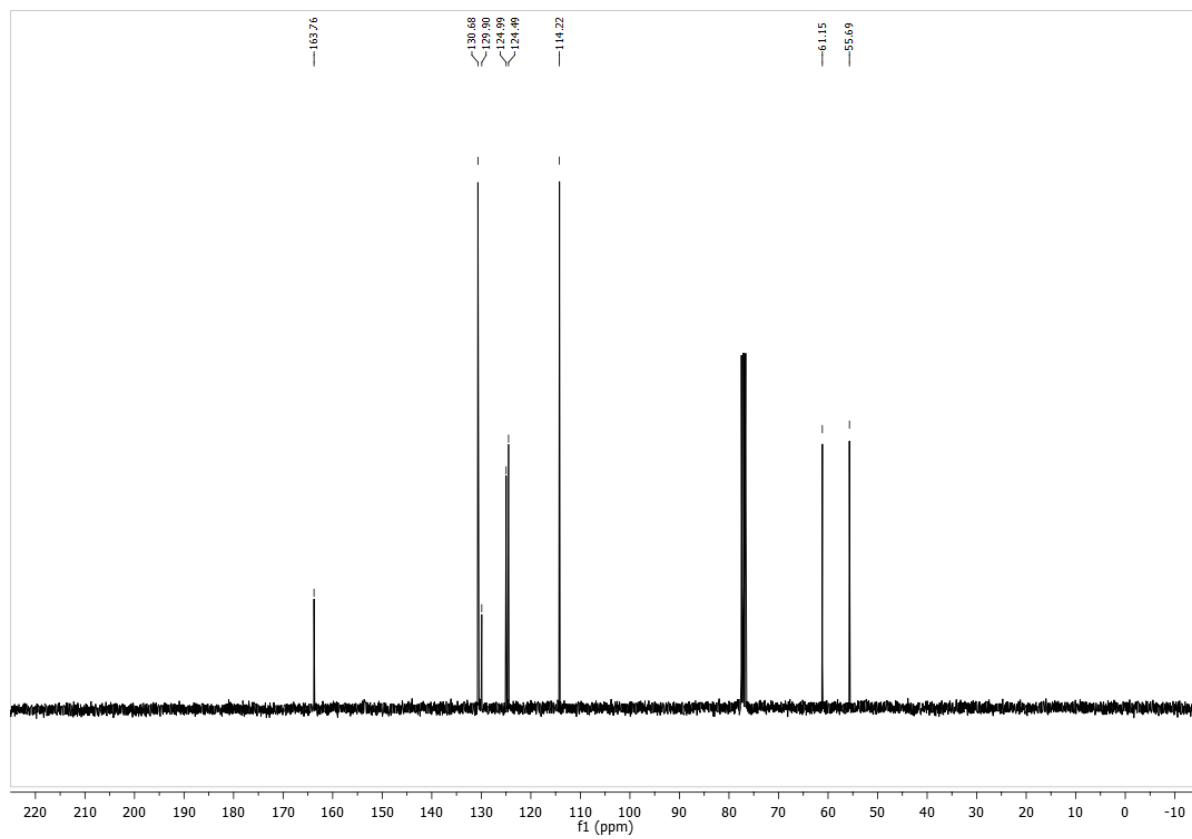
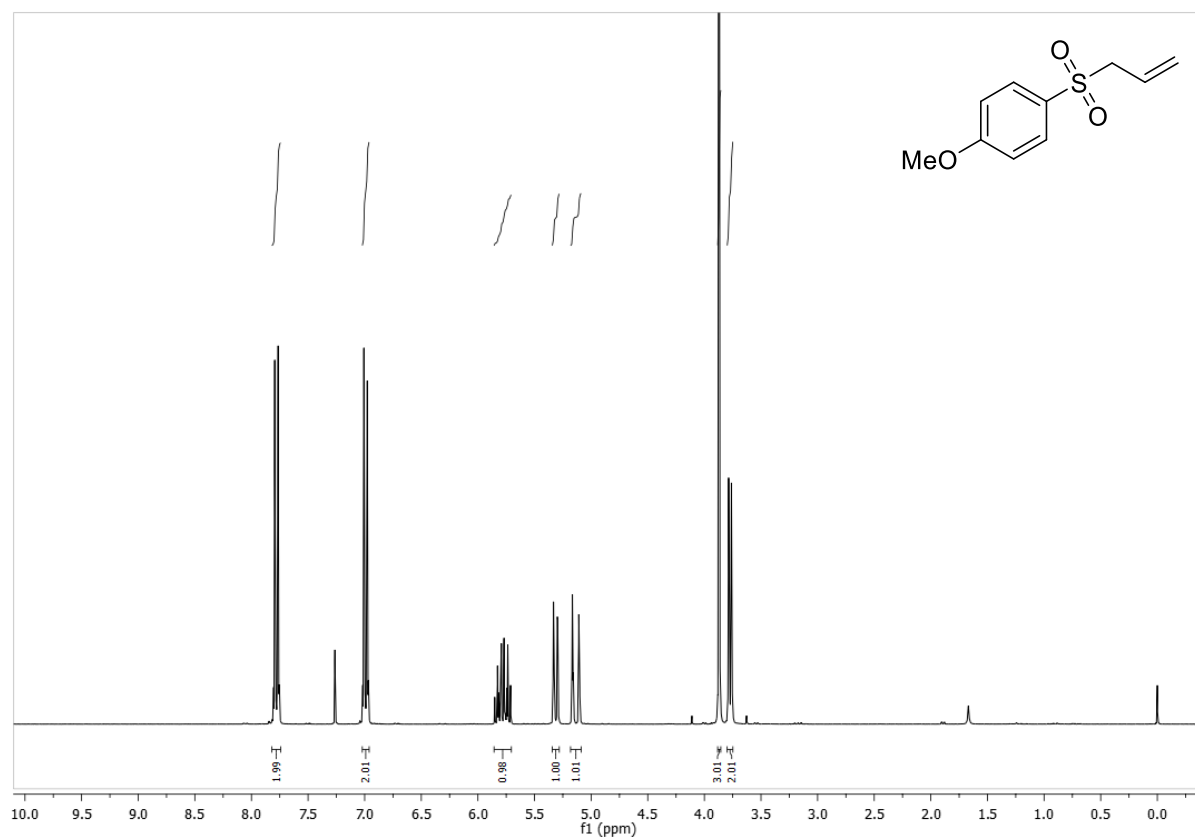


G Appendix



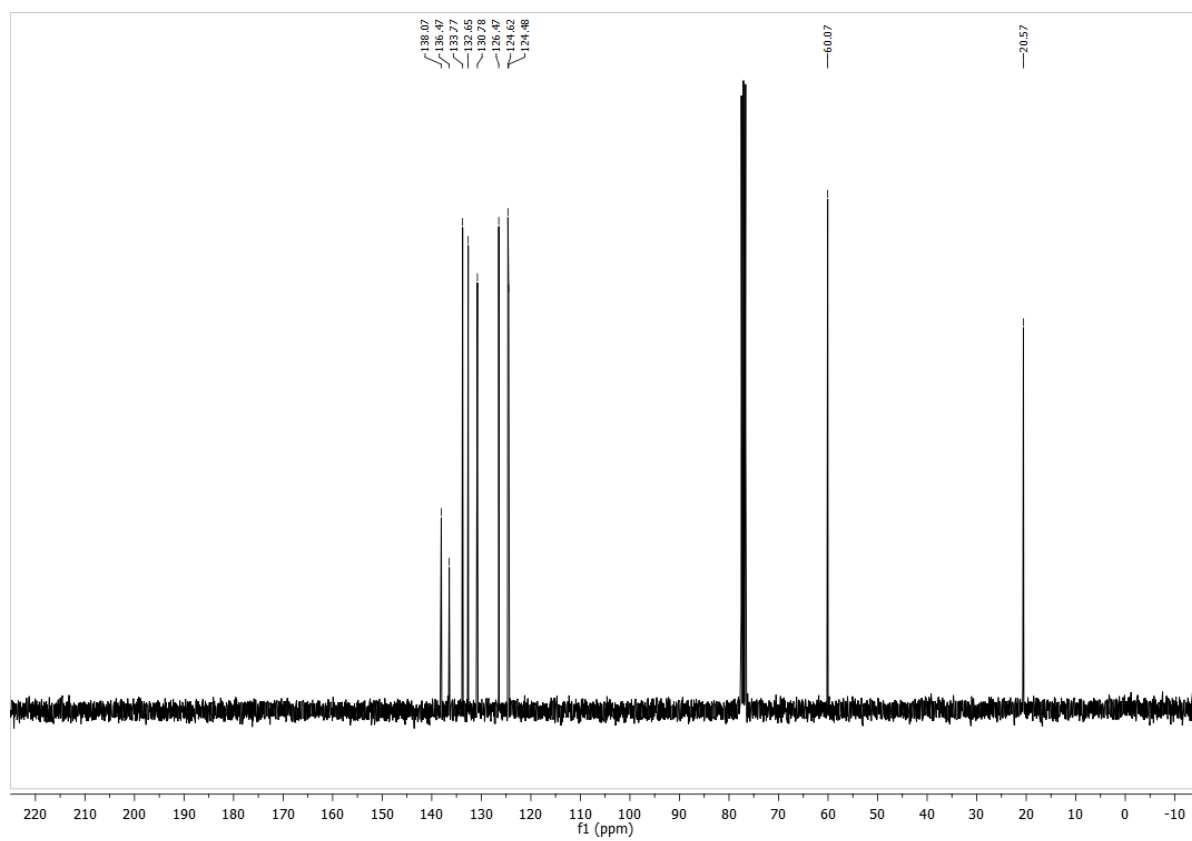
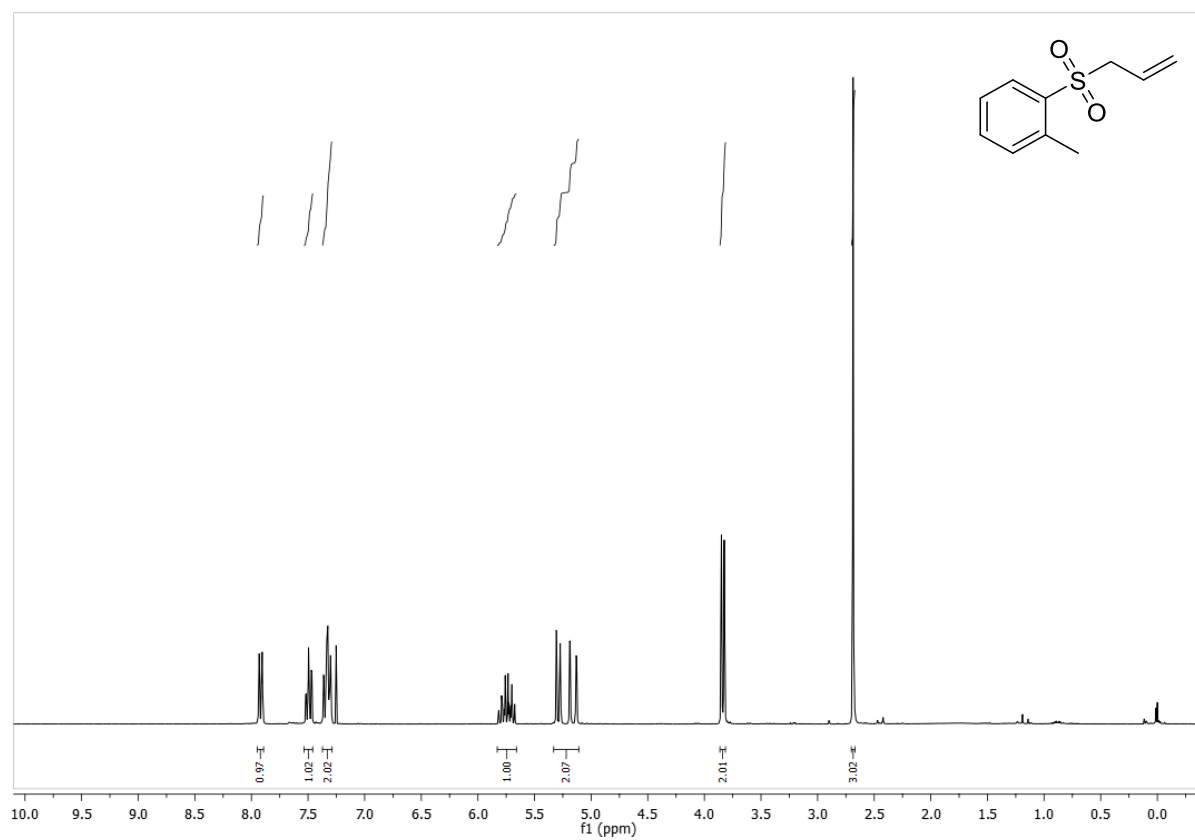
G Appendix

1-(allylsulfonyl)-4-methoxybenzene (192)



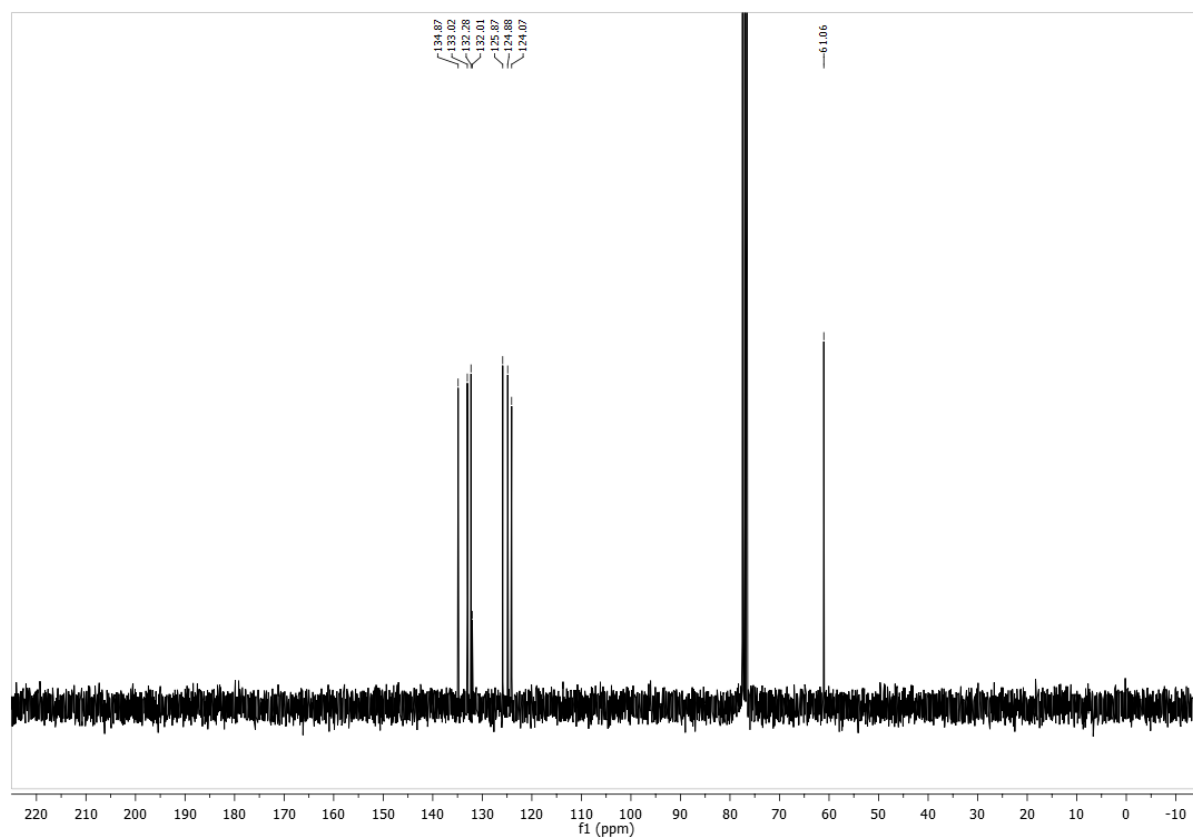
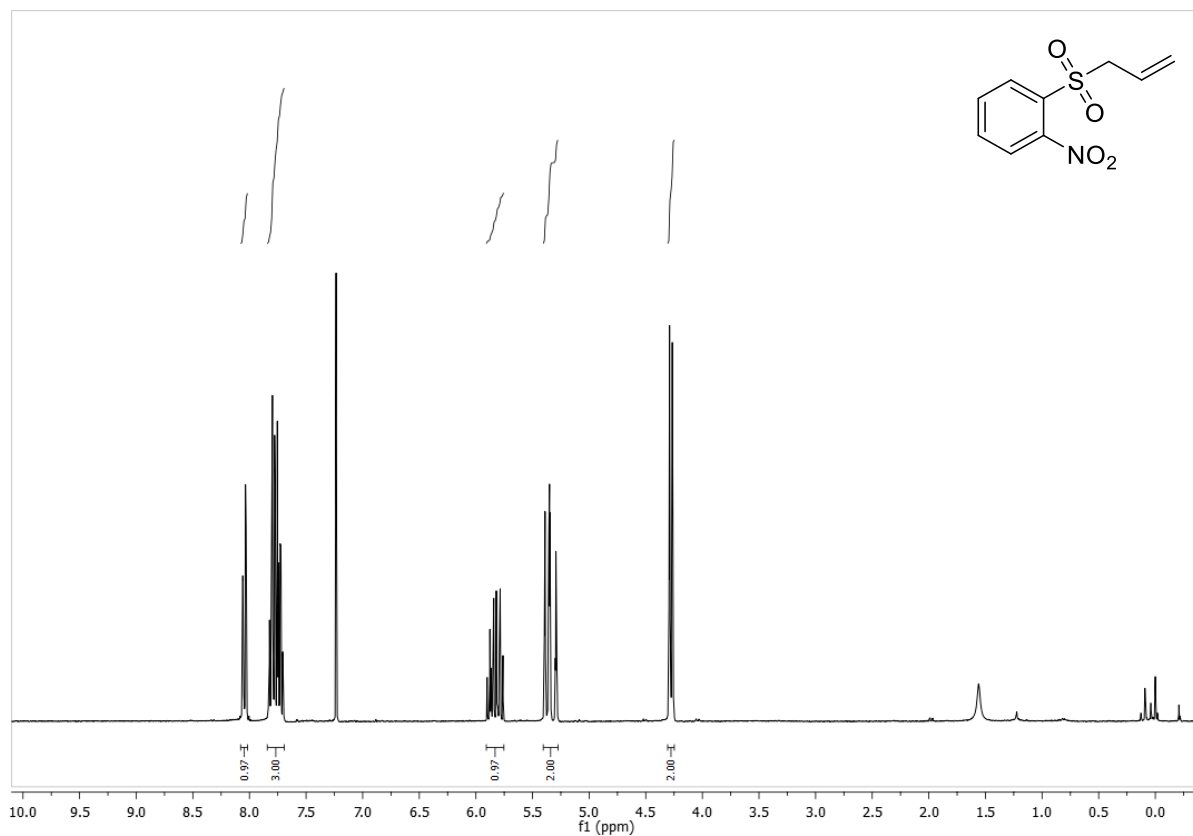
G Appendix

1-(allylsulfonyl)-2-methylbenzene (194)



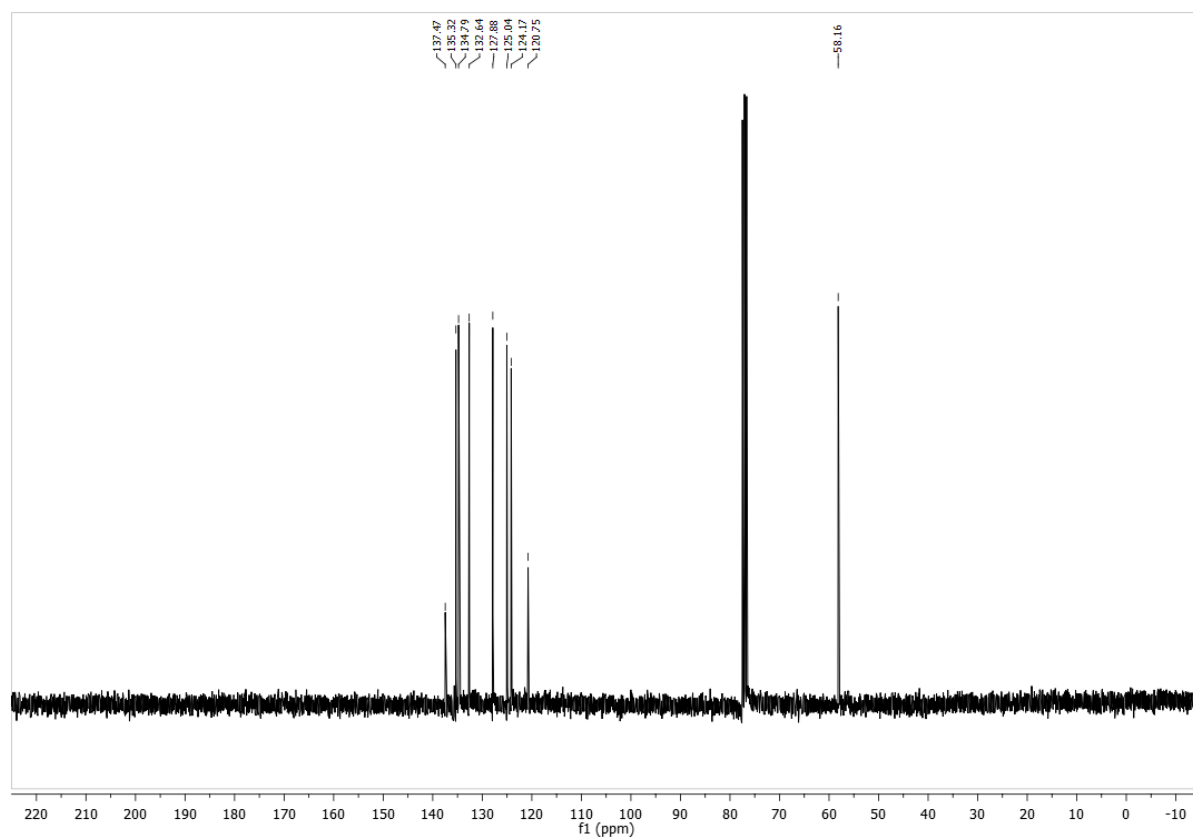
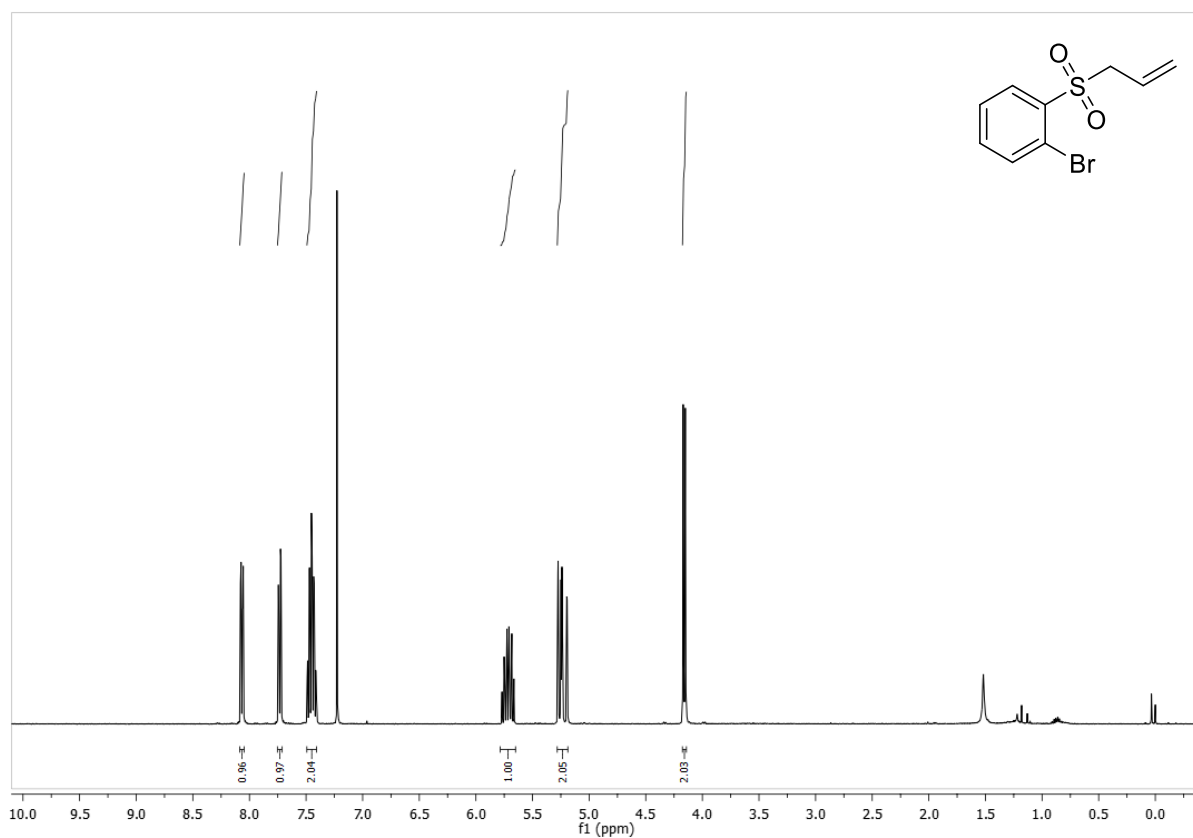
G Appendix

1-(allylsulfonyl)-2-nitrobenzene (196)



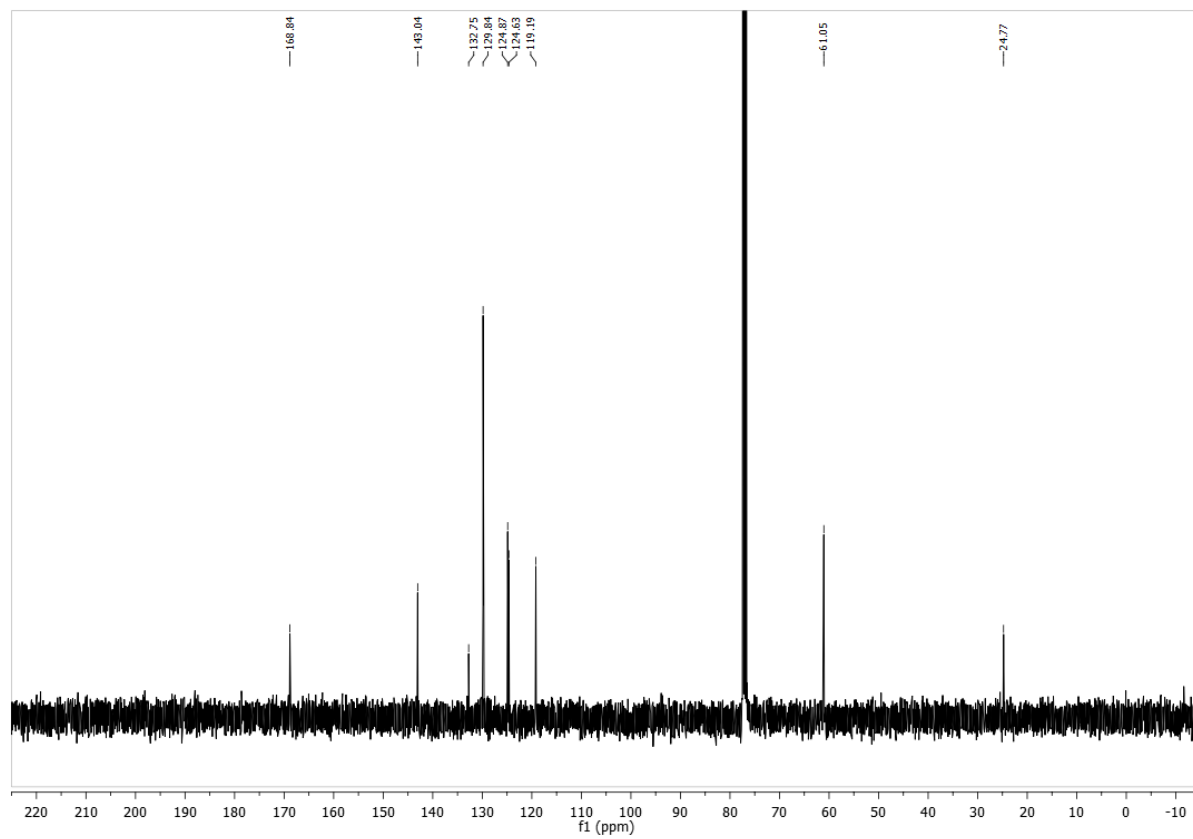
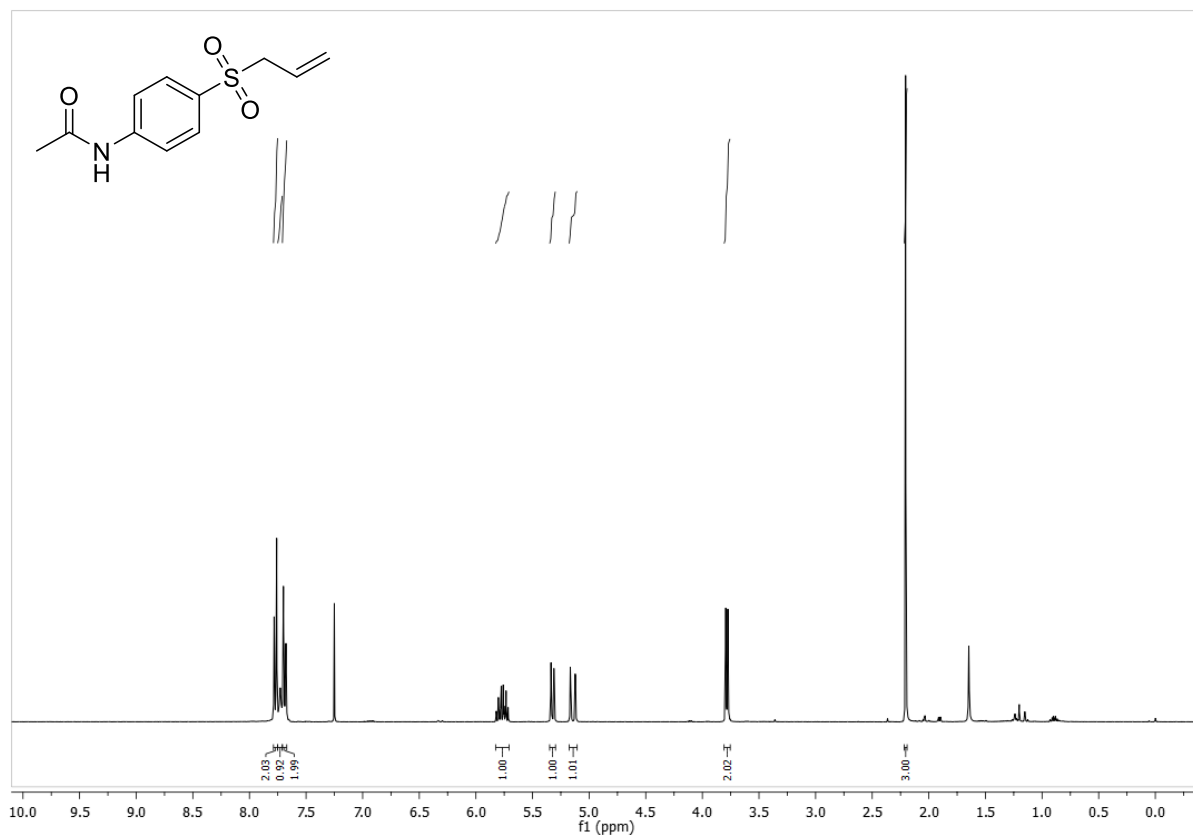
G Appendix

1-(allylsulfonyl)-2-bromobenzene (198)



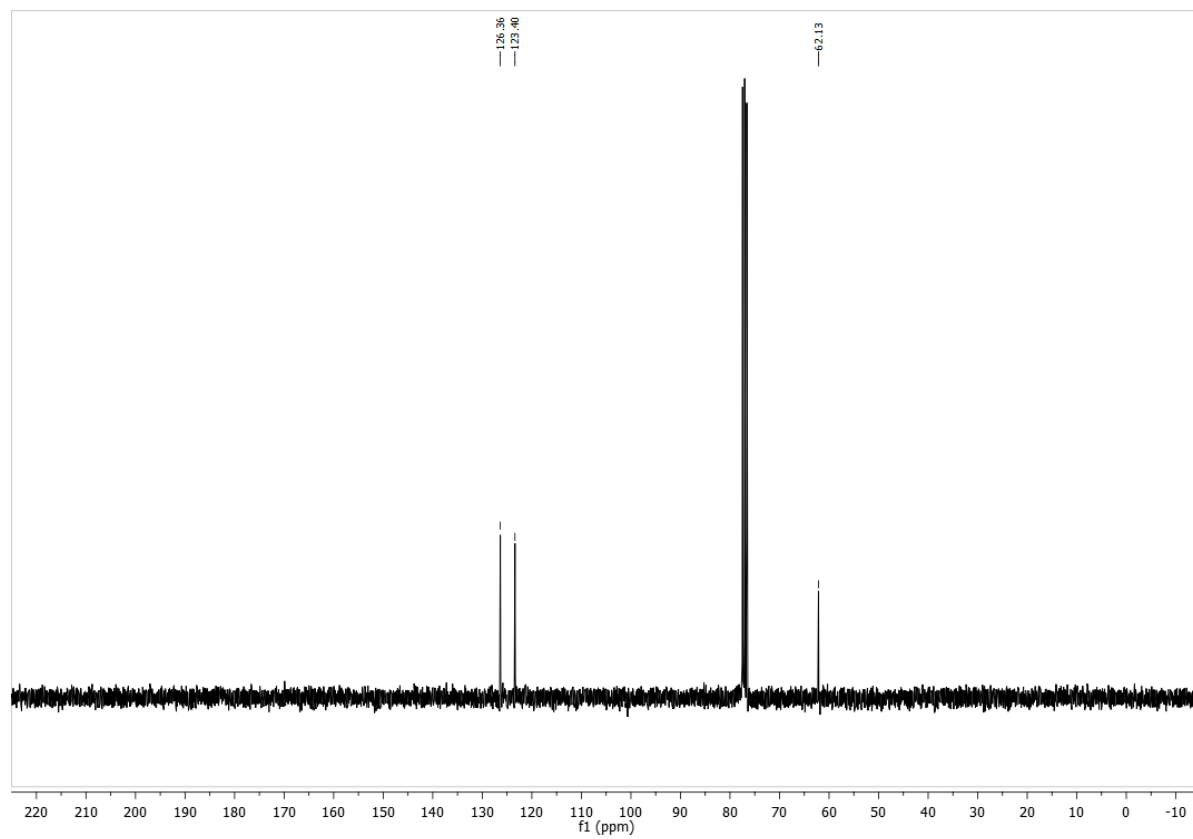
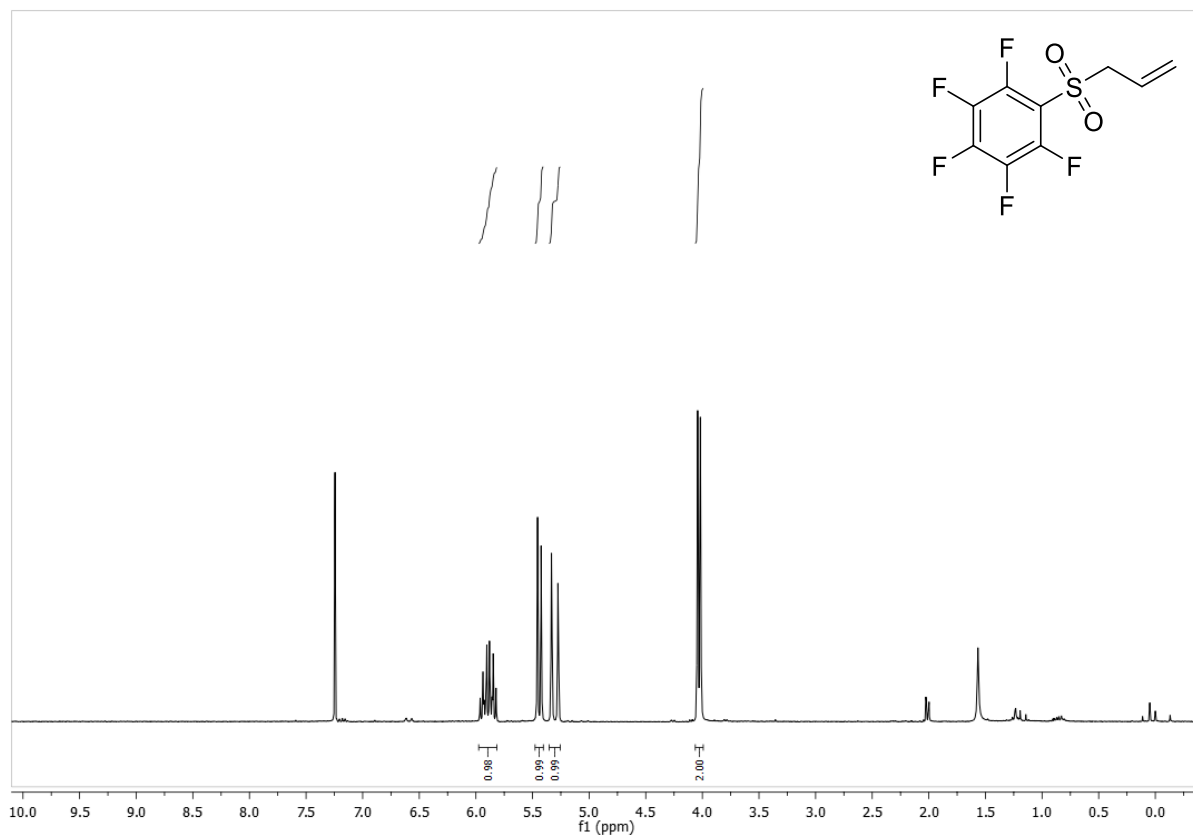
G Appendix

N-(4-(allylsulfonyl)phenyl)acetamide (200)

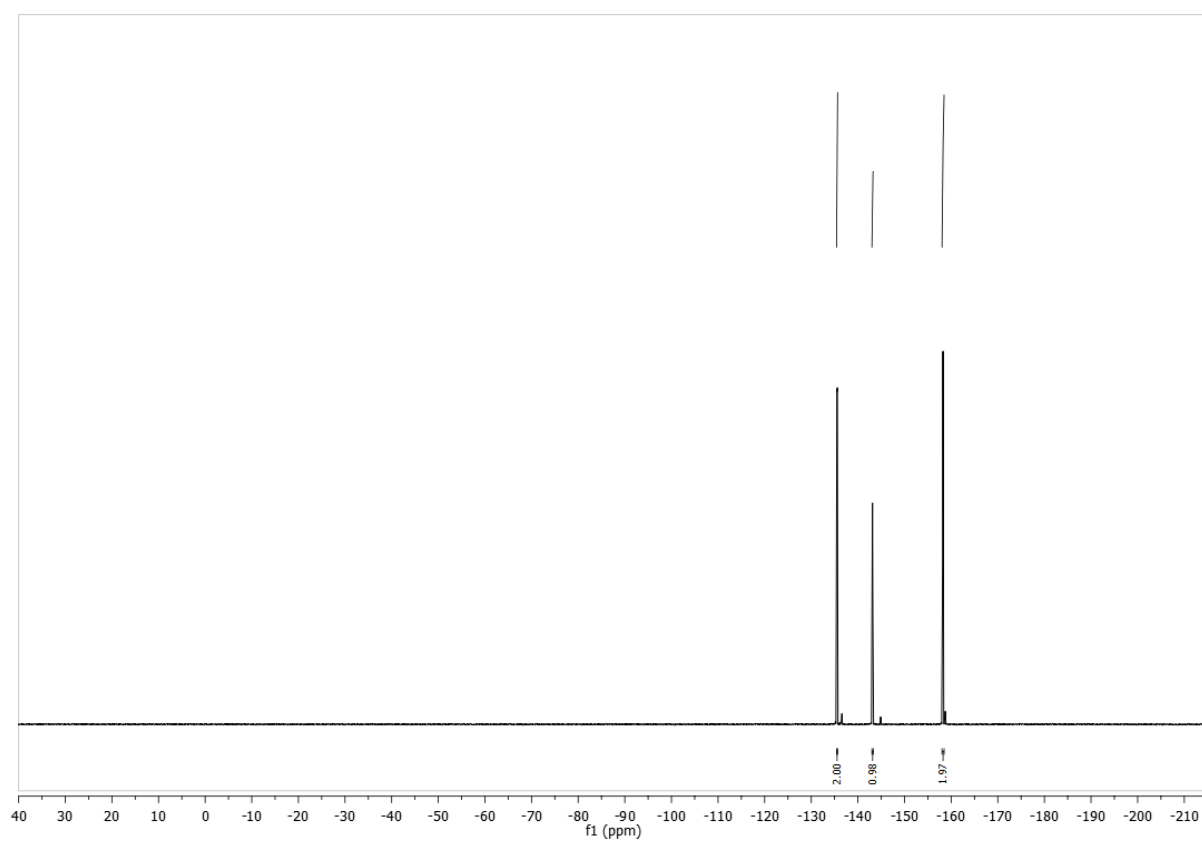


G Appendix

1-(allylsulfonyl)-2,3,4,5,6-pentafluorobenzene (202)

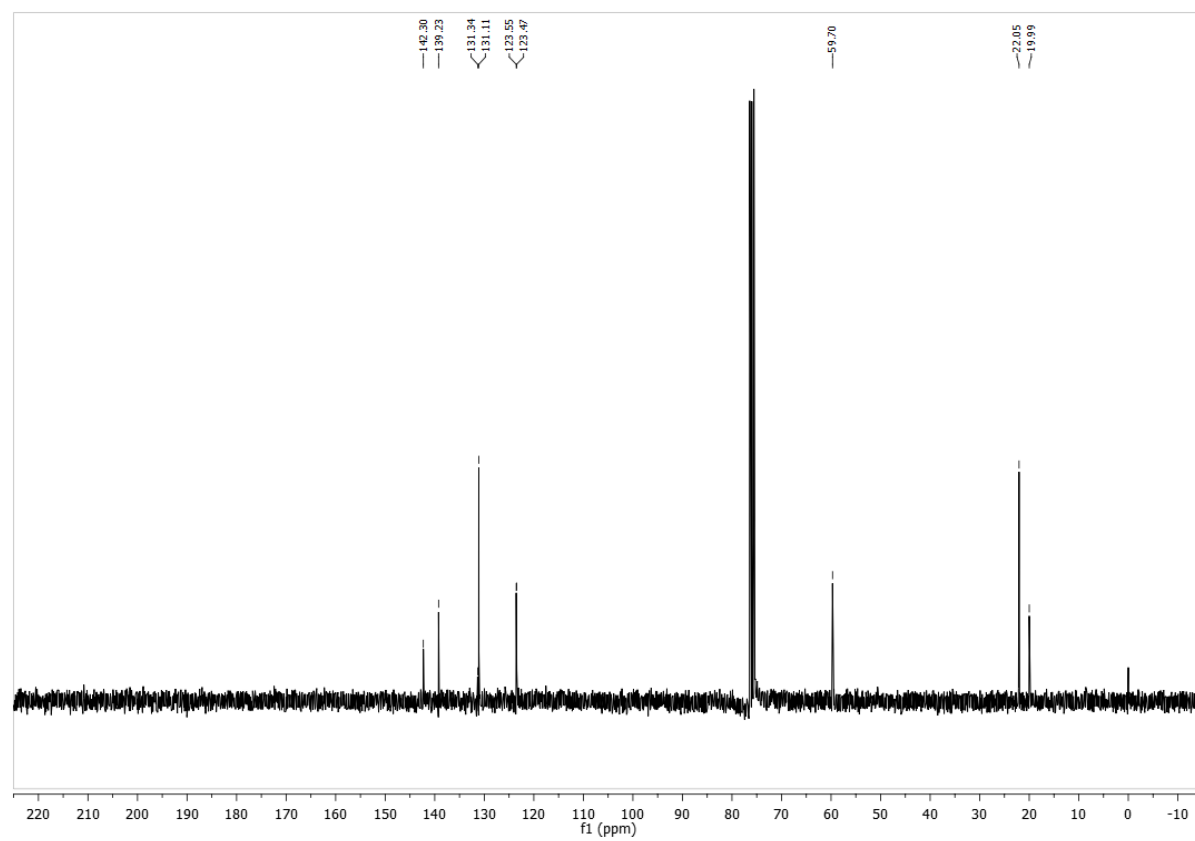
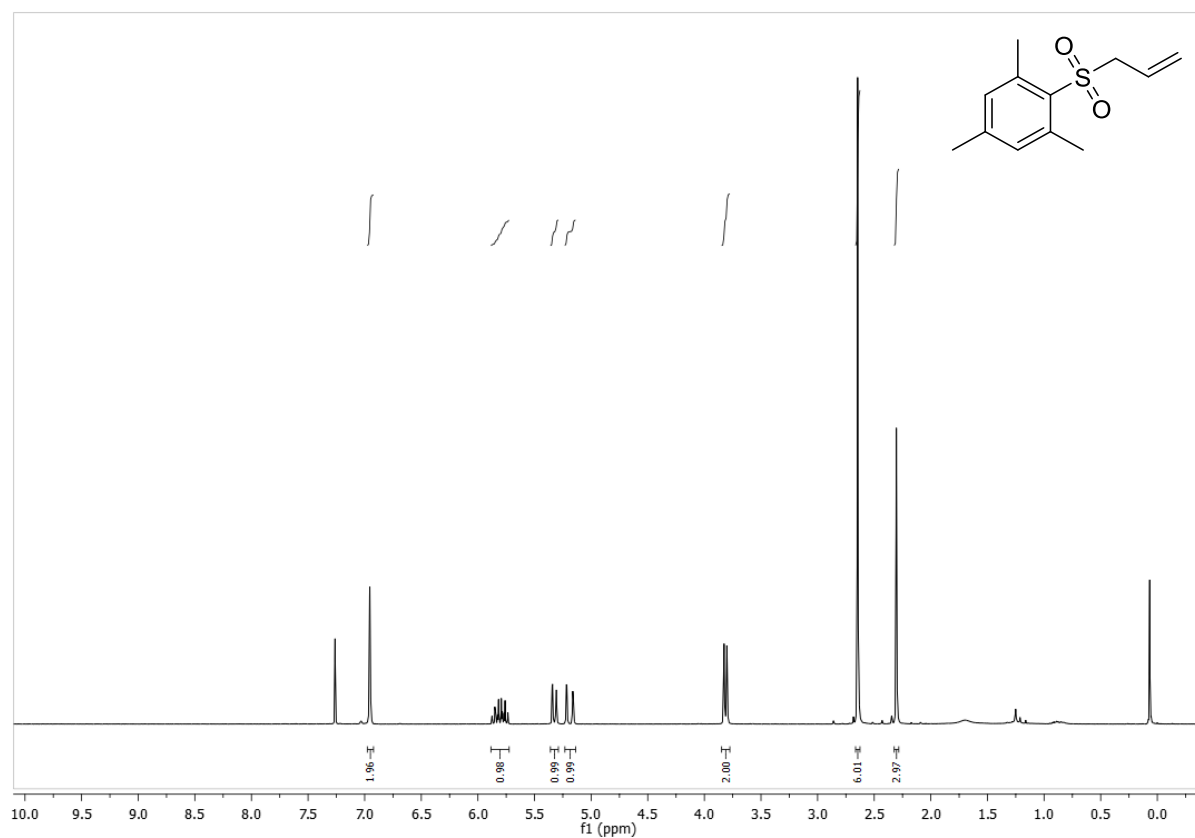


G Appendix



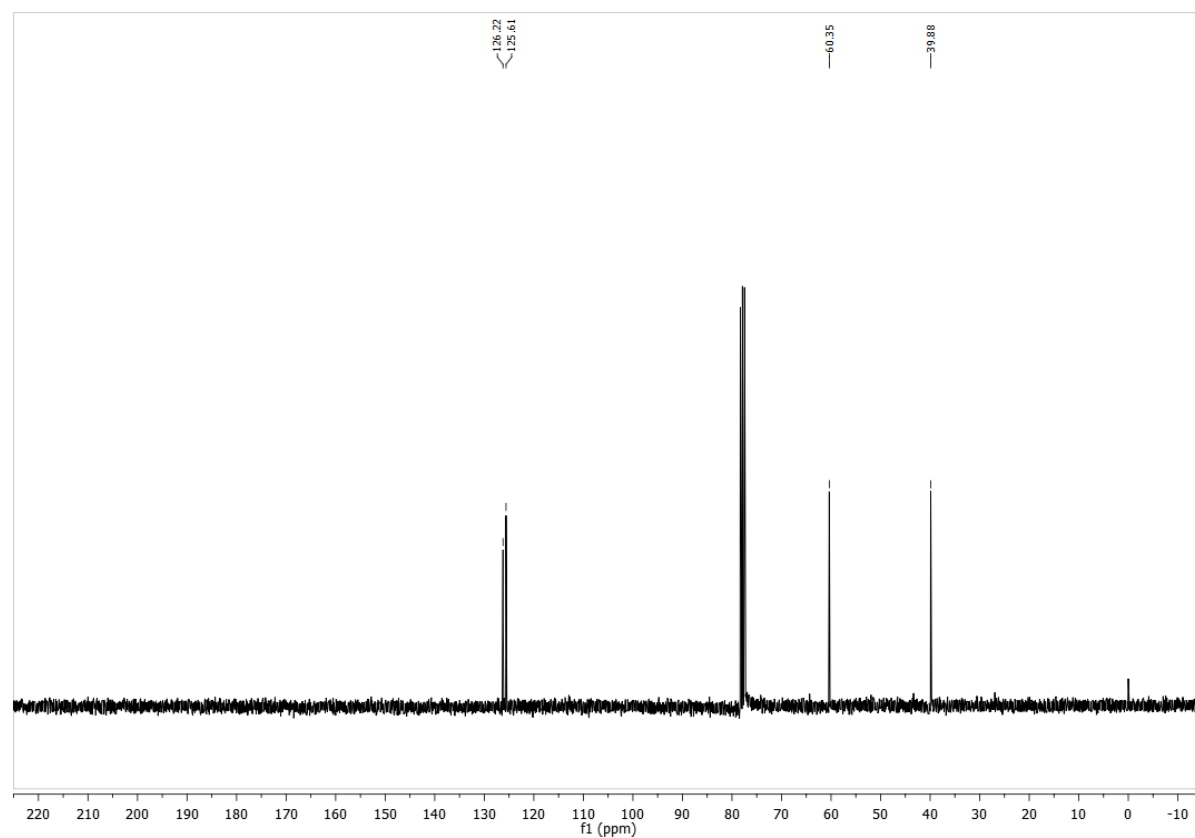
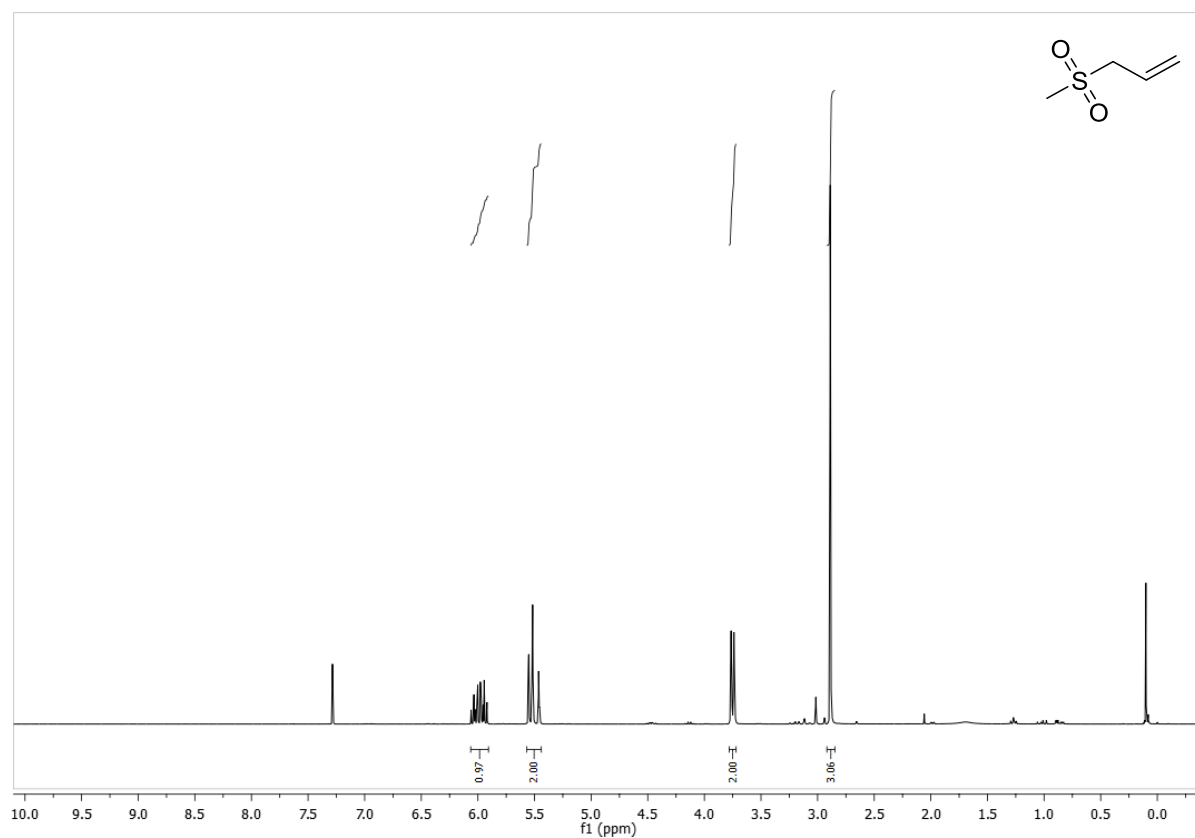
G Appendix

2-(allylsulfonyl)-1,3,5-trimethylbenzene (204)



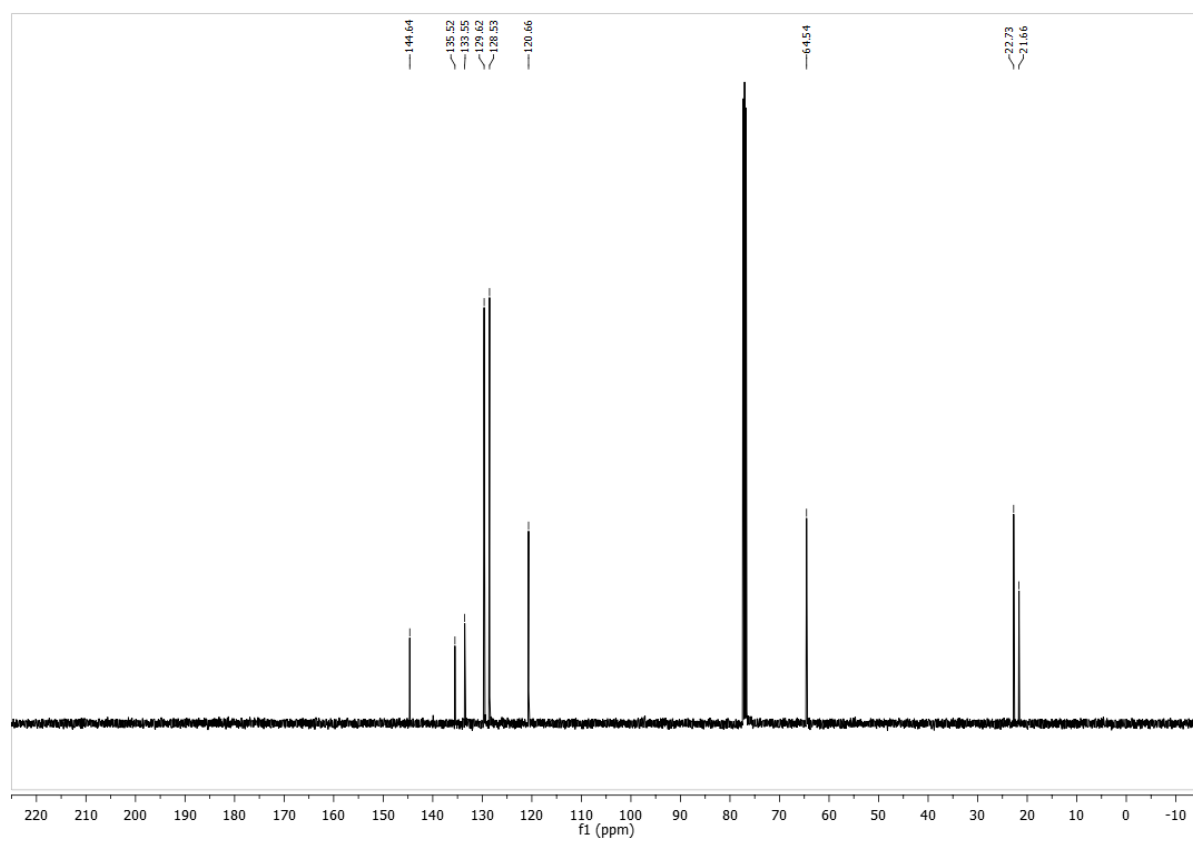
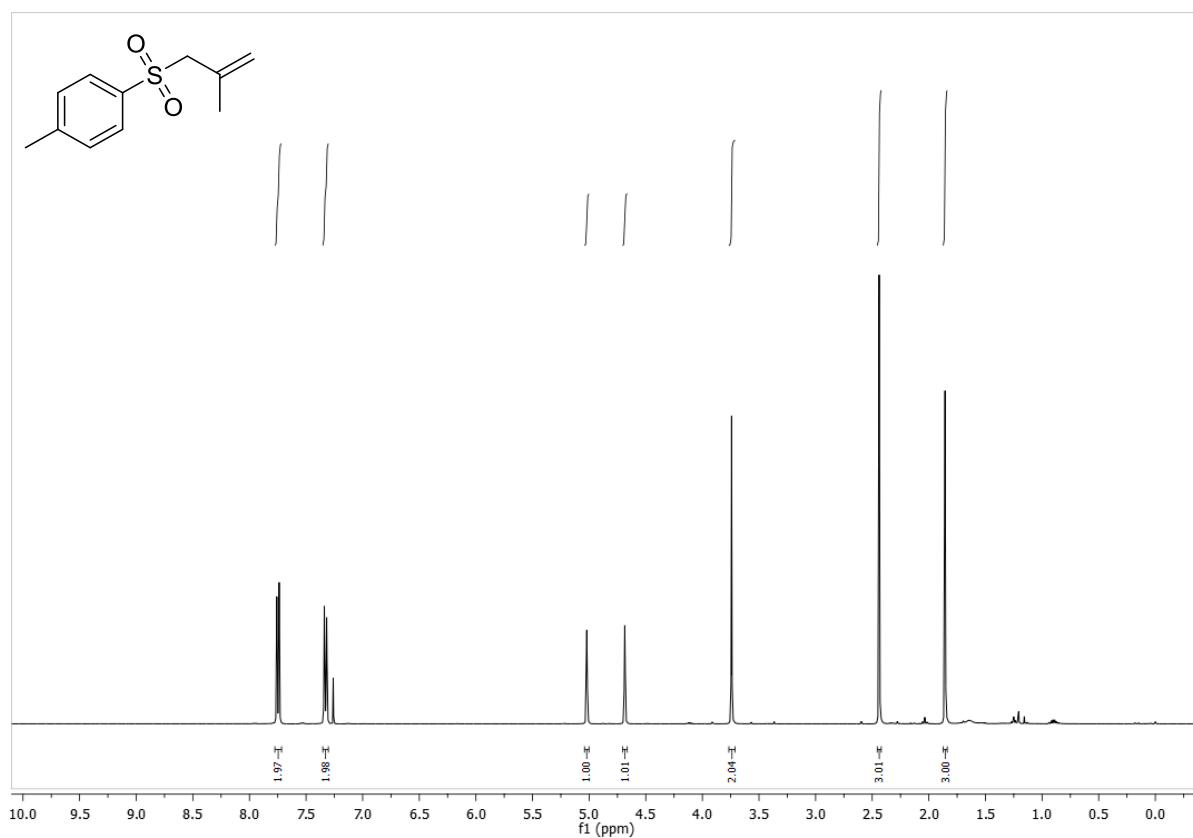
G Appendix

3-(methylsulfonyl)prop-1-ene (206)



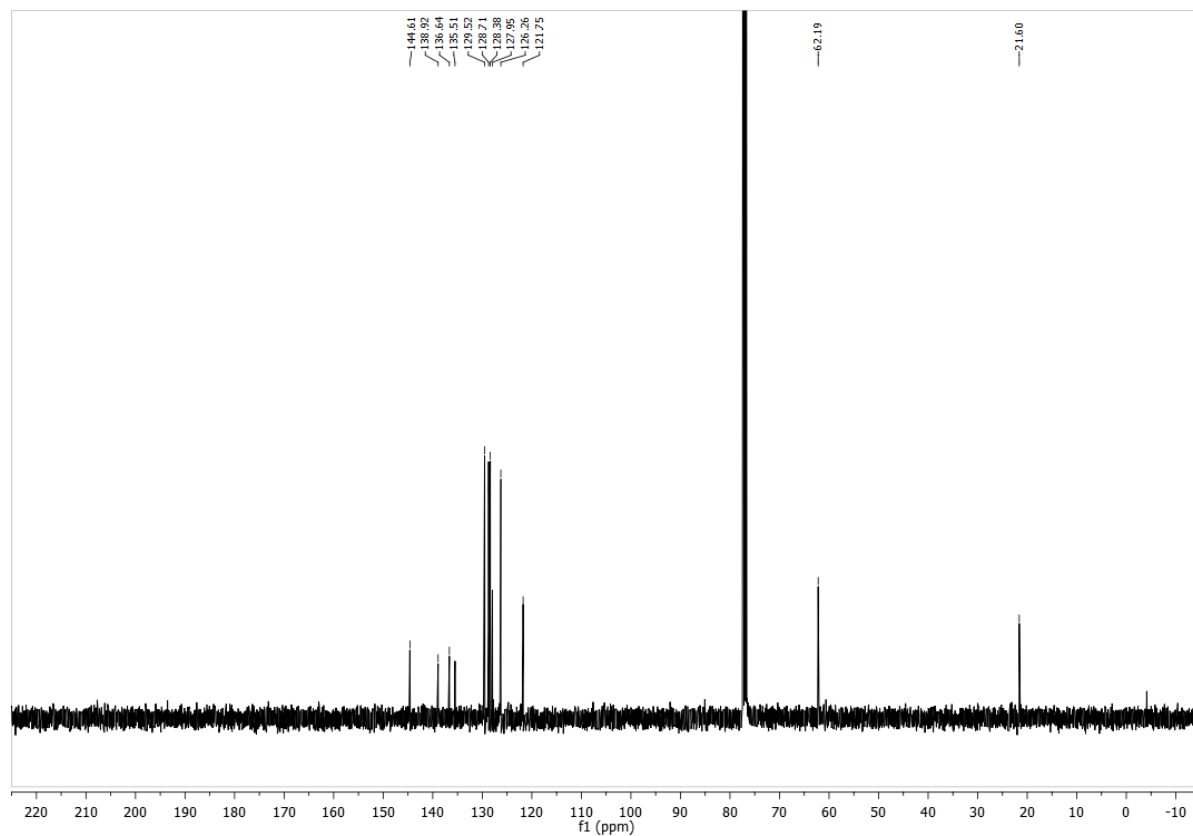
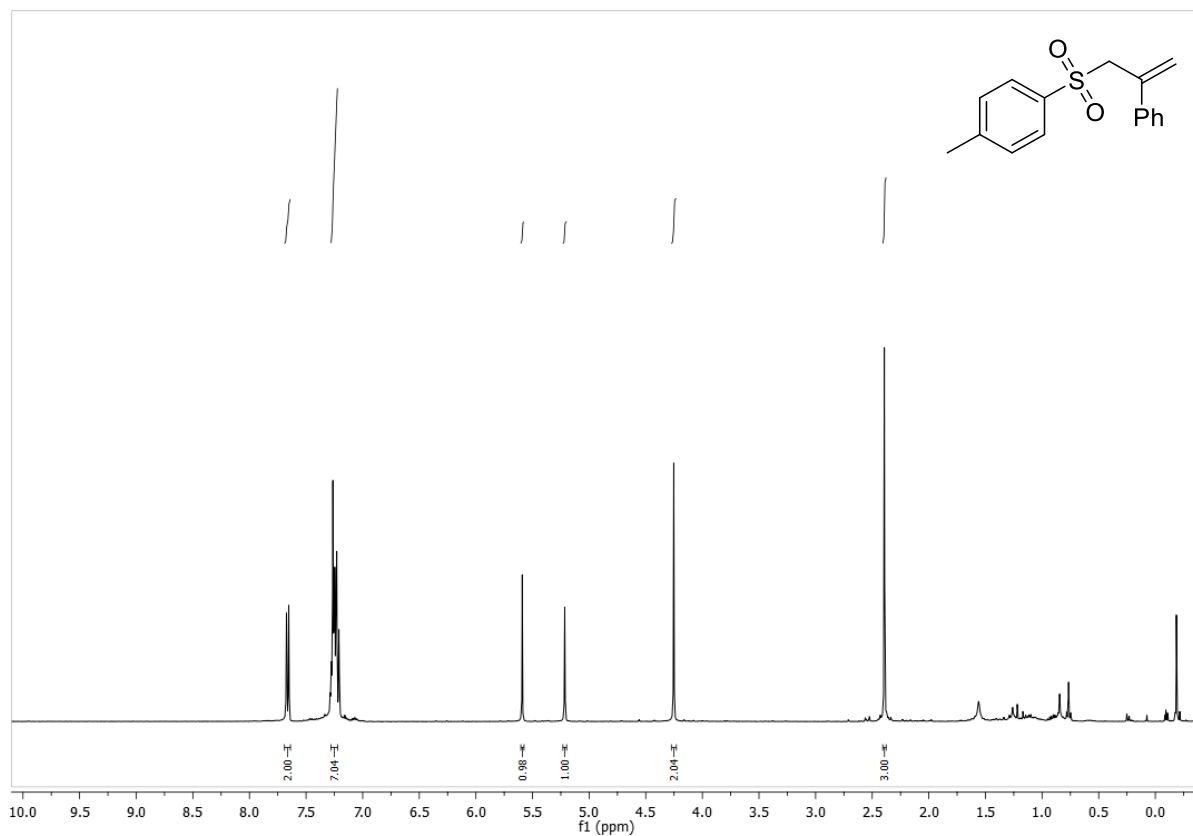
G Appendix

1-methyl-4-((2-methylallyl)sulfonyl)benzene (207)



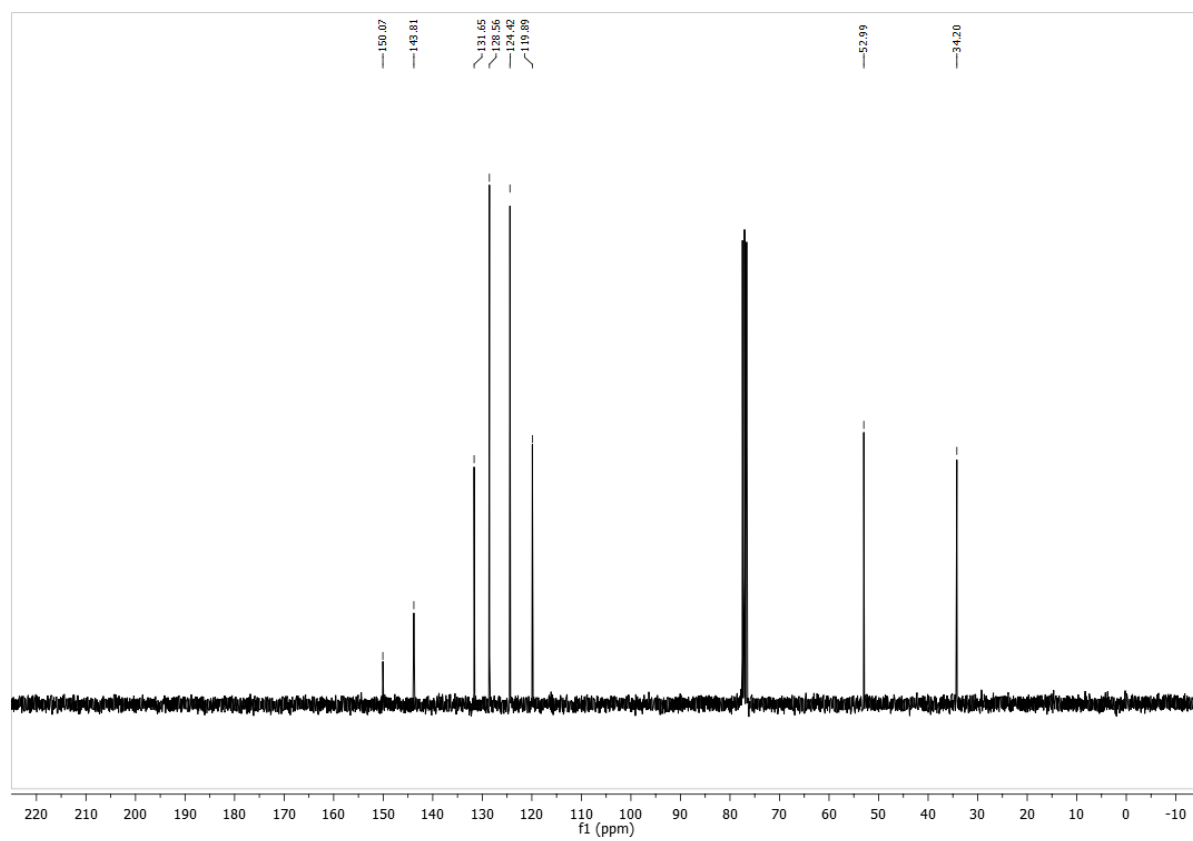
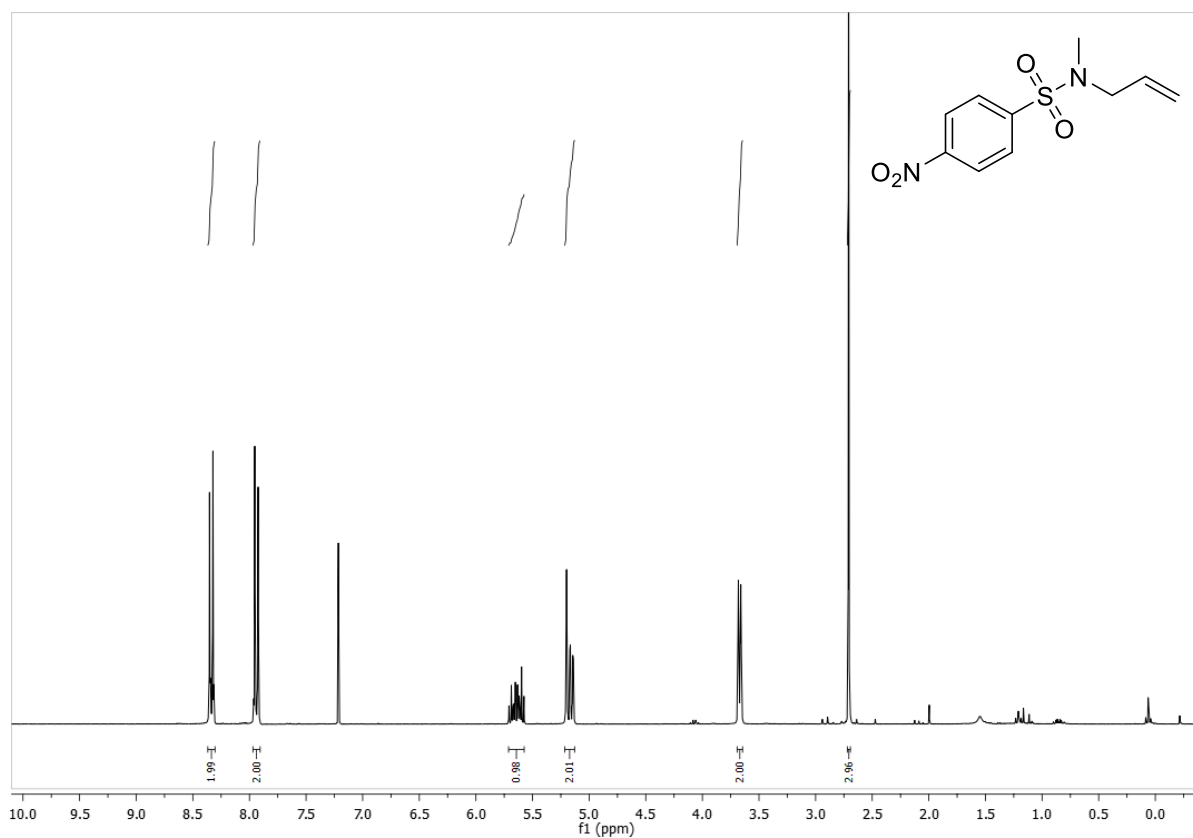
G Appendix

1-methyl-4-((2-phenylallyl)sulfonyl)benzene (208)



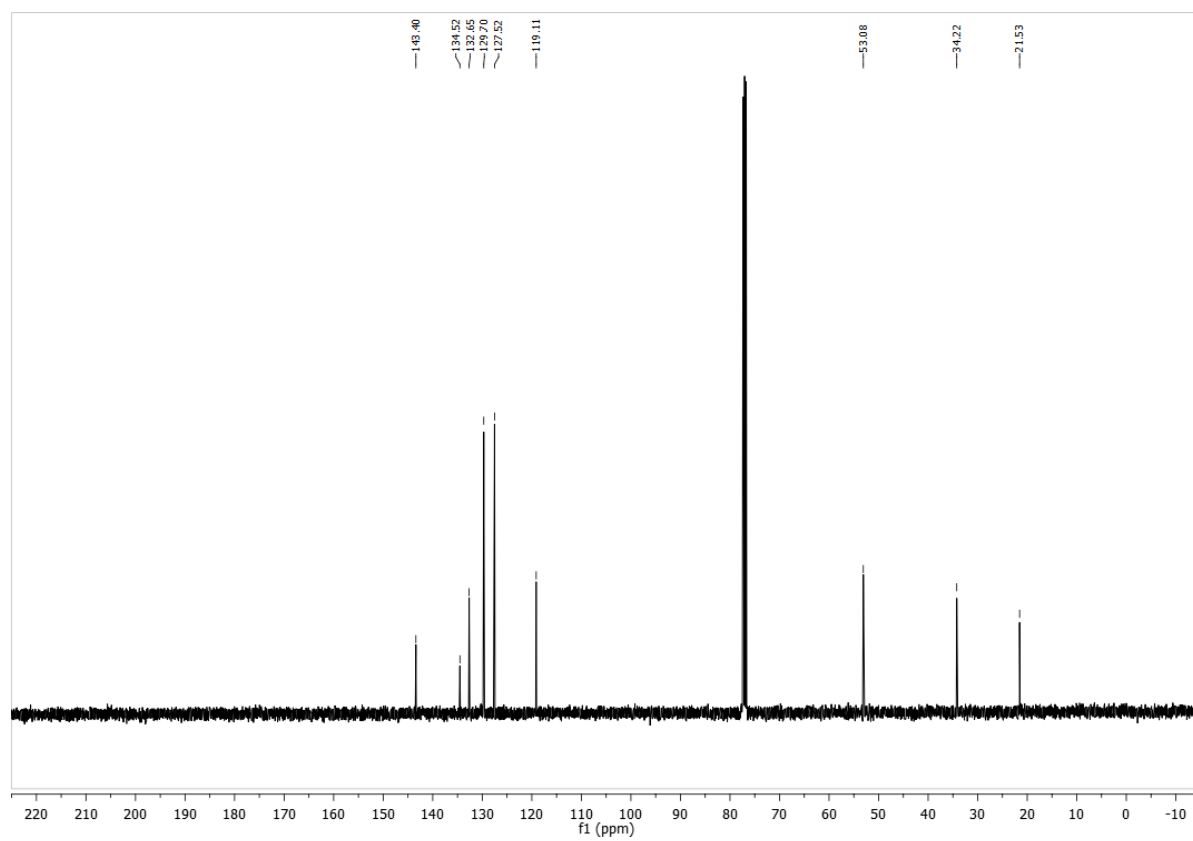
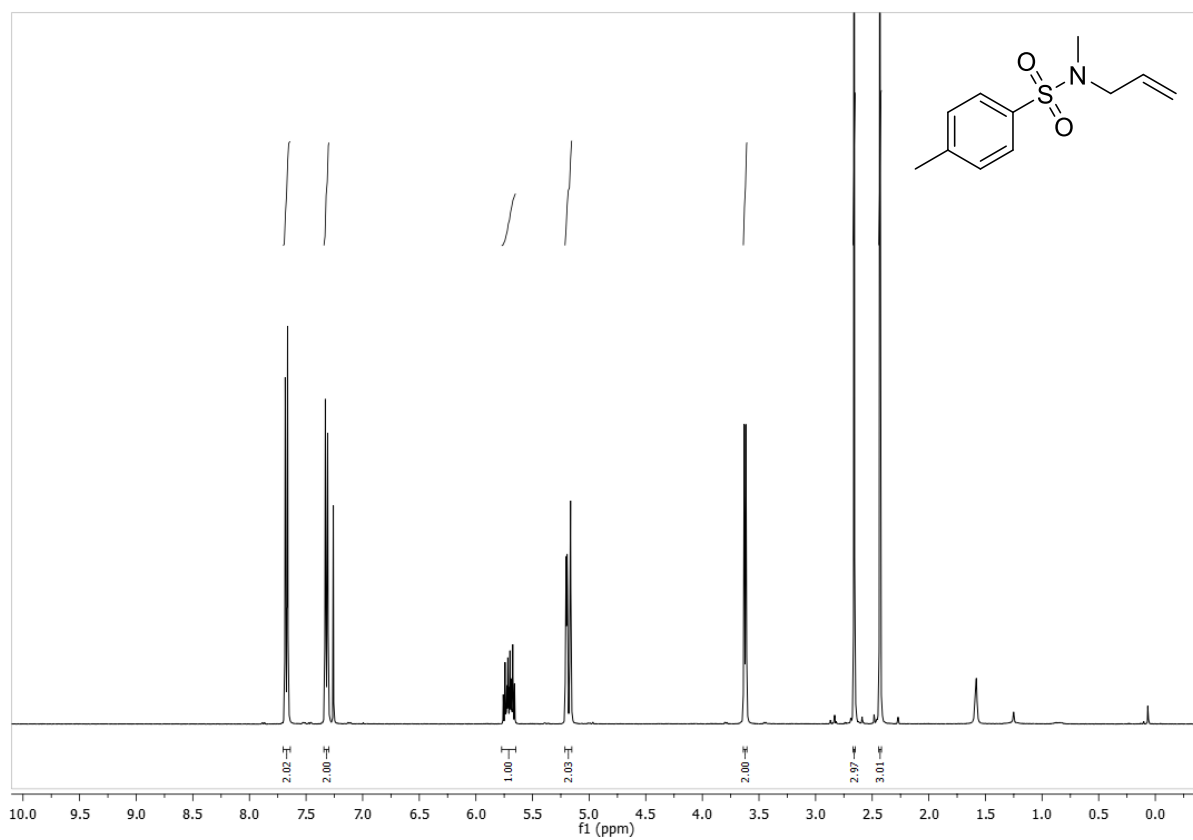
G Appendix

N-allyl-*N*-methyl-4-nitrobenzenesulfonamide (212)



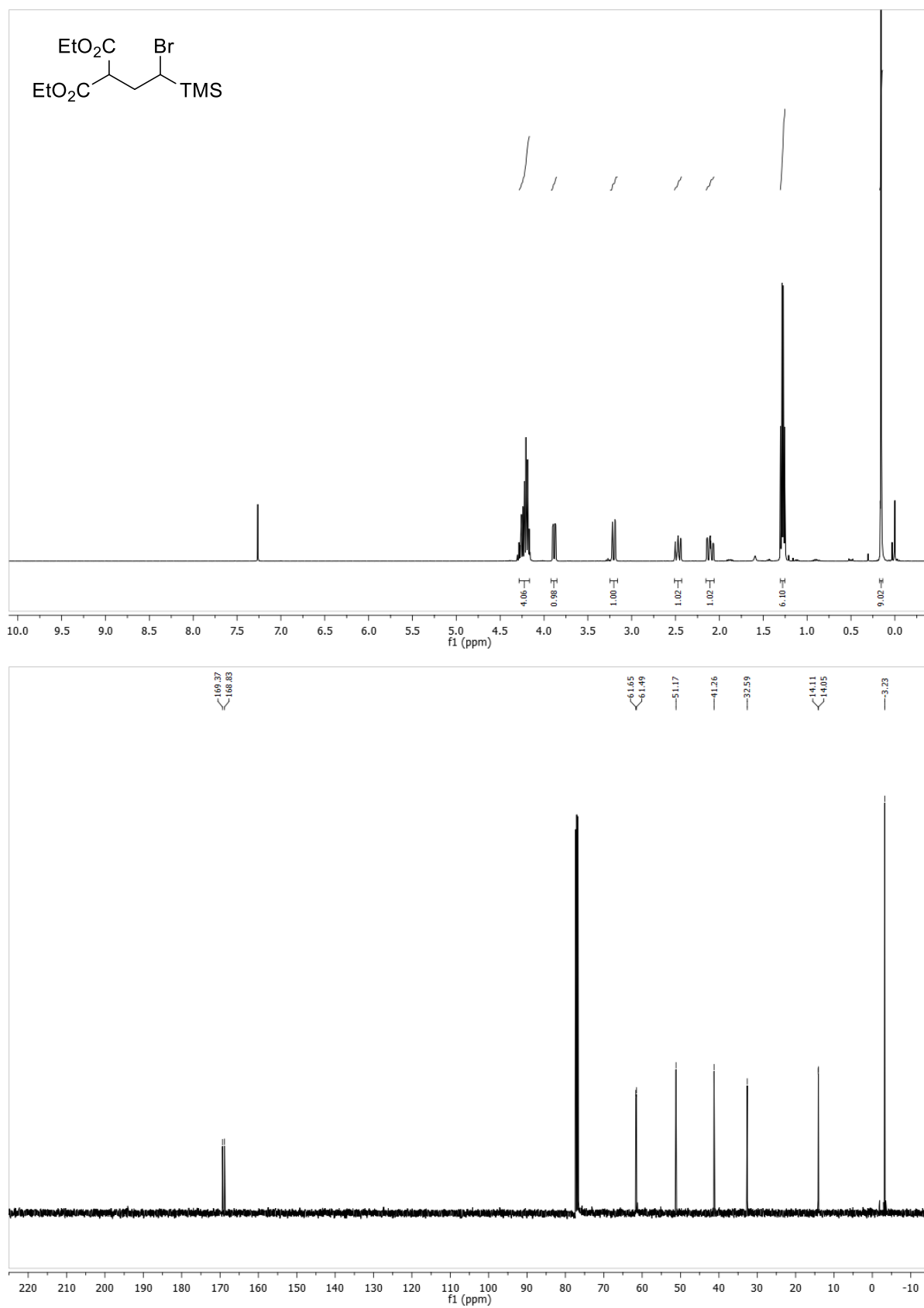
G Appendix

N-allyl-*N*,4-dimethylbenzenesulfonamide (214)



G Appendix

Diethyl 2-(2-bromo-2-(trimethylsilyl)ethyl)malonate (231)

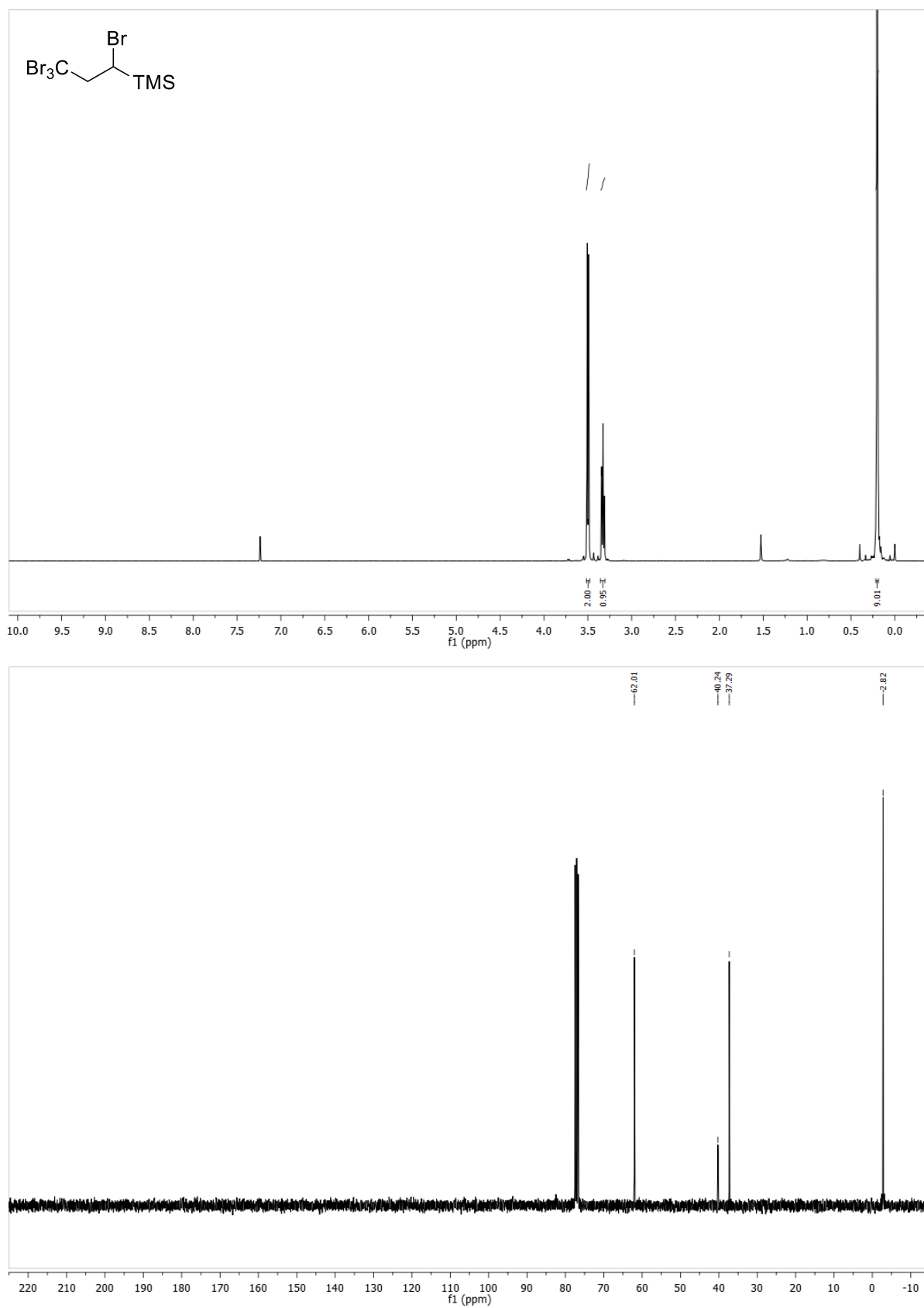


Diethyl 2-(2-bromo-2-(trimethylsilyl)ethyl)-2-methylmalonate (265)



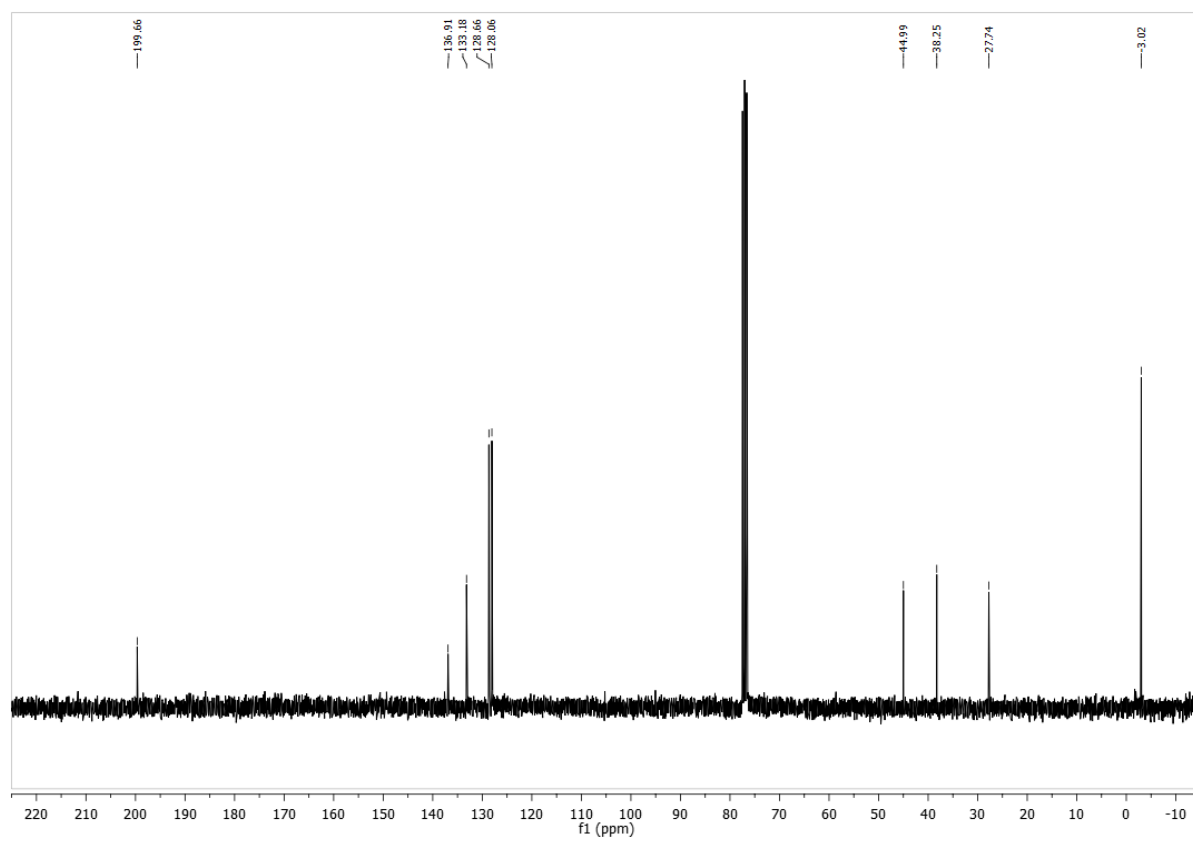
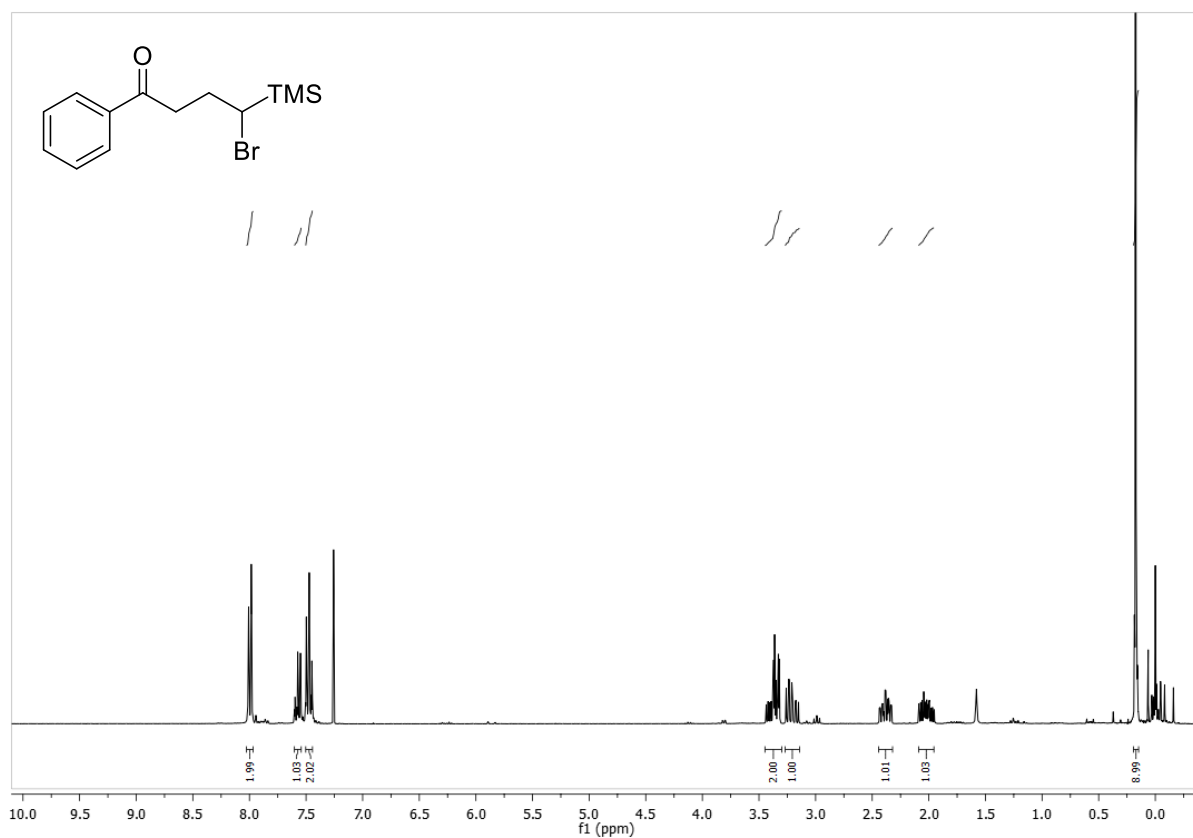
G Appendix

Trimethyl(1,3,3,3-tetrabromopropyl)silane (267)



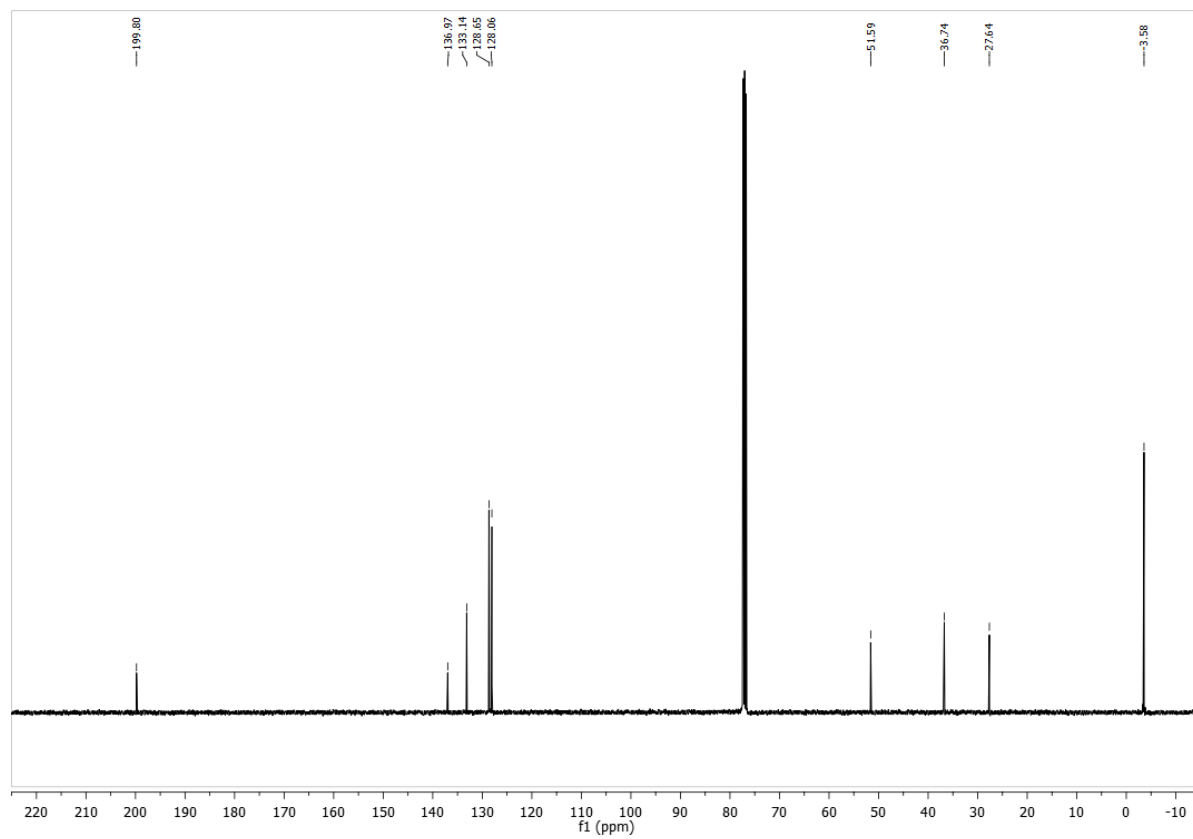
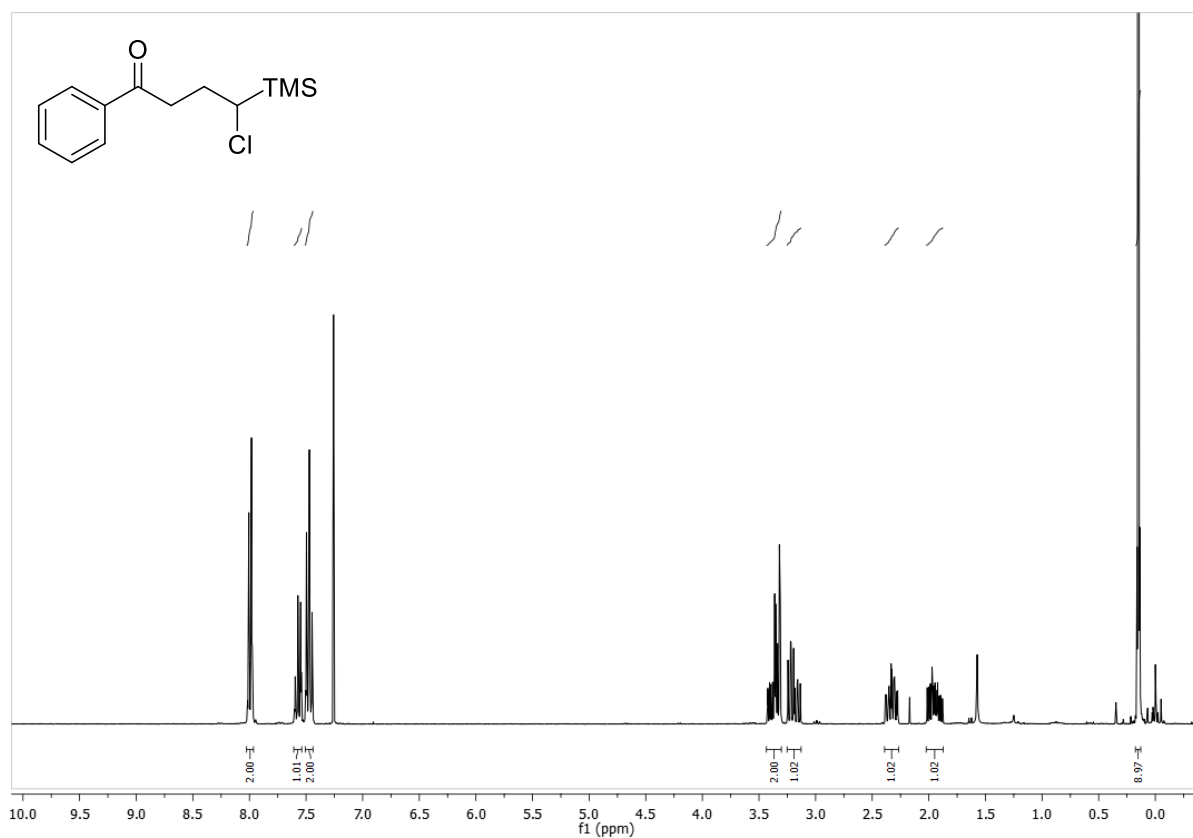
G Appendix

4-bromo-1-phenyl-4-(trimethylsilyl)butan-1-one (269)



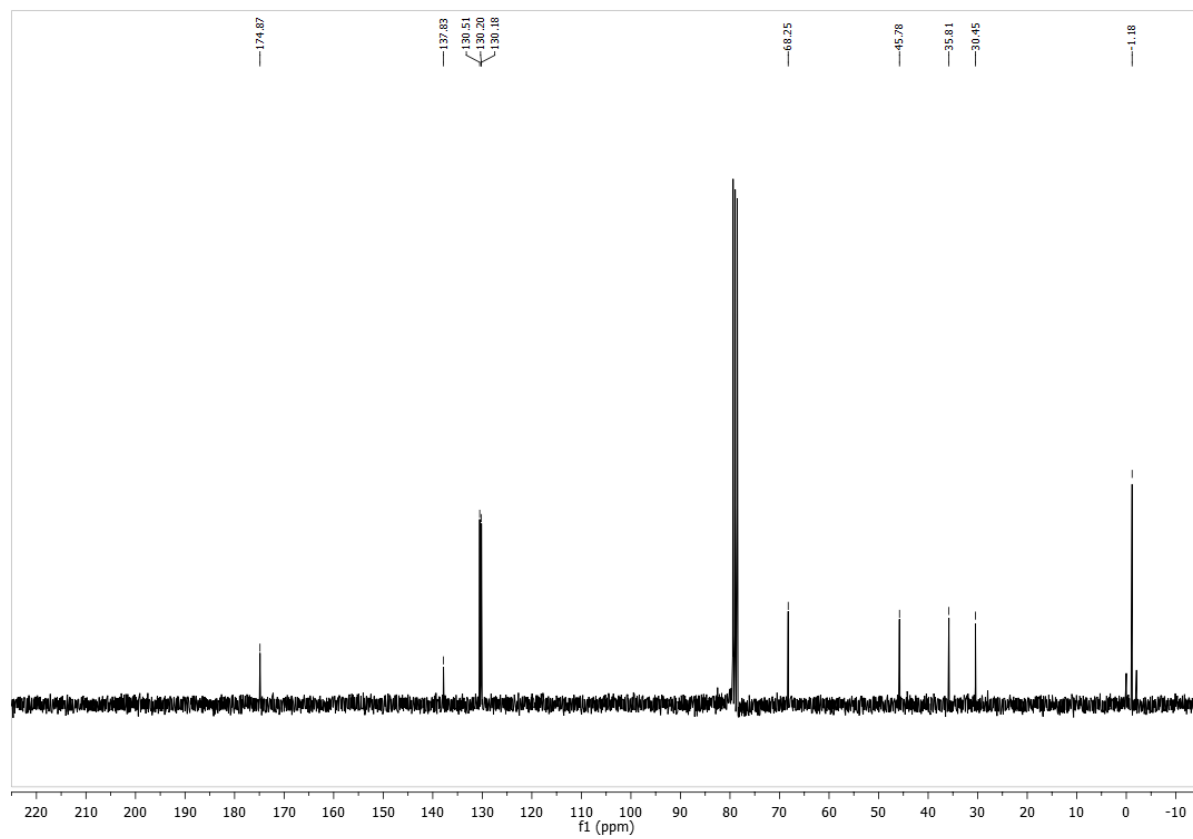
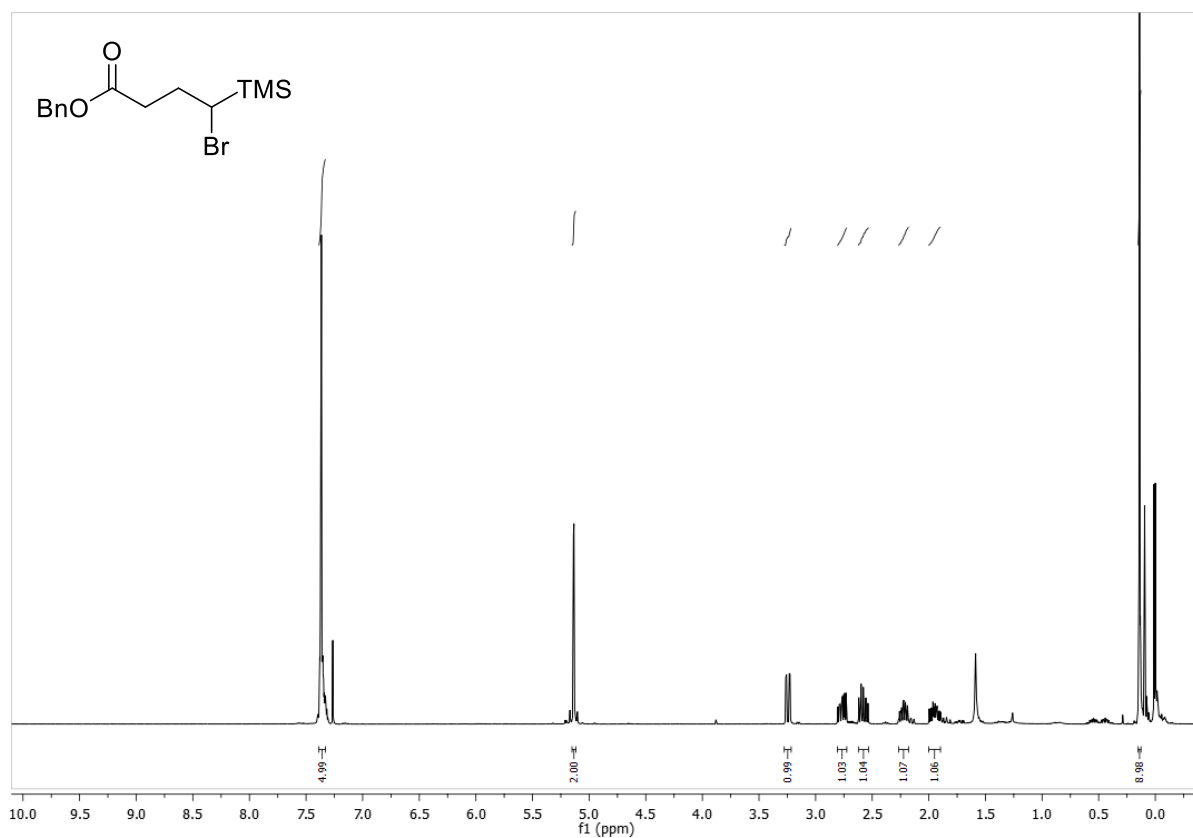
G Appendix

4-chloro-1-phenyl-4-(trimethylsilyl)butan-1-one (270)



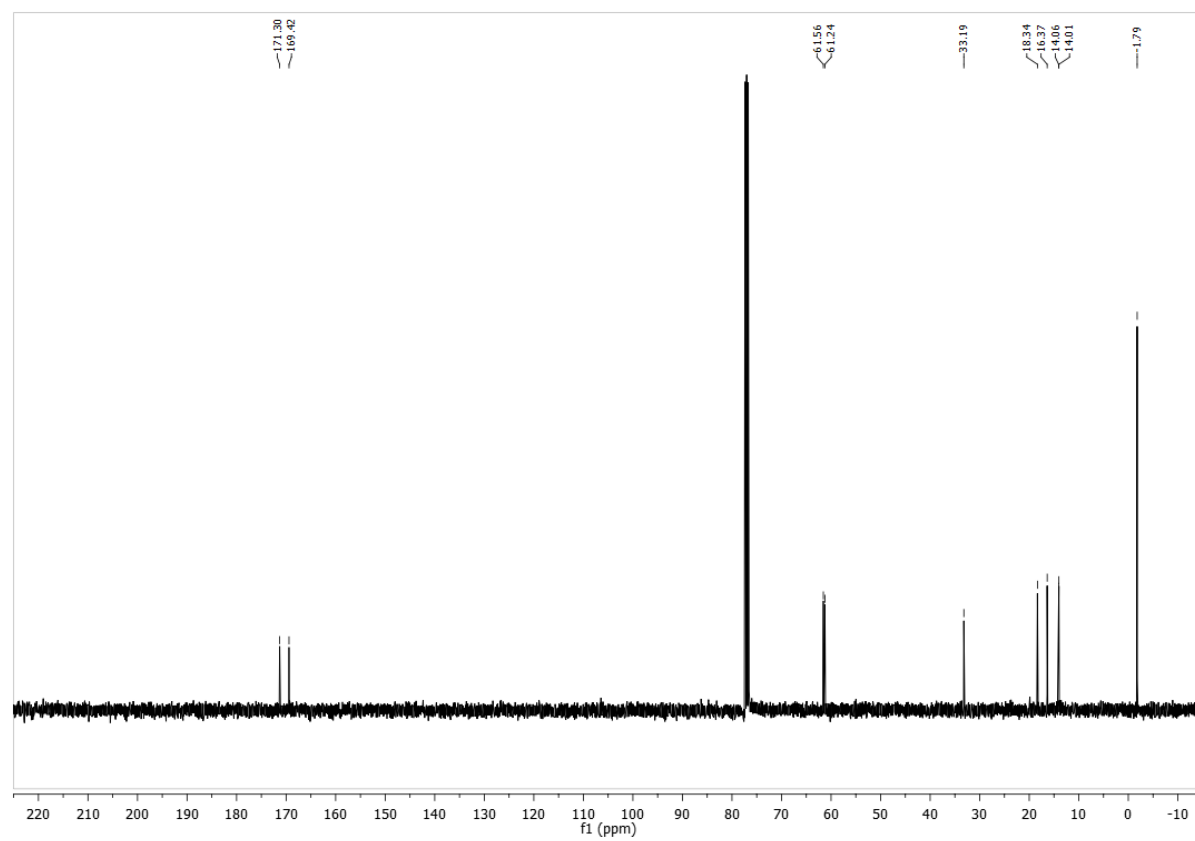
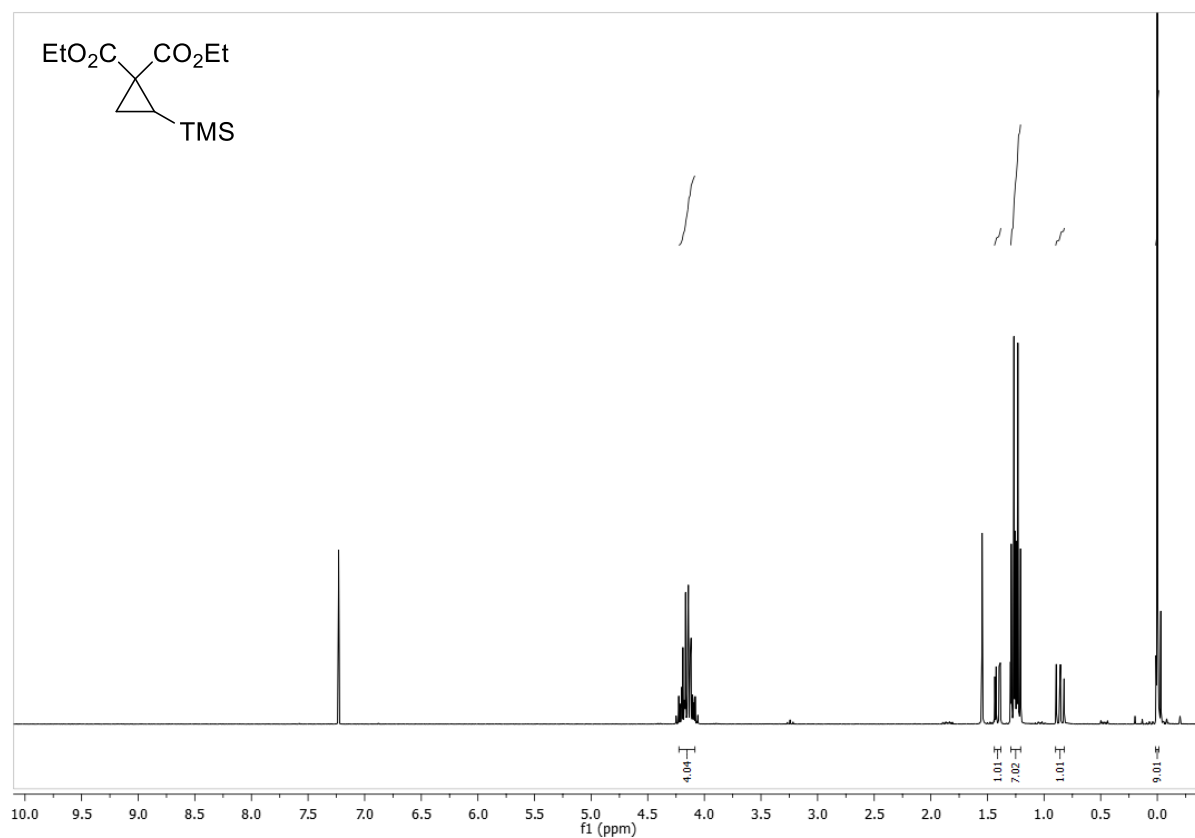
G Appendix

Benzyl 4-bromo-4-(trimethylsilyl)butanoate (271)



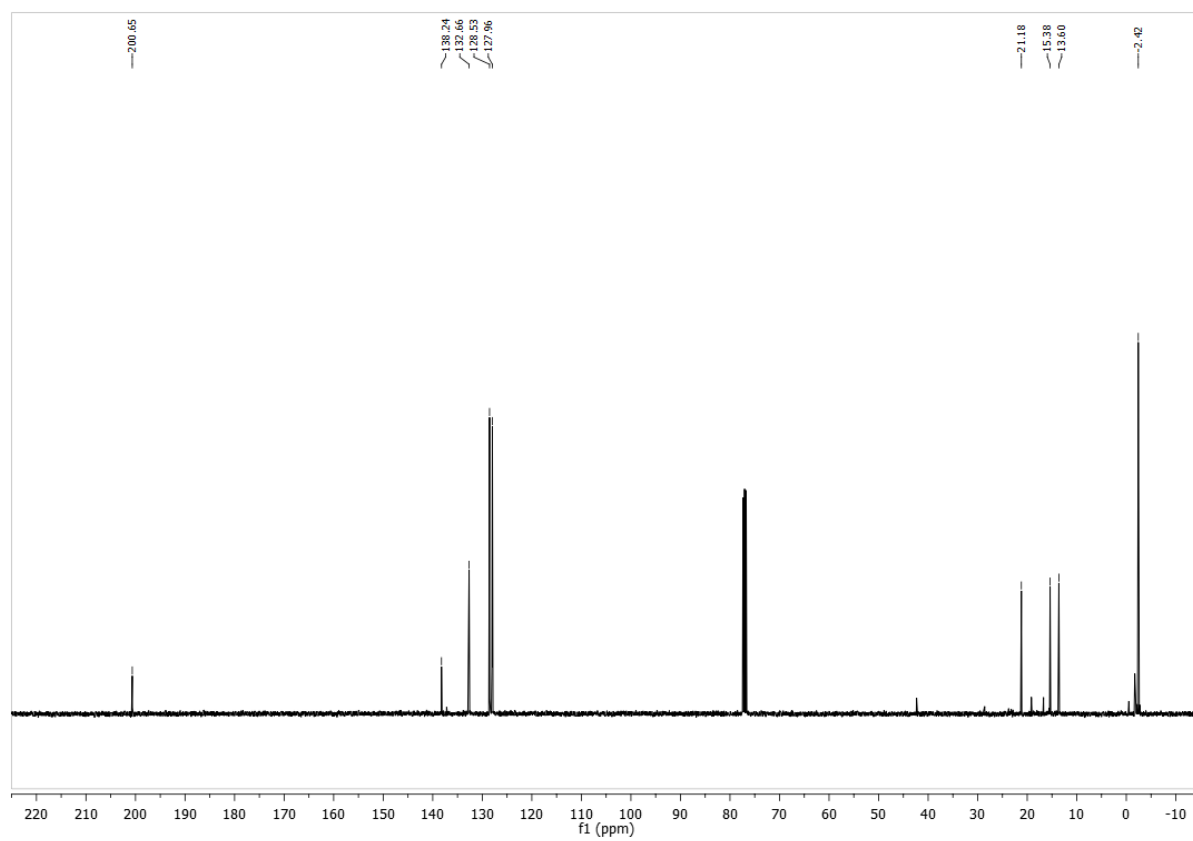
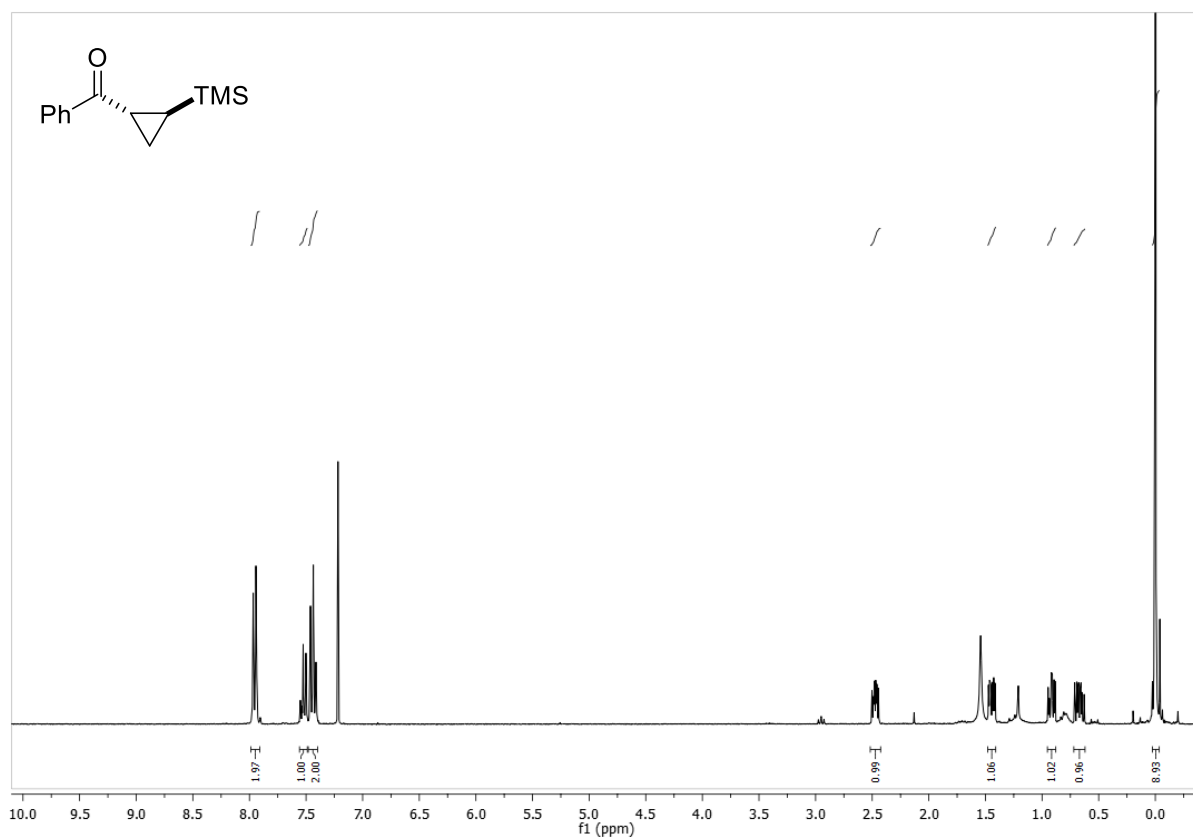
G Appendix

Diethyl 2-(trimethylsilyl)cyclopropane-1,1-dicarboxylate (300)



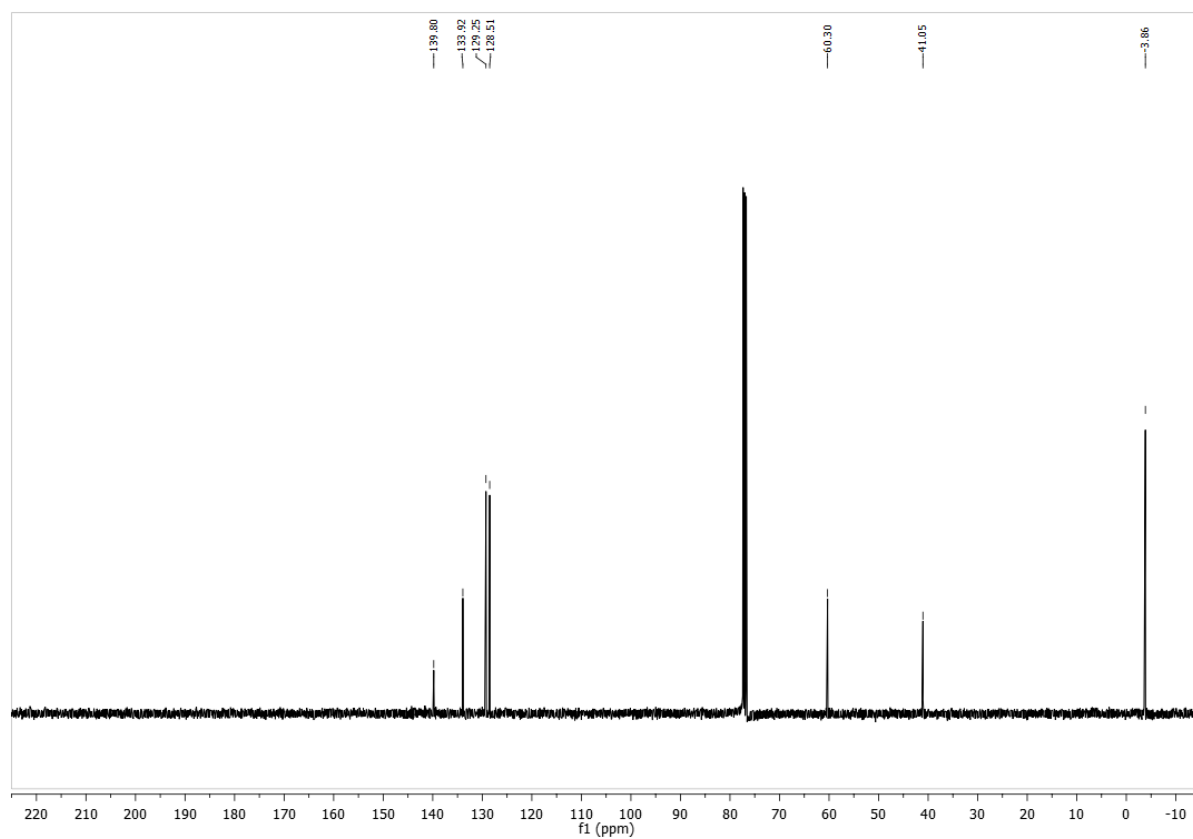
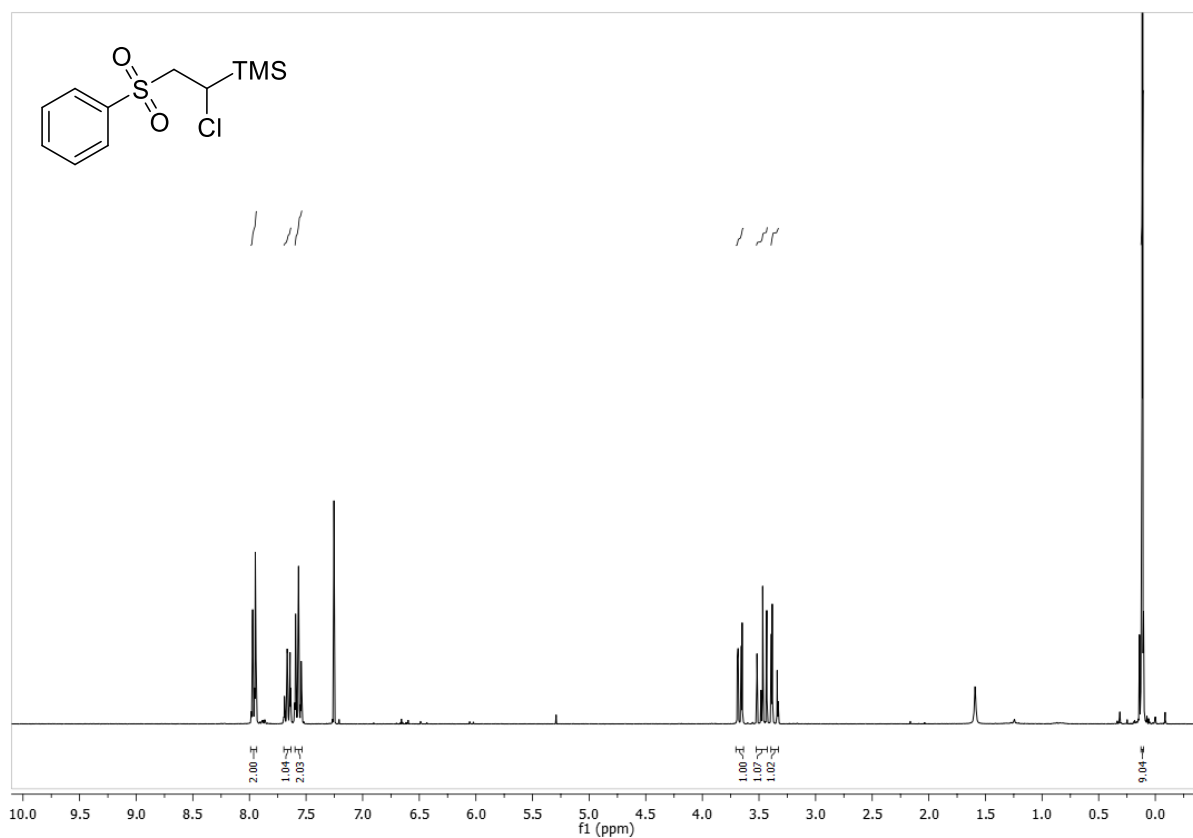
G Appendix

Phenyl-2-(trimethylsilyl)cyclopropyl)methanone (301)



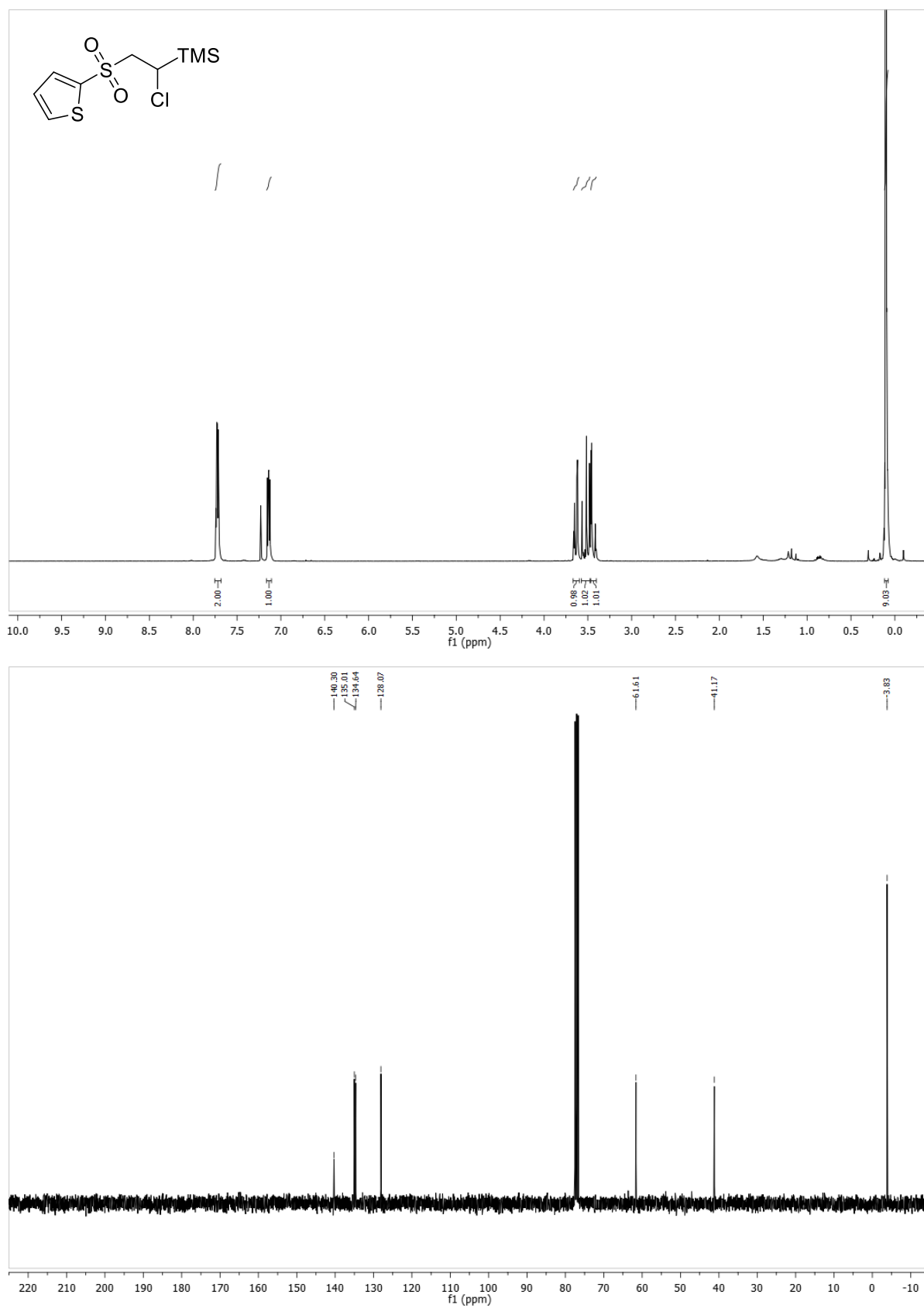
G Appendix

(1-chloro-2-(phenylsulfonyl)ethyl)trimethylsilane (245)



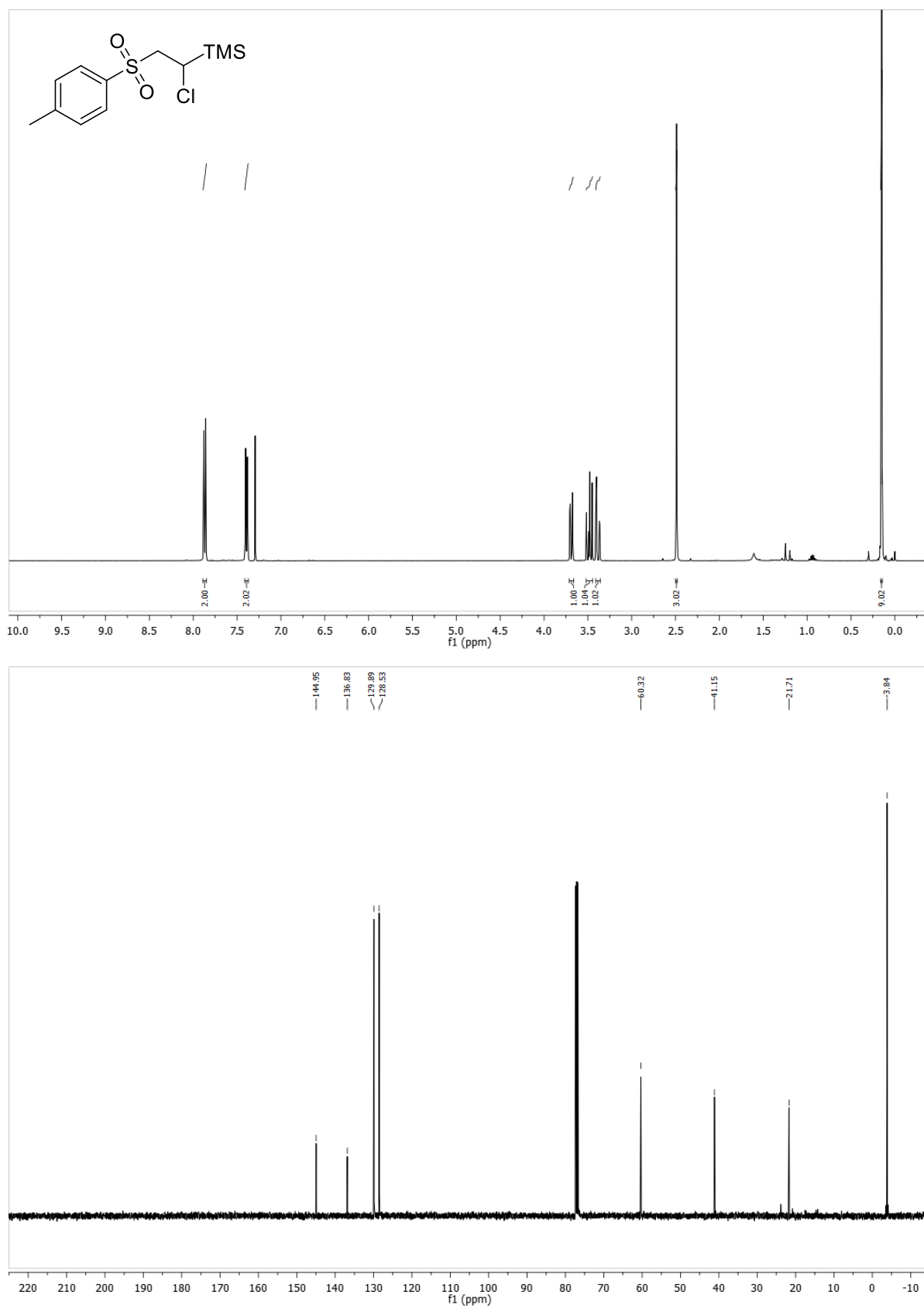
G Appendix

(1-chloro-2-(thiophen-2-ylsulfonyl)ethyl)trimethylsilane (273)



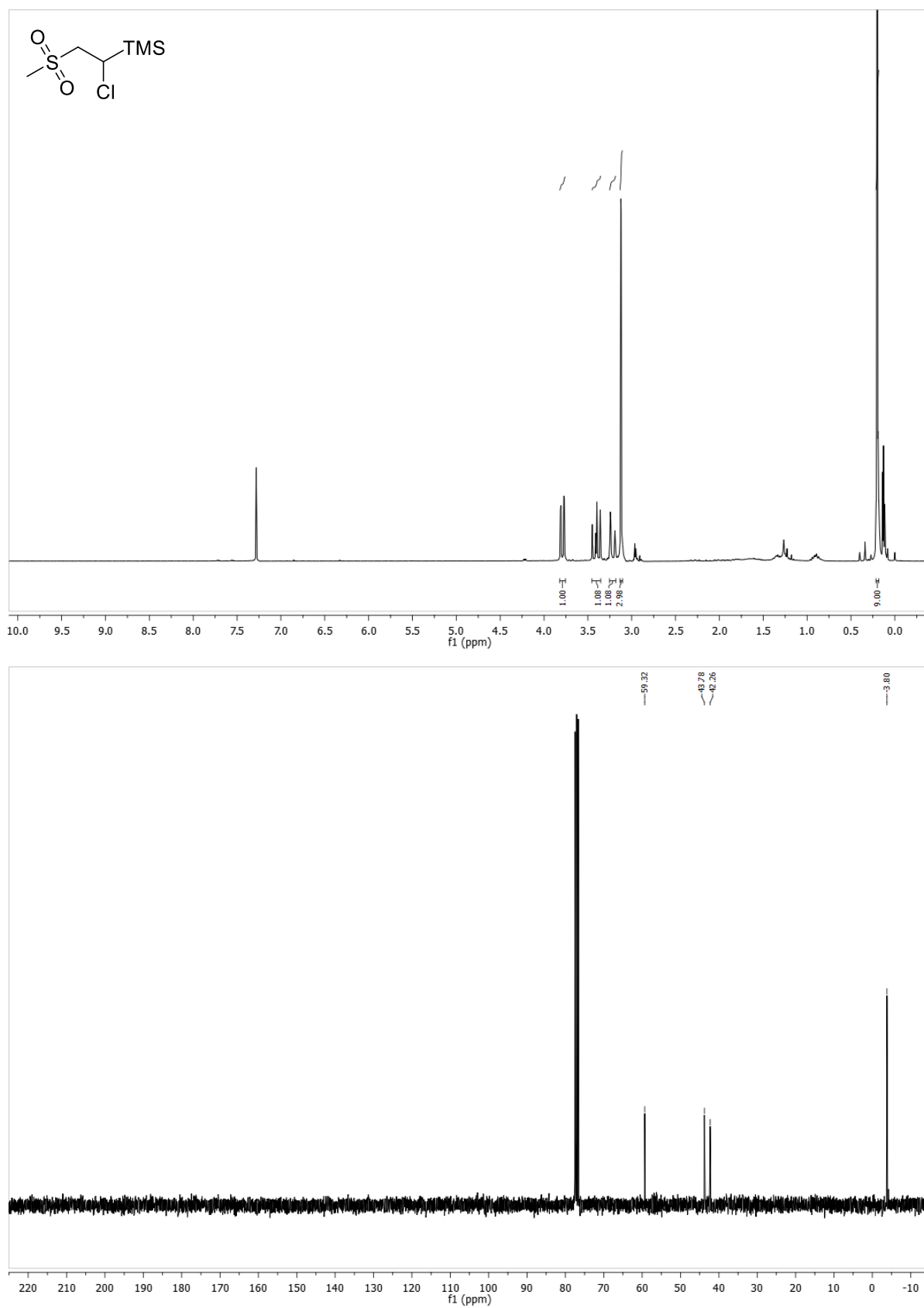
G Appendix

(1-chloro-2-tosylethyl)trimethylsilane (233)



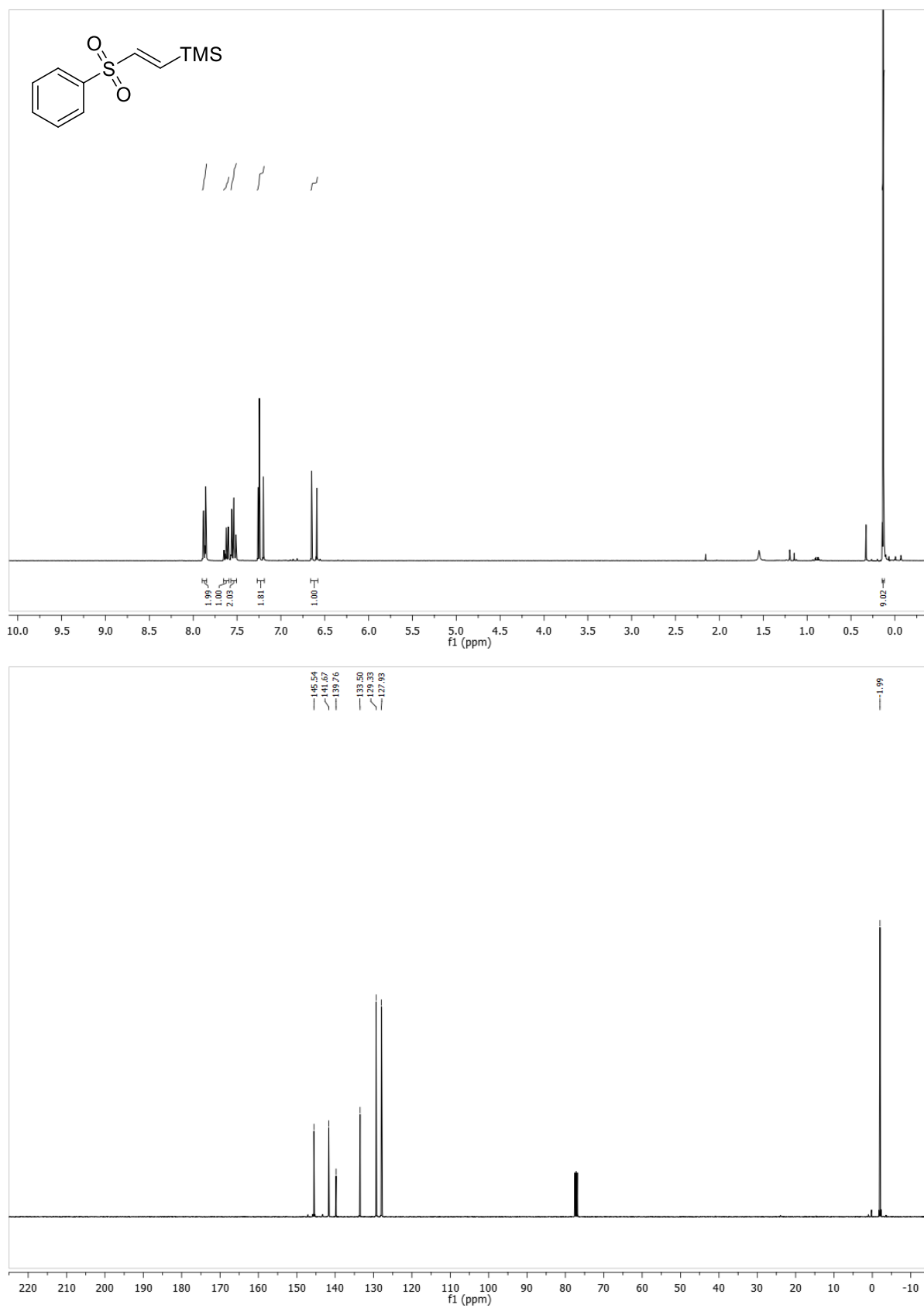
G Appendix

(1-chloro-2-(methylsulfonyl)ethyl)trimethylsilane (244)



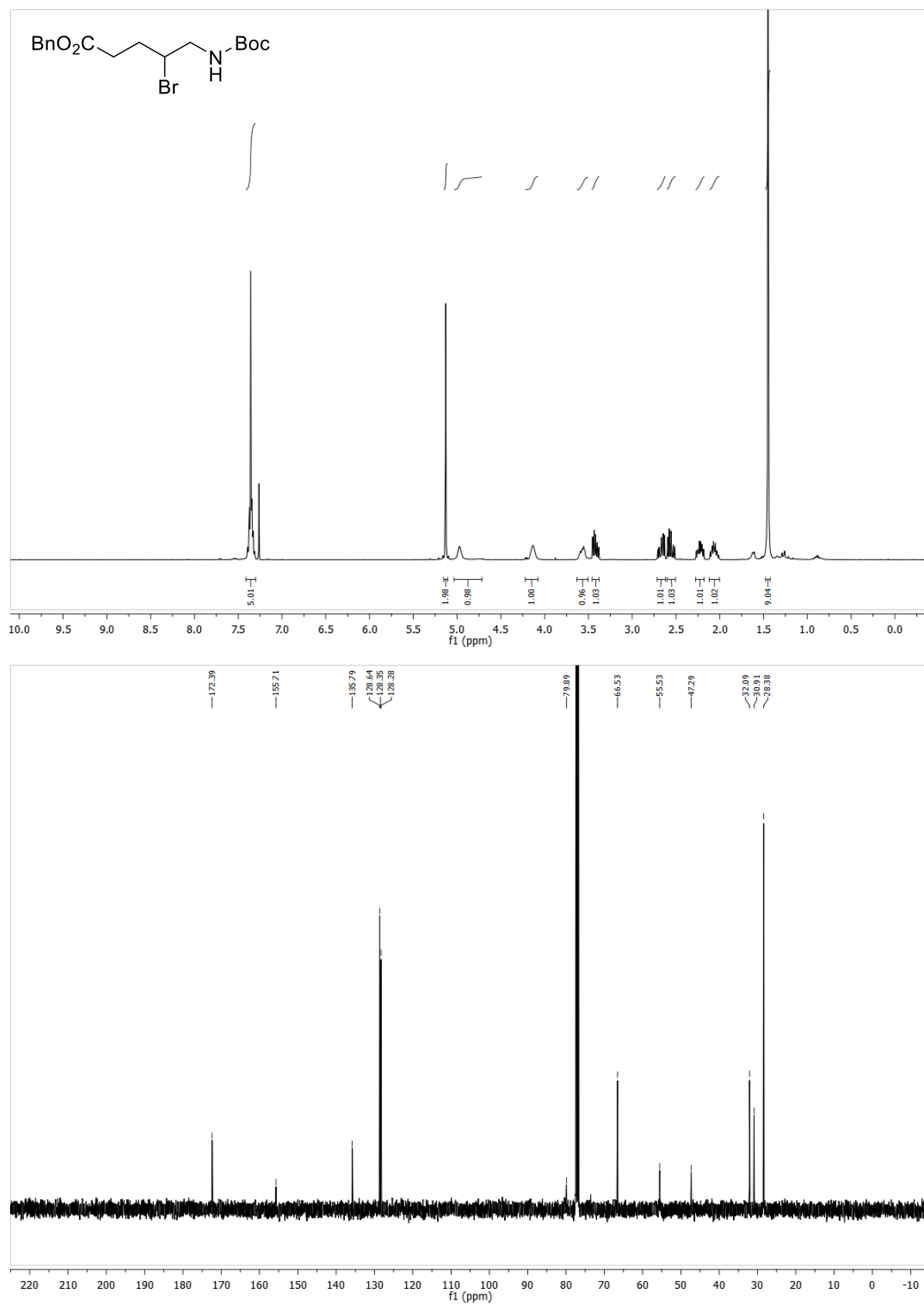
G Appendix

(*E*)-trimethyl(2-(phenylsulfonyl)vinyl)silane (278)



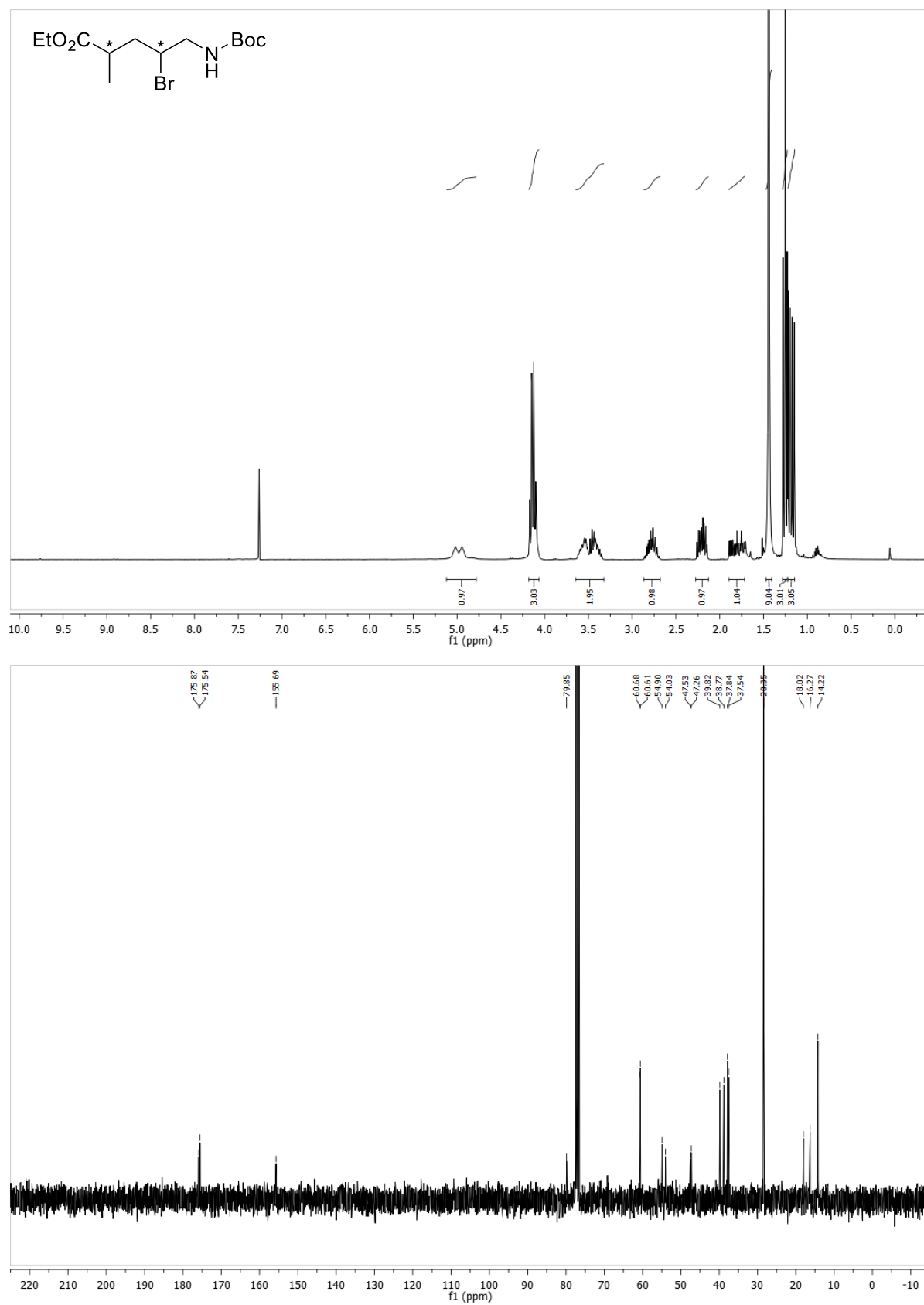
G Appendix

Benzyl 4-bromo-5-((*tert*-butoxycarbonyl)amino)pentanoate (317)



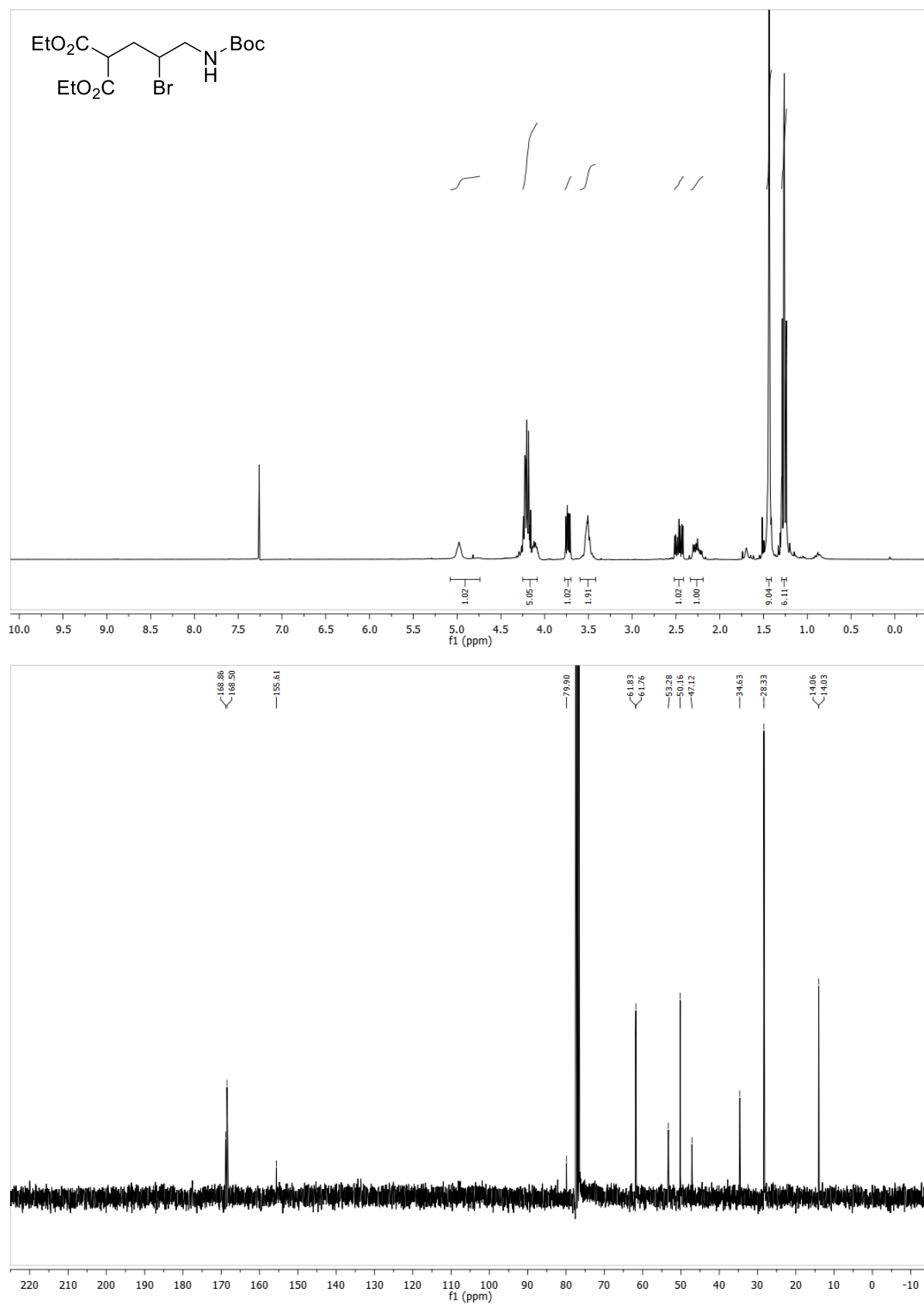
G Appendix

Ethyl 4-bromo-5-((*tert*-butoxycarbonyl)amino)-2-methylpentanoate (327)



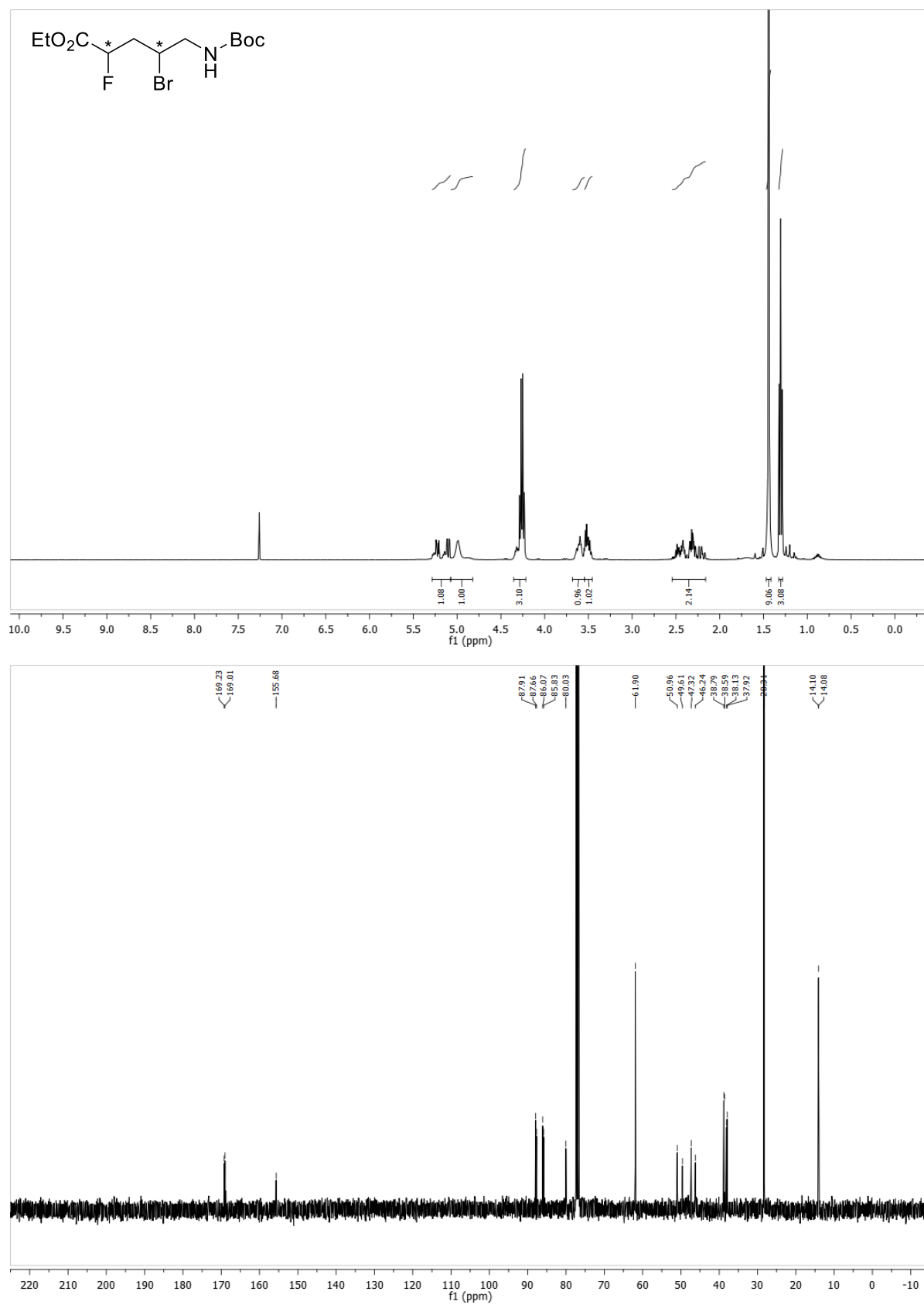
G Appendix

Diethyl 2-(2-bromo-3-((*tert*-butoxycarbonyl)amino)propyl)malonate (61)

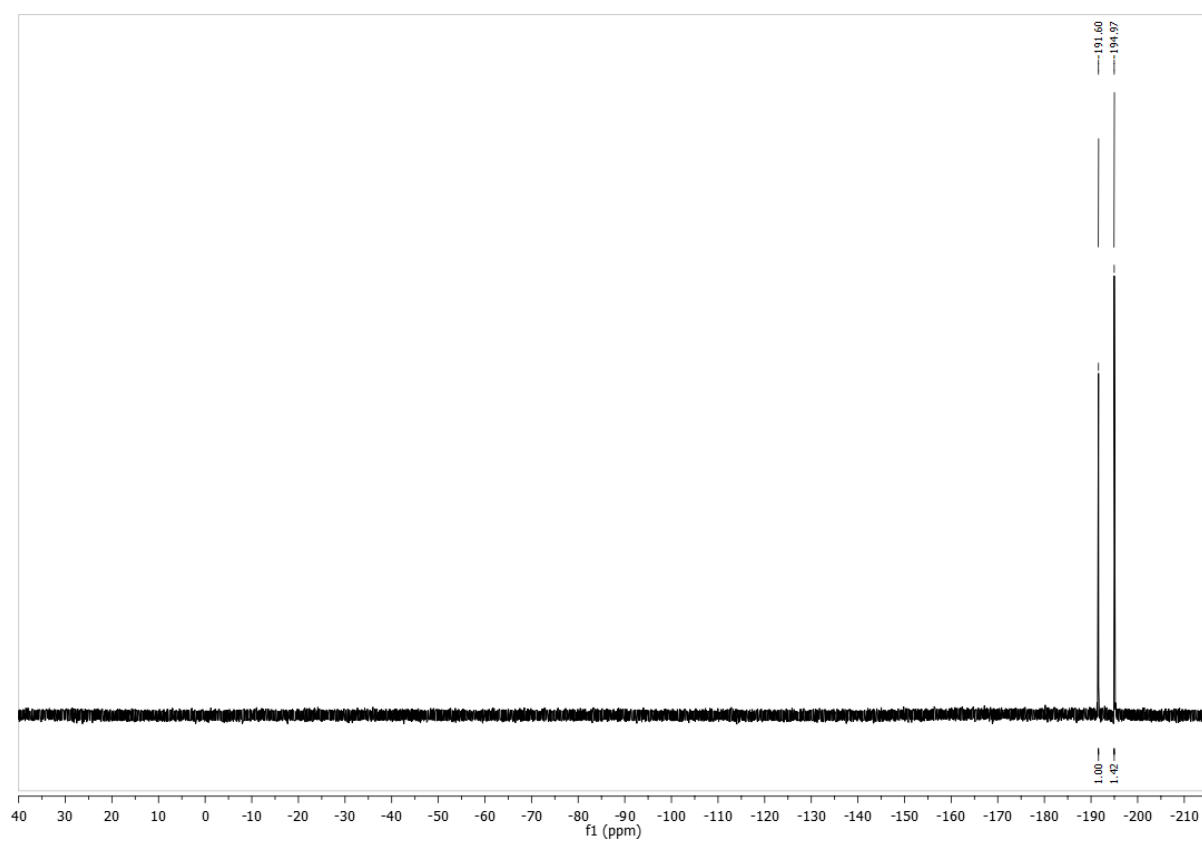


G Appendix

Ethyl 4-bromo-5-((*tert*-butoxycarbonyl)amino)-2-fluoropentanoate (329)

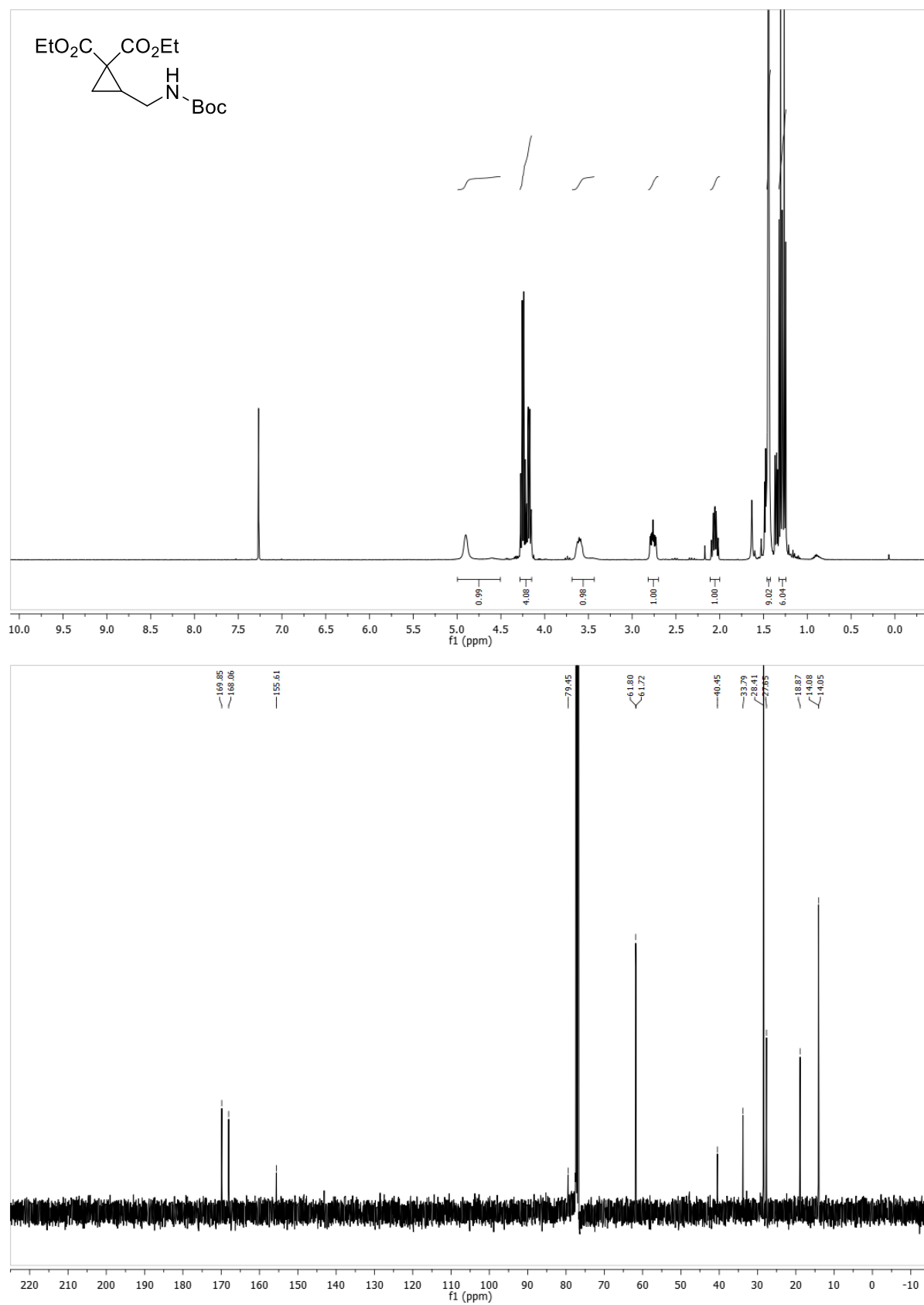


G Appendix



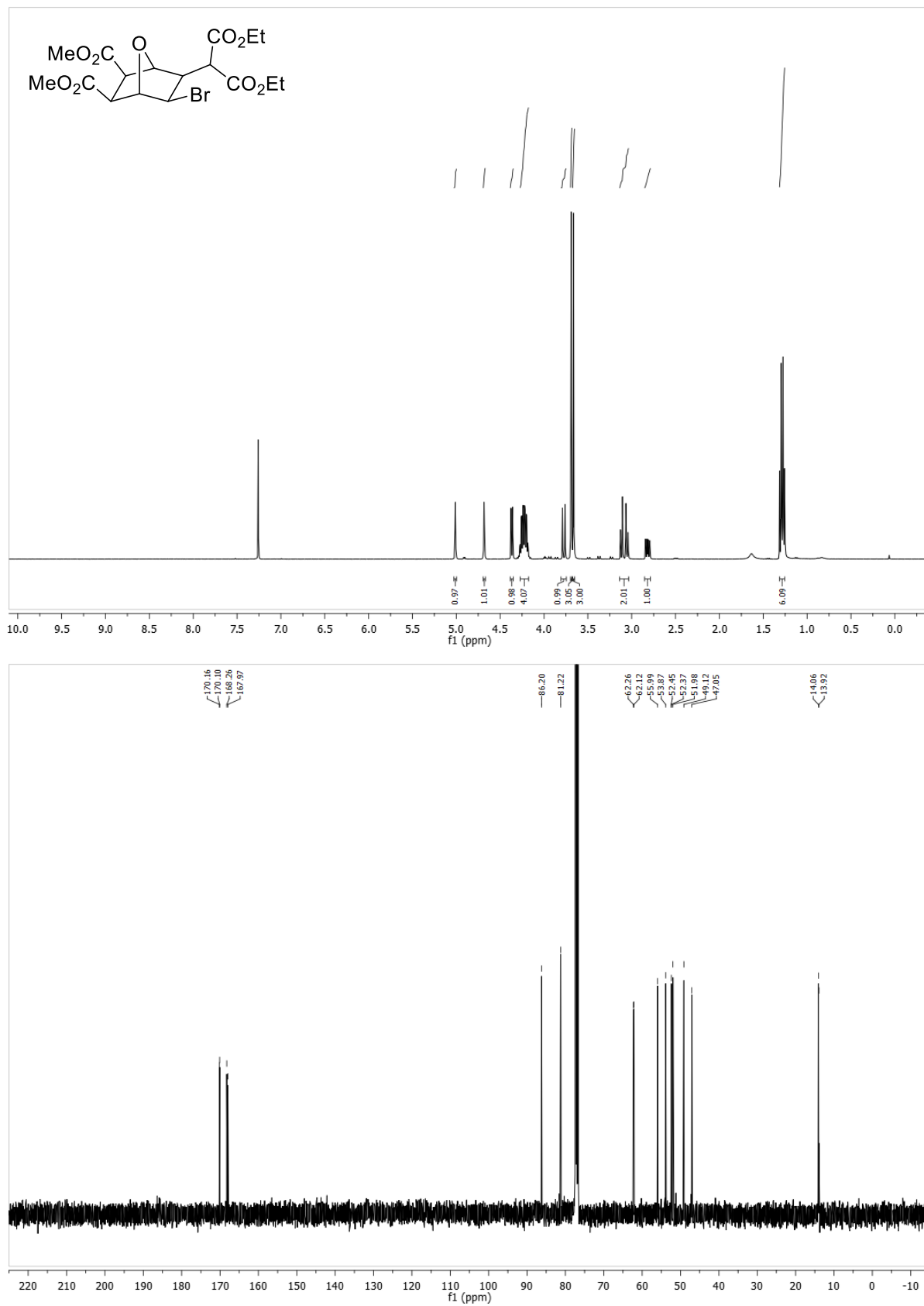
G Appendix

Diethyl 2-(((*tert*-butoxycarbonyl)amino)methyl)cyclopropane-1,1-dicarboxylate (332)



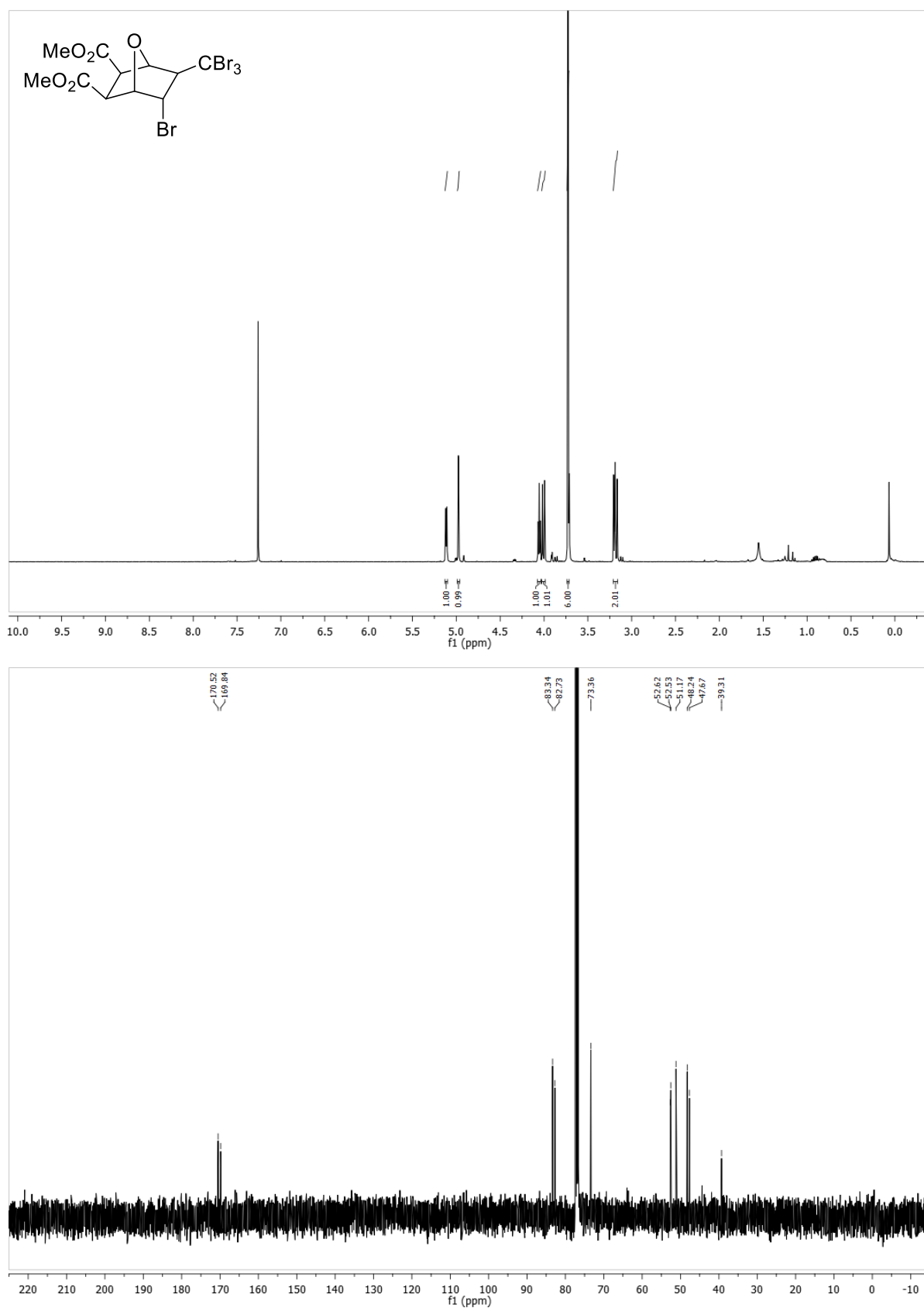
G Appendix

Dimethyl-(-5-bromo-6-(1-ethoxy-3-(ethylperoxy)-1-oxo-3 λ^2 -propan-2-yl)-7-oxabicyclo[2.2.1]heptane-2,3-dicarboxylate (352)



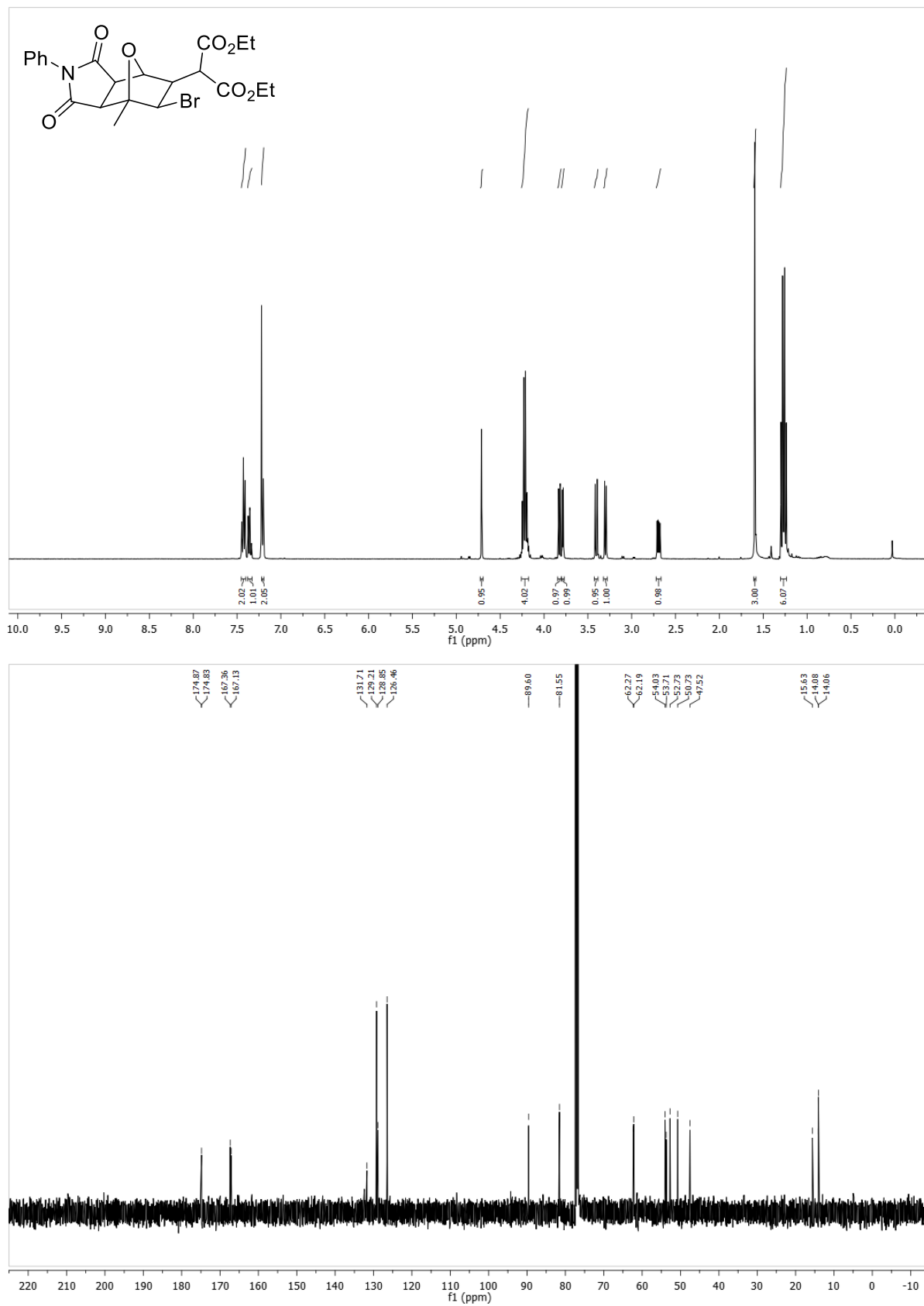
G Appendix

Dimethyl-(-5-bromo-6-(tribromomethyl)-7-oxabicyclo[2.2.1]heptane-2,3-dicarboxylate (353)



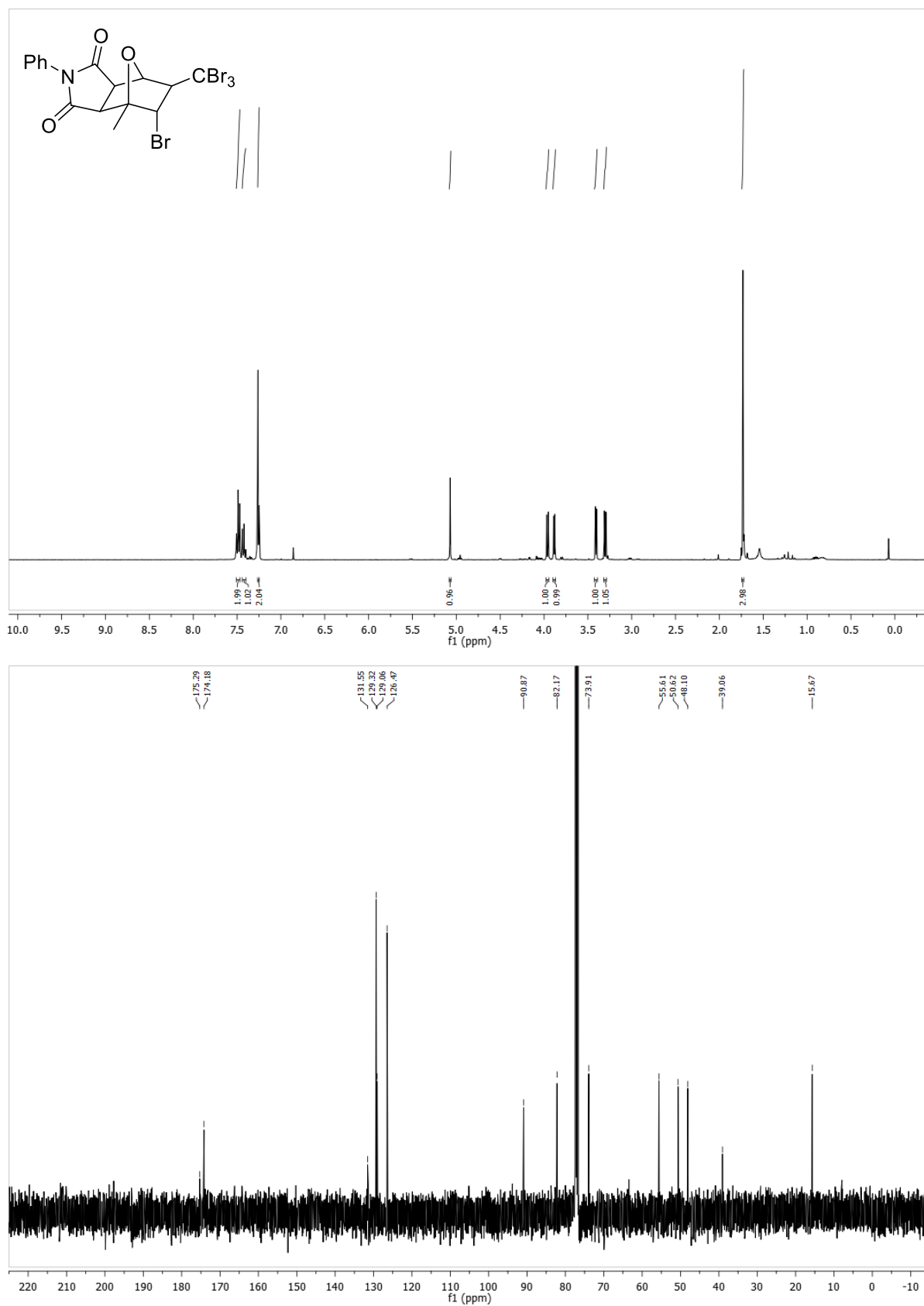
G Appendix

Ethyl-2-(6-bromo-7-methyl-1,3-dioxo-2-phenyloctahydro-1H-4,7-epoxyisoindol-5-yl)-3-(ethylperoxy)-3 λ^2 -propanoate (355)



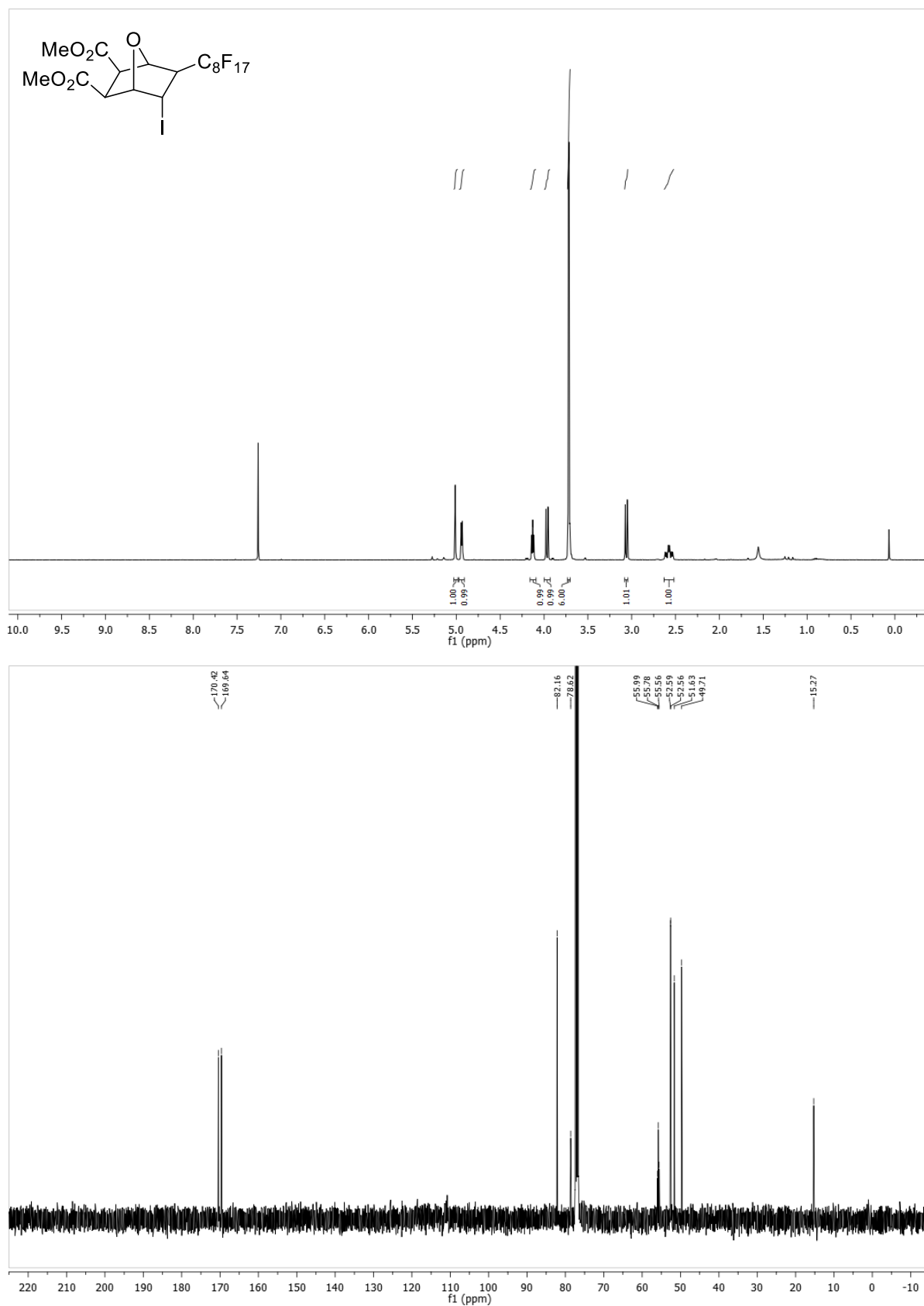
G Appendix

5-bromo-4-methyl-2-phenyl-6-(tribromomethyl)hexahydro-1*H*-4,7-epoxyisoindole-1,3(2*H*)-dione (356)

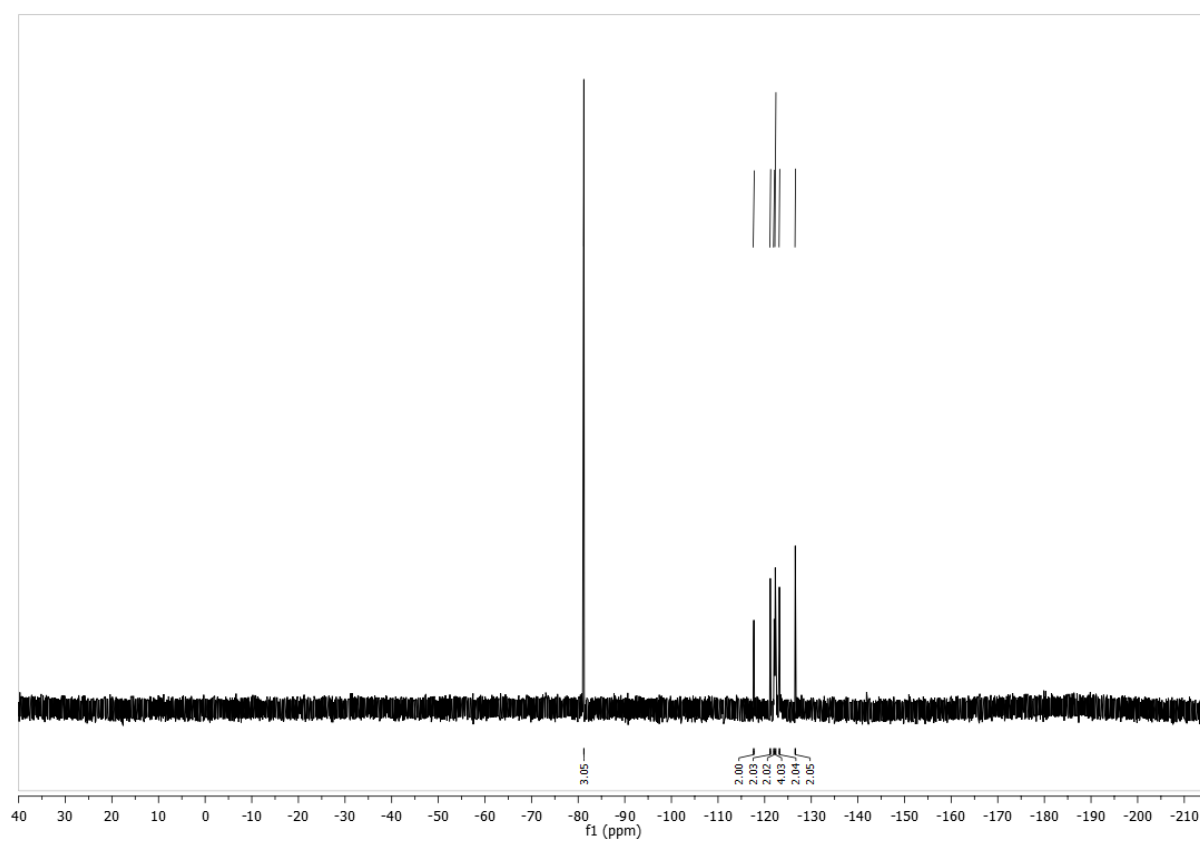


G Appendix

Dimethyl-(-5-iodo-6-(perfluorooctyl)-7-oxabicyclo[2.2.1]heptane-2,3-dicarboxylate (354)

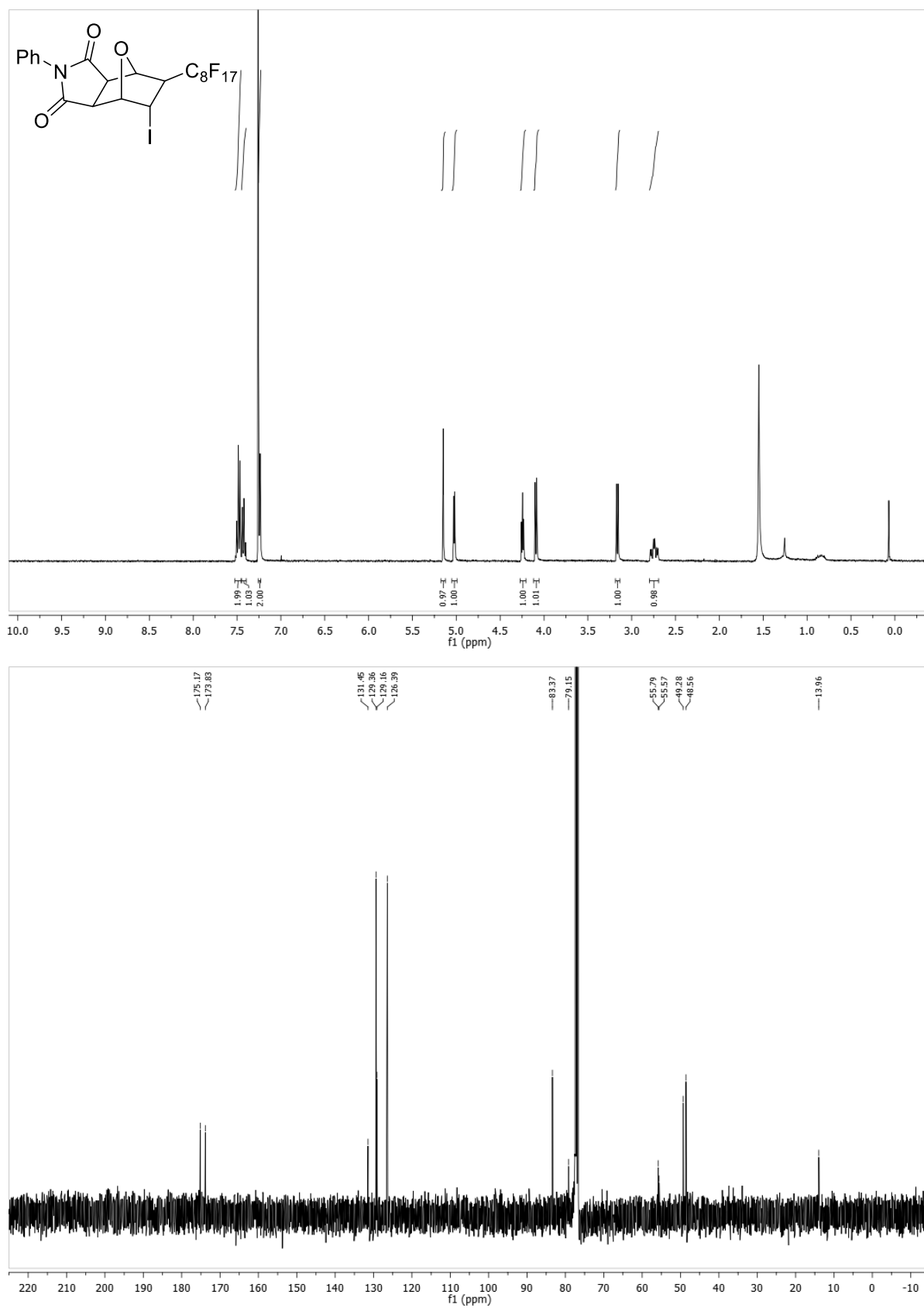


G Appendix

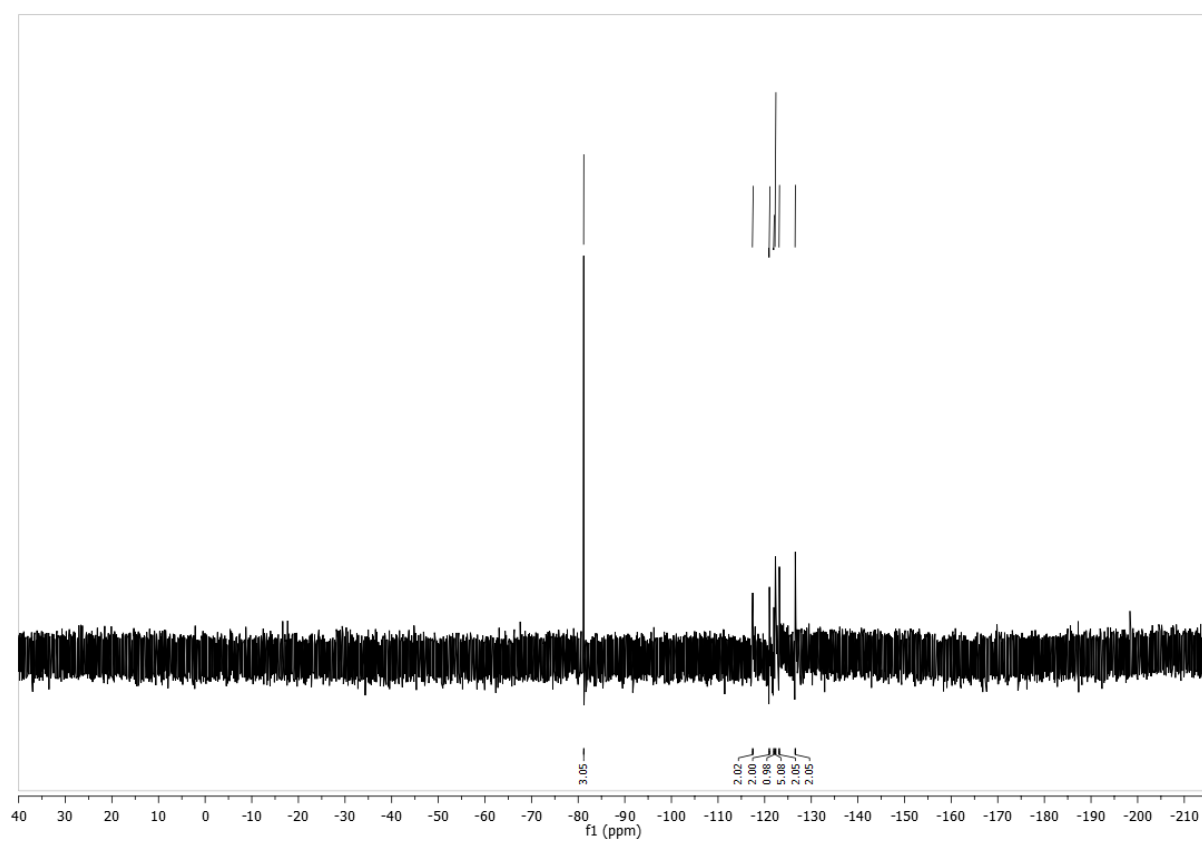


G Appendix

5-iodo-6-(perfluorooctyl)-2-phenylhexahydro-1*H*-4,7-epoxyisoindole-1,3(2*H*)-dione (360)

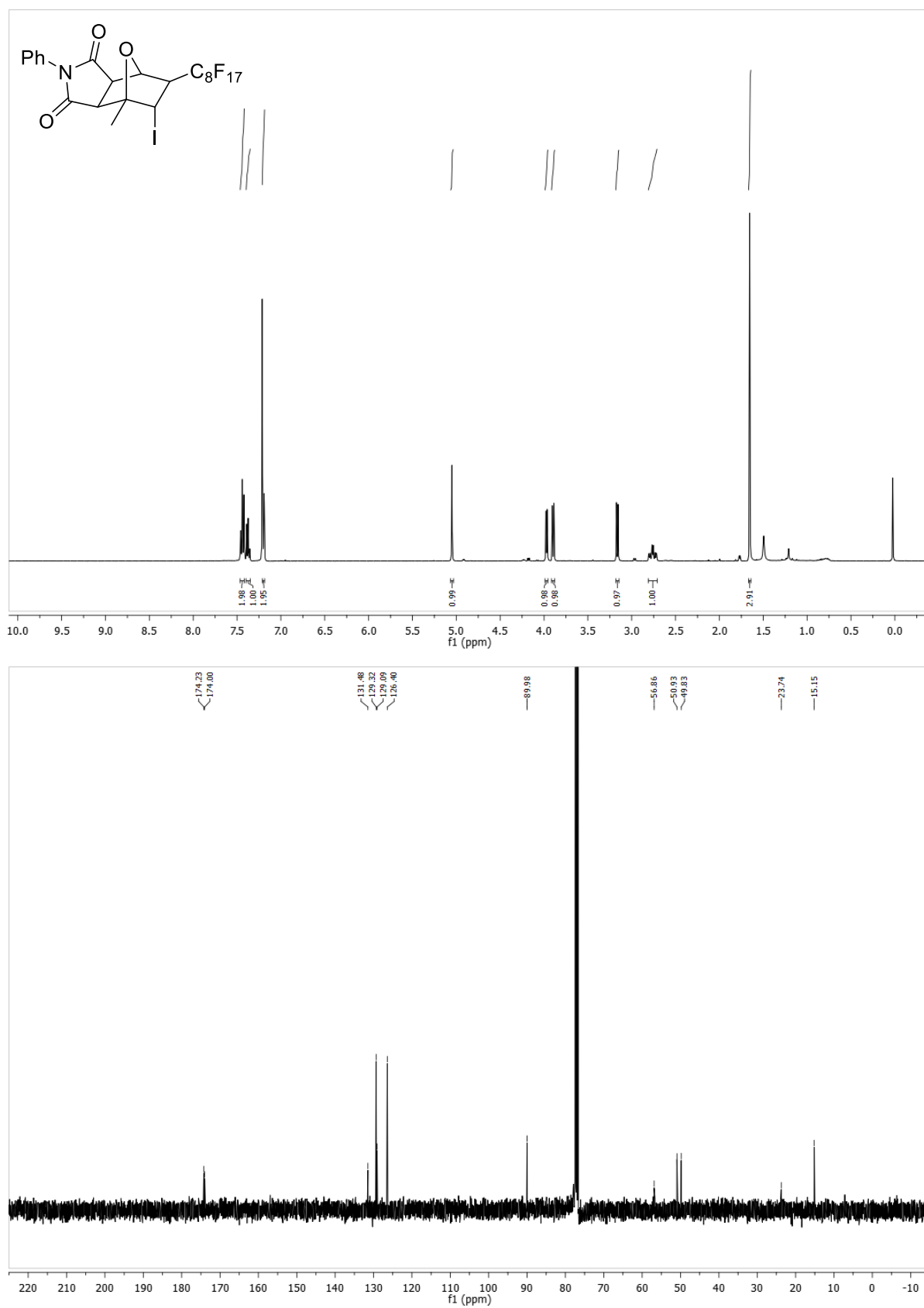


G Appendix



G Appendix

5-iodo-4-methyl-6-(perfluorooctyl)-2-phenylhexahydro-1*H*-4,7-epoxyisindole-1,3(2*H*)-dione (357)



H Acknowledgement

H Acknowledgement

Zuallererst möchte ich mich natürlich bei Prof. Dr. Oliver Reiser bedanken für die freundliche Aufnahme in seinen Arbeitskreis, das interessante und vielseitige Thema, seine fachliche Anleitung und Unterstützung während der Masterarbeit und Promotion.

Ein großer Dank geht vor allem auch an Dr. Peter Kreitmeier für seine fachliche Beratung, zügige Reparatur von defekten Geräten und zuverlässige Beschaffung von Chemikalien. Ein großes Dankeschön natürlich auch an unsere Mitarbeiter Brigitte Eichenseher, Klaus Döring, Helena Konkel, Johannes Floß und Roxane Harteis für die kräftige Unterstützung. Des Weiteren möchte ich mich bei unseren Sekretärinnen Antje Weigert und Michaela Schüle für die Hilfe im bürokratischen Alltag bedanken.

Außerdem gilt mein Dank den Mitarbeitern der Zentralen Analyse. Vor allem an Josef Kiermaier und Wolfgang Söllner für das Ausführen der zahlreichen Massenspektroskopien. Auch den Mitarbeitern der NMR-Abteilung, Fritz Kastner, Veronica Scheidler, Annette Schramm und Georgine Stühler möchte ich danken.

Für die wunderbare und herzliche Aufnahme in den Arbeitskreis sowie das stets heitere Klima und all die schönen Erlebnisse sowohl während als auch nach der Arbeitszeit möchte ich mich natürlich bei allen derzeitigen als auch ehemaligen Mitarbeitern und Gästen am AK Reiser herzlichst bedanken. Eine schönere Zeit als mit euch kann man sich gar nicht wünschen. Besonderer Dank geht dabei an Thomas Föll, Lisa Stadler, Michael Leitner, Andreas Hartl, Simon Budde, Lukas Traub, Christian Eichinger, Benjamin Kastl, Matthias Gnahn, Martin Hofmann, Eva Plut, Masa Kastner, Nejc Petek, Sebastian Engl, Christian Faderl, Thomas Ertl, Saerom Park, Asik Hossain, Daniel Dobler, Corina Eichenseher, Verena Lehner, Andreas Bergmann, Sabine Kerres, Daniel Rackl, Natalija Moor, Carina Sonnleitner, Robert Eckl, Thomas Weinbender, Alexander Reichle, Sebastian Fischer, Lisa Uhlstein, Anna Rustler, Andreas Ratzenböck, Tomislav Krolo, Tobias Babl und Anurag-Nitin Chinchole.

Auch außerhalb des AK Reiser gab es in der Fakultät Chemie viele nette Leute, mit denen man auch gerne mal nach der Arbeit fröhlich weiter über Chemie diskutiert, u.a. Philipp Nitschke, Andreas Graml, Alexander Wimmer, Matthias Schmalzbauer, Felix Riedlberger, Tobias Kahoun und Johannes Gramüller.

Mein größter Dank geht natürlich an alle meine Laborkollegen mit denen ich über all die Jahre eine wunderschöne Zeit im Labor 33.1.17 hatte. Zunächst besonders an Daniel Dobler der mich herzlich aufgenommen hat und mir den Einstieg in den Laboralltag sehr erleichtert hat. Dann möchte ich vor allem Thomas Föll und Eva Plut danken für die geile Zeit, die wir im Labor hatten, die abwechslungsreiche Musik, die wir genießen konnten und für die schönen Gespräche und Zusammenarbeit. Und natürlich möchte ich mich auch bei den zahlreichen weiteren Laborkollegen bedanken, die ich über die Jahre kennenlernen durfte: Adela Carillo, Matic Urlep, Victoria Scheidler, Urszula Klimczak, Pi Cheng, Martin Stinglhamer, Marco Henriquez und vor allem auch Alexander Reichle.

Ganz herzlich möchte ich mich auch bei Lisa Stadler bedanken. Dafür, dass sie mich in den letzten Monaten in ihrem Labor 33.1.11 so herzlich aufgenommen hat aber auch für die schöne Zeit während all der Jahre.

H Acknowledgement

Auch den Leuten aus dem Stammtischlabor 33.1.13, Andreas Hartl, Simon Budde, Christian Eichinger, Anna Rustler und Anurag-Nitin Chinchole möchte ich dafür danken, dass immer mal ein Plätzchen für mich frei war, wenn man jemanden zum Reden oder Diskutieren brauchte.

Ein besonderer Dank geht auch an Sebastian Engl für die zahlreichen „Fachgespräche“ und Unterstützung bei sämtlichen Problemen.

Meinen ehemaligen Forschungspraktikanten und Bacheloranten Susanne Märkl, Fabian Kellermeier, Tamara Woppmann, Dominik Kreutzer und vor allem Tomislav Krolo möchte ich herzlichst für ihre Unterstützung danken. Ebenso den Studenten aus den Laborpraktika mit denen ich immer eine schöne Zeit hatte.

Für das Korrekturlesen dieser Dissertation möchte ich nochmals Michael Leitner, Lisa Stadler, Simon Budde und Andreas Hartl meinen Dank aussprechen.

Doch auch einen herzlichsten Gruß möchte ich meinen guten Freunden Christian und Helena Hoidn, Markus Setzer, Angelika Dineiger, Max Lindner, Rene Thanabalan aber vor allem Rainer Herzog schicken für ihre Unterstützung in all den Jahren.

Der meiste Dank jedoch gilt meiner Familie, ohne die ich das nie schaffen hätte können. Vor allem meinen Eltern, die mich immer unterstützt haben und immer hinter mir standen, und meinen beiden Brüdern. Ich bin euch von ganzem Herzen dankbar.

I Declaration

I Declaration

Herewith I declare that this present thesis is a presentation of my original work prepared single-handed. Wherever contributions from others are involved, all of them are marked clearly, with reference to the literature, license, and acknowledgement of collaborative research.

Regensburg, 14.09.2021

Peter Ehrnsberger